

---

---

INHIBITING HEPATITIS B VIRUS GENE  
EXPRESSION WITH HAMMERHEAD RIBOZYMES  
THAT TARGET THE *HB<sub>x</sub>* OPEN READING FRAME

Marc Saul Weinberg

---

A thesis submitted to the Faculty of Health Sciences, University of the  
Witwatersrand, Johannesburg, in fulfilment of the requirements for the  
degree of  
Doctor of Philosophy

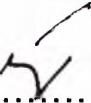
Johannesburg, 2002

---

---

## DECLARATION

I, Marc Saul Weinberg declare that this thesis is my own work. It is being submitted for the degree of Doctor of Philosophy in the University of the Witwatersrand, Johannesburg. It has not been submitted before for any degree or examination at this or any other University.

M. S. W 

.....

... 28<sup>th</sup> day of ..... October ..... 2002

---

...for my purpose holds  
To sail beyond the sunset, and the baths  
Of all the western stars, until I die.  
It may be that the gulfs will wash us down:  
It may be we shall touch the Happy Isles,  
And see the great Achilles, whom we knew.  
Though much is taken, much abides; and though  
We are not now that strength which in old days  
Moved earth and heaven; that which we are, we are;  
One equal temper of heroic hearts,  
Made weak by time and fate, but strong in will  
To strive, to seek, to find, and not to yield.

Tennyson, *Ulysses*, 62-70

**For my parents.**

---

---

## PUBLICATIONS AND PRESENTATIONS

The following articles, patents and conference presentations arose from work presented in this thesis.

### Research Articles

Passman M., Weinberg M.S, Kew M.C. and Arbuthnot P.B. (2000) In situ demonstration of inhibitory effects of hammerhead ribozymes that are targeted to the Hepatitis Bx sequence in cultured cells, *Biochem. Biophys. Res. Commun.* **268**: 728-733

Weinberg M.S., Passman M., Kew M.C. and Arbuthnot P.B. (2000) Hammerhead ribozyme-mediated inhibition of Hepatitis B virus X gene expression in cultured cells, *J. Hepatol.* **33**: 142-151

Weinberg M.S., Passman M., Kew M.C., and Arbuthnot P.B. (2002) Multimeric hammerhead ribozymes targeted to the Hepatitis B virus X open reading frame cleave HBx mRNA *in vitro* and inhibit HBV gene expression in cultured cells, (manuscript in preparation)

### Patents

Marc Weinberg and Patrick Arbuthnot, Ribozyme Therapy of HBV, 30<sup>th</sup> April 2001.  
South African Patent Application Number: 2002/3449

### Presentations

- 1) 2<sup>nd</sup> International Congress of Biochemistry and Molecular Biology, Potchefstroom, South Africa, September 30<sup>th</sup> to October 3<sup>rd</sup>, 1998, Ribozyme and Antisense Oligonucleotide-mediated Inhibition of the Hepatitis B Virus X Protein, a Potential Antiviral Therapy. M.S. Weinberg, M.C. Kew, P. B Arbuthnot
-



- 
- 2) 49<sup>th</sup> International Association for the Study of the Liver / American Association for the Study of Liver Diseases (ISAL/AASLD) conference, Chicago, USA, November 4<sup>th</sup>-6<sup>th</sup>, 1998, Ribozyme and Antisense Oligonucleotide-mediated Inactivation of Hepatitis B virus X protein in Cell Culture. M.S. Weinberg, M.C. Kew, P. B. Arbuthnot
  
  - 3) Molecular Biology of Hepatitis B Viruses, Institut Pasteur, Paris, France, September 18<sup>th</sup>-21<sup>st</sup>, 2000, Inhibition of HBV Gene Expression in Cultured Cells by Hammerhead Ribozymes that Target the X Open Reading Frame. M.S. Weinberg, M. Passman, C. Crowther, M.C. Kew, P. B. Arbuthnot
  
  - 4) Knowledge Foundation Conference – RNA in Drug Development: RNA as a Tool and Target, San Diego, USA, November 12<sup>th</sup>-13<sup>th</sup>, 2001, Multimeric Hammerhead Ribozymes Targeted To The Hepatitis B Virus X Open Reading Frame Cleave *HBx* mRNA *in vitro* And Inhibit HBV Gene Expression In Cultured Cells. M.S. Weinberg, M. Passman, M.C. Kew, P. B. Arbuthnot
-

---

## ABSTRACT

Hepatitis B virus (HBV) infection is endemic to several populous regions and is often complicated by cirrhosis and hepatocellular carcinoma (HCC). Present treatment of chronic HBV infection is usually ineffective and novel therapeutic approaches are an important medical objective. The X open reading frame (ORF) of HBV, *HBx*, is a conserved sequence that overlaps with the polymerase ORF and viral *cis*-elements, and is present within all viral transcripts. In addition, the *HBx* ORF encodes a 17 kDa transactivator protein, HBx, which is required for the establishment of viral infection and has been implicated in HBV-associated hepatocarcinogenesis. The *HBx* sequence thus represents a compelling target for applying nucleic acid hybridisation-based therapeutic agents for the inhibition of HBV gene expression and replication.

Hammerhead ribozymes are RNA enzymes that can be designed to hybridise to short complementary RNA sequences and catalyse the specific endonucleolytic cleavage of the phosphodiester backbone in *trans* at conserved 5' NUH 3' triplet sequences. *Trans*-cleaving hammerhead ribozymes have been applied as therapeutic agents to a number of different diseases for the targeted 'knockdown' of both viral and cellular gene expression. Although previous studies have shown that HBV RNA is susceptible to hammerhead ribozyme cleavage *in vitro*, the intracellular inhibitory effects of hammerhead ribozymes targeted to HBV remained unresolved.

Liver-derived cells were co-transfected with anti-HBx ribozyme expression vectors (along with catalytically inactive and antisense RNA control vectors) together with plasmids that constitutively express HBx or reconstitute intracellular HBV infection. Hammerhead ribozymes that were catalytically active *in vitro* were able to inactivate *HBx* mRNA, and inhibit HBx *trans*-activation function in cultured cells. Using a replication-competent HBV vector, ribozymes inhibited markers of HBV replication by inhibiting viral gene expression and decreasing the secretion of HBsAg and HBeAg into the culture medium. To confirm ribozyme antireplicative effects, a sensitive *in situ* measurement of ribozyme action in co-transfected Huh7 cells was assessed using an HBV vector, where the preS2/S region was replaced by DNA encoding enhanced green

---

fluorescent protein (EGFP). Ribozymes inhibited EGFP marker gene expression *in situ* and provided an accurate measurement of ribozyme antireplicative efficacy in cell culture. However, the data do not exclude a dominant antisense effect.

Vectors were developed that include head-to-tail concatamers of different ribozyme-encoding units, each with a respective 3'-flanked *cis* complementary target cleavage sequence. The aim was to generate expression cassettes encoding single transcripts with many *cis*-cleaving hammerhead ribozymes that retain the ability to cleave simultaneously in *trans*. All multimeric hammerhead ribozyme transcripts generated *in vitro*, self-cleaved to release 5' and 3' trimmed *trans*-acting hammerhead ribozymes. Expression vectors that encode multimeric *cis*- and *trans*-cleaving hammerhead ribozymes decreased HBsAg and HBeAg secretion when co-transfected along with HBV vectors in Huh7 cells. These ribozymes demonstrated an improved antireplicative effect when compared to previous single-unit, or catalytically defective ribozyme controls. The most elaborate multimeric hammerhead ribozyme expression vector, a 24-mer construct, that generates eight units of each of the three ribozymes, inhibited EGFP marker gene expression 10-15% more efficiently than single-unit ribozyme counterparts when measured *in situ* using a modified HBV EGFP vector.

In conclusion, the hammerhead ribozyme-encoding vectors generated represent a significant improvement on previously described anti-HBV ribozyme constructs. Moreover, the *HBx* ORF proved to be a suitable target site for hammerhead ribozyme-mediated inhibition of HBV gene expression and markers of replication in cell culture. For future use *in vivo*, expression cassettes encoding multimeric hammerhead ribozymes may be incorporated into liposomes or viral delivery vectors. Should the endogenously expressed hammerhead ribozymes presented in this thesis prove to be safe and efficacious in animal models of viral infection they may be further applied as therapeutic agents for the treatment of chronic HBV infection.

---

---

## ACKNOWLEDGEMENTS

The pursuit of new knowledge is never undertaken alone, and I am indeed indebted to a number of people who have helped both directly and indirectly in this thesis.

- 1) My gratitude extends foremost to my supervisor, colleague and friend, Prof. Patrick Arbuthnot, for embarking with me on a truly novel and rewarding project. Many thanks for all the sound advice and for consistent, thorough supervision. This has been an inspired and wonderful undertaking and thanks for enthusiastically seeing it through to the very end.
  - 2) I wish to thank my co-supervisor, Prof. Michael Kew whose support, supervision and encouragement I am grateful for. I am additionally grateful and privileged to have made use of the facilities within the Molecular Hepatology Research Unit.
  - 3) I would like to thank in particular my colleague Marc Passman for generating the EGFP-expression vector pCI neo GFP and the HBV modified vector pCH-EGFP. These vectors were invaluable in all transfection studies presented in this thesis. Thanks for often seeing to the health of the cells and for your crucial assistance in many of the transfections experiments.
  - 4) My gratitude extends to Alison Coppin and Mirriam Mashele of the National Institute of Communicable Diseases (formerly the National Institute for Virology) for assisting with the HBsAg and HBeAg measurements. Furthermore, I wish to acknowledge Dr. C. Wang for the gift of plasmid p $\beta$ -actin  $\beta$ -gal, Dr. Christian Bréchet for the plasmid pHBV *adw* HTD, and Dr. Michael Nassal for plasmid pCH-9/3091.
  - 5) I sincerely wish to thank my colleagues, Alexio Capovilla, Sergio Carmona, Naazneen Moolla and Thérèse Coetzer for many insightful comments, philosophical discussions, and for sharing my passion for molecular
-

---

biology. Thanks again to Thérèse for reading through an entire draft of my thesis. I also wish to acknowledge Dr. Anna Kramvis for the many occasions I've needed practical advice and for helping me use the GeneDoc™ program.

- 6) Financial support over the last five years is gratefully acknowledged in the form of scholarships/bursaries from: the University, the Loewenstein Endowment Trust, The National Research Foundation (formerly the Foundation for Research Development) and the Poliomyelitis Research Foundation. I also wish to acknowledge financial support from: the University Research Council, the Medical Faculty Research Endowment Fund, the Medical Research Council and the Cancer Association of South Africa.
- 7) To my parents, Alan and Grazia Weinberg, both professors, thanks for your love and support and for the arduous task of proofreading.
-

---

**TABLE OF CONTENTS**

	Page
TITLE PAGE.....	i
DECLARATION.....	ii
DEDICATION.....	iii
PUBLICATIONS AND PRESENTATIONS.....	iv
ABSTRACT.....	vi
ACKNOWLEDGEMENTS.....	viii
TABLE OF CONTENTS.....	x
LIST OF FIGURES.....	xv
LIST OF TABLES.....	xix

---

**CHAPTER 1.0: INTRODUCTION..... 1**


---

<b>1.1 Hepatitis B virus biology.....</b>	<b>2</b>
1.1.1 Hepadnaviruses.....	2
1.1.2 HBV structure, genome and transcripts.....	4
1.1.3 Viral gene products.....	6
1.1.3.1 Core and preC/eAg.....	6
1.1.3.2 Surface proteins.....	7
1.1.3.3 Polymerase.....	8
1.1.3.4 X protein, HBx.....	9
1.1.4 Viral <i>cis</i> -elements.....	10
1.1.4.1 HBV promoters and enhancers.....	10
1.1.4.2 Polyadenylation signal.....	12
1.1.4.3 Epsilon ( $\epsilon$ ).....	13
1.1.5 HBV life cycle.....	13
1.1.6 Serotypes and genotypes.....	16
1.1.6.1 Serotypes.....	16
1.1.6.2 Genotypes.....	16
1.1.7 Pathogenesis.....	17
1.1.7.1 Acute and chronic HBV infection.....	17
1.1.7.2 HBV and hepatocellular carcinoma (HCC).....	19
1.1.7.3 The role of HBx in HBV-associated HCC.....	20
<b>1.2 Treatment of chronic HBV infection.....</b>	<b>21</b>
1.2.1 Nucleoside analogues and immune system modulators.....	22
1.2.2 Novel molecular approaches to therapy.....	25
<b>1.3 Ribozymes.....</b>	<b>26</b>
1.3.1 Catalytic RNAs.....	26
1.3.2 Ribozymes and the origins of life debate.....	28
1.3.3 Hammerhead ribozymes.....	31
1.3.4 Hammerhead ribozyme structure and function.....	32
1.3.5 Hammerhead ribozymes that cleave in <i>trans</i> .....	35

---

1.3.5.1	Defining the <i>trans</i> -cleaving activity of hammerhead ribozymes	36
1.3.5.2	<i>In vitro</i> kinetics of <i>trans</i> -cleaving hammerhead ribozymes	36
1.3.6	Other small ribozymes designed to cleave in <i>trans</i> .....	40
1.4	<b>Nucleic acid-based therapy of HBV</b> .....	43
1.4.1	Presynthesized antisense oligodeoxynucleotides.....	44
1.4.2	Endogenously expressed antisense RNA.....	47
1.4.3	Ribozymes targeting HBV.....	48
1.4.4	Thesis objectives.....	51

---

**CHAPTER 2.0: HAMMERHEAD RIBOZYMES AND ANTISENSE RNAs TARGETED TO THE HBV *HBx* OPEN READING FRAME..... 54**

---

2.1	<b>Summary</b> .....	54
2.2	<b>Introduction</b> .....	55
2.3	<b>Materials and methods</b> .....	56
2.3.1	Hammerhead ribozymes and antisense RNA expression vectors.....	56
2.3.2	Target and reporter plasmids.....	58
2.3.3	<i>In vitro</i> transcription and cleavage.....	60
2.3.4	Cell culture.....	62
2.3.5	Detection of <i>HBx</i> mRNA in transfected cells.....	62
2.3.6	Transfection and detection of $\beta$ -galactosidase activity.....	64
2.4	<b>Results</b> .....	65
2.4.1	The selection of conserved regions of the <i>HBx</i> ORF for hammerhead ribozyme and antisense RNA hybridisation.....	65
2.4.2	Design of hammerhead ribozyme, antisense RNA and target vectors.....	66
2.4.3	Ribozyme-mediated cleavage of <i>HBx</i> RNA <i>in vitro</i> .....	66
2.4.4	Inhibition of <i>HBx trans</i> -activation by hammerhead ribozymes and antisense RNAs in cell culture.....	70
2.4.5	Ribozyme-expressing vectors decrease <i>HBx</i> mRNA in transfected cells.....	75
2.5	<b>Discussion and conclusions</b> .....	77

---



---

**CHAPTER 3.0: HAMMERHEAD RIBOZYME-MEDIATED  
INHIBITION OF HBV GENE  
EXPRESSION IN Huh7 HEPATOMA CELLS ..... 82**

---

3.1	<b>Summary</b> .....	82
3.2	<b>Introduction</b> .....	83
3.3	<b>Materials and Methods</b> .....	84
3.3.1	Target vectors.....	84
3.3.2	Northern blot.....	84
3.3.2.1	Preparation of HBV-specific probes	86
3.3.3	HBsAg and HBeAg secretion from transfected cells.....	86
3.3.4	<i>In situ</i> detection of hammerhead ribozyme activity.....	86
3.4	<b>Results</b> .....	87
3.4.1	Vectors expressing target sequences.....	87
3.4.2	The effects of ribozyme-expressing vectors on HBV RNA expression in transfected cells.....	87
3.4.3	Measurements of HBsAg and HBeAg secretion in co-transfected Huh7 cells.....	89
3.4.4	<i>In situ</i> detection of ribozyme activity in transfected Huh7 cells .....	91
3.4.4.1	Ribozyme modulation of EGFP expression	91
3.4.4.2	Ribozyme effects detected <i>in situ</i> and HBsAg secretion measurements in co- transfected Huh7 cells	94
3.5	<b>Discussion and conclusions</b> .....	95

---

**CHAPTER 4.0: MULTIMERIC CIS- AND TRANS-ACTING  
HAMMERHEAD RIBOZYMES THAT TARGET  
THE HBV HBx OPEN READING FRAME ..... 99**

---

4.1	<b>Summary</b> .....	99
4.2	<b>Introduction</b> .....	99
4.3	<b>Materials and Methods</b> .....	101
4.3.1	Plasmid vectors encoding multimeric ribozyme sequences.....	101
4.3.1.1	Plasmids containing single <i>cis</i> - and <i>trans</i> - cleaving ribozyme units	101
4.3.1.2	Multimeric <i>cis</i> - and <i>trans</i> -cleaving hammerhead ribozymes	107
4.3.1.3	Eukaryotic expression vectors producing multi-unit <i>cis</i> - and <i>trans</i> -cleaving ribozymes	108

---



4.3.2	<i>In vitro</i> transcription and cleavage reactions.....	110
4.3.2.1	Preparation of transcription template.....	110
4.3.2.2	Multimeric ribozyme <i>cis</i> -cleavage.....	110
4.3.2.3	Multimeric ribozyme <i>trans</i> -cleavage.....	112
4.3.3	<i>In situ</i> detection of multimeric hammerhead ribozyme activity.....	112
4.3.4	HBsAg and HBeAg assays.....	114
4.4	<b>Results</b> .....	114
4.4.1	Multimeric hammerhead ribozyme vectors.....	114
4.4.2	Proof of multimeric ribozyme efficacy.....	117
4.4.2.1	<i>In vitro</i> transcription and ribozyme cleavage.....	117
4.4.2.2	<i>In vitro trans</i> -cleavage activity of 5' and 3' monomeric hammerhead ribozymes generated by <i>cis</i> -cleavage.....	121
4.4.3	Multimeric ribozyme inhibitory effects on HBV gene expression in transfected liver-derived cells.....	121
4.4.3.1	The inhibitory effects of multimeric ribozymes <i>in situ</i> .....	124
4.4.3.2	Effects of multimeric ribozyme on HBV antigen secretion in cell culture supernatants.....	126
4.5	<b>Discussion and conclusions</b> .....	129
<hr/>		
<b>CHAPTER 5.0: GENERAL DISCUSSION AND CONCLUSION</b> .....		134
<hr/>		
5.1	<b>Hammerhead ribozymes and HBV</b> .....	134
5.1.1	Hammerhead ribozymes targeted to the <i>HBx</i> ORF.....	134
5.2.1	Hammerhead ribozymes and antiviral agents.....	135
5.2	<b>Designing therapeutic hammerhead ribozymes</b> .....	137
5.2.1	The effects of ribozyme flanking sequences.....	137
5.2.2	Finding suitable target sites for ribozyme cleavage.....	138
5.2.1.1	Probing RNA secondary structure using computer algorithms.....	139
5.2.1.2	The accessibility of target RNA for ribozyme cleavage <i>in vivo</i> .....	140
5.2.1.3	Combinatorial screening techniques for finding optimal ribozyme cleavage sites.....	140
5.2.3	Factors governing <i>in vivo</i> ribozyme activity.....	142
5.2.4	Summary.....	144
5.3	<b>Delivery of ribozymes</b> .....	145
5.3.3	Presynthesized hammerhead ribozymes.....	146
5.3.4	Viral-mediated delivery of ribozyme expression cassettes.....	147
5.3.4.1	Retroviral vectors.....	148
<hr/>		

---

5.3.4.2	Adenoviral vectors	149
5.3.4.3	Adeno-associated viruses (AAVs) and other viral systems	150
5.3.5	Cationic liposomes and non-viral delivery strategies.....	152
5.4	<b>Conclusion</b> .....	153

---

6.0	<b>APPENDICES</b> .....	157
-----	-------------------------	-----

---

A	<b>Standard Laboratory Methods</b> .....	157
A1	Bacterial transformation.....	157
A2	Plasmid DNA preparation.....	157
A3	RNA extraction and purification.....	159
A4	DNA/RNA purification.....	159
A5	Manual DNA sequencing.....	161
A6	Histochemical assay using X-gal.....	162
A7	Transfections into mammalian cells.....	162
B	<b>Solutions, Reagents and Buffers</b> .....	163
B1	Solutions.....	163
B2	Electrophoresis Buffers (Stock solutions).....	165
B3	Culture Media.....	166
C	<b>Other Appendices</b> .....	167
C1	Construction of multimeric <i>cis</i> - and <i>trans</i> -cleaving vectors.....	167
C2	Determination of equivalent transfection efficiencies.....	169
C3	HBx sequence variation for hammerhead ribozyme hybridisation and cleavage.....	170

---

7.0	<b>REFERENCES</b> .....	171
-----	-------------------------	-----

---

## LIST OF FIGURES

	Page
<b>Figure 1.1</b> A diagrammatic illustration of an infectious HBV virion or 'Dane' particle.....	4
<b>Figure 1.2</b> Transcriptional and translational organisation of the hepatitis B virus genome (strain <i>ayw</i> ).....	5
<b>Figure 1.3</b> Schematic illustration of the HBV infection and replicative cycle within the hepatocyte.....	8
<b>Figure 1.4</b> Essential steps involved in hepadnaviral DNA replication starting from a newly transcribed pgRNA template, with terminal repeats (R), 5' cap and a polyA tail.....	15
<b>Figure 1.5</b> Global maps showing the similarity between the geographical distributions of chronic hepatitis B virus infection and hepatocellular carcinoma.....	18
<b>Figure 1.6</b> The 'RNA World hypothesis' as envisioned by Cech and Golden (Cech and Golden, 1999).....	29
<b>Figure 1.7</b> A two-dimensional representation of the hammerhead ribozyme with all three helical arms terminated by nucleotide loops.....	34
<b>Figure 1.8</b> <i>Cis</i> - and <i>trans</i> -cleaving hammerhead ribozymes derived from the Haseloff-Gerlach model (Haseloff and Gerlach, 1988).....	37
<b>Figure 1.9</b> An illustration of the minimal kinetic description and reaction scheme for a <i>trans</i> -cleaving hammerhead ribozyme.....	38
<b>Figure 1.10</b> The general secondary structure depicting the minimal core sequences of both a <i>trans</i> -cleaving hairpin (Berzal-Herranz <i>et al.</i> , 1993) and antigenomic HDV ribozyme (Ananvoranich and Perreault, 1998) and their complementary substrates.....	42
<b>Figure 2.1</b> The catalytic sequences for hammerhead ribozymes <i>HBx</i> :Rz1 <sub>1473</sub> and <i>HBx</i> :Rz2 <sub>1651</sub> and hybridisation sequences for antisense RNAs <i>HBx</i> :At1 <sub>1473</sub> and <i>HBx</i> :At2 <sub>1651</sub> .....	59
<b>Figure 2.2</b> The target sequences for hammerhead ribozymes	

	<i>HBx</i> :Rz1 <sub>1473</sub> and <i>HBx</i> :Rz2 <sub>1651</sub> .....	61
<b>Figure 2.3</b>	Principle of the <i>HBx trans</i> -activation assay.....	64
<b>Figure 2.4</b>	The accessibility of <i>HBx</i> RNA sequences for hammerhead ribozyme and antisense RNA hybridisation.....	67
<b>Figure 2.5</b>	Hammerhead ribozyme-mediated cleavage of an <i>in vitro</i> transcribed <i>HBx</i> RNA substrate (HBV strain <i>ayw</i> ).....	69
<b>Figure 2.6</b>	Representative low power microscopic field of $\beta$ -galactosidase positive cells.....	71
<b>Figure 2.7</b>	Effect of ribozyme co-transfection on the number of $\beta$ -galactosidase positive Chang and PLC/PRF/5 cells.....	73
<b>Figure 2.8</b>	Effect of ribozyme and antisense co-transfection on the number of $\beta$ -galactosidase positive PLC/PRF/5 cells and hepatocytes derived from primary cultures of resected malignant liver tissue.....	74
<b>Figure 2.10</b>	Detection of <i>HBx</i> mRNA fom Huh7 cells transfected with ribozyme and <i>HBx</i> -encoding sequences.....	76
<b>Figure 3.1</b>	Plasmid constructs pCH-9/3091 and pCH-EGFP showing their open reading frames, respective transcripts and sites targeted by position of cleavage by <i>pHBx</i> :Rz1 <sub>1473</sub> and <i>pHBx</i> :Rz2 <sub>1651</sub> .....	85
<b>Figure 3.2</b>	Detection of HBV RNA fom Huh7 cells co-transfected with ribozyme vectors and an HBV replication competent vector.....	88
<b>Figure 3.3</b>	Secretion of HBsAg and HBeAg into the culture supernatant after transfection of Huh7 cells.....	90
<b>Figure 3.4</b>	Combined phase contrast and fluorescent microscopic field of Huh7 cells transfected with pCH-EGFP and either pCI neo, <i>pHBx</i> :Rz1 <sub>1473</sub> , <i>pHBx</i> :Rz1* <sub>1473</sub> as well as untransfected cells.....	92
<b>Figure 3.5</b>	Effect of ribozyme co-transfection on HBsAg production and on the number of EGFP positive Huh7 cells .....	93
<b>Figure 3.6</b>	Effect of ribozyme co-transfection on HBsAg production from plasmid pCH-9/3091.....	94
<b>Figure 4.1</b>	The principle of multimeric hammerhead ribozyme <i>cis</i> - and <i>trans</i> -cleavage action.....	102

---

<b>Figure 4.2</b>	Plus- and minus-strand sequences of a full-length <i>cis</i> - and <i>trans</i> -cleaving multimeric unit of ribozymes: <i>HBx</i> :Rz1 <sub>1473</sub> and <i>HBx</i> :Rz2 <sub>1651</sub> and <i>HBx</i> :Rz3 <sub>1607</sub> .....	103
<b>Figure 4.3</b>	A schematic illustration of the general structure of a multimeric <i>cis</i> - and <i>trans</i> -cleaving hammerhead ribozyme expression cassette.....	111
<b>Figure 4.4</b>	Sequences targeted by three hammerhead ribozymes <i>HBx</i> :Rz1 <sub>1473</sub> , <i>HBx</i> :Rz2 <sub>1651</sub> , and <i>HBx</i> :Rz3 <sub>1607</sub> .....	113
<b>Figure 4.5</b>	Restriction endonuclease digestion of multimeric hammerhead ribozyme plasmid constructs with <i>SpeI</i> and <i>XbaI</i> .....	115
<b>Figure 4.6</b>	DNA sequences of dimer series pBSKSII(+)-derived <i>cis</i> - and <i>trans</i> -cleaving hammerhead ribozyme vectors: pBS- <i>M2HBx</i> :Rz1 <sub>1473</sub> , pBS- <i>M2HBx</i> :Rz2 <sub>1651</sub> and pBS- <i>M2HBx</i> :Rz3 <sub>1607</sub> .....	116
<b>Figure 4.7</b>	<i>In vitro cis</i> -cleavage of multimeric <i>cis</i> - and <i>trans</i> -cleaving hammerhead ribozymes <i>HBx</i> :Rz1 <sub>1473</sub> and <i>HBx</i> :Rz3 <sub>1607</sub> .....	118
<b>Figure 4.8</b>	<i>Cis</i> -cleavage <i>in vitro</i> of transcripts containing multimeric hammerhead ribozymes.....	119
<b>Figure 4.9</b>	The <i>trans</i> -cleaving action <i>in vitro</i> of transcripts encoding multimeric <i>cis</i> - and <i>trans</i> -cleaving units of the same hammerhead ribozymes.....	122
<b>Figure 4.10</b>	The <i>trans</i> -cleaving action <i>in vitro</i> of transcripts encoding multimeric <i>cis</i> - and <i>trans</i> -cleaving units of different hammerhead ribozymes.....	123
<b>Figure 4.11</b>	<i>In situ</i> ribozyme modulation of EGFP activity in co-transfected Huh7 cells.....	125
<b>Figure 4.12</b>	An <i>in situ</i> quantitative comparison of the number of EGFP-positive Huh7 cells modulated by the transfection of various ribozyme-encoding expression vectors.....	126
<b>Figure 4.13</b>	Measurement of HBsAg and HBeAg secretion from Huh7 cells co-transfected with single-unit and multimeric ribozyme vectors (as well as antisense RNA) and a replication-competent HBV vector, pHTD <i>adw</i> HBV.....	127

---

---

<b>Figure 6.1</b>	A schematic illustration of the construction of a single-unit ( <i>M1</i> series) <i>cis</i> - and <i>trans</i> -cleaving hammerhead ribozyme cloning vector for each of the three hammerhead ribozymes.....	167
<b>Figure 6.2</b>	A schematic illustration of the construction of a multiple-unit ( <i>M2</i> series) <i>cis</i> - and <i>trans</i> -cleaving hammerhead ribozyme cloning vector for each of the three hammerhead ribozymes.....	168
<b>Figure 6.3</b>	An example of the number of EGFP-expressing Huh7 cells transfected with the plasmid pCI neo GFP for the determination of equivalent transfection efficiencies (transfection reported in 4.4.3.2).....	169
<b>Figure 6.4</b>	GeneDoc™ alignment of HBV variant RNA sense strand sequences (GenBank® accession numbers indicated) of genotypes A to G with HBV serotype ayw indicating hybridisation regions for ribozymes <i>HBx</i> :Rz1 <sub>1473</sub> , <i>HBx</i> :Rz2 <sub>1651</sub> and <i>HBx</i> :Rz3 <sub>1607</sub> .....	170

---

---

**LIST OF TABLES**

	Page
<b>Table 1.1</b> Naturally occurring ribozyme species (Cech and Golden, 1999; Doudna and Cech, 2002).....	27
<b>Table 2.1</b> Complementary sense (S) and antisense (A) oligonucleotide sequences for single unit hammerhead ribozymes and their respective cleavage-defective counterparts.....	56
<b>Table 2.2</b> Complementary sense (S) and antisense (A) oligonucleotide sequences for antisense RNA encoding vectors.....	57
<b>Table 2.3</b> Forward and reverse primers for <i>GAPDH</i> and <i>HBx</i> .....	63
<b>Table 4.1</b> Complementary oligonucleotides for single-unit <i>cis</i> -cleaving hammerhead ribozyme cassette <i>M1HBx:Rz2</i> <sub>1651</sub> .....	104
<b>Table 4.2</b> Complementary oligonucleotide sequences for 'long' and 'short' multimeric hammerhead ribozyme units of both <i>HBx:Rz1</i> <sub>1473</sub> and <i>HBx:Rz3</i> <sub>1607</sub> .....	106
<b>Table 4.3</b> pBSIIKS(+)-derived multimeric <i>cis</i> - and <i>trans</i> -cleaving hammerhead ribozyme vectors.....	109

---



---

## 1.0 INTRODUCTION

The hepatitis B virus (HBV) is an aetiological agent of both acute and chronic viral hepatitis. Chronic HBV infection represents a worldwide health problem. It is estimated that 375 million people are infected, that is, over 5% of the world's population (World Health Organisation, 1998). Endemic areas include sub-Saharan Africa, east and South-East Asia, and the western Pacific islands. In these regions between 8-15% of the population are chronic carriers (Beasley *et al.*, 1981). Although clinical manifestations of infection vary considerably, there is a strong correlation between chronic HBV infection and the risk of developing cirrhosis and hepatocellular carcinoma (HCC) (Robinson, 1994). In fact, nearly 25% of deaths in chronic carriers can be attributed to HCC (Beasley, 1988) which, along with cirrhosis, is the primary cause of morbidity and mortality in chronic HBV infected individuals.

Antiviral chemotherapy, using immune modulators and nucleoside analogues, remains presently the only treatment option for chronic HBV infection (Ganem, 1998; Lok, 2000). None of the many different chemotherapeutic strategies used at present and in the past has proven consistently successful. Moreover, chronic HBV infection continues to persist despite the availability of a suitable prophylactic vaccine for over 20 years. The global implementation of HBV vaccines, within the Expanded Programme on Immunisation (EPI), has not achieved the desired penetration, especially in sub-Saharan Africa.

An effective treatment of HBV remains elusive and represents an important medical objective. New knowledge will come from a better understanding of HBV replication and pathogenesis as well as from the propagation of new molecular tools for the treatment of viral diseases. One such approach is in the application of ribonucleic acid (RNA) catalysts, or ribozymes, which hold much promise as novel molecular therapeutic agents. The enzymatic effects of ribozymes have recently been examined for their therapeutic potential in a number of different acquired and inherited diseases (James and Gibson, 1998). Ribozymes can in principle be designed to inhibit HBV gene expression and viral replication and prevent the onset of disease-causing sequelae of chronic HBV infection. Of particular interest is the therapeutic potential of the

---



hammerhead ribozymes, which are the most versatile of the naturally occurring ribozymes (Birikh *et al.*, 1997b; Bramlage *et al.*, 1998). Although presynthesized hammerhead ribozymes can be constructed as therapeutic agents (Usman and Blatt, 2000), hammerhead ribozymes can be exploited to induce their potential antiviral effects as RNA generated endogenously from a ribozyme-encoding expression cassette.

In this thesis the antiviral potential of hammerhead ribozymes targeted to unique sequences within HBV was determined using cell culture models of HBV infection. Hammerhead ribozymes targeted to HBV have, to date, only been tested *in vitro*. Plasmid vectors were generated such that they expressed single-unit and/or multiple-unit hammerhead ribozymes. These ribozymes and their catalytically inactive ribozyme controls were tested along with antisense RNAs using assays that were specifically designed to test the efficacy of nucleic acid-mediated inhibition of HBV in cell culture. By characterising the effects of hammerhead ribozymes as intracellular inhibitors, the feasibility of these endogenously expressed nucleic acids was established for the future treatment of chronic HBV and the prevention of hepatocarcinogenesis.

## 1.1 Hepatitis B virus biology

### 1.1.1 *Hepadnaviruses*

HBV was first identified in 1965 by Blumberg as a new antigen in leukaemic sera of native Australians and was originally referred to as the “Australia antigen” (Blumberg *et al.*, 1965). Only later was this antigen shown to be the viral surface antigen or HBsAg. In 1970, Dane managed to isolate an infectious complete particle and identify it by electron microscopy (Dane *et al.*, 1970). Since then, significant strides have been made in characterising HBV biology, epidemiology and pathogenesis.

Human HBV represents the prototype of the *Hepadnaviridae*, a family of small DNA viruses that persistently infect liver cells and whose genome is the smallest known for mammalian viruses. The hepatocyte is the only confirmed site of replication for all members of this virus family. Nevertheless, HBV has been shown to infect bile ductule epithelial cells and a number of extrahepatic sites.

---

---

These include, but are not necessarily limited to, cells of the pancreas, kidney and lymphoid systems (Blum *et al.*, 1984; Nicoll *et al.*, 1997). HBV shares 70% sequence homology with mammalian hepadnaviruses discovered in woodchucks (Summers *et al.*, 1978) and in various ground squirrel species (Marion *et al.*, 1980). Old and New World primates possess wild-type infection of HBV subvariants that may prove to be species specific (Takahashi *et al.*, 2001). Human HBV is, however, capable of infecting chimpanzees, baboons and other great apes as well as various marsupials (Seeger and Mason, 2000). More distantly related viruses have been found in ducks (DHBV) (Mason *et al.*, 1980), wild herons (Sprengel *et al.*, 1988) and recently in white storks (Pult *et al.*, 2001). Domestic geese and other hosts are susceptible to infection from other avian hepadnaviral species (Marion *et al.*, 1987). Avian hepadnaviruses are grouped in the genus *avihepadnavirus* and share a similar genome structure, albeit with little sequence homology, to the mammalian hepadnaviruses, which belong to the genus *orthohepadnavirus*.

There are other significant differences between avian and mammalian hepadnaviruses. The genome of the avihepadnaviruses, which is slightly smaller than the orthohepadnaviruses, codes for two surface envelope proteins (as opposed to three in the mammalian viruses), and lacks the open reading frame (ORF) for a multifunctional protein termed HBx (Sprengel *et al.*, 1988). There does, however, appear to be a sequence vestige of the *HBx* ORF in the avihepadnaviruses, suggesting that HBx was present at some point in the evolution of the avian viruses (Lin and Anderson, 2000; Netter *et al.*, 1997). Both avian and mammalian viruses are often used as models to study the molecular biology of HBV, particularly with respect to the infection cycle, host immune response and disease-causing sequelae of chronic infection such as cirrhosis and liver cancer. More specifically, the woodchuck hepatitis virus (WHV) is used predominantly as a model of viral-induced hepatocarcinogenesis as DHBV-infected ducks or geese do not develop viral-associated HCC (Seifer *et al.*, 1991).

---

### 1.1.2 HBV structure, genome and transcripts

The genome of HBV, within virus particles or spherical virions (Dane particle), is composed of relaxed-circular, partially double-stranded DNA (pdsDNA) (Figures 1.1 and 1.2) (Robinson *et al.*, 1974). The long, full-length minus-strand is approximately 3200 nucleotides (nt) in length and has a protein (the viral polymerase) covalently bound to its 5' terminus. The plus-strand, which varies between 1700 and 2800 nt in length, depending on species and subtype, has a capped oligoribonucleotide at its 5' end. The plus-strand maintains genome circularity by a cohesive overlap across the 5' and 3' termini of the minus-strand.

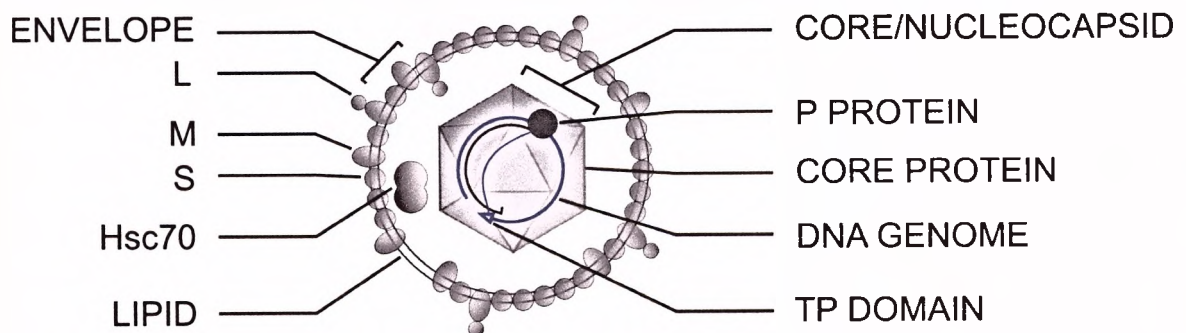


**Figure 1.1** A diagrammatic illustration of an infectious HBV virion or 'Dane' particle. The envelope bilayer contains the large (L), middle (M) and small (S) surface glycoproteins. The preS1 domain of L is displayed on both internal and external virion compartments (Prange and Streeck, 1995). The partially double stranded DNA (pdsDNA) genome is present within the icosahedral nucleocapsid. The 5' end of the complete minus-strand DNA is covalently linked to the terminal protein (TP) domain of Polymerase (P). Hsc70 represents a cellular chaperone, which co-purifies with virions and S particles (Nassal, 1999).

The HBV genome includes four ORFs that encode at least seven translation products through the use of varying in-frame initiation codons. These translation products include three surface antigens (HBsAg), the envelope glycoproteins preS1, preS2, and S; core (C or HBcAg) and e antigens (HBeAg); viral polymerase (P); and the X protein (HBx) (Figure 1.2). The genome is also replete with *cis*-elements required for the regulation of HBV gene expression and

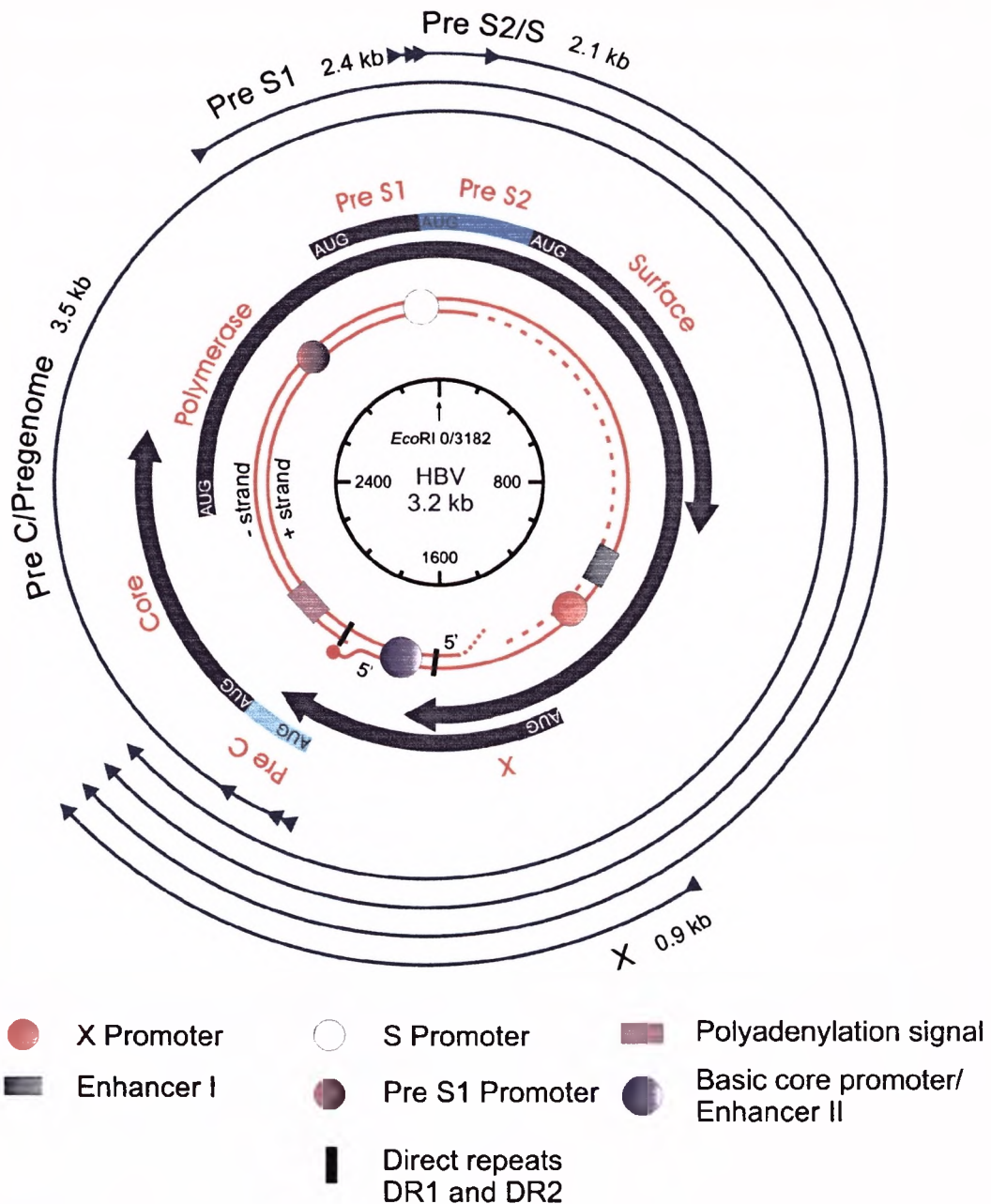


**Figure 1.2** Transcriptional and translational organisation of the hepatitis B virus genome (strain *ayw*). Co-ordinates of the genome are given relative to the single *EcoRI* restriction site. Partially double stranded (pds) HBV DNA comprises + and - strands with cohesive complementary 5' ends. Attached to the 5' end of the - DNA strand is a terminal protein (TP), whilst the 5' end of the + strand includes a short RNA oligomer cap. The *cis*-elements that regulate HBV transcription are represented by the circular and rectangular symbols. The positions of direct repeats DR1 and DR2 are indicated as black rectangles. Thick circular arrows immediately surrounding the genome indicate the viral open reading frames (with initiation codons) that encompass the entire genome. Four outer arrows, that give the 5' to 3' polarity, indicate the HBV transcripts. Multiple arrowheads at the 5' ends of the PreC/Pregenome and PreS2/S transcripts indicate heterogeneous transcription start sites. The common 3' end of all the HBV transcripts is depicted by the identical termination site and sequences that overlap with the HBx transcript.



replication. These include viral promoters, enhancers and signal regions. The 5' terminus of both strands contains regions of short (11 nucleotide) direct repeats, DR1 and DR2, which are essential for priming the synthesis of their respective DNA strands during replication. HBV's compact coding organisation ensures that every nucleotide falls within a transcribed region and that 50% of translated sequences are present in more than one ORF.

Covalently closed circular HBV DNA (cccDNA) is the template for both genomic and subgenomic viral transcript mRNAs, which are produced using cellular RNA polymerase II. The 5' terminus of the preC/pregenome and preS2/S transcripts both have heterogeneous transcription start sites. The *HBx* transcript, however, has only one unique start site. The preC and pregenomic RNA (preC/pgRNA) transcripts, which are approximately 3500 nt in size, are more than a full genome in length and contain terminal repeats at each end (Figure 1.2). The pgRNA transcript is unique in that, apart from being the genomic template for reverse transcription, it represents the mRNA for production of the core protein as well as the viral polymerase protein (Summers and Mason, 1982). Unlike the pgRNA, the genomic preC mRNA is not encapsidated (Jeong *et al.*, 2000; Nassal *et al.*, 1990). The S transcript is 2400 nt in length whilst the preS2 family of transcripts are roughly 2100 nt in size. The *HBx* mRNA is a single 900 nt transcript. The presence of a common 3' polyadenylation termination signal on the HBV genome results in all transcripts sharing the same 3' terminal sequences (see section 1.1.4.2).

### **1.1.3 Viral gene products**

#### **1.1.3.1 Core and preC/eAg**

The core ORF contains two in-frame initiation codons that divide it into the pre core (preC) and core (C) domains. Translation from the C initiation codon results in the formation of the viral core or capsid protein, C (or HBcAg). Core proteins dimerise and assemble independently to form an icosahedral nucleocapsid, which is 22 to 25 nm in diameter (Chang *et al.*, 1994). Short carboxy-terminal truncated core proteins can induce the formation of smaller nucleocapsid shells (Conway *et al.*, 1998). Translation from the preC initiation codon results in the synthesis of a fusion protein containing a signal peptide (Ou *et al.*, 1986). The

---

signal peptide targets the fusion protein for translocation through the lumen of the endoplasmic reticulum and onto a pathway where proteolytic cleavage of the carboxy- and amino-termini generates a soluble secreted product, the HBeAg (Bruss and Gerlich, 1988). Although the exact function of the eAg is unknown, its detection in serum is an important clinical marker as its presence indicates active viral replication.

### 1.1.3.2 Surface proteins

Surrounding the viral core is a lipid envelope which is derived from the host cell membrane and endoplasmic reticulum (Kamimura *et al.*, 1981). The infectious 42 nm virion or Dane particle contains an envelope with three classes of surface proteins embedded in the lipid membrane: small (S), middle (M) and large (L). All three surface proteins are glycosylated and form stable, transmembrane structures. The S protein (226 amino acids long) defines the S domain. The two larger proteins, M and L, contain S plus two additional amino terminal extensions (Seeger and Mason, 2000). The preS2 extension defines the extra domain of M, whilst L consists of both preS1 and preS2 domain extensions. Infectious particles are composed of up to 70% S, with the remainder of the particle constituted by approximately equal amounts of M and L (Heermann *et al.*, 1987). These envelope glycoproteins are also secreted in the form of small, non-infectious, non-DNA-containing, lipoprotein particles. These subviral particles are abundantly secreted and greatly outnumber the infectious HBV virions. Subviral particles are found in two forms: spheres, which consist of mainly S and M proteins; and filaments, which have slightly more L protein than spheres (Heermann *et al.*, 1984). Owing to the abundance of subviral particles in infected sera, they are thought to be largely responsible for the immune complex syndromes that occur in transient infections and may possibly act as decoys for anti-S neutralising antibodies (Seeger and Mason, 2000).

Although much remains to be ascertained, the specific function of the surface proteins appears to be in selectively transporting the nucleocapsid into and out of the host hepatocyte without causing cellular lysis. The preS1 domain appears to have a dual role in HBV biology. PreS1 is both a ligand to core

---

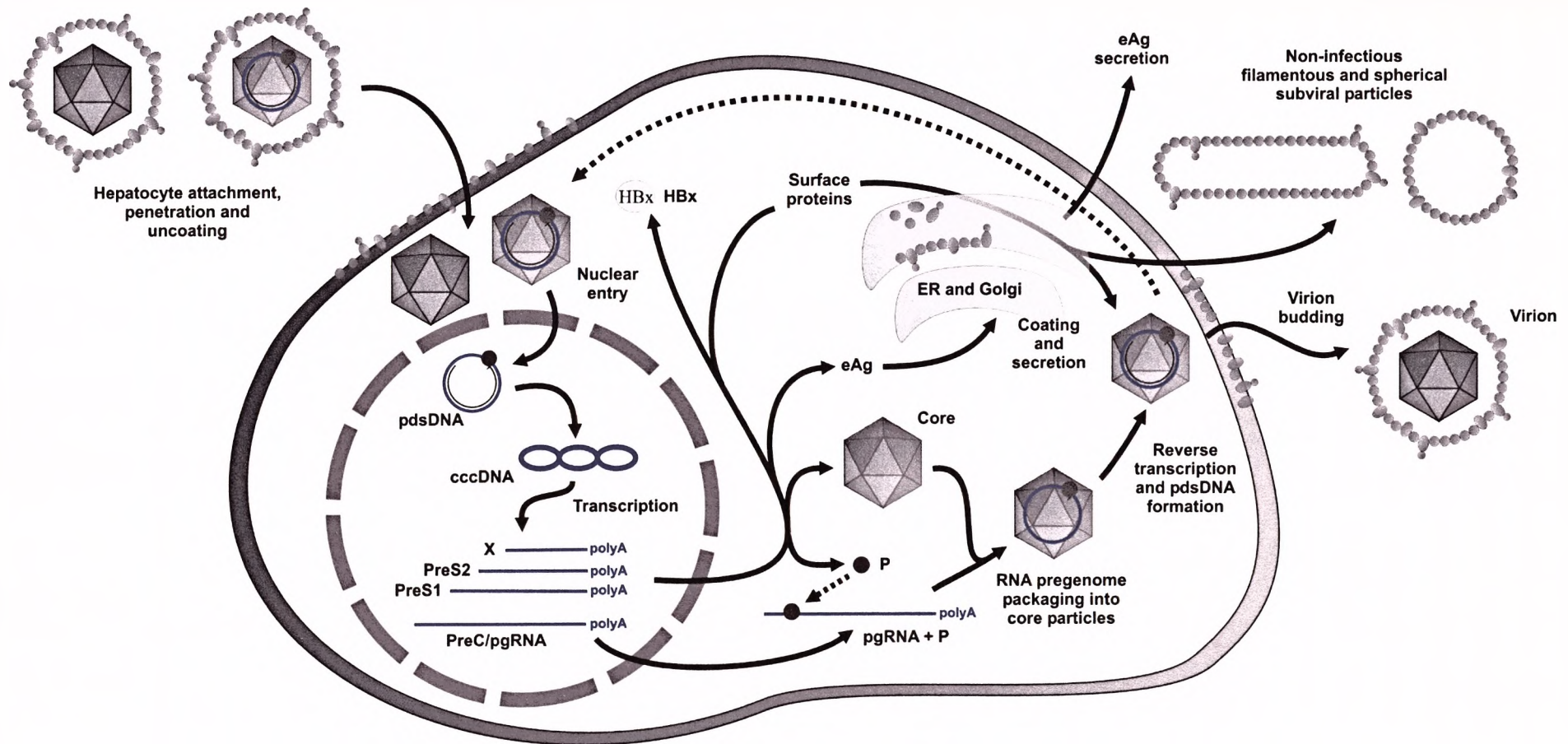


**Figure 1.3** Schematic illustration of the HBV infection and replicative cycle within the hepatocyte. Infectious virions attach to a cellular receptor(s) and uncoat, releasing nucleocapsids that migrate to the cell nucleus. The pdsDNA genome is converted to cccDNA, which is the template for the transcription of four viral transcripts. Translation occurs following transcript export to the cytoplasm. The pgRNA interacts with two gene products, Polymerase (P) and Core (C), to form immature, RNA packaged, nucleocapsids. The preC/pgRNA is reverse transcribed into DNA by P. The DNA genome can be either redelivered to the nucleus, or nucleocapsids can be coated by surface glycoproteins (in the Golgi and endoplasmic reticulum) before being exported as enveloped virions.

particles during viral envelope assembly (which is why a fraction of L particles display the preS1 domain towards the cytosolic interior), and a substrate to an unidentified host cell receptor during viral infection (Nassal, 1999) (Figure 1.3). Although antibodies to S alone provide sufficient protection against all strains of HBV, the preS1 epitope is also suited for the generation of virus-neutralising antibodies (Lambert, 1991). The precise function of preS2, however, is not as well understood but appears not to be required for viral infection (Fernholz *et al.*, 1993).

### 1.1.3.3 Polymerase

The *P* ORF encodes the viral polymerase, which is translated from an internal initiation codon on the viral preC/pgRNA. The *P* ORF is not in frame with the *C* ORF (Chang *et al.*, 1989) and the *P* gene is transcribed as part of a second cistron of the preC or pgRNA transcript and thus lacks its own direct upstream promoter element. Regulation of *P* appears, therefore, to be at the level of translation. Translation of *P* requires ribosomal 'scanning' of the preC/pgRNA and thus *P* is produced less efficiently than either eAg or *C* proteins (Seeger and Mason, 2000).

HBV polymerase is responsible for both DNA- and RNA-dependent DNA polymerase activity during viral DNA replication (Toh *et al.*, 1983). *P* is further endowed with two functional domains: the terminal protein (TP) at its amino terminal, and RNase H-like activity at its carboxy-terminal (Radziwill *et al.*, 1990). The TP is found covalently linked to the 5' end of HBV minus-strand DNA and is important for the packaging of the RNA pregenome as well as acting as a primer for reverse transcription (Wang and Seeger, 1993).

The viral polymerase is principally responsible for reverse transcription of pgRNA to produce minus-strand DNA, concomitant degradation of the RNA template, and synthesis of plus-strand DNA. *P* is also required as a structural component for the packaging of pgRNA into immature core particles (Bartenschlager *et al.*, 1990) and may play a role in orchestrating entry into the host cell nucleus for early replication (Wang and Seeger, 1993).



#### 1.1.3.4 X Protein, HBx

Considering the efficient utilisation of sequence space by HBV, with significant portions of the viral genome coding for more than one protein, it is expected that a coding region unique to hepadnaviruses would reveal a protein whose function is obvious in the biology of the virus. However, understanding the biological role of the X protein, HBx, has been far from simple. The name, 'X' gene, was assigned when no amino acid sequence homology was observed with the existing database of viral or cellular proteins (Miller and Robinson, 1986).

HBx is a small, 17 kDa protein and although poorly immunogenic, produces antibodies in sera of infected humans and naturally infected animals (Feitelson and Clayton, 1990). Although the specific function of HBx in natural infection remains elusive, its presence is necessary for the establishment of viral infection *in vivo* in animals (Chen *et al.*, 1993; Zoulim *et al.*, 1994). HBx appears to possess a multitude of activities *in vitro*, although few of these define a specific role for this protein during viral replication.

HBx has been shown to activate the transcription of a variety of viral and host cellular genes (Caselmann, 1996; Rossner, 1992). This indiscriminate or 'promiscuous' *trans*-activation activity appears to be via an indirect process. HBx, without DNA-binding domains, cannot act alone. Although it appears that *trans*-activation is supplementary to HBx's intended primary function, recent studies suggest a more prominent role for this function in the HBV life cycle as HBx was shown to activate transcription of the core gene *in vivo* in HBx transgenic mice (Reifenberg *et al.*, 1999). Apart from modulating transcription, HBx is a multifunctional viral regulator that adapts cell responses to genotoxic stress (by modulating or affecting DNA repair and apoptosis), protein degradation, signalling pathways, and cell cycle checkpoints (reviewed in Arbuthnot *et al.*, 2000). These modulations affect viral replication, directly or indirectly, and in turn provide insight into the possible role of HBx in the aetiology of HBV-induced carcinogenesis (see section 1.1.7.3). The overwhelming array of host-cell factors that are associated with HBx (as well as other viral factors) underscores the exquisite sensitivity and specificity which HBV enjoys in its natural cellular environment.

---

### 1.1.4 Viral cis-elements

#### 1.1.4.1 HBV promoters and enhancers

Transcription of the four ORFs is controlled by four promoter elements: preS1, preS2, core and X promoter (Figure 1.2). Two viral enhancer elements, enhancers I (EnhI) and II (EnhII), located upstream of the core promoter (CP), as well as *cis*-acting negative regulatory elements, are necessary for regulation of all viral genes (Schaller and Fischer, 1991b). The basic (basal) core promoter (BCP) along with an upstream regulatory region (URR), constitute the major functional elements of the core promoter. Although the BCP lacks the canonical TATA box sequence, distinct TATA-box like sequences form part of two partially overlapping yet genetically distinct *cis*-acting elements that independently drive the transcription of both preC and pgRNA transcripts (Yu and Mertz, 1996). URR can be further divided into positive and negative regulatory regions (Guo *et al.*, 1993). The core upstream regulatory sequence (CURS) region contains several domains (*cis*-elements) that stimulate BCP activity. Two domains in the CURS region (CURS-A and CURS-B) span most of the EnhII sequence. However, unlike CURS, which is position and orientation dependent in activating BCP, EnhII activates preS1, preS2 and X promoters alone and functions indifferently to its position and orientation (Kramvis and Kew, 1999). Further upstream of the BCP and CURS is a negative regulatory element (NRE), which acts to suppress BCP and EnhII activity (Lo and Ting, 1994). In addition, a number of liver-derived transcription factors bind to the BCP and its upstream regulatory sequence as well as other viral promoters in order to modulate viral transcription (reviewed by Kramvis and Kew, 1999, and Schaller and Fischer, 1991a).

The preS1 and preS2 promoters control the expression of the surface transcript mRNAs and accurately regulate the abundance of each of the three surface glycoproteins. The preS1 promoter regulates transcription of the entire S ORF, which is translated into the large surface protein (L). The preS2 promoter controls transcription of a family of transcripts resulting in middle (M) and small (S) surface proteins upon translation. Unlike the preS1 promoter, the preS2 promoter lacks a TATA box and is contained within two ORFs (Schaller and Fischer, 1991a). Although present on all viral transcripts, the *HBx* ORF encodes a unique *HBx* transcript, which is under its own transcriptional control. Uniquely,

the X promoter overlaps with the 3'-end sequence of EnhI. However, the minimal X promoter can be separated from EnhI whilst retaining its function (Guo *et al.*, 1991). Since EnhI dramatically influences the transcription of preC/pgRNAs and HBx mRNA (Hu and Siddiqui, 1991), the virus must avoid the impact of promoter occlusion. Seeger and Mason speculate that different cccDNA templates, which behave like mini-chromosomes, may differentiate promoter-coupled transcription events (Seeger and Mason, 2000). Additionally, the X promoter contains *cis*-elements for binding of transcription factors, some of which are liver-specific. This includes the tumour suppressor protein, p53, which has been shown to downregulate the function of the X promoter.

#### 1.1.4.2 Polyadenylation signal

All HBV transcripts share the same 3' termini due to the presence of a common polyadenylation signal on the cccDNA viral genome. PreC/pgRNA transcripts are larger-than-genome-length since RNA polymerase II skips the polyadenylation signal on the first pass. The polyadenylation signal is only recognised on the second encounter (Russnak, 1991). The resultant transcripts possess terminal sequence repeats at both their 5' and 3' termini. The greater-than-genome-length pgRNA sequence is necessary for viral replication and packaging into nucleocapsids (see sections 1.1.4.3 and 1.1.5). A number of factors possibly affect the termination of transcription. The HBV polyadenylation signal (5' UAUAAA 3') is known to be less effective than the canonical eukaryotic polyadenylation signal sequence 5' AAUAAA 3', suggesting a necessary adaptation for the differential use by HBV (Russnak, 1991). More specifically, DHBV cccDNA possesses a *cis*-element or positive effector of transcription (PET), which is located within the 5' transcribed region of the pgRNA-encoding sequence. The presence of PET ensures that RNA polymerase II skips the transcription termination site during first passage of pregenome transcription (Huang and Summers, 1994). Termination of transcription during the second encounter appears to be regulated by a second *cis*-element, termed negative effector of transcription (NET) (Beckel-Mitchener and Summers, 1997).

#### 1.1.4.3 Epsilon ( $\epsilon$ )

The terminal repeats of the pgRNA contain a stem-loop sequence, or epsilon ( $\epsilon$ ), which plays a key role in HBV DNA encapsidation and reverse transcription. The location of  $\epsilon$  was determined by fusing heterologous genes to various regions of the HBV genome and by observing subsequent encapsidation (Junker-Niepmann *et al.*, 1990; Pollack and Ganem, 1993). Despite the presence of terminal repeats on the pgRNA, only the 5'  $\epsilon$  retains functionality resulting in encapsidation of the pgRNA transcript, notwithstanding the fact that all HBV transcripts have the  $\epsilon$  coding region at their 3' ends. Analysis of  $\epsilon$  shows a series of inverted repeats that fold into a three-dimensional stem-loop structure. This stem-loop is conserved among all hepadnaviruses irrespective of differences in the primary sequence (Junker-Niepmann *et al.*, 1990). Polymerase recognises and directly interacts with  $\epsilon$ , initiating both encapsidation as well as reverse transcription of the HBV pgRNA (Fallows and Goff, 1995).

#### 1.1.5 HBV life cycle

Although knowledge of the HBV replicative cycle is comprehensive, a number of important questions remain unanswered. Surprisingly, little is known about the mode of receptor-mediated infection of host hepatocytes. Most pertinently, the absence of cell lines susceptible to hepadnavirus infection has prevented an accurate understanding of the initial stages of viral infection. A large membrane glycoprotein termed gp180 or p170 (a protein of the carboxypeptidase D [CPD] family) has been identified as a component of the cellular receptor for DHBV (Breiner *et al.*, 1998; Urban *et al.*, 1998). Although human homologues of CPD have been identified, it appears that further receptor components are necessary for HBV-mediated infections in hepatocytes (Seeger and Mason, 2000).

Once inside the nucleus, using host-dependent factors, the virus converts its partially double-stranded genome into covalently closed circular DNA (cccDNA) through an as yet unknown mechanism of DNA repair. The presence of cccDNA in hepatocytes indicates a successful initiation of infection (Ruiz-Opazo *et al.*, 1982). CccDNA is the template for transcription of genomic and subgenomic viral mRNAs. The greater-than-genome-length pgRNA, which is

---

transcribed by cellular RNA polymerase II, represents the mRNAs (along with preC mRNAs) for the translation of P and C proteins as well as being the template for reverse transcription of minus-strand DNA (Schaller and Fischer, 1991a). The pgRNA interacts, possibly simultaneously, with both its gene products, C and P. Translation of P and pgRNA packaging are tightly coupled events. Polymerase binds to the 5' end  $\epsilon$  (Figure 1.4A), and triggers the addition of core complex dimers, which allows for packaging into capsids (Figure 1.3) (Bartenschlager *et al.*, 1990; Junker-Niepmann *et al.*, 1990). Reverse transcription takes place during capsid formation (Figure 1.4) (Nassal and Schaller, 1993).

A unique polymerase-linked DNA primer consisting of three or four nucleotides is synthesized using the bulge region of the stem-loop  $\epsilon$  as template (Tavis *et al.*, 1994; Wang and Seeger, 1993) (Figure 1.4B). Following priming, the first of three template switches occurs. The short primer translocates to a homologous three/four-nucleotide sequence, which is part of direct repeat DR1, at the 3' end of the pgRNA (Figure 1.4C). Subsequently, minus-strand DNA synthesis continues within the immature nucleocapsid (Havert and Loeb, 1997). RNase H activity of P then degrades the pgRNA which is hybridised to the minus-strand DNA (Summers and Mason, 1982) (Figure 1.4D). Degradation is complete except for a short stretch at the 5' terminus (16-18 nt) which acts as the primer for synthesis of the complementary plus-strand viral DNA (Loeb *et al.*, 1991; Seeger *et al.*, 1986). This primer RNA is translocated to the second direct repeat (DR2) where the synthesis of plus-strand DNA is initiated (Figure 1.4E). Plus-strand DNA is extended to the physical end of minus-strand DNA using a short terminal repeat  $r$  followed by a template switch from the 5'- to the 3'-end of the minus-strand DNA (Havert and Loeb, 1997). Failure to translocate, referred to as *in situ* priming (Staprans *et al.*, 1991), leads to the synthesis of a double-stranded linear form of the viral genome, which is often observed in tissue culture. A third template switch enables the synthesis of the partially double-stranded DNA genome found in mature, infectious virions (Seeger *et al.*, 1986) (Figure 1.4F). The plus-strand DNA maintains genome circularity through a cohesive overlap across the 5' and 3' ends of the minus-strand DNA.

Within the viral replicative cycle there are a number of potential targets for drug development. However, many of these await the identification of both



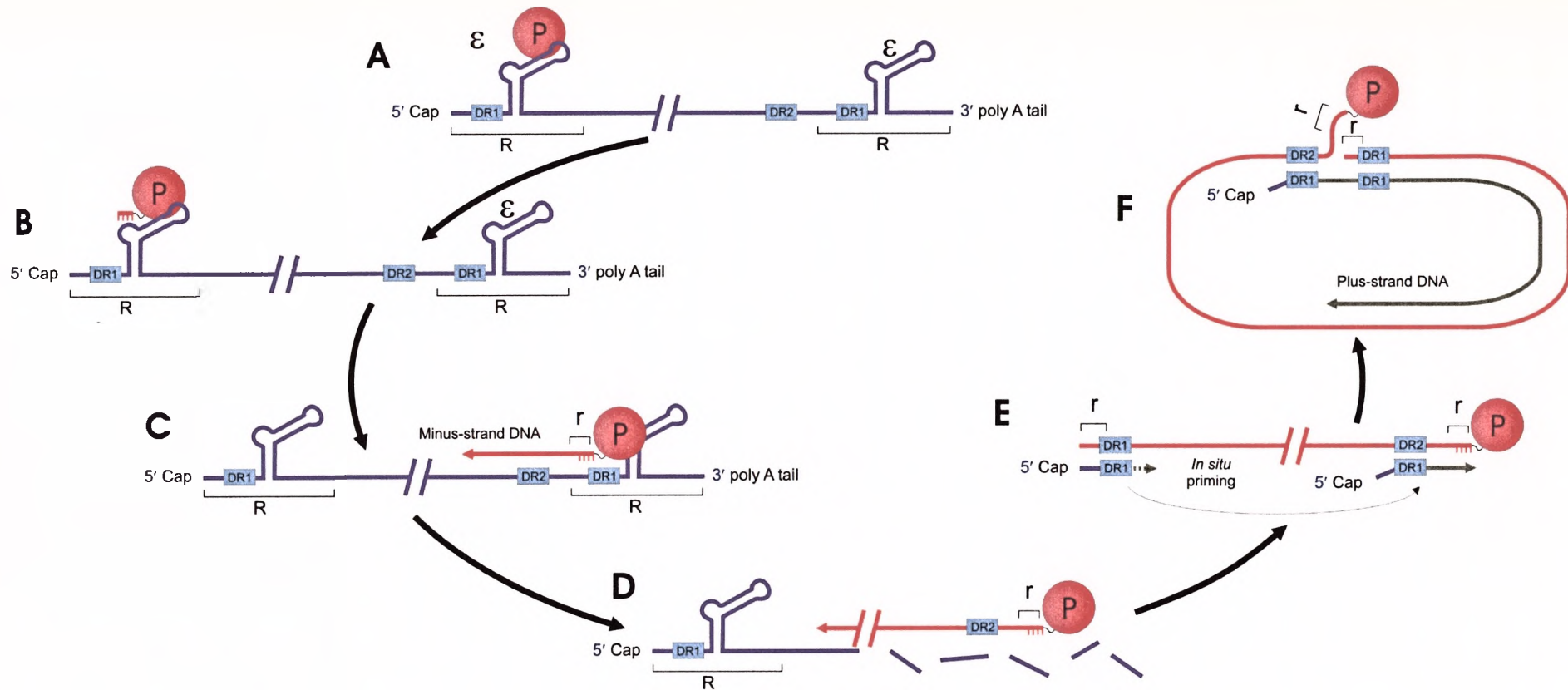


**Figure 1.4** Essential steps involved in hepadnaviral DNA replication starting from a newly transcribed pgRNA template, with terminal repeats (R), 5' cap and a polyA tail. **A)** The reverse transcriptase (P) binds to the epsilon ( $\epsilon$ ) stem-loop structure near the 5' terminus of the pgRNA (blue). **B)** Reverse transcription is by a protein priming mechanism, utilising a tyrosine located near the amino terminus of the reverse transcriptase itself (Zoulim and Seeger, 1994). **C)** Following the synthesis of three or four bases in the bulge region of  $\epsilon$ , P translocates to the 3' terminus of the RNA template, where the four bases can anneal with a complementary sequence. **D)** Elongation of the minus-strand DNA (red) to the 5' end is concomitant with RNase H degradation of the pregenome sparing the 5' cap and DR1, which remain hybridised to the minus-strand. Completion of minus strand produces a short (~9 nt) terminal repeat (r) in the - strand DNA. **E)** The remaining oligoribonucleotide fragment serves as primer for plus-strand DNA synthesis (green), following its translocation to DR2. Failure to translocate leads to a double-stranded, linear form of the viral genome (a process referred to as *in situ* priming). **F)** A third translocation occurs when the plus-strand DNA reaches the 5' terminus of the minus-strand, circularising the molecule and allowing continued plus-strand elongation. This translocation is facilitated by the short terminal repeat on the minus strand DNA (r) (Nassal, 1999).

viral and cellular determinants that are involved in each step of the viral life cycle. Antiviral strategies to date have focused on inhibiting viral DNA polymerase or reverse transcriptase. Future antiviral targets under consideration include: viral attachment to the host cell, penetration and translocation to the nucleus, and uncoating of the viral nucleocapsid. More accessible targets include: viral transcription and translation, viral genome packaging, maturation of the viral nucleocapsid, and envelope formation. Of particular interest are the antiviral strategies that target HBV nucleic acid sequences. Since HBV sequences are distinct from that of the host hepatocyte, targeting the inhibition of viral gene expression and replication can be highly specific. The HBV genome life cycle uses both DNA and RNA as replicative intermediates. Consequently, therapeutic strategies that make use of nucleic-acid hybridisation may suppress viral replication and gene expression by degrading viral RNA intermediates or by blocking translation of important proteins necessary for viral propagation.

### **1.1.6 Serotypes and genotypes**

#### **1.1.6.1 Serotypes**

Four serotypes, also known as subtypes of HBsAg, were initially defined by two mutually exclusive determinant pairs, *d/y* and *w/r*, and a common *a* determinant (Le Bouvier and McCollum, 1970). Nine different subtypes were identified following further subdivision of the *w* subdeterminant into *w1* through to *w4*, and the acquisition of the *q* determinant. Thus in total, eleven subtypes have been identified: *ayw*, *ayw2*, *ayw3*, *ayw4*, *adw2*, *adw4* (*adw4q<sup>+</sup>* and *adw4q<sup>-</sup>*), *adr*, *ayr*, and *adr* (*adrq<sup>+</sup>* and *adrq<sup>-</sup>*). Further modifications were later made by adding two compound subtypes: *adyr* and *adwr* (Courouce-Pauty *et al.*, 1983).

#### **1.1.6.2 Genotypes**

To determine a molecular basis for the serological variations of HBsAg, variants of the HBV S gene were sequenced and compared. HBV sequence data established a phylogenetic relationship between HBV variants resulting in the definition of six HBV genotypes: A to F (Norder *et al.*, 1993; Okamoto *et al.*, 1988). A possible seventh genotype, G, appears to correlate with the serotype

---

*adw2* (Stuyver *et al.*, 2000). However, in general, the interrelation between the nine subtypes and the seven genotypes remains unclear. Genotypes A and D are prevalent in sub-Saharan Africa (Bollyky and Holmes, 1999; Bowyer *et al.*, 1997; Norder *et al.*, 1994). The most divergent genotype is F, which is geographically distributed in South America. The F genotype differs by up to 14% from other HBV genomes (Norder *et al.*, 1993).

### **1.1.7 Pathogenesis**

#### **1.1.7.1 Acute and chronic HBV infection**

Primary infection of HBV can result in both acute and chronic hepatitis. Acute hepatitis represents a transient infection which generally runs a course of one to six months, and which includes an asymptomatic period characterised by high-titre viraemia ( $10^{10}$  per ml). Both cellular and humoral immune responses to HBV-encoded antigens are responsible for viral clearance, and have been extensively reviewed elsewhere (Chisari and Ferrari, 1995).

The risk of developing a persistent or chronic infection following a usually mild acute infection is inversely correlated with age and immunocompetence (Hyams, 1995). Infections occur in less than 5% of adult individuals and in approximately 90% of neonates. The latter is usually through perinatal infection. Chronic infection is defined as the persistence of HBsAg in the serum of an individual for six months or longer (Evans and London, 1998). As HBV is not cytopathic, liver damage from chronic HBV infection is thought to be largely immune-mediated, in which various mechanisms are involved. These may include recognition of viral antigens (both expressed on hepatocytes and secreted) by B cell immunoglobulin receptors, and recognition of short, processed viral antigen peptides associated with human leucocyte antigen (HLA) molecules of the  $\alpha$ - $\beta$  heterodimer receptors on T cells (Chisari and Ferrari, 1995). Viral peptide fragments, processed within the infected hepatocyte, are presented along with HLA class I to CD8<sup>+</sup> cytotoxic T cells, leading to both cytolytic and noncytolytic inhibition of viral replication (Guidotti *et al.*, 1996).

In chronically infected patients with little to no serum HBeAg levels, viral persistence appears to be through a 'non-replicative' mechanism as the rate of viral replication is low. HBV mutations in the preC gene can, however, result in

---



viral infection occurring in the absence of detectable serum HBeAg (Carman *et al.*, 1989) and may be responsible for 95% HBeAg-negativity rate in sub-Saharan asymptomatic carriers of infection (Kramvis *et al.*, 1997).

#### 1.1.7.2 HBV and hepatocellular carcinoma (HCC)

The correlation between chronic HBV infection and the development of HCC is well established globally with several lines of evidence implicating the virus and its persistent infection in the aetiology of hepatocyte tumorigenesis (reviewed by Arbuthnot and Kew, 2001; Sherlock *et al.*, 1970). In a cohort study in Taiwan, HBV chronic carriers showed a greater than 100-fold increased relative risk of developing HBV-associated HCC (Beasley *et al.*, 1981), thus ranking chronic HBV infection as one of the worst environmental carcinogenic risk-factors known to humans. The relative risk of HBV-associated HCC varies depending on a number of factors, some of which include geographical environment, age and method of infection, the presence or absence of HBeAg, and the presence of cirrhosis (Figure 1.5 correlates the geographical distribution of HBV with HCC; reviewed by Arbuthnot and Kew, 2001).

Both direct and indirect processes are involved in establishing HBV-associated HCC. Integration of HBV into the chromosomes of infected hepatocytes, although not required for HBV replication, represents a direct mechanism of establishing HCC. Evidence of viral integration is observed in infected hepatocytes during the course of chronic infection with a higher proportion of viral integrants detected in HBV-associated HCC tumours (Bréchet *et al.*, 1981; Takada *et al.*, 1990). Infected hepatocytes are susceptible to chromosomal integration of HBV DNA via an illegitimate recombination mechanism. The linear, double-stranded HBV DNA produced by *in situ* priming is the predominant precursor for integration (Gong *et al.*, 1995; Yang and Summers, 1995). Integration often results in several heterogeneous rearrangements of the viral genome causing significant disruption of the expression of viral genes. Core and polymerase coding regions are usually interrupted while envelope protein reading frames and their promoters, as well as the HBx ORF, often remain intact (although fewer than 50% of integrants have a complete HBx sequence) (Miyaki *et al.*, 1986; Paterlini *et al.*, 1995; Robinson, 1994).

---

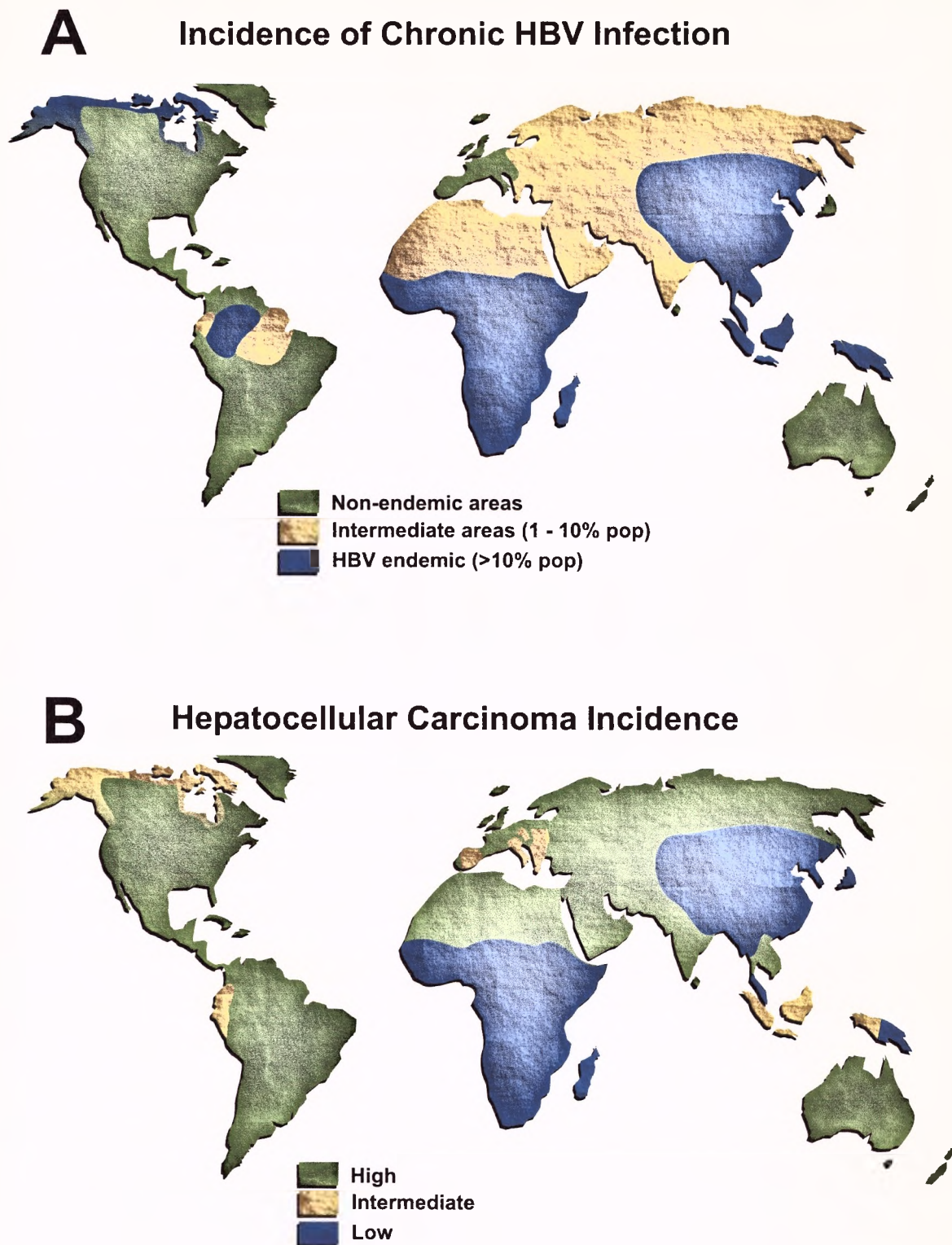


**Figure 1.5** Global maps showing the similarity between the geographical distributions of chronic hepatitis B virus infection (A) and hepatocellular carcinoma (B).

Integration may stimulate tumorigenesis through the *cis*-activation of cellular genes. This is certainly true for woodchuck infections where WHV integration appears to be near or in *c-myc* and *N-myc* proto-oncogenes in 50% of WHV-associated HCC (Hsu *et al.*, 1988). There is a direct correlation between viral integration and activation of the *myc* family of genes in woodchucks (Fourel *et al.*, 1990). No such correlation exists in HBV-associated HCC. Viral surface proteins M and L possess *trans*-activation properties if truncated at the carboxy-terminal and have been shown to *trans*-activate several cellular oncogenes. For the most part, *cis*-activation of oncogenes appears to be rare in human HBV infections. An alternative model for HBV-associated tumorigenesis implies that HBV, like tumour viruses, contains an oncogene. One of the principle candidates for a viral oncogene is the HBx protein.

#### 1.1.7.3 The role of HBx in HBV-associated HCC

The HBx protein has been widely studied in the development of HBV-associated HCC and has been the subject of recent reviews (Arbuthnot *et al.*, 2000; Caselmann, 1996). This is mainly due to the plethora of activities displayed by HBx both *in vitro* and in cell culture. HBx is a non-specific transcriptional *trans*-activator and is believed to *trans*-activate a large variety of viral and host cell *cis*-elements (Caselmann, 1996; Rossner, 1992). *Trans*-activation by HBx involves 1) interaction with transcriptional factors and 2) activation of cell signalling pathway activity.

Several viral transcription regulatory elements, such as EnhI, are responsive to HBx-induced *trans*-activation (Spandau and Lee, 1988). Host genes that are activated by HBx include, *inter alia*, those of the major histocompatibility complex (Zhou *et al.*, 1990), *c-myc* (Balsano *et al.*, 1991), *c-fos* (Avantaggiati *et al.*, 1993), *c-jun* (Twu *et al.*, 1993),  $\beta$ -interferon (Aufiero and Schneider, 1990; Twu and Schloemer, 1987) and tRNA<sup>Ala</sup> (Aufiero and Schneider, 1990; Twu and Schloemer, 1987). HBx mediates transcription responses to cAMP by binding to cAMP-responsive element binding protein (CREB) thus affecting DNA binding through the interaction with transcription factors such as ATF-2 and NF- $\kappa$ B (Maguire *et al.*, 1991; Twu and Robinson, 1989). Other HBx *trans*-activation activities include stimulation of the mitogen-

activated protein kinase (MAP) and Janus family tyrosine kinase (JAK)/ signal transducer and activator of transcription (STAT) signal transduction pathways (Benn and Schneider, 1994; Kekule *et al.*, 1993), and interactions with the tumour suppressor protein p53 (Feitelson *et al.*, 1993). These latter interactions implicate HBx in the regulation of cell cycle control (Benn and Schneider, 1995) and programmed cell death (reviewed in Arbuthnot *et al.*, 2000).

Lastly, HBx may be directly responsible for hepatocarcinogenesis by modulating DNA repair in the host cell (for a recent review, refer to Arbuthnot *et al.*, 2000). HBx has been shown to compromise the repair of UV-damaged DNA and is known to interact with factors that participate in cellular DNA repair pathways (Becker *et al.*, 1998; Capovilla *et al.*, 1997; Lee *et al.*, 1995). Intracellular factors, which are known to interact with HBx, include the tumour-suppressor protein p53 (thus affecting the p53-mediated repair pathway), and damaged DNA binding protein, DDB (Becker *et al.*, 1998).

## 1.2 Treatment of chronic HBV infection

As stated previously, treatment of HBV infection remains largely ineffective. Although HBV immunisation usually prevents HBV infection, those who are already chronically infected with the virus continue to be at risk for developing cirrhosis and liver cancer. Most therapeutic agents under clinical evaluation belong to a new generation of immune system modulators and nucleoside or nucleotide analogues. These agents may deliver therapeutic benefits in the short-term. However, it remains to be seen whether these will overcome the serious concerns regarding long-term efficacy and tolerability.

Most anti-HBV agents developed to date target the inhibition of viral DNA synthesis. Since the HBV polymerase possesses multiple functions, some of which are unique to hepadnaviruses, it represents an ideal target for antiviral agents. Deoxy- and dideoxynucleoside analogues specifically inhibit the RNA-dependent DNA polymerase action of HBV polymerase by competing with natural substrates and leading to truncated DNA synthesis. Other strategies rely on boosting the immune system response to viral infection. Patients who develop HBV chronic infection appear to have a deficient immune response to HBV antigens (Chisari and Ferrari, 1995). The immune system modulators developed

---



to date possess both a direct antiviral and an immune modulatory action (Vilcek and Sen, 1996).

### 1.2.1 Nucleoside analogues and immune system modulators

The second generation nucleoside analogue lamivudine or 3TC ( $\beta$ -L-2',3'-dideoxy-3'-thiacytidine) is a deoxycytidine analogue with an unnatural levorotatory 'L' configuration and is currently the only approved alternative to interferon-alpha (IFN- $\alpha$ ) treatment. Lamivudine is part of a new generation of biochemically novel nucleoside analogues that was originally developed to combat human immunodeficiency virus (HIV) and members of the herpes simplex virus family. Although lamivudine appears to be a well-tolerated inhibitor of HBV replication, it has been established that short-term lamivudine monotherapy is ineffective in clearing residual viral infection. A twelve-month course of lamivudine monotherapy was found to achieve clearance of HBeAg in 20-30% of eAg-positive chronic patients and virological remission in more than 65-70% of HBeAg-negative chronic carriers (Papatheodoridis *et al.* 2002). However, for the latter, relapses were observed in the majority of responders following the cessation of therapy. Although long-term lamivudine therapy appears to be relatively safe, prolonged therapy (for longer than twelve months) is associated with a progressive increase in the rate of viral resistance to lamivudine (Ling *et al.*, 1996). Virological breakthrough usually develops after six months of lamivudine monotherapy and that rate varies between 15-30% after twelve months, and exceeds 50% after three years of therapy in both HBeAg positive and negative chronic carriers (Delaney *et al.*, 2001). The propensity to develop resistant HBV strains is likely the result of a combination of high viral turnover and HBV polymerase function. HBV polymerase, like most retroviral polymerases, lacks proof-reading ability and as a result is prone to a high error rate. It has not been firmly established whether resistant HBV mutant strains exist prior to therapy or whether these occur during the course of therapy. However, there does appear to be some evidence supporting the hypothesis that lamivudine-resistant strains are present *ab initio* and are then selected immediately following treatment.

---

The first lamivudine-resistant HBV strains presented mutations within the YMDD motif (tyrosine-methionine-aspartate-aspartate) of the HBV polymerase. This motif is in catalytic region C of the HBV polymerase and is conserved in all viral reverse transcriptases. The most common nucleotide substitutions result in a change from leucine (L) at position 526 to methionine (M), and M to valine (V) at position 550 (L526M and M550V, respectively) (Ling *et al.*, 1996; Tipples *et al.*, 1996). Many mutations have been identified in different regions of HBV polymerase yet the next most common resistance mutation is the substitution of M with isoleucine (I) at position 550 (M550I) (Tipples *et al.*, 1996). Other mutations of HBV polymerase have been described predominantly within catalytic regions B and C, but their significance towards resistance remains undetermined (Delaney *et al.*, 2001). The replication rate of lamivudine-resistant mutant strains in cell culture is a lot lower than that of wild-type HBV. A single mutation at position 550 (M550V or M550I) was found to decrease significantly the rate of viral replication (Dienstag *et al.*, 1999; Lai *et al.*, 1998), whereas this does not seem to be affected by additional mutations at position 526 (L526M). Lamivudine-resistant mutant strains suffer from a selective disadvantage in the absence of antiviral pressure, which may explain why wild-type HBV reappears a few months after the discontinuation of lamivudine therapy (Chayama *et al.*, 1998).

The clinical impact of lamivudine resistant mutations has not been clarified. Biochemical evidence for viral breakthrough, which is usually expressed as an increase in serum transaminase levels, appears several months after the first detection of lamivudine resistant strains (Liaw *et al.*, 1999). This may be either after or before the peak detection of HBV viraemia levels. Nevertheless, several studies recommend that patients who develop resistant strains should continue to be treated with lamivudine since resistant strains are less aggressive than wild-type HBV (Honkoop *et al.*, 2000).

Among newer HBV antivirals in clinical studies, the purine derivatives such as adefovir dipivoxil and entecavir, and the pyrimidine derivative emtricitabine, appear to be at least as potent as lamivudine in suppressing HBV replication. The carbocyclic deoxyguanosine analogue famciclovir has recently undergone Stage III clinical trials. However, famciclovir appears to have a relatively limited efficacy for general use in patients with chronic HBV. Extensive

clinical trials are necessary for the development of any new nucleoside/tide analogues since some have been shown to be severely toxic *in vivo* and have even resulted in death (McKenzie *et al.*, 1995).

Of serious concern to the future of nucleoside/tide analogues are the results obtained from *in vitro* studies which indicate that mutations found in lamivudine- and famciclovir-resistant HBV strains (in particular, the YMDD mutations of viral polymerase) can confer cross-resistance to emtricitabine, and the pyrimidine derivative  $\beta$ -L-Fd4C (2',3'-dideoxy-2',3'-didehydro- $\beta$ -L-5-fluorocytidine). Notwithstanding the above concerns, preliminary studies using adefovir dipivoxil show that clinical efficacy is possible following the development of lamivudine resistance (Xiong *et al.*, 2000). A number of nucleoside analogues, which include adefovir dipivoxil and entecavir, suppress replication of YMDD mutant HBV (Delaney *et al.*, 2001; Perrillo *et al.*, 2000). However, since only short-term studies have been completed to date, it remains to be seen whether these nucleoside/nucleotide analogues will develop their own mutant-resistant HBV quasi-species *in vivo*. The most likely future outcome will include combination-based therapies for treatment of chronic HBV infection using various nucleoside/nucleotide analogues in combination with the immune modulator interferon-alpha (IFN- $\alpha$ ). These combinations may be augmented at a later stage by novel molecular approaches to therapy. However, the ease with which drug-resistant strains develop and the added toxicity of combination therapy must be worrying factors for the future development of these antiviral chemotherapeutic agents (Delaney *et al.*, 2001).

Present therapy for chronic HBV infection includes the immune modulator IFN- $\alpha$ . Positive results have been reported in only a limited number of cases. A subgroup of patients with active viral replication (HBeAg positive), with elevated serum transaminases, and low viraemia, appear to respond well to IFN- $\alpha$  treatment. But, for the vast majority of chronic carriers IFN- $\alpha$  therapy remains ineffective. Interferon therapy is also associated with unfavourable dose-limiting side effects (Niedermaier *et al.*, 1996). Although a number of other immune modulators have been tested for their effects against chronic HBV infection, such as interferon-gamma (Guidotti *et al.*, 2002), thymosin alpha1 (Lau, 2000), and interleukin-12 (Zeuzem and Carreno, 2001), it is obvious that a better

understanding of the antiviral effects of the immune modulators is needed in order to improve their therapeutic efficacy and tolerability.

### **1.2.2 Novel molecular approaches to therapy**

Significant progress is being made in establishing entirely novel treatment strategies for chronic HBV infection. Owing to the emergence of various cellular and animal models of viral infection, as well as to advances in the field of molecular biology, a number of different and innovative molecular approaches have been tested for their therapeutic potential against chronic HBV infection. Many review articles deal with the emergence of these novel molecular or gene-based approaches to therapy (Nassal, 1997; von Weizsäcker *et al.*, 1997; Wands *et al.*, 1997; Zoulim and Trepo, 1999). Most putative molecular therapeutic strategies are presently in an early stage of development, and many remain untested hypotheses. However, some of these novel molecular therapies appear to represent an improvement on existing pharmacological treatment regimes and have imminent clinical application, particularly with regard to specificity and toxicity. Promising candidates include antisense oligonucleotides, naked DNA vaccines, hairpin and hammerhead ribozymes, and decoy attenuated viruses (dominant negative mutants). Of these candidates, the therapeutic effects of hybridising nucleic acids will be explored, namely antisense oligoribonucleotides and ribozymes.

As potentially novel therapeutic agents, antisense RNA molecules can inactivate viral nucleic acid by Watson-Crick hybridisation to complementary viral RNAs, thereby inducing viral RNA degradation or preventing the translation of viral proteins. Catalytic RNAs, or ribozymes, differ from antisense molecules in that they function as endonucleolytic enzymes, targeting and degrading viral RNA in a sequence-specific manner. Both nucleic acid approaches to therapy of chronic HBV infection are explored. However, this thesis specifically focuses on the antiviral effects of hammerhead ribozymes, which are the most therapeutically versatile of the ribozyme species.

---



## 1.3 Ribozymes

This section briefly reviews the discovery of catalytic RNAs and their significance with regard to the origins of biomolecular replicators and the early evolution of life. The vast array of research conducted on hammerhead ribozymes is explored, emphasising the efforts made to engineer this RNA species into potentially viable antiviral therapeutic agents.

### 1.3.1 Catalytic RNAs

Since their discovery over 100 years ago, proteins were regarded as the only macromolecule capable of fulfilling the role of biological catalysts. For all life, proteins represent a ubiquitous and versatile catalyst. Enzymes are so intimately coupled to their protein nature that they have always been unambiguously defined as proteins. Yet, until relatively recently, there has been little appreciation of the scope and biological contribution of other macromolecular biocatalysts, in other words, of non-protein enzymes.

Although early studies on the nature and function of the ribosome suggested a role for RNA in the catalytic functions of this organelle, it was not until the early 1980's that Thomas Cech, Sydney Altman and colleagues discovered independent RNA catalysts. These were reported in 1982 for group I intervening sequences (introns) of *Tetrahymena* (Kruger *et al.*, 1982) and in 1983 for the RNA subunit component of ribonuclease P (RNase P), which is necessary for tRNA maturation (Guerrier-Takada *et al.*, 1983). The name 'ribozyme' was thus coined to denote all ribonucleic acid sequences with enzyme-like functions. There are seven different types of naturally existing ribozymes (Table 1.1). These are conveniently divided into two groups, namely the large and small ribozymes. Large ribozymes include group I and II introns and the catalytic RNA subunit of RNase P (Guerrier-Takada *et al.*, 1983; Kruger *et al.*, 1982; Peebles *et al.*, 1986). Small ribozymes include hammerhead (Forster and Symons, 1987; Uhlenbeck, 1987), hairpin (Wu *et al.*, 1989), hepatitis delta virus (HDV) (Buzayan *et al.*, 1986; Dange *et al.*, 1990) and the *Neurospora* mitochondrial Varkud Satellite (VS) ribozymes (Saville and Collins, 1990).

---

**Table 1.1** Naturally occurring ribozyme species (Cech and Golden, 1999; Doudna and Cech, 2002).

Category	Number Sequenced	Biological Source	Reaction performed <sup>a</sup>
<b>Self splicing RNAs:</b>			
Group I	>1500	Eukaryotes (nuclear and organellar), prokaryotes and bacteriophages	<i>Trans</i> -esterification (3' - OH)
Group II	>700	Eukaryotes (organellar) and prokaryotes	<i>Trans</i> -esterification (3' - OH)
<b>Self-cleaving:</b>			
Group I-like	6	<i>Didymium, Naeglaria</i>	Hydrolysis (3'-OH)
<b>Small self-cleavers:</b>			
Hammerhead	11	Plant viroids, virusoids and Satellite RNAs (newts & cave crickets)	<i>Trans</i> -esterification (2', 3' >p)
Hairpin	1	Satellite RNAs of tobacco ringspot virus	<i>Trans</i> -esterification (2', 3' >p)
Hepatitis $\delta$ Virus (HDV)	2	Human hepatitis virus	<i>Trans</i> -esterification (2', 3' >p)
Varkud Satellite	1	<i>Neurospora</i> mitochondria	<i>Trans</i> -esterification (2', 3' >p)
<b>RNase P RNAs</b>			
Various	>500	Eukaryotes (nuclear and organellar), prokaryotes	Hydrolysis (3'-OH)

<sup>a</sup>As seen from the reaction products.

Recent studies suggest that the ribosomal RNA as well as the RNA component of the spliceosome is a ribozyme (Cech, 2000; Collins and Guthrie, 2000; Nissen *et al.*, 2000). In nature, however, the catalytic repertoire of ribozymes is limited to RNA processing reactions. Ribozymes generally catalyse the endonucleolytic *trans*-esterification of the phosphodiester bond backbone of RNA, requiring structural and/or catalytic divalent metal ions under physiological conditions. The group I and II introns are found in bacteria and in organelles of higher plants, fungi and algae (Cech and Herschlag, 1996; Michel *et al.*, 1989). These large ribozymes cleave RNA phosphodiester linkages, using an external nucleophile in a two-step reaction to splice-out their primary transcripts. The 5' splice site is attacked by the 3'-OH of the external guanosine in group I introns, or by the 2'-OH of internal adenosine for group II introns. RNase P is an endonuclease that, in a simpler reaction, generates the mature 5' end of tRNAs (Takagi *et al.*, 2001). The bacterial RNase P RNA subunit has catalytic activity independent of its protein subunit component. However, both components are necessary for catalysis *in vivo*. By contrast, the small ribozymes use an internal nucleophile (usually the 2' oxygen of the ribose moiety at the cleavage site) for a non-hydrolytic cleavage reaction, which results in the formation of 2',3'-cyclic phosphate and 5'-hydroxyl termini (Takagi *et al.*, 2001).

### 1.3.2 ***Ribozymes and the origins of life debate***

The central dogma of molecular biology, that biological information flows from DNA to RNA (transcription) and from RNA to proteins (translation), defines the role of nucleic acids as molecules of information storage and retrieval. An evolutionary paradox is established, since each component of the biological information pathway requires catalysis, a role previously the sole preserve of protein enzymes. Molecules capable of sustaining early life require, theoretically, two fundamental criteria: catalytic function as well as information storage and retrieval. It is not surprising then that catalytic RNAs, or ribozymes, which possess both these requirements, fulfil the role of candidate progenitor molecule for all life. The storage, transfer and replication of information allow any system to undergo natural selection and improve biological viability. Equally important is

---

catalytic function. At the very least the information-carrying molecules require enzymatic properties in order to copy their information from generation to generation. The enzymatic process must be specific and proceed with high fidelity, but a frequency of errors is necessary for the diversity to drive adaptation and evolution. It is now thought that the evolution of life did include a phase where RNA was the predominant biological macromolecule, predating both proteins and DNA. Today, a multitude of evidence supports RNA as a precursor hereditary biological molecule in what has been termed “The RNA World” hypothesis (Figure 1.6) (Di Giulio, 1997; Gilbert, 1986).

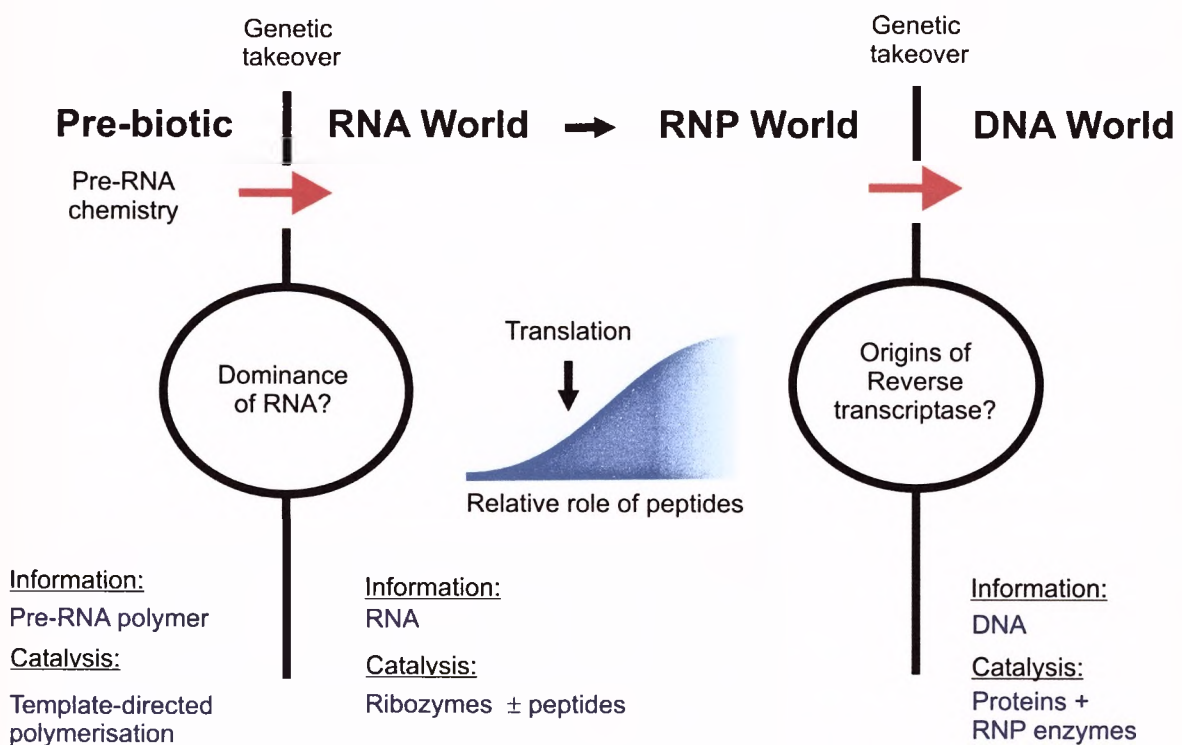


**Figure 1.6** The ‘RNA World hypothesis’ as envisioned by Cech and Golden (Cech and Golden, 1999). The RNA World predates both DNA and proteins and suggests that all life, both extant and extinct, derives from RNA-based self-replicators. In the RNA World, the two important prerequisites for life, information storage and catalytic power, is in the domain of RNA. Later, the development of specialised roles may have resulted in the transference of catalytic activity to RNA-protein complexes and ultimately to proteins alone. Similarly, information storage may have been transferred from RNA to the domain of DNA. Today, all of life lies within the ‘DNA World’. Yet a prebiotic world or pre-RNA environment, which is speculated to involve more simple catalysts, must have preceded the RNA World. This is likely due to the difficulties in developing complex RNA-based reactions *in vitro*. These reactions are implicit in the chemistry of the RNA World. There is, however, no direct evidence from extant life of a pre-RNA World.

---

Two major hurdles persist in the analysis of the RNA World. Firstly, few ribozymes from extant species possess the catalytic repertoire necessary for even the most basic of replication reactions. Secondly, RNA is a complex macromolecule and is unlikely to self-assemble by random molecular evolution even under a highly reducing environment (lack of free oxygen) (Mojzsis *et al.*, 1999). For this reason, there is general consensus that a pre-biotic condition must have preceded the RNA World (Mojzsis *et al.*, 1999). However, the exact nature of such a pre-RNA World environment remains speculative. Although the second hurdle still remains unsolved, the first hurdle has been tackled by *in vitro* experiments, which aim to increase the catalytic variability of ribozymes. Techniques have been developed which improve the repertoire of ribozyme-catalysed reactions, thus exploring the chemical boundaries of the RNA World. Since any sequence change to the ribozyme backbone directly results in a different phenotype (as the catalytic action is altered), specific ribozyme phenotypes can be selected from a pool of random RNA sequences. Successive rounds of *in vitro* selection and evolution mould and refine the creation of artificially desired phenotypic traits (Green *et al.*, 1990; Joyce, 1989). Briefly, a large combinatorial library of different RNA sequences is chemically challenged to express a particular phenotypic trait. The molecules that succeed are amplified and reselected. Through successive iterations of challenging, selecting and re-amplifying generations of RNA molecules, new enzymatic traits are created (Green *et al.*, 1990; Joyce, 1989). This represents a useful way of mining sequence space (up to  $10^{15}$  different oligoribonucleotides can be screened). Newly identified nucleic acid catalysts may shed light on previously extinct enzymatic functions or offer completely new traits altogether. *In vitro* selection/evolution has greatly improved the catalytic repertoire of RNA (and DNAs). Some of the catalytic activities that have been selected *in vitro* include RNAs that utilise nucleoside triphosphate substrates (Ekland and Bartel, 1996; Lorsch and Szostak, 1994), make and break amide bonds (Dai *et al.*, 1995; Wiegand *et al.*, 1997), alkylate a nucleoside or a thiophosphate (Wilson and Szostak, 1995), and add an amino acid to a nucleoside via an ester linkage (Illangasekare *et al.*, 1995). Although these reactions all utilise RNA as a substrate, other substrates have been tested. Notably, RNAs have been selected to catalyse a classical chemistry reaction, Diels-Alder cycloaddition, in the

---



presence of  $\text{Cu}^{2+}$  ions (Tarasow *et al.*, 1997), and have been selected to insert metal ions into porphyrin rings (Conn *et al.*, 1996).

Perhaps the most intriguing developments to date are in the efforts to develop an *in vitro* RNA replicator. An RNA-dependent RNA polymerase was generated and selected *in vitro* that repeatedly extends an RNA chain up to 14 nucleotides from a specified template (Johnston *et al.*, 2001). Apart from their value to studies aimed at understanding the role of RNA in the early history of life, experiments of this nature may lead to the development of *in vitro* self-replicating systems. These systems are likely to facilitate the discovery of new RNA enzymes by automating Joyce and Green's *in vitro* evolution technique (Green *et al.*, 1990; Joyce, 1989).

### 1.3.3 Hammerhead ribozymes

Hammerhead ribozymes are the smallest known RNA catalysts capable of directing the site-specific *trans*-esterification of a phosphodiester bond in the presence of divalent metal ion cofactors. These ribozymes were discovered in the RNA genomes of several different small plant pathogens possessing site-specific self-cleavage activity. The hammerhead ribozyme catalytic motif was first identified in viroid RNA (Hutchins *et al.*, 1986) and later in virusoids (Forster and Symons, 1987) and in small satellite RNAs (Miller *et al.*, 1991). Hammerhead ribozymes have also been found in RNA transcripts of satellite DNA tandem repeat sequences in several newt (Koizumi *et al.*, 1988), schistosome (Ferbeyre *et al.*, 1998) and cave cricket species (Rojas *et al.*, 2000). In contrast to the catalytic activity of hammerhead ribozymes in the newt, schistosome, and cave cricket (which are all associated with transcribed repetitive DNA sequences in animals), hammerhead ribozyme activity in the small plant pathogens is well defined and appears to be an integral component for genomic replication. The observed RNA processing involves the site-specific, self-cleavage of linear RNA intermediates (multimeric RNA precursors). These pregenomic viral concatamers represent the precursor RNA multiples of monomeric plus and minus RNA template strands that undergo site-specific internal RNA editing (Bratty *et al.*, 1993; Symons, 1992). Spliced monomers then join head-to-tail to form a circularised single-stranded RNA genome. This form of the rolling-circle

replication mechanism is a feature shared by all ribozyme-containing RNA pathogens.

Recent evidence from experiments using *in vitro* selection techniques suggests that the hammerhead ribozyme catalytic motif is ubiquitously conserved for the catalysis of phosphodiester bond hydrolysis. The divergent organisms may thus have derived their hammerhead ribozyme function independently (Salehi-Ashtiani and Szostak, 2001). The biological role of hammerhead ribozymes in newt, schistosomes and cave crickets remains speculative. These ribozymes were found to be active *in vivo* and appear to impact RNA processing events at the riboprotein complex (Denti *et al.*, 2000; Luzi *et al.*, 1997). More specifically, with respect to the newt hammerhead ribozyme, dimeric and multimeric RNA transcripts, which are generated by all somatic tissues as well as in the testes, self-cleave into monomers at the hammerhead domain. Monomeric units contain intact hammerhead ribozyme sequences. These sequences associate with the newt ovary riboprotein complex with the help of a protein that specifically binds to the ovarian form of the newt ribozyme (Cremisi *et al.*, 1992; Denti *et al.*, 2000).

#### **1.3.4 Hammerhead ribozyme structure and function**

The hammerhead ribozyme, in its wild-type conformation, consists of roughly forty nucleotide sequences and folds into a secondary structure containing three distinct domains that form stem-loop helical motifs. These domains are designated helix I, II and III. The consensus sequence requisite for the catalytic core consists of at least thirteen conserved nucleotides at the junction of three duplex stems (Figure 1.7) (Forster *et al.*, 1990; Forster and Symons, 1987; Haseloff and Gerlach, 1988). Endonucleolytic cleavage of a phosphodiester bond then takes place 3' of the 5' NUH 3' catalytic core, where N represents any base, U represents a conserved uridine and H represents any base except G, to generate sequences terminating in 2',3'-cyclic phosphate and 5'-hydroxyl termini (Shimayama *et al.*, 1995; Zoumadakis and Tabler, 1995). Recent experiments determining hammerhead ribozyme sequence specificity at the cleavage site have resulted in the reformulation of the 5' NUH 3' rule to 5' NHH 3' (Kore *et al.*, 1998). The hammerhead ribozyme is a metalloenzyme and requires the presence

---



of divalent metal ion cofactors for catalysis to occur. Although in nature,  $Mg^{2+}$  is the most commonly found metal ion cofactor,  $Co^{2+}$ ,  $Mn^{2+}$  and  $Ca^{2+}$  have proven to be effective substitutes (Dahm and Uhlenbeck, 1991). Studies have also shown that ribozymes are catalytically active using high concentrations of monovalent cations (Murray *et al.*, 1998).

The distinctive shape of the hammerhead ribozyme was first observed in the stable conformation computations of two-dimensional RNA folding patterns (Forster and Symons, 1987; Symons, 1992). Evidence for this particular conformation was also later observed in thermodynamic studies and NMR measurements (Heus *et al.*, 1990; Odai *et al.*, 1990; Pease and Wemmer, 1990). More recent configurations derived from X-ray diffraction data (Pley *et al.*, 1994; Scott *et al.*, 1995) and fluorescent resonance energy transfer (FRET) studies (Tuschl *et al.*, 1994), indicate a three-dimensional  $\gamma$  or 'wishbone' shape, where helices II and III are part of the same axis and where helix I lies adjacent to helix II (see Figure 1.7B). X-ray crystal analyses have provided a wealth of information regarding the overall function and structure of the hammerhead ribozyme. Structurally, the hammerhead ribozyme's catalytic core, which resides predominantly in helix II, is well defined and is divided into two domains (Hertel *et al.*, 1992). The hammerhead ribozyme numbering system is defined according to Hertel *et al.* (1992) and refers to the nucleotides in the catalytic core essential for hammerhead ribozyme function. These include domain I comprising nucleotides 5' C<sub>3</sub>U<sub>4</sub>G<sub>5</sub>A<sub>6</sub> 3' and domain II comprising nucleotides 5' G<sub>12</sub>A<sub>13</sub>A<sub>14</sub> 3' and 5' U<sub>7</sub>G<sub>8</sub>A<sub>9</sub> 3' (shaded in blue in Figure 1.7A & B). Nucleotides 5' U<sub>16</sub>H<sub>17</sub> 3', however, form part of the catalytic core on the complementary RNA strand (red italicised letters in Figure 1.7A & B). The three-dimensional configuration of the hammerhead ribozyme described by Pley *et al.* (1994) and Scott *et al.* (1995) elucidates its putative catalytic action (Birikh *et al.*, 1997b) and proposes domain II as the location for  $Mg^{2+}$  ion binding sites. The exact sites, however, remain to be determined.

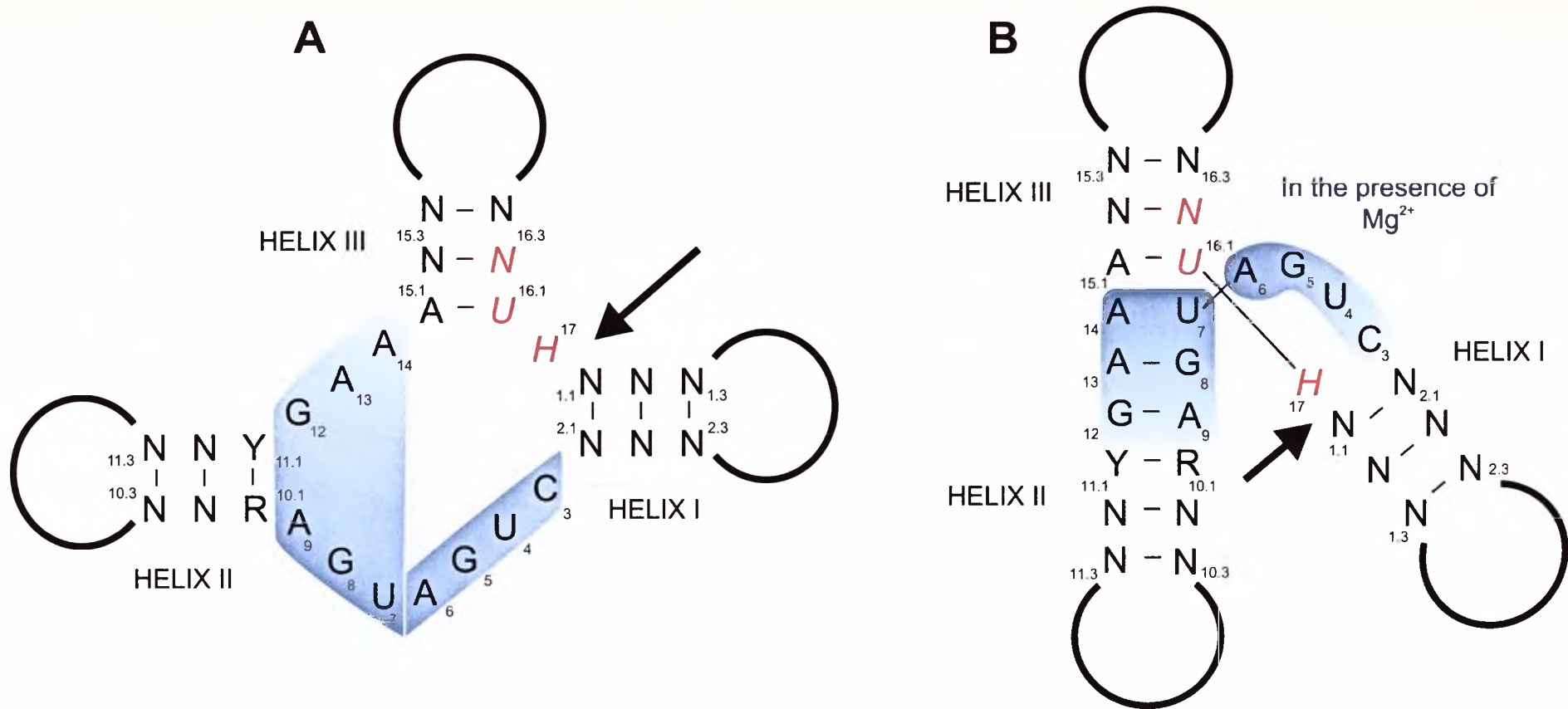


**Figure 1.7** A two-dimensional representation of the hammerhead ribozyme with all three helical arms terminated by nucleotide loops. Conserved nucleotides are shaded (blue). The cleavage triplet is italicised and shown in red. N represents any nucleotide; H represents any nucleotide except G. The dashes represent Watson-Crick base pairs. The helix II catalytic core is shaded and consists of domain I (C<sub>3</sub>-A<sub>6</sub>) and domain II (U<sub>7</sub>-A<sub>9</sub> and G<sub>12</sub>-A<sub>14</sub>). The arrow indicates the cleavage site. Outlined letters are conserved nucleotides and are labelled according to Hertel *et al.* (1992). **A**) Two dimensional structure without the presence of Mg<sup>2+</sup> ions. **B**) X-ray crystal structure showing the  $\gamma$ -shaped structure that results from both Watson-Crick and reversed-Hoogsteen base pairing. This diagram is an adaptation from Birikh *et al.* (1997b).

### 1.3.5 Hammerhead ribozymes that cleave *in-trans*

The wild-type hammerhead ribozyme has two of its three helical arms terminated by nucleotide loops allowing for intramolecular (*cis*) cleavage only. Intermolecular (*trans*) cleaving ribozymes, however, can be created synthetically by removing a loop terminating one of the helical arms. The *trans*-acting ribozyme thus requires the hybridisation of two independent RNA strands. *Trans*-cleaving hammerhead ribozymes have been constructed from two RNA strands in a number of ways: with helix III closed and helices I and II open-ended (Clouet-D'Orval and Uhlenbeck, 1996), with helix I closed and helices II and III open-ended (Jeffries and Symons, 1989; Uhlenbeck, 1987), and similarly with helix II closed and helices I and III open-ended (Haseloff and Gerlach, 1988).

The hammerhead ribozyme described by Haseloff and Gerlach (1988), where a nucleotide loop terminates helix II, is the most versatile of the *trans*-cleaving hammerhead ribozymes and has been shown to cleave substrates more efficiently than other constructs (Ruffner *et al.*, 1989). In this example, most of the conserved sequences necessary for the hammerhead ribozyme catalytic core (the RNA sequence containing a closed helix II) are present on one strand. The target complementary RNA strand, which forms helices I and III upon hybridisation, requires only the cleavage triplet (as described above) to generate an active site for effective catalysis. The Haseloff-Gerlach ribozyme has the least sequence constraints when defining its 'substrate' RNA strand, making it the best model for applications that require the targeting of ribozymes to foreign RNA substrates. Strictly speaking, the hammerhead ribozyme requires both RNA strands to contribute elements of the hammerhead ribozyme catalytic core for cleavage activity to occur. This is to say, the presence of all three helices is necessary for the hammerhead ribozyme to act catalytically. The Haseloff-Gerlach hammerhead ribozyme, however, distinguishes the RNA strand harbouring most of the catalytic core as the 'enzyme' or 'ribozyme' component from the cleaved target complementary RNA strand which is defined as the 'substrate' component. By definition, a true enzyme requires sequential catalysis for substrate to product turnover. Identifying two RNA molecules as distinct moieties, one of which is regarded as the enzyme and the other the substrate, allows for the study of hammerhead ribozyme enzyme kinetics (Haseloff and

---

Gerlach, 1988; Koizumi *et al.*, 1989; Koizumi *et al.*, 1988). The separation of substrate from enzyme in the Haseloff-Gerlach model has allowed the use of hammerhead ribozymes for the site-specific intermolecular cleavage of an array of RNA targets. The targeted 'knockdown' of specific RNA molecules represents the single most important innovation for the potential use of ribozymes as novel therapeutic agents.

#### 1.3.5.1 *Defining the trans-cleaving activity of hammerhead ribozymes*

The consensus sequence requisite for the target RNA is a 5' NUH 3' triplet. The sequences either side of the helix II active site on the hammerhead ribozyme strand are complementary to the target substrate sequence adjacent to the cleavage triplet (Figure 1.8). These sequences form hammerhead ribozyme helices I and III respectively and bind the ribozyme to its substrate. The only requirement for helices I and III are that they bind through Watson-Crick base complementation with their respective substrate. By altering the sequence of the ribozyme arms that form helices I and III, it is theoretically possible to design synthetic hammerhead ribozymes that cleave substrate RNAs of any sequence. Random RNA sequences are replete with 5' NUH 3' cleavage triplet sites, hence any RNA species is theoretically accessible for hammerhead ribozyme cleavage. The most common naturally occurring cleavage triplet is 5' GUC 3', which statistically appears once every 64 nucleotides. Other naturally occurring hammerhead ribozyme cleavage triplets include 5' GUA 3' and 5' AUA 3' (Miller *et al.*, 1991). There are only slight differences in catalytic efficiency with regard to the nucleotide composition of the cleavage triplet. However, for conditions that include saturated levels of ribozyme and substrate, the most catalytically efficient hammerhead ribozyme cleavage site remains 5' GUC 3' (Shimayama *et al.*, 1995).

#### 1.3.5.2 *In vitro kinetics of trans-cleaving hammerhead ribozymes*

Hammerhead ribozyme steady state kinetics lends itself to Michaelis-Menten analysis *in vitro* in the same way as do kinetics studies of protein-based enzymes

---

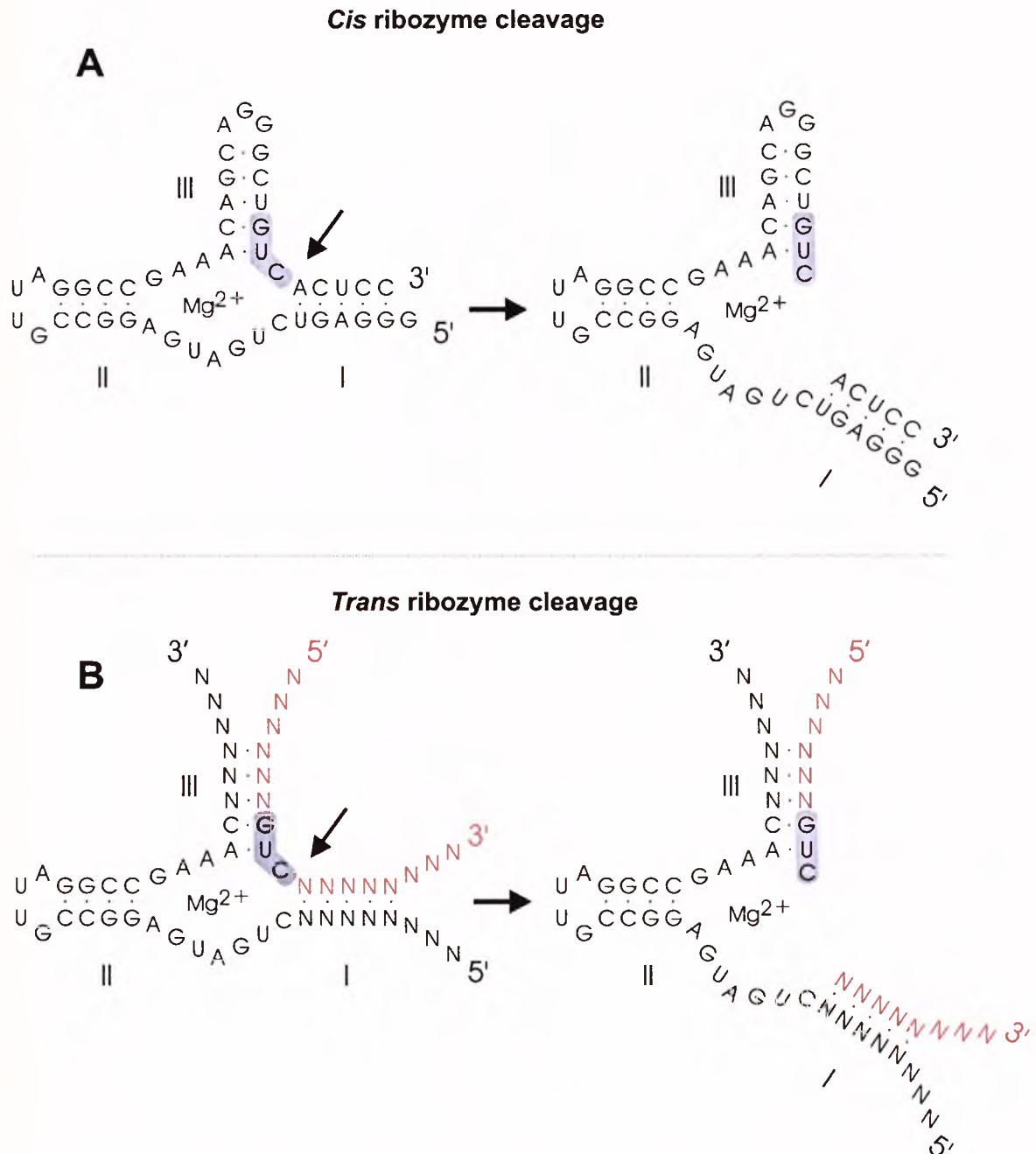


**Figure 1.8** *Cis*- and *trans*-cleaving hammerhead ribozymes derived from the Haseloff-Gerlach model (Haseloff and Gerlach, 1988). **A)** *Cis*-cleaving ribozyme with helix III closed. Cleavage of the same strand yields two cleavage products. **B)** *Trans*-cleavage ribozyme where helical arms I and III hybridise prior to cleavage. The consensus sequence of helix II, which is not part of the active site, is shown in its native form.  $Mg^{2+}$  is required for catalysis. Watson-Crick hybridisation is shown as points between nucleotides. The cleavage triplet is highlighted in black. Cleavage is shown 3' of the 5' GUC 3' triplet (shaded in blue) by a black arrow.



(Perreault *et al.*, 1990; Uhlenbeck, 1987). The enzymatic parameters  $k_{\text{cat}}$  (chemical turnover) and  $K_m$  (ribozyme-substrate affinity) allow for mechanistic studies of the ribozyme enzymatic reaction. The minimal kinetic mechanism for hammerhead ribozyme catalytic action can be summarised in three reversible reaction steps. Ribozyme (Rz) and substrate (S) assemble into an enzyme-substrate complex (Rz.S) followed by cleavage of the phosphodiester bond generating 5' and 3' end products with a 2',3'-cyclic phosphate terminus (P1) and a 5'-hydroxyl terminus (P2) respectively, and followed lastly by the release of both products (Figure 1.9). Defining each step, where each represents the

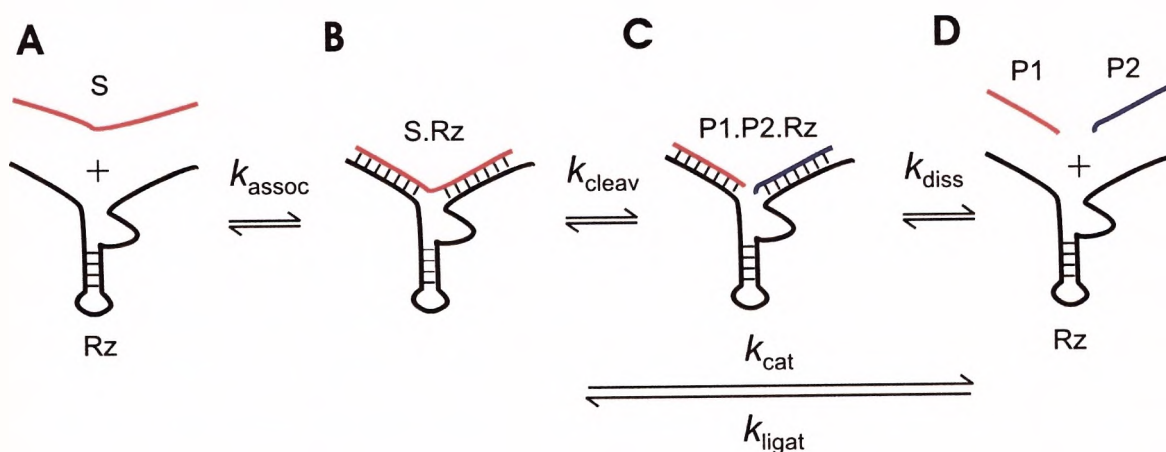


**Figure 1.9** An illustration of the minimal kinetic description and reaction scheme for a *trans*-cleaving hammerhead ribozyme. The ribozyme catalysed reaction consists of *at least* three reversible steps: **A)** and **B)** Together with  $\text{Mg}^{2+}$  ions, the substrate RNA (S) first binds to the ribozyme (Rz) ( $k_{\text{assoc}}$ ) followed by **C)**  $\text{Mg}^{2+}$ -induced cleavage of the phosphodiester bond of the bound substrate ( $k_{\text{cleav}}$ ). **D)** The cleaved products (P1 and P2) fragments then dissociate from the ribozyme allowing the liberated ribozyme to engage in new catalytic events ( $k_{\text{diss}}$ ) (Hertel *et al.*, 1994; Hertel and Uhlenbeck, 1995).

elemental rate constants in both the forward and reverse reaction, facilitates the analysis of individual catalytic parameters for every stage of the reaction. Although such an analysis yields important information, it still represents a simplified model as both the parameters of turnover and affinity, respectively  $k_{\text{cat}}$  and  $K_m$ , may unwittingly be affected by indistinguishable contributions from several of the reversible reaction steps. These include the folding of ribozyme



and substrates into alternative inactive conformations (Clouet-D'Orval and Uhlenbeck, 1996; Fedor and Uhlenbeck, 1992; Hertel *et al.*, 1994) or unusually slow release (dissociation) of reaction products (Fedor and Uhlenbeck, 1990). Hence determining an accurate kinetic scheme for hammerhead ribozyme catalysis necessitates the delineation of rate constants for each individual reaction step. Most importantly, it is necessary to separate the rate of chemical cleavage activity from the rates of substrate binding and substrate-product dissociation (Hertel *et al.*, 1994).

Under multiple turnover conditions where ribozyme concentrations are small relative to that of substrate, *in vitro* kinetic studies have shown that the rate limiting step,  $k_{\text{cat}}$ , occurs during bond cleavage, where the cleavage rate ( $k_{\text{cleav}}$ ) is less than the rate of product dissociation ( $k_{\text{diss}}$ ) (Sawata *et al.*, 1993; Takagi and Taira, 1995). Substrate binding and product dissociation is relatively fast as long as ribozyme helices I and III contain fewer than six nucleotides each. However, substrate binding and product release can become rate limiting even with the modest elongation of both helices I and III to 8 nucleotides each. The lengthening of the helical arms appears to result in protracted binding and increased ribozyme stability, which concomitantly increases ribozyme-substrate specificity. The association/dissociation rate for both substrates and products decreases drastically, resulting in a decrease in the overall catalytic rate ( $k_{\text{cat}} < 0.008 \text{ min}^{-1}$ ). The dissociation rate,  $k_{\text{diss}}$ , becomes rate limiting and the reaction kinetics change to that described under single-turnover conditions, where the ribozyme is present in excess over substrate (Hertel *et al.*, 1994; Hertel and Uhlenbeck, 1995). It can be seen that, along with changes in pH or divalent metal ion concentration (Dahm *et al.*, 1993; Dahm and Uhlenbeck, 1991), the binding nature of helices I and III plays the largest role in affecting the reaction rate constants. Varying the sequence length and nucleotide composition of the substrate-binding arms is an important tool for modulating the rate of substrate and product dissociation (Fedor and Uhlenbeck, 1992) (see section 5.2.1). The general nucleotide composition and the sequence encoding the hammerhead ribozyme catalytic core, by contrast, have a very limited effect on the rates of substrate and product binding. Although the cleavage reaction is reversible under standard conditions (10 mM  $\text{MgCl}_2$ , 40-50 mM Tris-Cl pH 7.5 at 25°C), the formation of products from substrates is 130-fold more favourable at reaction equilibrium for ribozymes

containing a total of 16 complementary annealing nucleotides. In this case the rate of ligation,  $k_{\text{ligat}}$ , is approximately  $0.008 \text{ min}^{-1}$ . This is due to an increase in entropy subsequent to bond cleavage of the bound ribozyme-substrate complex (Hertel and Uhlenbeck, 1995). The binding and release of substrate and products, on the other hand, follow the kinetics expected from a Watson-Crick dissociation curve.

Wild-type cleavage rates for most of the described hammerhead ribozymes as well as other small ribozyme species (for example, hairpin and VS ribozyme) are remarkably similar, with typical catalytic turnover approximating one molecule per minute ( $k_{\text{cat}} \approx 1 \text{ min}^{-1}$ ) (McKay and Wedekind, 1999). Evident is the fact that ribozyme catalytic rates in general are paltry when compared to protein-based enzymes, suggesting that ribozymes are intrinsically adapted to perform a single catalytic reaction in their wild-type conformation. This, perhaps, underscores their function and biological origin as intramolecular (*in-cis*) cleaving enzymes, which have a higher emphasis on specificity rather than turnover.

### 1.3.6 Other small ribozymes designed to cleave *in-trans*

Of the naturally occurring small ribozymes, the hairpin (Hampel *et al.*, 1990), HDV (Been, 1994) and *Neurospora* VS (Guo and Collins, 1995) ribozymes have all been converted to cleave *in-trans*. The construction of these *trans*-acting ribozymes was achieved by adopting a similar approach to that used for hammerhead ribozymes. Sequences were selected that allow the ribozyme to be distinguished into substrate and enzyme components. The substrate sequence selected contains the minimal number of nucleotides necessary to complement the nucleotides provided by the ribozyme sequence for proper catalytic core function.

A number of different hairpin (Kruger *et al.*, 1982; Ojwang *et al.*, 1992) and HDV ribozymes (Ananvoranich and Perreault, 1998; Kato *et al.*, 2001) have been adapted and used extensively to cleave RNA molecules *in-trans*. Their enzymatic properties are discussed in detail elsewhere (Takagi *et al.*, 2001). Of the naturally occurring small ribozymes, the *Neurospora* VS *trans*-cleaving ribozyme is the least understood and is unlikely to be immediately applied as a therapeutic agent (James and Gibson, 1998).

---

Hairpin ribozymes are unique among the small ribozymes in that they do not require  $Mg^{2+}$  ions for catalysis (Chowrira *et al.*, 1993; Hampel and Cowan, 1997). This ribozyme species is composed of four helical regions interspersed by two nonduplexed regions. The *trans*-cleaving hairpin ribozyme hybridises with its substrate forming helices I and II. A nonduplexed region lies between the two helices (Berzal-Herranz *et al.*, 1993). The substrate RNA requires a minimal sequence necessary to complement the hairpin ribozyme catalytic core for cleavage, namely, 5' RYNGHYB 3' (where N = any base; R = A,G; Y = C,U; B = C,G,U; H = A,C,U; V = A,C,G) (Figure 1.10A). Cleavage occurs immediately 5' of the guanosine in the nonduplexed region of the substrate sequence. Like the hammerhead ribozyme, the hairpin ribozyme has been widely applied for its potential as a therapeutic agent (James and Gibson, 1998). Although the hammerhead ribozyme is reversible with cleavage being favoured over ligation, hairpin ribozymes favour ligation ten-fold over cleavage in the presence of excess products (Hegg and Fedor, 1995; Nesbitt *et al.*, 1997). This is assumed to be the result of a more rigid cleavage reaction, which constrains the products within the cleavage site (McKay and Wedekind, 1999).

Both genomic and antigenomic HDV ribozymes possess a pseudoknot secondary structure consisting of four helices and three single-stranded regions (Ferre-D'Amare *et al.*, 1998; Takagi *et al.*, 2001). The *trans*-cleaving ribozyme (Figure 1.10B) is divided at the junction of helices I and II (referred to as P1 and P2). P1, consisting of 7 bp in the wild-type HDV ribozymes, has a cleavage site at the 5'-end of the cleavage recognition sequence 5' GN<sub>6</sub> 3' (G followed by six nucleotides) (Roy *et al.*, 1999). Like hammerhead ribozymes, the HDV ribozyme requires divalent metal ions for catalysis. Their catalytic properties are different to hammerhead ribozymes in that a cytosine (or pyrimidine) base distal to the cleavage site is thought to act as a general acid during catalysis (Takagi *et al.*, 2001). Helices II and III (P2 and P3) retain the catalytic core structure while helix IV (P4) acts to stabilise the active site conformation. However, studies have shown that P4 is dispensable in the function of the *trans*-cleaving HDV ribozyme (Bartolomé *et al.*, 1995).

Since the natural host of HDV is the human hepatocyte, HDV ribozymes have the unique advantage of acting naturally within an intracellular

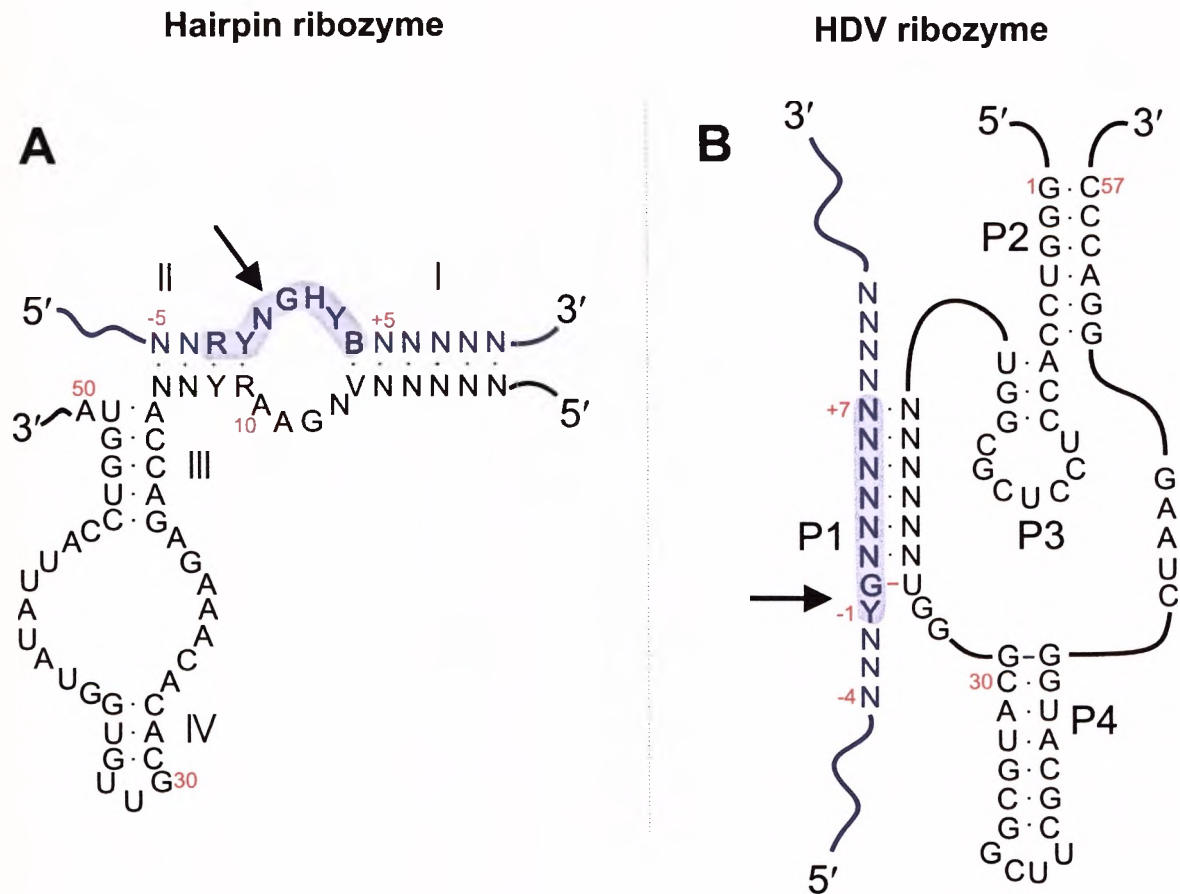


**Figure 1.10** The general secondary structure depicting the minimal core sequences of both a *trans*-cleaving **A**) hairpin (Berzal-Herranz *et al.*, 1993) and **B**) antigenomic HDV ribozyme (Ananvoranich and Perreault, 1998) and their complementary substrates. The hairpin catalytic region is defined by helices III and IV, whilst recognition of the substrate is by Watson-Crick base pairing within helices I and II. The pseudoknot HDV structure is numbered according to Perrotta and Been (Perrotta and Been, 1991). The minimal substrate strand for both hairpin and HDV ribozymes is labelled in blue with the essential cleavage recognition region shaded (light blue). Single dots represent Watson-Crick base pairing. A red dash represents the G-U wobble basepair in the P1 helix, while a blue dash denotes a homopurine basepair at the top of the P4 helix. The black arrows indicate the cleavage sites. IUB codes are used: N = any base; R = A,G; Y = C,U; B = C,G,U; H = A,C,U; V = A,C,G.



environment. These ribozymes are especially attractive in targeting HBV given that the HDV infection life cycle is dependent on the presence of HBV, as HDV makes use of HBV-generated envelope proteins. Interestingly, HDV has been proposed as a vector for the delivery of ribozymes specific for chronic HBV infection (Hsieh and Taylor, 1992). Yet, little is known about the aetiology of HDV-associated liver disease and the possibility of cytopathic effects induced by HDV ribozyme sequences in the course of infection. There exists a 75% homology between the antigenomic HDV self-cleavage region and the first 55 nucleotides of human 7SL RNA (Negro *et al.*, 1991; Negro *et al.*, 1989), which is an essential component of the signal recognition particle (SRP), a small cytoplasmic ribonucleoprotein that targets nascent secretory and membrane proteins, to the rough endoplasmic reticulum (Walter and Blobel, 1982). HDV ribozymes may induce cytopathic effects on the host cell through an antisense mechanism by hybridising to 7SL RNA (Bartolomé *et al.*, 1995).

Clearly other small ribozymes can be designed to act as therapeutic agents. Nevertheless, their unique features do not, at this moment, appear to add value to the *trans*-cleaving effects of hammerhead ribozymes, which have a more simple structure and can be designed to cleave almost any RNA backbone with exquisite specificity (Kato *et al.*, 2001).

In summary, the hammerhead ribozyme is the most amenable ribozyme species for experimental study owing to its size and versatility (Kato *et al.*, 2001; Sczakiel and Nedbal, 1995). It has been extensively applied as a tool to understand the molecular evolution of biological life. Furthermore, X-ray crystal analyses of the hammerhead ribozyme have revealed the intricacies of RNA catalysis, facilitating the study of ribozyme mechanics and enzyme kinetics. It is, however, as a potential therapeutic agent that the hammerhead ribozyme offers interesting prospects in the treatment of HBV infection.

## 1.4 Nucleic acid-based therapy of HBV

Ribozymes and antisense molecules are examples of hybridising nucleic acid sequences that can be designed to inhibit the expression of specific genes. Targeted inhibition or 'knockdown' of gene expression represents the most potent therapeutic application of both antisense and ribozyme approaches. Like

---



ribozymes, antisense DNA or RNA oligonucleotides are designed specifically to hybridise to the target 'sense' mRNA by virtue of Watson-Crick hybridisation. Unlike ribozymes, which inactivate target substrate RNA through both antisense binding and endonucleolytic cleavage, antisense oligonucleotides form double-stranded DNA-RNA (antisense DNA) or RNA-RNA (antisense RNA) duplexed hybrids that prevent RNA replication, reverse transcription or block translation of mRNA. Additionally, double-stranded RNA-RNA or RNA-DNA duplexed hybrids elicit the action of RNase H, which degrades these duplexed hybrids, thereby inactivating target RNA (Agrawal and Zhao, 1998).

Ribozymes possess a significant pharmacological advantage over antisense molecules because of their enzymatic properties. Unlike antisense molecules, which behave like conventional competitive inhibitors, ribozyme molecules can cleave multiple RNA substrates, and are thus theoretically more efficient. Considering the parallels between ribozymes and antisense mechanisms, studies using antisense oligonucleotides for the inactivation of gene expression hold valuable information for the construction of ribozymes. Of particular importance are results obtained from antisense research regarding optimal target site selection. Even though antisense oligonucleotide therapeutic strategies preceded the use of ribozymes, antisense RNAs are still integrated into ribozyme studies as additional experimental controls. Antisense approaches that target HBV will be discussed first as a prelude to a review of anti-HBV ribozymes.

#### **1.4.1 Presynthesized antisense oligodeoxynucleotides**

Antisense approaches include both presynthesized oligodeoxynucleotides (ODNs) and endogenously expressed RNAs. Goodarzi and colleagues were the first to apply presynthesized antisense molecules to inhibit HBV gene expression (Goodarzi *et al.*, 1990). In their study, a range of presynthesized antisense ODNs of 15 nt in length were directed to the preS2/S ORF of HBV. These antisense ODNs inhibited HBsAg production by up to 96% in the HCC cell line, PLC/PRF/5, which contains several copies of integrated HBV DNA. The results obtained by Goodarzi *et al.* (1990) were later confirmed using HBV-transfected Huh7 human hepatoma cells (Blum *et al.*, 1991a). In the latter experiments, both the

---

production of HBsAg and HBeAg were significantly inhibited by antisense ODNs (Blum *et al.*, 1991a).

Later studies, testing 56 different antisense target sites, showed that antisense ODNs targeting the HBV encapsidation signal ( $\epsilon$ ) were the most effective inhibitors of the generation of nascent viral particles (Korba and Gerin, 1995). None of the antisense ODNs examined had any effect on HBV transcript RNA levels, indicating that its therapeutic action was through the blocking of translation and not necessarily by degrading the target RNA (Korba and Gerin, 1995). Antisense ODNs targeted to the core ORF, including the sequences complementary to the polyadenylation signal of HBV, were specifically directed to liver cells via their asialoglycoprotein receptors (Wu and Wu, 1992). This was achieved by complexing DNA to polycations, namely poly-L-lysine conjugated to asialo-orosomucoid. In this case, cellular uptake of complexed DNA was significantly faster than for uncomplexed antisense DNA. Furthermore, complexed antisense ODNs proved to be more effective in reducing HBsAg secretion and viral replication than the uncomplexed counterparts. All ODNs constructed were linked together by phosphorothioate bonds resulting in reduction of their susceptibility to nuclease degradation (Wu and Wu, 1992). In a later study it was also noted that pre-exposure of cells to targeted complexed antisense DNA blocked viral gene expression and replication following transfection of HBV DNA (Nakazono *et al.*, 1996). A similar approach targeting ODNs to avian liver cells was attempted using complexes of unmodified human adenoviral particles and a protein conjugate consisting of modified bovine serum albumin, streptavidin and poly-L-lysine (Madon and Blum, 1996). With this delivery system, an antisense ODN targeted to the encapsidation site of the HBV pregenome caused a modest inhibition of HBV replication in transfected cells.

The first *in vivo* application of anti-hepadnaviral antisense ODNs was reported for the inhibition of Peking duck hepatitis B virus (DHBV) in Peking ducks. The most effective antisense ODN was directed against the 5' region of the preS gene and resulted in a significant inhibition of viral replication and gene expression *in vivo* (Offensperger *et al.*, 1993). Following on from earlier *in vitro* work by Wu and colleagues (Wu and Wu, 1992), antisense ODNs complexed to asialo-orosomucoid poly-L-lysine conjugates were adapted to target the polyadenylation region and adjacent upstream sequences of the pregenome of

woodchuck hepatitis virus (WHV) *in vivo* (Bartholomew *et al.*, 1995). Woodchucks presenting with hepatitis were injected with both complexed and uncomplexed antisense DNA, which resulted in a significant decrease in circulating viral DNA for up to 25 days post treatment. Uncomplexed antisense ODNs and random DNA sequences did not reduce circulating viral DNA levels (Bartholomew *et al.*, 1995).

Using a mouse model for HCC, which is transgenic for the *HBx* gene of HBV, phosphorothioate antisense ODNs were targeted to two sites, including the initiation codon and 5' coding region of the *HBx* ORF. Significantly, antisense DNAs were able to inhibit the expression of HBx and prevented the development of preneoplastic lesions in the liver of treated mice (Moriya *et al.*, 1996). In another study, an animal model expressing HBV markers was developed in order to test phosphorothioate antisense ODNs targeting HBV *in vivo* (Yao *et al.*, 1996). Athymic BALB/c nude mice were transplanted subcutaneously with the hepatoma cell line, HepG2 2.2.15. This HBV transfected hepatoma cell line continuously replicates HBV and produces infectious particles which resulted in the formation of tumours after two weeks. Antisense DNA, which was injected directly into the tumour that developed post-transplantation, resulted in a decrease in the presence of viral antigens, HBsAg and HBeAg, ten days after treatment (Yao *et al.*, 1996).

Most studies thus far have used phosphorothioate-modified ODNs in order to prevent the degradative effects of serum and cellular nucleases. However, their use in human therapy is hampered by questions regarding toxicity. Of particular concern is the risk that chemically modified nucleosides will be incorporated into cellular DNA (Agrawal and Zhao, 1998; Plenat, 1996). Robaczewska and colleagues used a polymeric DNA-binding cation, namely linear polyethylenimine (IPEI), as a synthetic carrier of natural unmodified antisense ODNs (Robaczewska *et al.*, 2001). DHBV-infected Pekin ducklings were injected with natural antisense DNA complexed to IPEI targeting the initiation codon of the large surface protein. The unmodified antisense DNA/IPEI conjugates were better at targeting hepatocytes than antisense molecules alone and were able to inhibit viral replication and protein expression. However, the results were not as significant as those achieved using phosphorothioate modified antisense DNA (Robaczewska *et al.*, 2001).

### 1.4.2 Endogenously expressed antisense RNA

Presynthesized oligonucleotides must be given continuously and in large quantities in order to suppress viral gene expression and replication. Furthermore, as has been indicated these molecules, especially phosphorothioates, often have undesired toxic and immunological effects (Branch, 1998; Stein, 1995). These effects have been reported in animal models and include: decreased blood clotting, white blood cell count, and heart rate (Guidotti and Chisari, 1996). The constitutive expression of antisense RNA from a DNA expression cassette may negate many of the toxicity and efficacy concerns of antisense ODNs and phosphorothioates. Antisense gene therapy may potentially provide long-term protection against the pathogenic effects of chronic HBV infection.

Wu and Gerber (1997) were the first to test the therapeutic effects of expressed antisense RNAs as antiviral agents against HBV. Initially prokaryote expression vectors were used to express three RNAs, which were targeted to inhibit the translation of HBsAg mRNA *in vitro*. In addition, the secretion of HBsAg was significantly inhibited in an HBsAg-secreting cell line transfected with antisense RNA-expressing vectors. The inhibitory effects lasted for many months post-transfection (Wu and Gerber, 1997). Using a retroviral vector delivery system, two antisense RNAs targeting the preC/C and preS2/S regions of HBV were expressed in the HepG2 2.2.15 cell line (Ji and Si, 1997). Antisense RNA targeted to preS2/S inhibited HBsAg and HBeAg secretion by 71% and 23% respectively in transduced cells, while the antisense RNA targeted to preC/C inhibited secretion of HBsAg and HBeAg by 23% and 59% respectively (Ji and Si, 1997).

A comprehensive study was conducted using five subgenomic fragments of the HBV genome to generate antisense and sense RNAs. These were tested for their ability to interfere with HBV replication in cultured cells (zu Putlitz *et al.*, 1998). A replication-competent HBV vector was transfected into human HCC cells, in order to reconstitute viral replication. Antisense RNAs of approximately 300 nt in length targeting the preS2/S and the C/P regions inhibited viral antigen secretion and HBV replication by between 60% to 75%. Unlike the Wu and Gerber study, there was no significant reduction of HBV

---



transcript RNA, indicating that the antisense molecules were exerting their antiviral effects via the blocking of translation. However, an antisense RNA complementary to preS2/S was able to prevent the encapsidation of viral pregenomic RNA (zu Putlitz *et al.*, 1998). Apart from the problems regarding the general safety and efficacy of presynthesized oligonucleotides (see section 5.3.3), there are other concerns associated with the therapeutic application of both antisense DNA and RNA that warrant consideration. Although evidence in eukaryotic cells is slight, it is generally accepted that expressed RNAs deploy their antisense-mediated antiviral effects via Watson-Crick hybridisation with viral RNAs. Apart from impeding translation (referred to as 'translational arrest') and becoming substrates for rapid degradation by double-strand-specific RNases, duplexed RNA-DNA or RNA-RNA hybrids may also elicit unwanted non-specific or 'non-antisense' effects. The latter include the degradation of alternative, non-targeted RNAs by cellular RNase H. Since most expressed antisense RNAs are several hundred nucleotides in length and since only ten hybridised nucleotides are enough to elicit an RNase H response, the potential for antisense RNAs to inactivate cellular mRNAs is considerable (Branch, 1996; Branch, 1998).

Additional concerns include the fact that duplexed RNA-RNA species may also first serve as substrates for cellular deaminases, which modify RNA sequences within the duplex (Polson *et al.*, 1996); and secondly, activate components of the interferon-associated antiviral pathway whose products in turn are known to activate the usually latent endonuclease, RNase L (Baglioni, 1979; Desai *et al.*, 1995). While it is clear from most of the antisense studies that inhibition of HBV gene expression and replication is possible, few have adequately addressed these non-antisense effects. In order for antisense approaches to be given therapeutic credence, non-antisense effects need to be mitigated in any future applications.

### **1.4.3 Ribozymes targeting HBV**

Ribozymes were first observed to cleave HBV RNA *in vitro* in 1992 (von Weizsäcker *et al.*, 1992). In contrast to research conducted using antisense oligonucleotides, there have only been a handful of studies exploring the potential of ribozymes as anti-HBV therapeutic agents.

---



The first anti-HBV ribozyme study made use of a triple hammerhead ribozyme construct. A single transcript RNA encompassing a total length of 44 antisense nucleotides was produced from a single DNA template (von Weizsäcker *et al.*, 1992). These linked ribozymes were targeted to three adjacent cleavage triplet sites on the C ORF of HBV. All three ribozymes efficiently cleaved a transcribed HBV RNA substrate in a cell-free system *in vitro*. The study found that 80% cleavage of a short target RNA was possible using a 1:1 molar ratio of ribozyme to substrate under physiological conditions. Furthermore, the cleavage efficiency and kinetics of the triple ribozyme transcript was similar to that previously described for single ribozymes. The authors speculate that this is due to the fact that cleavage products were able independently to dissociate from the cleavage complex, thus reducing the dissociation rate of the remaining complementary antisense hybridising arms. However, the hammerhead ribozymes developed by von Weizsäcker *et al.* (1992) showed cleavage *in vitro* using either artificial or truncated RNA substrates. These substrates prevent a native secondary structure conformation resulting in ribozyme cleavage conditions different to those found *in vivo*. In a later study, Beck and Nassal (1995) were able to express high levels of hammerhead ribozymes, which were driven by an RNA Polymerase III (RNA Pol III) U6 snRNA promoter in transfected cells. These ribozymes were directed to cleave the highly conserved encapsidation signal ( $\epsilon$ ) of HBV. In intact cells, ribozymes were unable to reduce the steady-state levels of full-length HBV pgRNA, which was expressed from a co-transfected DNA construct. Nevertheless, ribozymes cleaved target expressed RNA in extracts of transfected cells *in vitro* since prior to cleavage, the cellular extracts were treated with proteinase K and phenol, and supplemented with additional  $MgCl_2$ . These results indicate that some unknown factor(s), possibly proteins, prevented the intracellular hybridisation of hammerhead ribozymes to the  $\epsilon$  region of the pgRNA transcript. It also appears that low intracellular  $Mg^{2+}$  concentration limited the efficiency of intracellular ribozyme activity (Beck and Nassal, 1995). However,  $Mg^{2+}$  ions are critical for the establishment of the active form of the ribozyme-substrate complex. It was concluded that intracellular  $Mg^{2+}$  ion concentration is limiting in cases where ribozyme-substrate annealing is hampered by a highly structured target, such as the viral encapsidation signal. This result does not preclude the possibility that alternative sites on the HBV

genome are susceptible to ribozyme cleavage. The  $\varepsilon$  region of HBV is known to be highly structured and to bind to viral polymerase, which may have compromised the activity of hammerhead ribozymes.

To date, the antiviral effects of hammerhead ribozymes have not been characterised *in vivo*. Other studies were able to assess the antiviral effects of hairpin ribozymes targeting HBV in an intracellular context. A retroviral-mediated delivery system was constructed in order to express three hairpin ribozyme-encoded sequences in hepatoma cells (Welch *et al.*, 1997). In this study, HCC cells were co-transfected with a plasmid vector containing a replication-competent dimer of HBV. This vector reconstitutes HBV infection in transfected hepatocyte cell cultures. Hairpin ribozymes, which were targeted to three regions on the viral pgRNA, reduced the level of viral particle production by 66% using an endogenous polymerase assay (Welch *et al.*, 1997). To find accessible ribozyme cleavage sites on the HBV genome, a library of modified hairpin ribozymes with randomised substrate binding domains was constructed (zu Putlitz *et al.*, 1999). This hairpin library was challenged to cleave target sites on a full-length *in vitro* transcribed HBV pgRNA substrate. Primer extension analysis revealed cleavage products which define potential candidate cleavage sites. Of the 40 sites identified, 17 conserved sites were selected for further study. Selected ribozyme constructs were transfected, expressed from both RNA Pol II and Pol III promoter elements, and tested for their antiviral effects in cultured cells. Accessible cleavage sites were clustered around three regions of the HBV genome: the 5' end of the C ORF, several sites in preS2/S, and between DR1 and DR2 on the HBx ORF. Four hairpin ribozymes targeting the preS2/S region were selected for their ability to inhibit viral replication and gene expression in transfected cells in culture and were shown to inhibit HBV replication and antigen synthesis by up to 80%. Although three of the four ribozymes selected were driven by the U6 snRNA Pol III promoter, there did not appear to be a significant difference in either the intracellular levels of ribozyme expression or in ribozyme-mediated antireplicative effects using different promoter systems.

Both studies using hairpin ribozymes offer valuable information regarding target-site accessibility. Further information was obtained from the observation of ribozyme-mediated antiviral effects in cell culture transfection and transduction experiments. However, hairpin ribozymes have a significantly

---

different catalytic mode of action compared to hammerhead ribozymes, and results obtained for the hairpin ribozymes cannot necessarily be interpreted for hammerhead ribozymes.

#### 1.4.4 Thesis objectives

There are unique features of the hepatitis B virus that make it receptive to the targeting effects of therapeutic nucleic acids. The HBV genome consists of overlapping ORFs that cover the entire 3200 nt length of the viral genome. The sequence heterogeneity among hepadnaviral species is modest in comparison to other RNA viruses such as HIV. Conserved regions of the compact HBV genome may encode more than one protein as well as HBV *cis*-elements required for viral replication (Tiollais *et al.*, 1981). Moreover, HBV replicates its genome from a pregenomic RNA template and produces numerous subgenomic transcripts. Both pregenomic and preC RNA species are greater-than-genome-length and encompass the entire 3200 nt genomic sequence of HBV. Other important RNA species include the 2100 and 2400 nt preS/S and the 900 nt HBx transcripts. Since all HBV transcripts are indispensable in the viral life cycle, any viral RNA entity is a potential target for attack using therapeutic nucleic acids.

Many of the viral transcripts share the same sequences, ensuring that ribozyme and antisense molecules can be exploited simultaneously to orchestrate the targeted inactivation of multiple viral RNAs. Even though there appears to be numerous antisense recognition sequences suitable for targeting, it is important to select sequences implicated in multiple functions in the life cycle of the virus, since the targeting of conserved sequences is less likely to result in the generation of ribozyme-resistant viral variants. Moreover, oncogenic viral proteins such as HBx and preS2/S are often expressed endogenously in non-replicative HBV chronic individuals. Viral integration into the chromosomes of the host hepatocyte usually renders the virus incapable of replicating. The onset of disease-causing complications of viral infection may be caused by persistent gene expression and is not necessarily dependent on viral replication. Therefore, it may also be necessary to target those viral transcripts in which translational products are potentially carcinogenic.

---

The inhibitory effects of therapeutic hammerhead ribozymes targeting HBV infection have not been characterised in a cellular environment. For the present thesis, the multifunctional *HBx* region was chosen as a target for antisense and hammerhead ribozyme-mediated attack. Previous studies using antisense DNA/RNA and hairpin ribozymes have indicated that the *HBx* region of HBV is accessible to nucleic acid hybridisation (Moriya *et al.*, 1996; Welch *et al.*, 1997; zu Putlitz *et al.*, 1999). Thus, this thesis broadly encompassed the following objectives:

- 1) Mammalian expression vectors were generated to constitutively express RNA encoding: hammerhead ribozymes, catalytically inactive ribozyme controls, and antisense RNA targeted to two sites of the *HBx* ORF of HBV.
  - 2) The functional endonucleolytic cleavage activities of various hammerhead ribozyme transcripts were determined *in vitro*. Hammerhead ribozyme-mediated cleavage of target *HBx* RNA substrate at specific sites was assayed in an *in vitro* cleavage reaction.
  - 3) Endogenously expressed hammerhead ribozymes and antisense RNAs were tested to inhibit *HBx* mRNA expression and *HBx trans*-activation function in transfected liver-derived cells.
  - 4) The efficacy of hammerhead ribozymes for the inhibition of viral gene expression and markers of viral replication was determined in transfected cells that reconstitute HBV infection following co-transfection with a replication-competent vector of HBV.
  - 5) The antireplicative effects of the anti-*HBx* ribozymes were assayed *in situ* in transfected cells by measuring the expression of a marker gene for Enhanced Green Fluorescent Protein (EGFP). The *EGFP* ORF was used to substitute the preS2/surface ORF in a vector that constitutively expressed all HBV pregenomic and subgenomic transcripts.
  - 6) Multimeric *cis*- and *trans*-cleaving hammerhead ribozyme vectors were generated to increase the intracellular concentration anti-*HBx* hammerhead ribozymes and improve their efficacy *in vivo*. *Cis*- and *trans*-cleavage activities were determined using *in vitro* transcribed multimeric ribozyme transcripts and substrate *HBx* RNA.
-

- 7) The antireplicative effects of multimeric ribozymes targeted to the *HBx* ORF of HBV was assessed in transfected cells using the EGFP/HBV reporter assay and using vectors which reconstitute viral infection in transfected cells.

Some of the approaches used to modify hammerhead ribozymes for therapeutic use are discussed later in section 5.2. Of particular interest to this thesis are the methods used to deliver ribozyme therapeutic genes to their target tissue or cells and the methods employed to maintain their intracellular expression and concentration once acquired. These issues are discussed in the view of applying hammerhead ribozymes for the future treatment of chronic HBV infection.

---



## 2.0 HAMMERHEAD RIBOZYMES AND ANTISENSE RNAs TARGETED TO THE HBV *HBx* OPEN READING FRAME

### 2.1 Summary

The multifunctional *HBx* ORF of HBV encodes a 17 kDa protein, *HBx*, which is necessary for viral infection and implicated in HBV-associated hepatocarcinogenesis. In this study, the *HBx* ORF of HBV was chosen as a target for hammerhead ribozyme hybridisation and cleavage. Oligonucleotides encoding two selected hammerhead ribozymes and sequences encoding respective antisense RNA as well as catalytically inactive ribozyme sequences, were cloned into the mammalian expression vector pCI neo to generate plasmids *pHBx:Rz1*<sub>1473</sub> and *pHBx:Rz2*<sub>1651</sub>.

Hammerhead ribozymes *HBx:Rz1*<sub>1473</sub> and *HBx:Rz2*<sub>1651</sub>, cleaved their target *HBx* sequences *in vitro* within 60 minutes under standard physiological conditions. *HBx:Rz1*<sub>1473</sub> was slightly more efficient than *HBx:Rz2*<sub>1651</sub> and suggested that the site targeted by *HBx:Rz1*<sub>1473</sub> was more accessible for cleavage. The efficacy of the two endogenously expressed hammerhead ribozymes and their antisense RNA controls were tested in co-transfections of various liver-derived hepatoma cells. The target vectors included a plasmid that constitutively expresses *HBx* and a replication-competent dimer of HBV, which reconstitutes HBV infection in transfected Huh7 cells. Both ribozyme-encoding expression vectors, *pHBx:Rz1*<sub>1473</sub> and *pHBx:Rz2*<sub>1651</sub>, inactivated *HBx* mRNA, and concomitantly inhibited *HBx trans*-activation of the reporter plasmid p $\beta$ -actin  $\beta$ -gal, which expresses  $\beta$ -galactosidase under control of the *HBx*-inducible  $\beta$ -actin promoter. *HBx trans*-activator function was inhibited in Chang and PLC/PRF/5 cells and in primary hepatocellular carcinoma cultures that express endogenous *HBx*. However, since the antisense RNA control *pHBx:At2*<sub>1651</sub> was equally as effective as *pHBx:Rz2*<sub>1651</sub>, it is evident that, for this ribozyme species at least, antisense effects were likely to be largely responsible for ribozyme-mediated inhibition in cell culture.

## 2.2 Introduction

The *HBx* open reading frame (ORF) represents an ideal target for nucleic acid-based hybridisation. *HBx* is required for viral replication and the *HBx* sequence encodes multiple functions in the HBV genome (see sections 1.1.3.4 and 1.1.7.3) (Chen *et al.*, 1993; Tiollais *et al.*, 1985; Zoulim *et al.*, 1994). The multifunctional *HBx* sequence overlaps with the 3'-terminal sequence of the polymerase ORF as well as HBV sequences encoding the essential basic core promoter (BCP), which is relatively conserved amongst the mammalian hepadnaviruses (Chen *et al.*, 1993; Tiollais *et al.*, 1985; Zoulim *et al.*, 1994). These factors restrict sequence plasticity of the *HBx* ORF and limit the ability of the virus to evade therapeutic nucleic acid hybridisation. All viral transcripts share a common 3' end owing to the presence of a single polyadenylation signal on the viral genome (Figure 1.2). As a result, the sequence of the smallest *HBx* transcript is fully included in the 3'-end sequences of all HBV transcripts including the pregenome (Tiollais *et al.*, 1985). Targeting the *HBx* ORF allows for the simultaneous inactivation of the template RNA necessary for viral replication, along with all viral transcript mRNA species.

Although the function of *HBx* in the life cycle of the virus remains unclear, *HBx* is directly implicated in HBV-associated hepatocarcinogenesis (section 1.1.7.3) (Arbuthnot *et al.*, 2000). As a preventative measure against the onset of HCC in chronic HBV individuals, inactivating the expression of viral proteins that are potentially carcinogenic, which include *HBx*, is an important medical objective. Since *HBx* can be expressed from replication-incompetent viral integrants, the presence of *HBx*-encoding sequences may be independently responsible for the onset of hepatocarcinogenesis, irrespective of whether successful suppression of viral replication is achieved. Reducing the intracellular presence of *HBx* may improve the long-term prognosis of chronically infected individuals.

In this chapter, two hammerhead ribozymes targeting different sites of the *HBx* ORF were investigated for the potential to cleave *HBx* mRNA transcribed *in vitro*. Moreover, these ribozymes were targeted to inhibit *HBx* *trans*-activator function in co-transfected liver-derived cell cultures. Two regions of the *HBx* ORF were chosen as targets for nucleic acid hybridisation and cleavage based on conserved sequences and computer predictions of accessible RNA secondary

structures. Two antisense RNA expression vectors, which anneal to the same sites as their hammerhead ribozyme counterparts, were used in addition to defective ribozyme variants as ribozyme-negative controls.

## 2.3 Materials and methods

### 2.3.1 Hammerhead ribozyme and antisense RNA expression vectors

Plasmids producing ribozyme sequences (*pHBx:Rz1*<sub>1473</sub> and *pHBx:Rz2*<sub>1651</sub>), their catalytically inactive counterparts (*pHBx:Rz1\**<sub>1473</sub> and *pHBx:Rz2\**<sub>1651</sub>) and antisense oligonucleotides sequences (*pHBx:At1*<sub>1473</sub> and *pHBx:At2*<sub>1651</sub>) directed to the *HBx* ORF were generated in the pCI neo mammalian expression vector (Promega, WI, USA). Oligonucleotides designed to encode the ribozyme and antisense sequences were synthesized using standard phosphoramidite chemistry (Ransom Hill, USA). Complementary sense and antisense oligonucleotide sequences for hammerhead ribozyme cassettes *HBx:Rz1*<sub>1473</sub> and *HBx:Rz2*<sub>1651</sub>, and their respective catalytically-defective counterparts *HBx:Rz1\**<sub>1473</sub> and *HBx:Rz2\**<sub>1651</sub> are presented in Table 2.1. Complementary sequences for antisense oligonucleotide cassettes *HBx:At1*<sub>1473</sub> and *HBx:At2*<sub>1651</sub> are presented in Table 2.2. Altered bases in the sequences encoding catalytically inactive ribozymes are underlined. Oligonucleotides were annealed after heating to 95°C for 5 minutes followed by slow cooling to room temperature. Double stranded DNA, with 5' *EcoRI* and 3' *XbaI* cohesive ends, was cloned into the equivalent restriction sites of the pCI neo vector.

Plasmid pCI neo was digested with *EcoRI* and *XbaI*. The vector backbone fragment was excised and eluted from a 1% agarose gel. Following extraction with chloroform/phenol (Appendix A4-1), the DNA was precipitated with ethanol (see Appendix A4-2). A ligation reaction containing a 50:1 molar ratio of annealed fragment to vector (0.6 pmol vector backbone to 30 pmol annealed fragment insert) was incubated at room temperature for 1 hour in a 20 µl reaction volume containing 20 U T4 DNA Ligase (New England Biolabs, MA, USA). Aliquots (10 µl) of the ligation reaction were used to transform competent

**Table 2.1** Complementary sense (S) and antisense (A) oligonucleotide sequences for single unit hammerhead ribozymes and their respective cleavage-defective counterparts.

<b><i>HBx:Rz1</i><sub>1473</sub> S</b>	5' AATTCTCCCAAGCCTGATGAGTCCGTGAGGACGAAACCCCG AGT 3'
<b><i>HBx:Rz1</i><sub>1473</sub> A</b>	5' CTAGACTCGGGGTTTCGTCCTCACGGACTCATCAGGCTTGG GAG 3'
<b><i>HBx:Rz1*</i><sub>1473</sub> S</b>	5' AATTCTCCCAAGCCT <u>A</u> ATGAGTCCGTGAGGACG <u>A</u> ACCCCG AGT 3' <sup>a</sup>
<b><i>HBx:Rz1*</i><sub>1473</sub> A</b>	5' CTAGACTCGGGG <u>T</u> CGTCCTCACGGACTC <u>A</u> TAGGCTTGG GAG 3' <sup>a</sup>
<b><i>HBx:Rz2</i><sub>1651</sub> S</b>	5' AATTCTTATGTAAGTATGAGTCCGTGAGGACGAAACCTTGGGT 3'
<b><i>HBx:Rz2</i><sub>1651</sub> A</b>	5' CTAGACCCAAGGTTTCGTCCTCACGGACTCATCAGTTACATAAG 3'
<b><i>HBx:Rz2*</i><sub>1651</sub> S</b>	5' AATTCTTATGTAAGT <u>A</u> ATGAGTCCGTGAGGACG <u>A</u> ACCTTGGGT 3' <sup>a</sup>
<b><i>HBx:Rz2*</i><sub>1651</sub> A</b>	5' CTAGACCCAAGG <u>T</u> CGTCCTCACGGACTC <u>A</u> TAGTTACATAAG 3' <sup>a</sup>

<sup>a</sup> Underlined nucleotides indicate the alterations made to the ribozyme catalytic site rendering hammerhead ribozymes *HBx:Rz1\**<sub>1473</sub> and *HBx:Rz2\**<sub>1651</sub> catalytically defective (see Figure 2.1).

**Table 2.2** Complementary sense (S) and antisense (A) oligonucleotide sequences for antisense RNA encoding vectors.

<b><i>HBx:At1</i><sub>1473</sub> S</b>	5' AATTCTCCCAAGCGAACCCCGAGT 3'
<b><i>HBx:At1</i><sub>1473</sub> A</b>	5' CTAGACTCGGGGTCGCTTGGGAG 3'
<b><i>HBx:At2</i><sub>1651</sub> S</b>	5' AATTCTTATGTAAGACCTTGGGT 3'
<b><i>HBx:At2</i><sub>1651</sub> A</b>	5' CTAGACCCAAGGTCTTACATAAG 3'

*Escherichia coli* XL1-Blue™ (Stratagene, CA, USA), which were plated on Luria Bertani ampicillin positive (100 µg/ml ampicillin; Gibco BRL, United Kingdom) agar plates (see Appendices B3-1, B3-2). To identify correctly cloned ribozyme-encoding plasmids, individual colonies ( $\pm 10$ ) were cultured in 50 ml of ampicillin positive medium (Appendix B3-1). Plasmids were prepared by silica mini-prep plasmid purification (see Appendix A2-1) and digested with *EcoRI* and *XbaI*. Digested fragments were run on non-denaturing 8% polyacrylamide gels along with 30 pmol of annealed dsDNA oligonucleotides encoding *HBx*:Rz1<sub>1473</sub> as a molecular weight control. Gels were soaked for 5 minutes in 0.5 µg/ml ethidium bromide solution in 1xTAE buffer (Appendix B2-1) prior to viewing on a UV transilluminator. Successfully cloned plasmids were sequenced using the Sequenase™ Version 2.0 Kit (USB, OH, USA) to confirm the fidelity of sequence (Appendix A5-1). The resulting cassettes produce transcripts from the cytomegalovirus (CMV) immediate early promoter/enhancer. Transcripts derived from *pHBx*:Rz1<sub>1473</sub>, *pHBx*:Rz1\*<sub>1473</sub> and *pHBx*:At1<sub>1473</sub> contain complementary sequences to HBV *ayw* co-ordinates 1465-1481; similarly, the *HBx*:Rz2<sub>1651</sub> and *HBx*:Rz2\*<sub>1651</sub> and *HBx*:At2<sub>1651</sub> RNAs include sequences complementary to co-ordinates 1643-1661 (GenBank® accession number J02203) (Figure 2.1).

### 2.3.2 Target and reporter plasmids

Plasmids pBS-X and pCI neo *HBx* have been previously described (Capovilla *et al.*, 1997). In summary, DNA encoding *HBx* from HBV strain *ayw* was amplified using PCR. The sequence was cloned into the *EcoRI* and *BamHI* sites of the pBluescript II™ KS(+) (pBSII KS[+]; Stratagene, CA, USA) multiple cloning site to produce pBS-X. The *HBx* sequence was then excised from pBS-X and inserted into the mammalian expression vector pCI neo (Promega, WI, USA) to produce pCI neo *HBx*. In this plasmid, *HBx* expression is under control of the constitutively active CMV promoter.



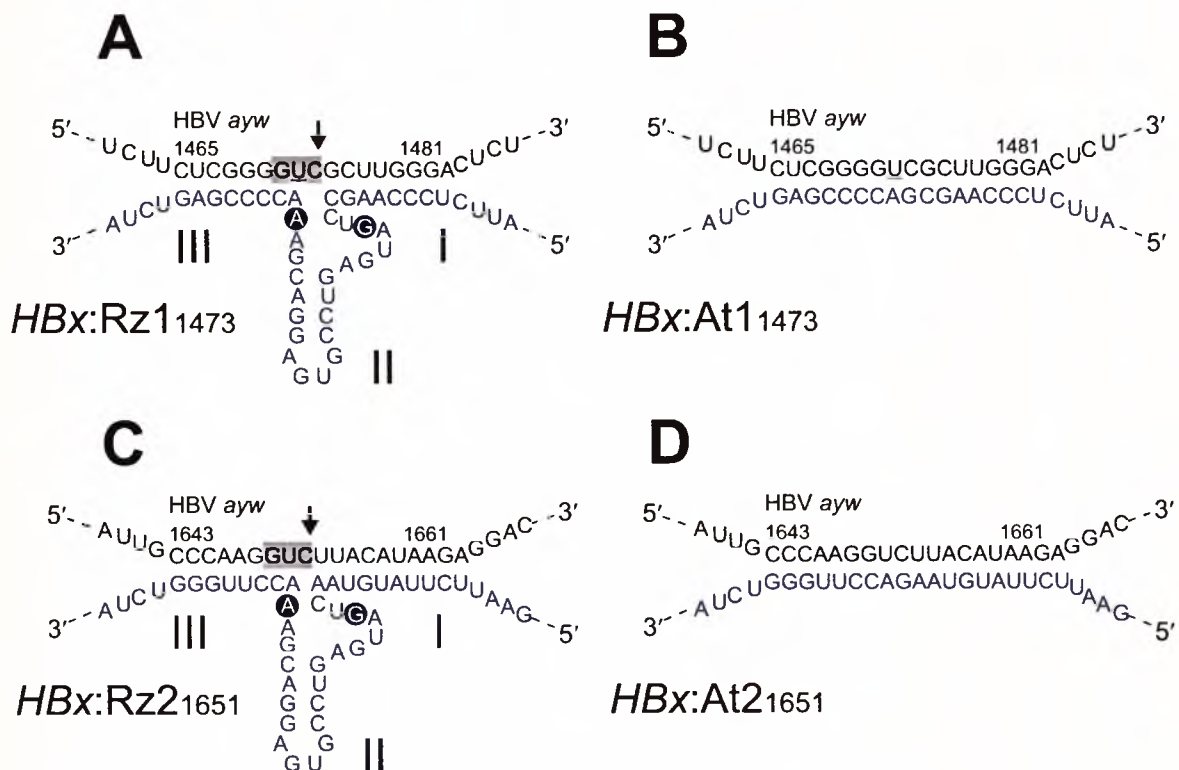


**Figure 2.1** The catalytic sequences for hammerhead ribozymes *HBx:Rz1*<sub>1473</sub> and *HBx:Rz2*<sub>1651</sub> and hybridisation sequences for antisense RNAs *HBx:At1*<sub>1473</sub> and *HBx:At2*<sub>1651</sub>. **A)** and **C)** The HBV *ayw* sequences targeted by *HBx:Rz1*<sub>1473</sub> and *HBx:Rz2*<sub>1651</sub> are indicated with the pairing ribozyme sequences of the helix I and helix III domains. *HBx:Rz1*<sub>1473</sub> is complementary to HBV *ayw* bases from co-ordinates 1465 to 1481 and *HBx:Rz2*<sub>1651</sub> is complementary to bases 1643 to 1661. The 5' GUC 3' cleavage motifs are shaded and the arrows indicate the sites of cleavage. The ribozyme catalytic cores are located within the helix II domains. The underlined U residue of the *HBx:Rz1*<sub>1473</sub> cleavage motif is substituted for a C in HBV subtype *adw*. Circled G and A bases are substituted for A and C residues respectively in the sequences encoding catalytically inactive ribozymes *HBx:Rz1*<sup>\*</sup><sub>1473</sub> and *HBx:Rz2*<sup>\*</sup><sub>1651</sub>. **B)** and **D)** The HBV *ayw* sequences targeted by antisense control molecules *HBx:At1*<sub>1473</sub> and *HBx:At2*<sub>1651</sub>. These sequences both lack ribozyme helix II domains and thus exert their inhibitory activity by hybridisation (antisense effects).

Plasmid pHBV *adw* HTD has been described previously (Blum *et al.*, 1991b), and is a HBV replication competent plasmid that comprises a head-to-tail dimer of the entire HBV genome (strain *adw*) cloned into pGEM 7F+ (Promega, WI, USA). The plasmid p $\beta$ -actin  $\beta$ -gal contains an expression cassette with the  $\beta$ -galactosidase reporter gene under control of the  $\beta$ -actin promoter (Wang and Stiles, 1994). The reporter plasmid pCI neo GFP expresses the gene for Enhanced Green Fluorescence Protein (EGFP) under constitutive control of the CMV promoter (Passman *et al.*, 2000; Weinberg *et al.*, 2000).

### 2.3.3 *In vitro* transcription and cleavage

The *HBx*-encoding plasmid, pBS-X, ribozyme plasmids p*HBx*:Rz1<sub>1473</sub> and p*HBx*:Rz2<sub>1651</sub> and their catalytically inactive counterparts p*HBx*:Rz1\*<sub>1473</sub> and p*HBx*:Rz2\*<sub>1651</sub> were linearised by digestion with *Xba*I. Linearised DNA templates were eluted from a 1% agarose gel, and extracted using phenol/chloroform as described in 2.3.1 and Appendix A4-1. DNA pellets were resuspended in H<sub>2</sub>O to a final concentration of 1  $\mu$ g/ $\mu$ l. Radiolabelled target *HBx* RNA was transcribed from *Xba*I-linearised pBS-X. The reaction mixture contained 2  $\mu$ g of template DNA, 10 mM dithiothreitol, 40 mM Tris-HCl (pH 8.0), 8 mM MgCl<sub>2</sub>, 2 mM spermidine, 20 U RNasin (Promega, WI, USA), 0.5 mM ATP, 0.5 mM TTP, 0.5 mM UTP, 12.5  $\mu$ M GTP, 25  $\mu$ Ci of  $\alpha$ -<sup>32</sup>P GTP (3000 Ci/mmol; NEN du Pont, USA), and 20 U of T3 RNA Polymerase (Promega, WI, USA) in 20  $\mu$ l. After incubating at 37°C for 1 hour, 20 U of DNase I (Promega, WI, USA) were added to the reaction mixture for 20 minutes at 37°C. RNA fragments were purified using the Qiagen RNeasy (Qiagen, CA, USA) RNA purification kit according to the manufacturers instructions. *In vitro* transcription reactions for ribozymes and their catalytically inactive controls were performed at 37°C for 1 hour in a 20  $\mu$ l reaction mixture containing 2  $\mu$ g of template DNA, 10 mM dithiothreitol, 40 mM Tris-HCl (pH 8.0), 8 mM MgCl<sub>2</sub>, 2 mM spermidine, 20 U RNasin (Promega, WI, USA), 0.5 mM NTPs (0.5 mM each ATP, TTP, UTP and GTP), 20 U of T7 RNA Polymerase (Roche, Germany). Similarly, 20 U of DNase I (Promega, WI, USA) were added to the reaction mixture for 20 minutes followed by RNA purification

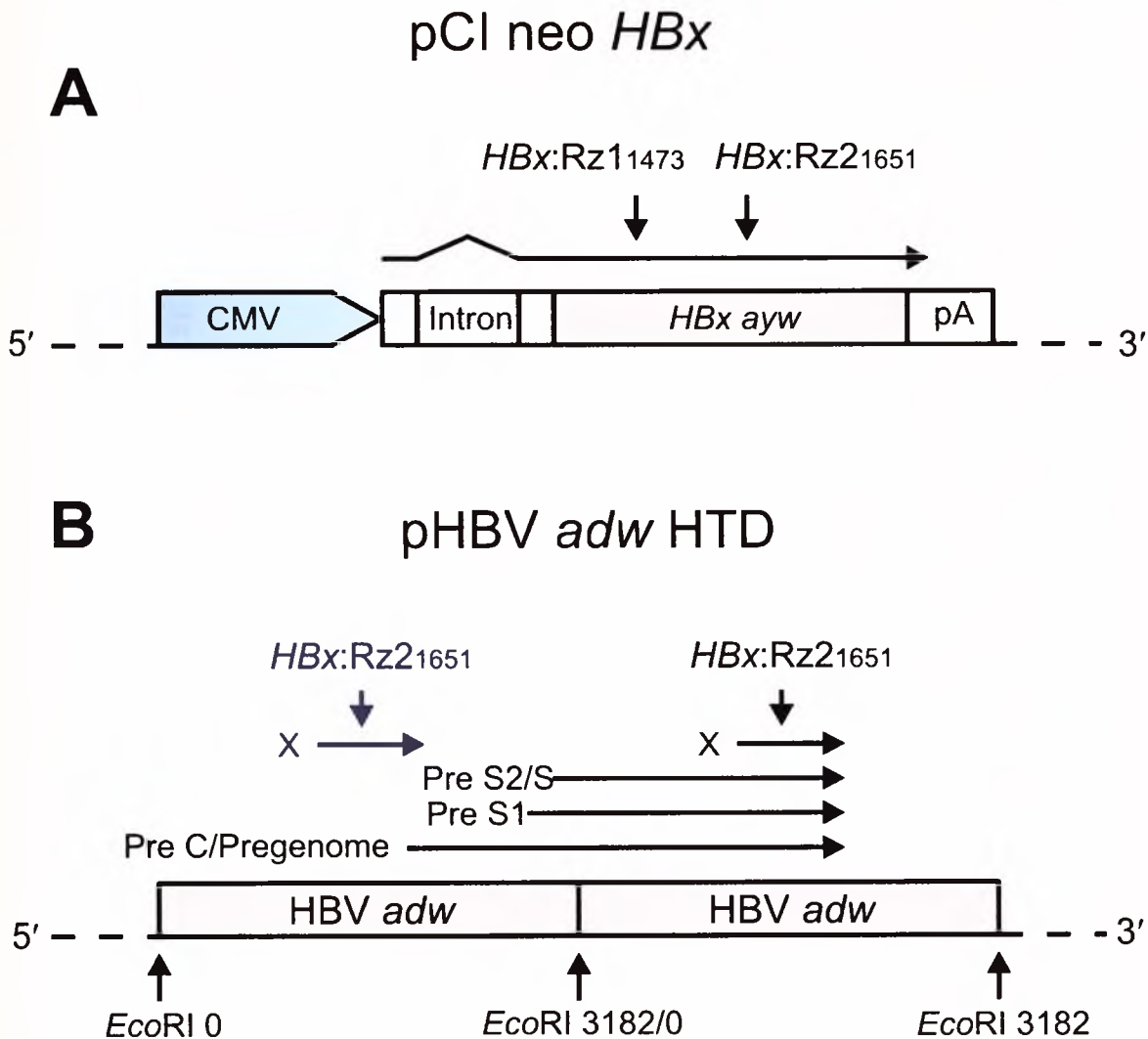


**Figure 2.2** The target sequences for hammerhead ribozymes *HBx:Rz1<sub>1473</sub>* and *HBx:Rz2<sub>1651</sub>*. Both antisense RNAs *HBx:At<sub>1473</sub>* and *HBx:At<sub>21651</sub>* (not shown above) target the same sequence region for hybridisation as their respective ribozymes: *HBx:Rz1<sub>1473</sub>* and *HBx:Rz2<sub>1651</sub>* **A)** The pCl neo HBx vector is shown with ribozyme targets of the ayw HBx transcript. The cytomegalovirus immediate early promoter/enhancer (CMV), intron and polyadenylation signal (pA) of the expression cassette are also indicated. **B)** The pHBV adw HTD vector is represented by the head-to-tail dimer of the HBV adw genome. The HBV transcripts (horizontal arrows) and *HBx:Rz2<sub>1651</sub>* target are indicated.

as above. The cleavage reaction was carried out in a 40  $\mu$ l reaction mixture containing a five-fold molar ratio of ribozyme to radiolabelled target RNA in the presence of 20 mM  $MgCl_2$ , 50 mM Tris-Cl (pH 8.0) and incubated at 37°C. Aliquots (10  $\mu$ l) were removed after incubation for 5 and 60 minutes and then added to 3  $\mu$ l of RNA loading buffer (see Appendix B2-3). Samples were resolved on a 6% polyacrylamide, 7 M urea denaturing gel at 60 W (until the bromophenol blue dye front reached the end of the gel) and autoradiographed.

### 2.3.4 Cell Culture

PLC/PRF/5, Chang and Huh7 cell lines were maintained in Dulbecco's modified Eagle's medium (DMEM) supplemented with 10% foetal calf serum (FCS), penicillin (50 IU/ml) and streptomycin (50  $\mu$ g/ml) (Gibco BRL, UK). Primary cultures of malignant hepatocytes were prepared from a resected tumour of a HBV chronic carrier patient with hepatocellular carcinoma. The patient's serum was positive for HBsAg but negative for HBeAg on testing with Ausria and AxSYM kits (Abbott Laboratories, IL, USA). After resection, the tissue was rinsed in HEPES buffered saline containing collagenase (0.025% collagenase, Sigma grade I; 0.075%  $CaCl_2 \cdot 2H_2O$ ; 161 mM NaCl; 3.15 mM KCl; 0.7 mM  $Na_2HPO_4$ ; 33 mM HEPES, pH 7.65). To dissociate the cells and remove fibrous material, the tissue was teased and passed through a fine stainless steel mesh. The cells collected after this treatment were washed and cultured in Ham's F12 medium (and plated at 90% confluency) supplemented with 10% foetal calf serum (FCS), penicillin (50 IU/ml) and streptomycin (50  $\mu$ g/ml).

### 2.3.5 Transfection and detection of HBx mRNA in cultured cells

On the day prior to transfection, Huh7 cells were seeded at one fifth of their confluent density. Transfections were performed according to the calcium phosphate method (Graham and van der Eb, 1973) (Appendix A7-1). Cells in 100 mm diameter culture dishes were co-transfected with a combination of 20  $\mu$ g of pCl neo HBx and 10  $\mu$ g of either pHBx:Rz1<sub>1473</sub>, pHBx:Rz1\*<sub>1473</sub>, pHBx:Rz2<sub>1651</sub>, pHBx:Rz2\*<sub>1651</sub> or pCl neo. Similar quantities (10  $\mu$ g) of the reporter plasmid pCl neo GFP were also included in each transfection. Prior to RNA extraction,

equivalent transfection efficiencies were verified by fluorescence microscopy that detected similar numbers of EGFP expressing cells in each culture dish (Appendix C2). Seventy-two hours after transfection, total cellular RNA was isolated from the cells using the Guanidinium Thiocyanate method (see Appendix A3) (Schaller and Fischer, 1991a).

To detect *HBx* mRNA using reverse transcriptase (RT) and PCR, first strand cDNA synthesis was performed at 42°C for 1 hour in a 20 µl reaction mixture containing 1 µg of total cellular RNA, 0.8 µg oligo (dT)<sub>15</sub> (Promega, WI, USA), 1 mM each of dATP, dCTP, dTTP and dGTP, 2.5 mM MgCl<sub>2</sub>, 10 mM Tris-HCl (pH 8.3), 50 mM KCl, 5 U RNase inhibitor (Roche, Germany) and 4 U AMV Reverse Transcriptase (Promega, WI, USA). Aliquots (4 µl) of the cDNA reaction mixture were used to amplify *HBx* and glyceraldehyde-3-phosphate dehydrogenase (*GAPDH*) sequences separately. The PCR reaction mixtures included 2.5 µCi of α-<sup>32</sup>P dATP (3000 Ci/mmol; ICN, CA, USA), 50 mM KCl, 10 mM Tris-HCl (pH 9 at 25°C), 0.1% Triton X-100, 1.5 mM MgCl<sub>2</sub>, 0.2 mM each of dATP, dCTP, dTTP and dGTP, 10 pmol each of forward and reverse primers, and 2.5 U of REDTaq™ DNA polymerase (Sigma, MO, USA). Sequences of forward and reverse *GAPDH* and *HBx* primers are given in Table 2.3.

**Table 2.3** Forward and Reverse primers for *GAPDH* and *HBx*.

<b><i>GAPDH</i> F</b>	5' CCCTTCATTGACCTCAACTACATG 3'
<b><i>GAPDH</i> R</b>	5' CATGCCAGTGAGCTTCCCGTTCAG 3'
<b><i>HBx</i> F</b>	5' CCCTTCATTGACCTCAACTACATG 3'
<b><i>HBx</i> R</b>	5' CATGCCAGTGAGCTTCCCGTTCAG 3'

After an initial denaturing step at 92°C for 3 minutes, thermal cycling reactions were conducted at 92°C for 30 seconds, 57°C for 30 seconds and 72°C for 1 minute. Aliquots were removed from the PCR reaction mixtures during the



exponential phase of amplification after 15 and 25 cycles. Samples were resolved using 8% polyacrylamide gel electrophoresis for  $\pm 1.5$  hours at 100 V and then subjected to autoradiography overnight.

### 2.3.6 Transfection and detection of $\beta$ -galactosidase activity

On the day prior to transfection of PLC/PRF/5 and Chang liver cells, approximately  $2 \times 10^5$  cells were seeded at one tenth of their confluent density. Primary cultures of malignant hepatocytes were plated at 90% confluence. All cells were seeded in 35 mm diameter culture dishes. Transfections, as described in section 2.3.5, were carried out with a combination of 2  $\mu$ g reporter plasmid (p  $\beta$ -actin  $\beta$ -gal), 8  $\mu$ g of a target plasmid (pCI neo HBx or pHBV *adv* HTD) and

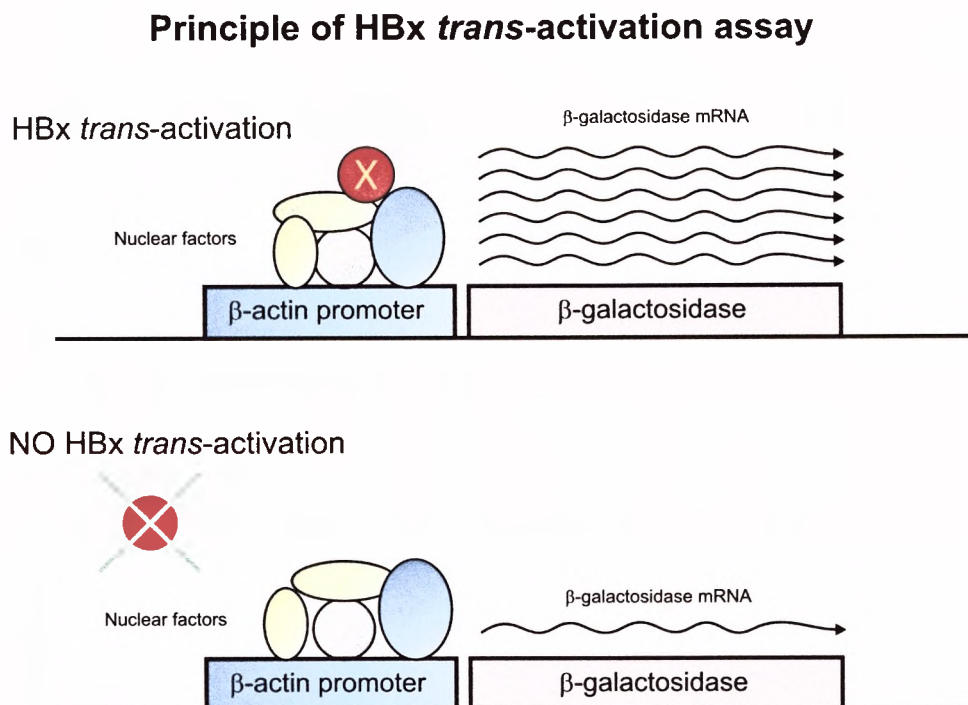


**Figure 2.3** Principle of the HBx *trans*-activation assay. HBx activates the  $\beta$ -actin promoter inducing an increased expression of the downstream  $\beta$ -galactosidase gene. Thus, the presence of HBx can be measured by assaying for  $\beta$ -galactosidase activity using histochemical staining techniques (X-gal is the chromogenic substrate for  $\beta$ -galactosidase).

8  $\mu\text{g}$  of ribozyme (*pHBx:Rz1<sub>1473</sub>* and/or *pHBx:Rz2<sub>1651</sub>*) or control plasmid (*pCI neo*). Seventy two hours after transfection, the cells were fixed and stained with X-gal solution (Sanes *et al.*, 1986) (see Appendix B1-9).

Cells that had a dominant blue colouration on microscopic examination were assessed as positive. The number of positive cells was counted from an entire dish and verified by an independent observer. Duplicate transfections were performed on the primary cultures. The means and standard errors of the means (SEM) were calculated from the data of six independent transfections of PLC/PRF/5 and Chang cells. The analysis of variance was calculated using Dunnett's multiple comparisons test with the number of  $\beta$ -galactosidase-positive cells detected in the transfections with *p $\beta$ -actin  $\beta$ -gal* and *pCI neo HBx* without ribozyme as the control for comparison. This value was normalised to 100%.

## 2.4 Results

### 2.4.1 *The selection of conserved regions of the HBx ORF for hammerhead ribozyme and antisense RNA hybridisation*

Of the possible twelve 5' GUC 3' hammerhead ribozyme cleavage triplets in the *HBx* ORF of HBV strain *ayw* (Figure 2.4B), two sites were selected as candidate target regions for complementary hammerhead ribozymes and antisense RNAs. These include regions 1465-1481 and 1643-1661 for hammerhead ribozyme *HBx:Rz1<sub>1473</sub>* and *HBx:Rz2<sub>1651</sub>* (or antisense RNA *HBx:At1<sub>1473</sub>* and *HBx:At2<sub>1651</sub>*) respectively. The hammerhead ribozyme cleavage triplet sites 1473 and 1651 correspond to the position 3' of the 5' GUC 3' cleavage triplet on the *HBx* ORF of HBV *ayw*. The RNA folding program, Mfold<sup>®</sup> (Genetics Computer Group, WI, USA) was used to predict the putative secondary structure of the *HBx* ORF to ascertain accessible regions for the annealing of complementary ribozyme and antisense sequences. The *HBx* sequence appears to conform to a highly structured secondary structure and the sites indicated in Figure 2.4A were only modestly accessible for nucleic acid hybridisation in the secondary structure predictions of the *HBx* ORF RNA sequence. As a result, the target cleavage sites were primarily selected on the basis of their relative position in conserved regions

within the HBx coding sequence (Appendix C3). Hammerhead ribozyme *HBx*:Rz1<sub>1473</sub> cleaves within a region shared by both *HBx* and *P* ORFs, while *HBx*:Rz2<sub>1651</sub> cleaves within the BCP/Enh II sequence on the HBV genome.

#### 2.4.2 Design of hammerhead ribozyme, antisense RNA and target vectors

Two eukaryotic expression vectors, *pHBx*:Rz1<sub>1473</sub> and *pHBx*:Rz2<sub>1651</sub>, encoding ribozyme sequences that hybridise to targets surrounding 5' GUC 3' cleavage motifs within *HBx*, were constructed (Figure 2.1). The ribozymes included 8 (*pHBx*:Rz1<sub>1473</sub>) or 10 (*pHBx*:Rz2<sub>1651</sub>) complementary bases in helix I, while in both ribozymes there were 8 complementary bases in the helix III domain. Sequence changes in the helix II domain were introduced to propagate the enzymatically inactive control vectors. To inhibit *HBx* expression, the eukaryotic expression vectors were generated to express hammerhead ribozyme RNA sequences under control of the constitutively active CMV immediate early promoter/enhancer (Figure 2.1A and C). Moreover, these sequences were cloned between T3 and T7 RNA promoters for preparation of ribozyme RNA *in vitro*. Equivalent vectors encoding catalytically inactive ribozymes (Figure 2.1A and C) and antisense RNAs (Figure 2.1B and D) were also generated. Plasmids expressing the target *HBx* sequences are depicted in Figures 2.2A and 2.2B. Plasmid *pCl neo HBx* contains the *HBx* sequence from HBV strain *ayw* cloned downstream of the CMV immediate early promoter/enhancer. *pHBV adw* HTD is a replication competent HBV plasmid that contains two head-to-tail copies of the entire HBV genome (*adw* strain). In this plasmid, *HBx* gene expression is similar to that of replicating HBV. The triplet cleavage motif of *HBx*:Rz1<sub>1473</sub> is substituted with a 5' GCC 3' sequence in *pHBV adw* HTD.

#### 2.4.3 Ribozyme-mediated cleavage of HBx RNA in vitro

To test the endonucleolytic cleavage activities of the two designed hammerhead ribozymes *in vitro*, ribozyme and target RNAs were transcribed from linearised templates using T7 and T3 RNA polymerase respectively. A 584 nt substrate

**A** *HBx* ORF (HBV *ayw*) - RNA secondary structure

Mfold<sup>®</sup> (Genetics Computer Group, Madison, WI)  
 $\delta G = -142.49$  (initially -157.7)

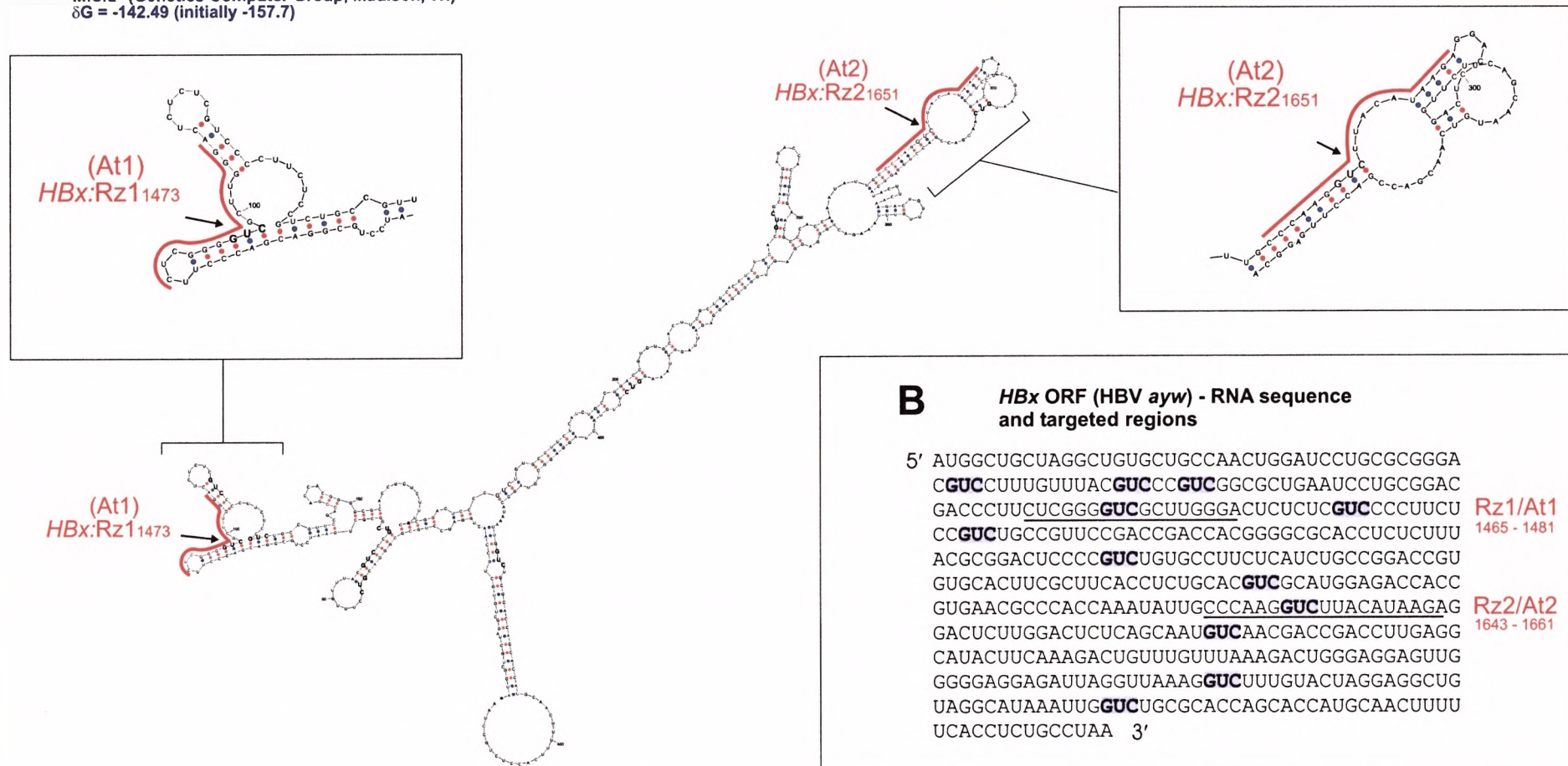


**Figure 2.4** The accessibility of *HBx* RNA sequences for hammerhead ribozyme and antisense RNA hybridisation. **A)** The most energetically favourable ( $\delta G$ ) secondary structure of the *HBx* RNA ORF sequence (HBV *ayw*, GenBank<sup>®</sup> accession number: J02203) obtained using Mfold<sup>®</sup>. The 12 5' GUC 3' cleavage triplets are shown (bold). Cleavage sites (arrows) and hybridisation regions are annotated. **B)** *HBx* ORF RNA sequence showing all twelve 5' GUC 3' cleavage triplets. Underlined are the hybridisation sites for both hammerhead ribozyme and antisense RNA sequences.



RNA encoding the *HBx* ORF was subjected to cleavage by both hammerhead ribozymes *HBx*:Rz1<sub>1473</sub> and *HBx*:Rz2<sub>1651</sub> under single turnover conditions (a five-fold molar excess of ribozyme over substrate RNA). Ribozyme and target RNA were incubated for up to 60 minutes under standard physiological conditions. Both ribozymes cleaved their target substrate at the predicted cleavage sites (Figure 2.5A and 2.5B). These results indicate that both ribozyme target sites are accessible for cleavage *in vitro* and that the designed ribozymes are able to display their wild-type phenotypic behaviour.

Hammerhead ribozyme *HBx*:Rz1<sub>1473</sub> cleaved the 584 nt target RNA yielding products of 168 and 416 nt in length. Similarly, *HBx*:Rz2<sub>1651</sub> generated cleavage products of 350 and 234 nt in length (Figure 2.5A). No cleavage was observed for the catalytically inactive ribozyme counterparts for both hammerhead ribozymes *HBx*:Rz1<sub>1473</sub> and *HBx*:Rz2<sub>1651</sub>. Helix II bases G<sub>5</sub> and A<sub>14</sub> (nomenclature according to Hertel *et al.*, 1992) are substituted for A and C residues respectively in the sequences encoding catalytically inactive ribozymes *HBx*:Rz1\*<sub>1473</sub> and *HBx*:Rz2\*<sub>1651</sub>. The mutant ribozymes theoretically retain the ability to hybridise by the complementary base-pairing of helices I and III, while being catalytically inactive. Both ribozymes cleaved their respective target sequences while the catalytically inactive ribozyme variants were ineffective *in vitro*. Hammerhead ribozyme *HBx*:Rz2<sub>1651</sub> appears to be less effective than ribozyme *HBx*:Rz1<sub>1473</sub>, which may be more accessible for ribozyme cleavage due to a favourable secondary structure conformation of the substrate RNA *in vitro*.

For all ribozyme reactions, 5'-end cleavage products were present in greater abundance than 3'-end products. This is likely the result of an inefficient transcription reaction *in vitro*, which can produce truncated transcripts containing variable 3' ends. Incomplete transcription of the substrate RNA may also be due to a lack of unradiolabelled GTP during the T3 RNA polymerase reaction. Moreover, there did appear to be some degradation of the RNA throughout the incubation. This was particularly evident for reactions involving the defective ribozyme species.



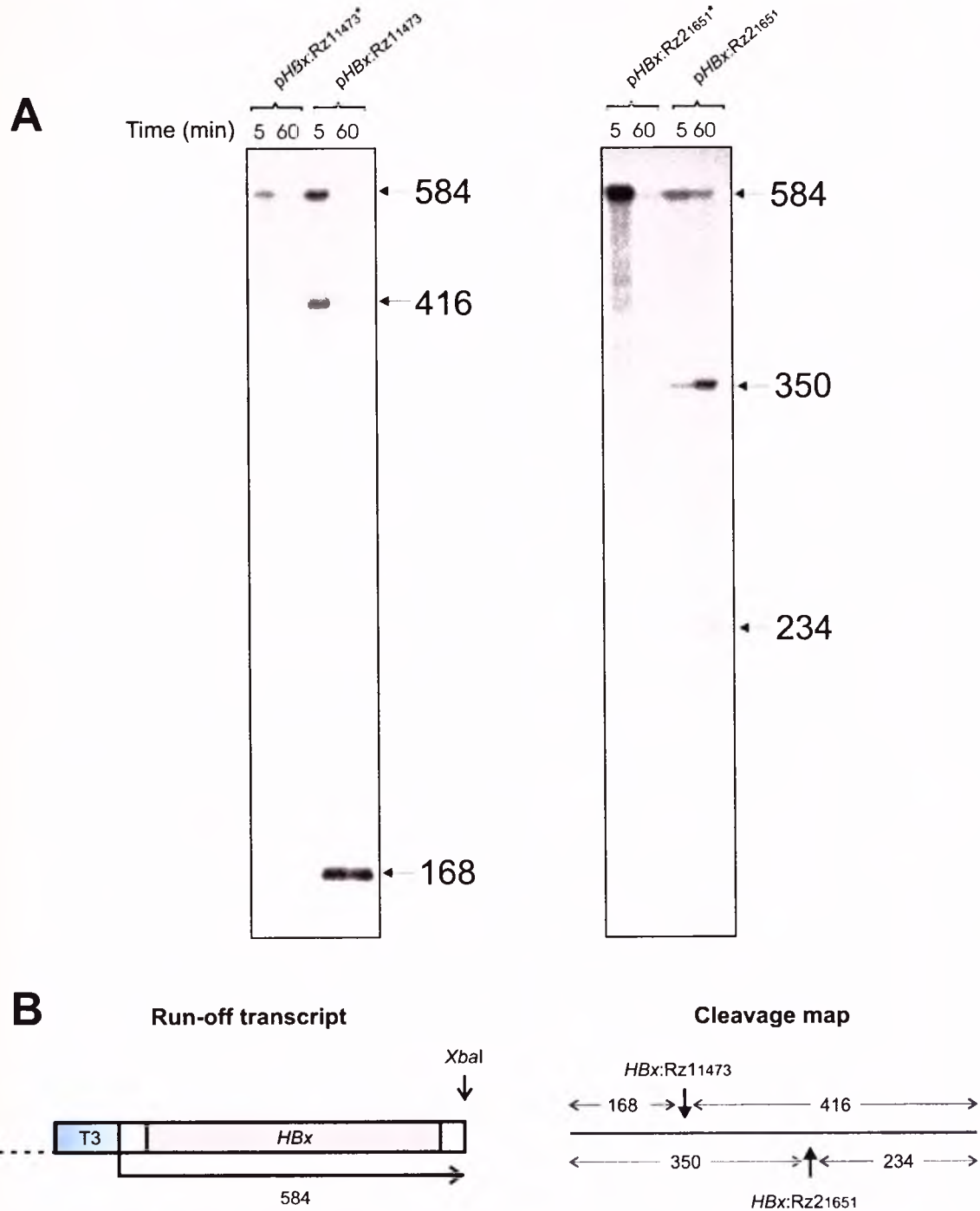


**Figure 2.5** Hammerhead ribozyme-mediated cleavage of an *in vitro* transcribed *HBx* RNA substrate (HBV strain *ayw*). **A)** *In vitro* cleavage of *HBx* RNA by ribozymes and their catalytically inactive counterparts. The cleavage reaction was carried-out as a 5:1 molar ratio of ribozyme to target. The lengths in bases of the substrate and cleavage products are annotated to the right of the autoradiograph. **B)** Schematic representation of T3 RNA polymerase generated run-off transcripts encoding *HBx*. The expected cleavage products for hammerhead ribozymes *HBx:Rz1*<sub>1473</sub> and *HBx:Rz2*<sub>1651</sub> are shown on a cleavage map.

#### 2.4.4 Inhibition of HBx trans-activation by hammerhead ribozymes and antisense RNAs in cell culture

Transcriptional activation of the  $\beta$ -actin promoter and increased expression of  $\beta$ -galactosidase mediated by HBx were used to mark cells expressing the viral protein. The cells shown in Figure 2.6 were co-transfected with a combination of either pCI neo and p $\beta$ -actin  $\beta$ -gal or pCI neo HBx and p $\beta$ -actin  $\beta$ -gal (Figure 2.3). When co-transfected with pCI neo HBx, the number of cells that was histochemically positive for  $\beta$ -galactosidase expression was consistently 8 and 20 fold higher in Chang and PLC/PRF/5 liver cells respectively (Figure 2.6). Thus, under the assay conditions, not all cells transfected with pCI neo and p $\beta$ -actin  $\beta$ -gal were positive for  $\beta$ -galactosidase activity, and the number of positive cells increased significantly as a result of *trans*-activation by HBx. Histochemically detectable  $\beta$ -galactosidase-positive cells in the transfections with pCI neo in the absence of HBx may reflect an increase in the intracellular copy number of p $\beta$ -actin  $\beta$ -gal in these cells. Uptake of vector molecules by individual cells during calcium phosphate transfection is variable. In cells where the intracellular copy number of the marker plasmid is high,  $\beta$ -galactosidase expression would be sufficient to produce histochemically positive cells without  $\beta$ -actin promoter *trans*-activation by HBx. To enable comparison of the ribozyme effects on PLC/PRF/5 and Chang liver cell lines, the mean number of positive cells in the series transfected with pCI neo HBx (positive control) has been normalised to 100%. This corresponds to an average of 255  $\beta$ -galactosidase-positive PLC/PRF/5 cells and 184  $\beta$ -galactosidase-positive Chang cells per dish of transfected cells. This indirect histochemical method of detecting cells expressing  $\beta$ -galactosidase and HBx appears to be more specific and sensitive than immunohistochemical detection of HBx. The effects of transfecting the ribozyme vectors on the number of Chang and PLC/PRF/5 cells that are histochemically positive for  $\beta$ -galactosidase activity are depicted graphically in Figure 2.7 and 2.8. After co-transfection of Chang cells with either pHBx:Rz1<sub>1473</sub> or pHBx:Rz2<sub>1651</sub>, the number of positive cells diminished significantly when compared with the cells expressing HBx without ribozyme ( $P < 0.01$ ) (Figure 2.7A). The inhibitory effect of pHBx:Rz1<sub>1473</sub> was more marked than that of pHBx:Rz2<sub>1651</sub>.

---

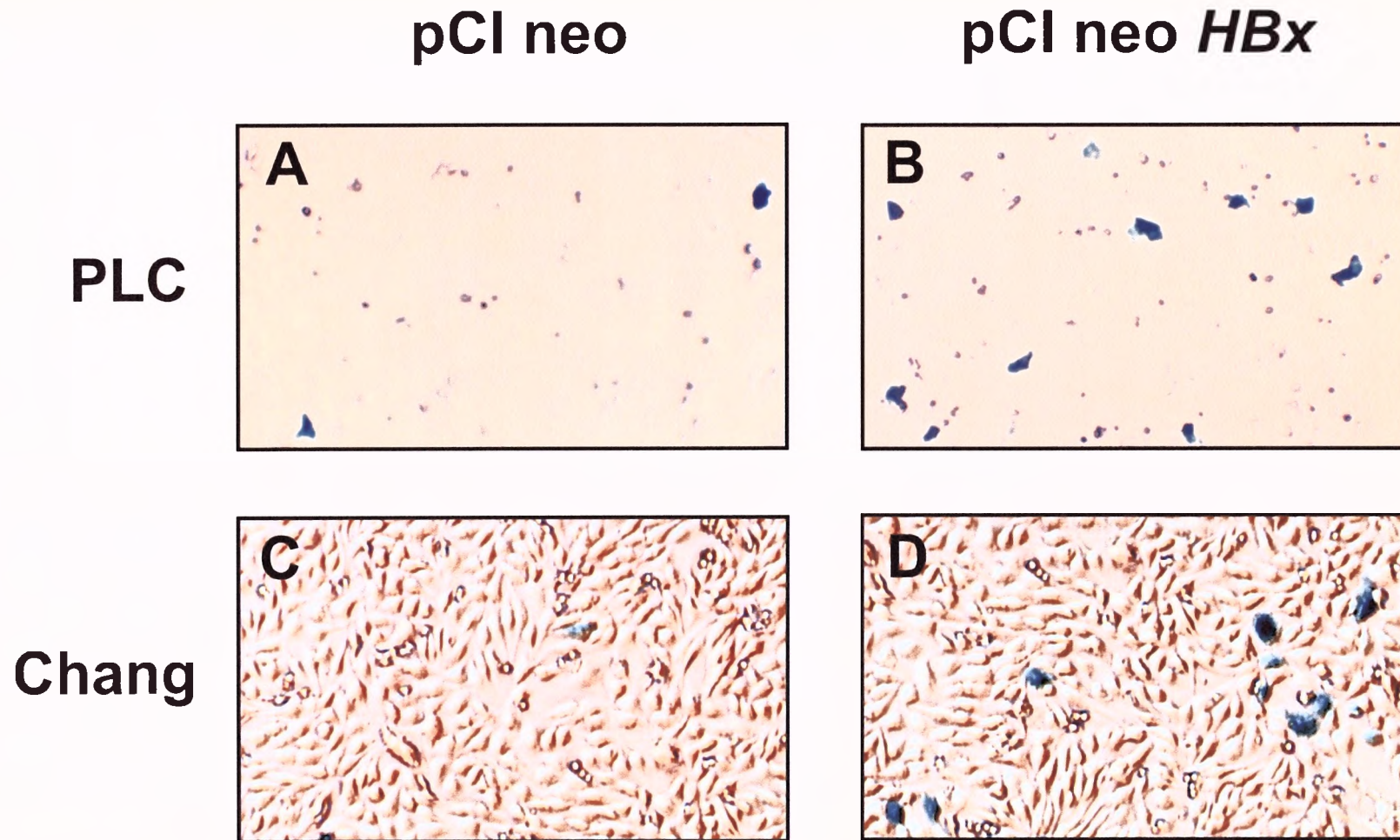


**Figure 2.6** Representative low power microscopic field of  $\beta$ -galactosidase positive PLC/PRF/5 (A and B) and Chang (C and D) cells transfected with  $\rho\beta$ -actin  $\beta$ -gal and pCI neo (A and C) or  $\rho\beta$ -actin  $\beta$ -gal and pCI neo *HBx* (B and D).

Transfection of Chang cells with *pHBx:Rz1<sub>1473</sub>* and *pHBx:Rz2<sub>1651</sub>* in combination had a similar effect to that of *pHBx:Rz1<sub>1473</sub>* alone. Furthermore, there was no significant difference ( $P > 0.01$ ) between the number of  $\beta$ -galactosidase-positive cells detected in the negative control (pCI neo with p $\beta$ -actin  $\beta$ -gal) and in the co-transfections with *pHBx:Rz1<sub>1473</sub>* alone or together with *pHBx:Rz2<sub>1651</sub>*. In PLC/PRF/5 cells (Figure 2.7B), *pHBx:Rz2<sub>1651</sub>* alone or in combination with *pHBx:Rz1<sub>1473</sub>* diminished the number of  $\beta$ -galactosidase positive cells significantly ( $P < 0.01$ ) and *pHBx:Rz2<sub>1651</sub>* was more effective than *pHBx:Rz1<sub>1473</sub>*. The number of positive cells detected after co-transfection with *pHBx:Rz2<sub>1651</sub>* or the two ribozyme plasmids together was not significantly different to the number detected in the negative control (reporter plasmid with pCI neo) (Figures 2.8A and B). Co-transfection of the pCI neo backbone vector with pCI neo *HBx* and the reporter did not change the number of positive cells (not shown). These data indicate that both ribozyme expressing plasmids inhibit *HBx trans*-activation in transfected PLC/PRF/5 and Chang cells.

The inhibitory effects of both antisense encoding plasmids, *pHBx:At1<sub>1473</sub>* and *pHBx:At2<sub>1651</sub>* were compared in similar co-transfection experiments in PLC/PRF/5 cells (Figure 2.8A and B). Unlike the ribozyme-encoding plasmid *pHBx:Rz1<sub>1473</sub>*, *pHBx:At1<sub>1473</sub>* did not reduce the number of  $\beta$ -galactosidase-positive cells. However, the addition of *pHBx:At2<sub>1651</sub>* reduced the number of positive cells to the levels detected for the negative control (Figure 2.8A). This observation suggests that an antisense effect generated by *pHBx:At2<sub>1651</sub>* is equally as effective as the ribozyme-encoding sequence counterpart, *pHBx:Rz2<sub>1651</sub>*. Without being able to determine cleavage conditions *in vivo*, it cannot be ruled out that the ribozyme-encoding sequences are generating their inhibitory effects through an antisense mechanism alone. However, there is a clear difference between the effects of *pHBx:Rz1<sub>1473</sub>* and *pHBx:At1<sub>1473</sub>*, which may indicate that ribozyme cleavage is directly responsible for the greater inhibitory power of *pHBx:Rz1<sub>1473</sub>*.

To determine the effects of *pHBx:Rz2<sub>1651</sub>* and *pHBx:At2<sub>1651</sub>* on *HBx* expressed in the context of normal HBV sequences, PLC/PRF/5 cells were co-transfected with the HBV replication competent plasmid, pHBV *adw* HTD (Figure 2.2B). Relative to the baseline expression of reporter in the negative control



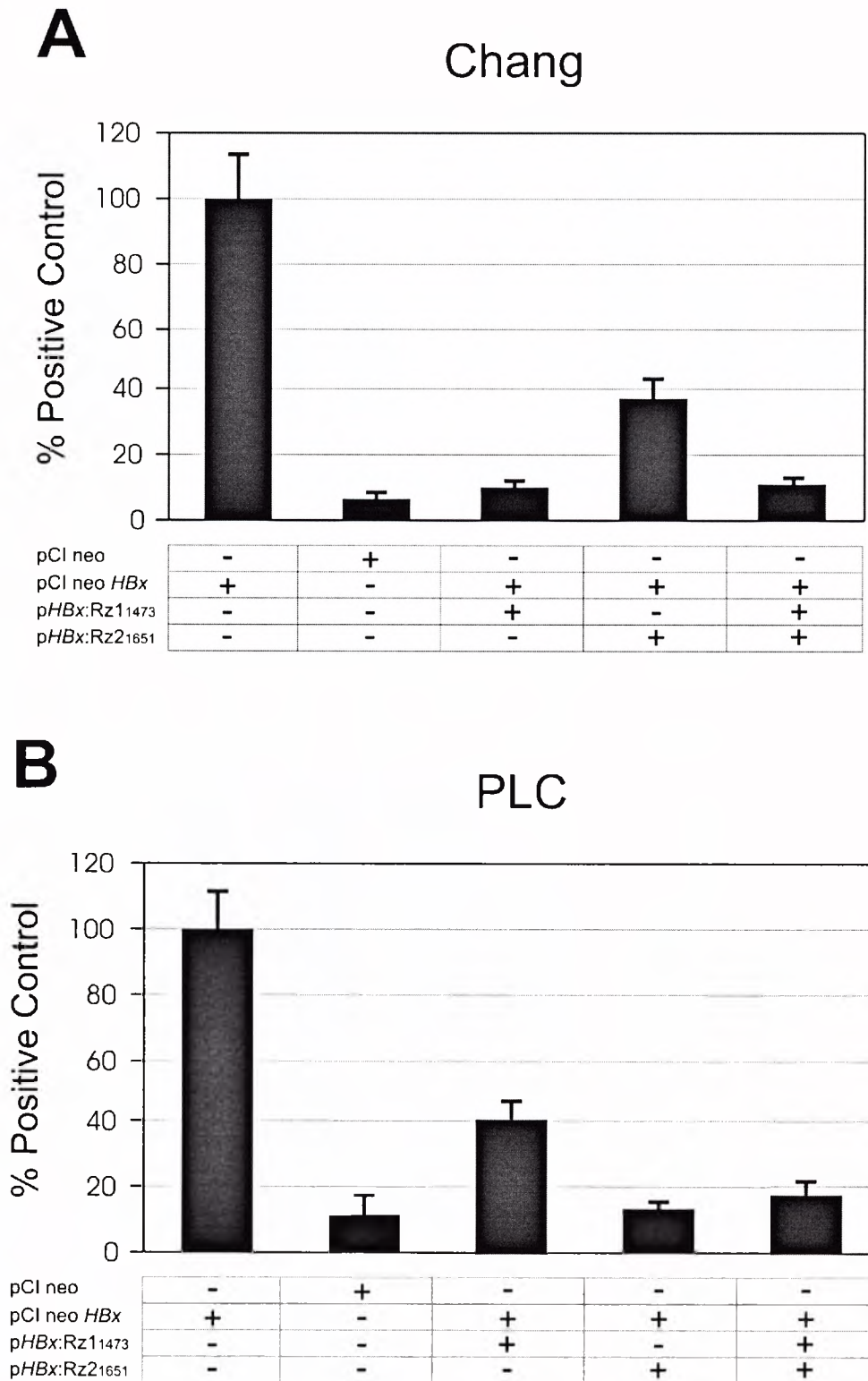


**Figure 2.7** Effect of ribozyme co-transfection on the number of  $\beta$ -galactosidase positive Chang cells (**A**) and PLC/PRF/5 cells (**B**). The data in each column are given relative to the mean number of  $\beta$ -galactosidase positive cells transfected with p $\beta$ -actin  $\beta$ -gal and pCl neo HBx (positive control of 100%). The plasmids co-transfected with p $\beta$ -actin  $\beta$ -gal are indicated below each column. The means and standard errors from six independent experiments are given in **A** and **B**.



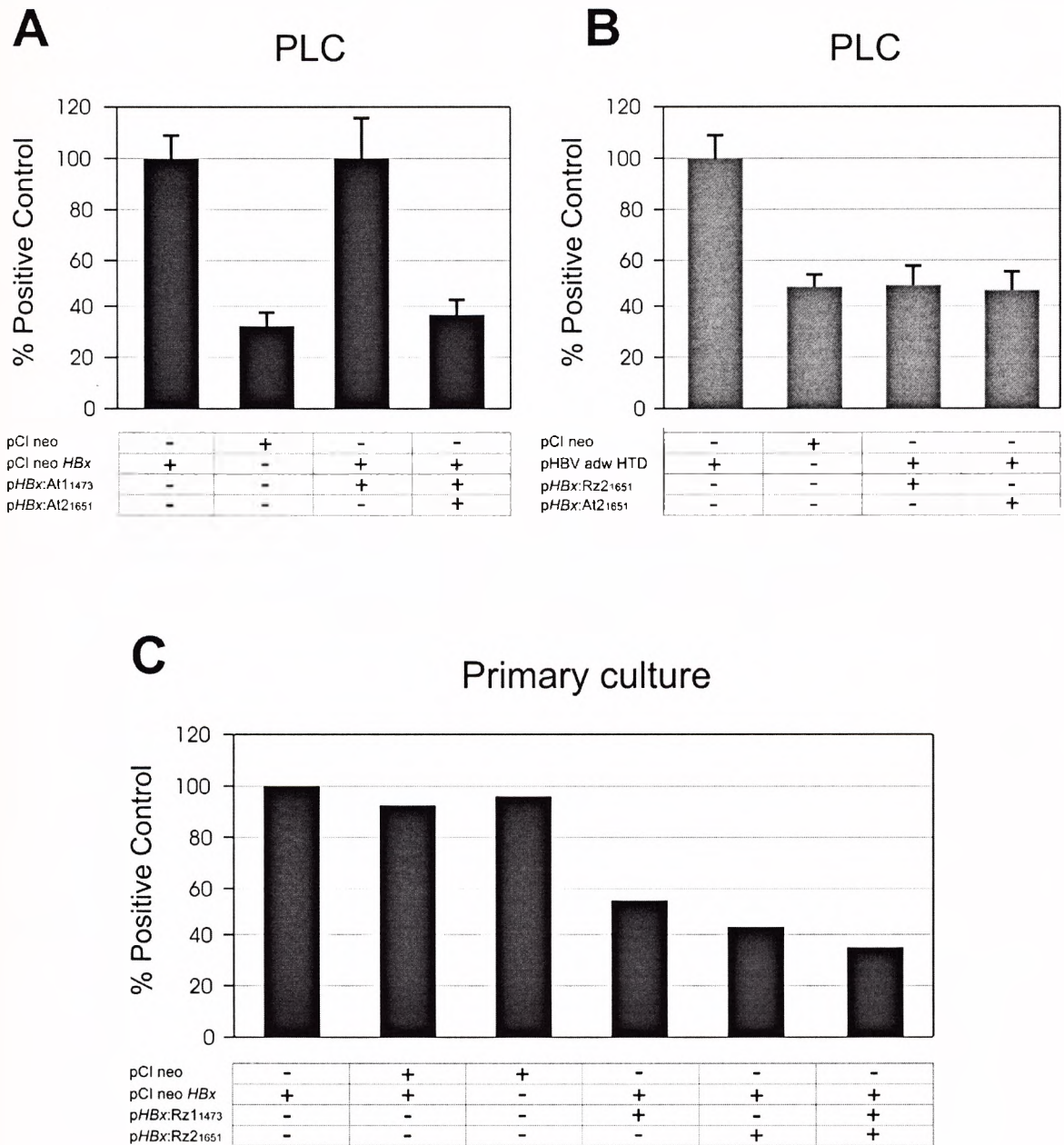


**Figure 2.8** Effect of ribozyme and antisense co-transfection on the number of  $\beta$ -galactosidase positive PLC/PRF/5 cells (**A** and **B**) and hepatocytes derived from primary cultures of resected malignant liver tissue (**C**). The data in each column are given relative to the mean number of  $\beta$ -galactosidase positive cells transfected with p $\beta$ -actin  $\beta$ -gal and pCI neo HBx (positive control of 100%). The plasmids co-transfected with p $\beta$ -actin  $\beta$ -gal are indicated below each column. The means and standard errors from six independent experiments are given in **A** and **B**. The data in **C** represent the means from two independent transfections (the positive control consists of a mean value of 263 histochemically positive cells per plate).

vector, pCl neo, the number of positive cells resulting from transfections with the vector pHBV *adw* HTD was approximately 60% that of pCl neo *HBx* (data not shown). Relative to the number of positive cells generated by the vector pHBV *adw* HTD (reflected as a positive control of 100% in Figure 2.8B), baseline cell numbers that were histochemically positive for  $\beta$ -galactosidase activity were in the order of 40%. This difference is expected since the CMV promoter is likely to be more powerful than the endogenous *HBx* promoter (Schaller and Fischer, 1991a). Co-transfection of pHBV *adw* HTD with the vectors expressing *pHBx:Rz2<sub>1651</sub>* and *pHBx:At2<sub>1651</sub>* diminished the number of positive cells to a level similar to that of the negative control (pCl neo). Additionally, this result suggested that for *pHBx:Rz2<sub>1651</sub>* and *pHBx:At2<sub>1651</sub>*, ribozyme and antisense-mediated effects are largely indistinguishable.

Co-transfection experiments were performed on a primary culture of malignant hepatocytes derived from a tumour resected from a patient who was a non-replicative chronic carrier of HBV (HBsAg positive, HBeAg negative, HBeAb positive). In these cultures, the number of histochemically positive cells transfected with pCl neo and the reporter plasmid was similar to the number from transfection with pCl neo *HBx* and p $\beta$ -actin  $\beta$ -gal (Figure 2.8C). These data suggest that there is endogenous expression of *HBx* and are in keeping with the frequent finding of *HBx* and *HBx* RNA in HBV related HCC (Paterlini *et al.*, 1995; Su *et al.*, 1998). PCR analysis confirmed that *HBx* is integrated into the genome of these malignant cells (not shown, see acknowledgements). *pHBx:Rz1<sub>1473</sub>* and *pHBx:Rz2<sub>1651</sub>* each diminished the number of transfected cells expressing  $\beta$ -galactosidase to 35% and 45% of the transfections with pCl neo and/or pCl neo *HBx*. The two ribozyme plasmids in combination further decreased the number of cells that were positive for  $\beta$ -galactosidase activity.

#### **2.4.5 Ribozyme-expressing vectors decrease *HBx* mRNA in transfected cells**

Total cellular RNA was extracted from transfected Huh7 liver cells to determine the effects of the two anti-*HBx* ribozymes on *HBx* mRNA expressed from transiently transfected pCl neo *HBx*. A sensitive method employing reverse

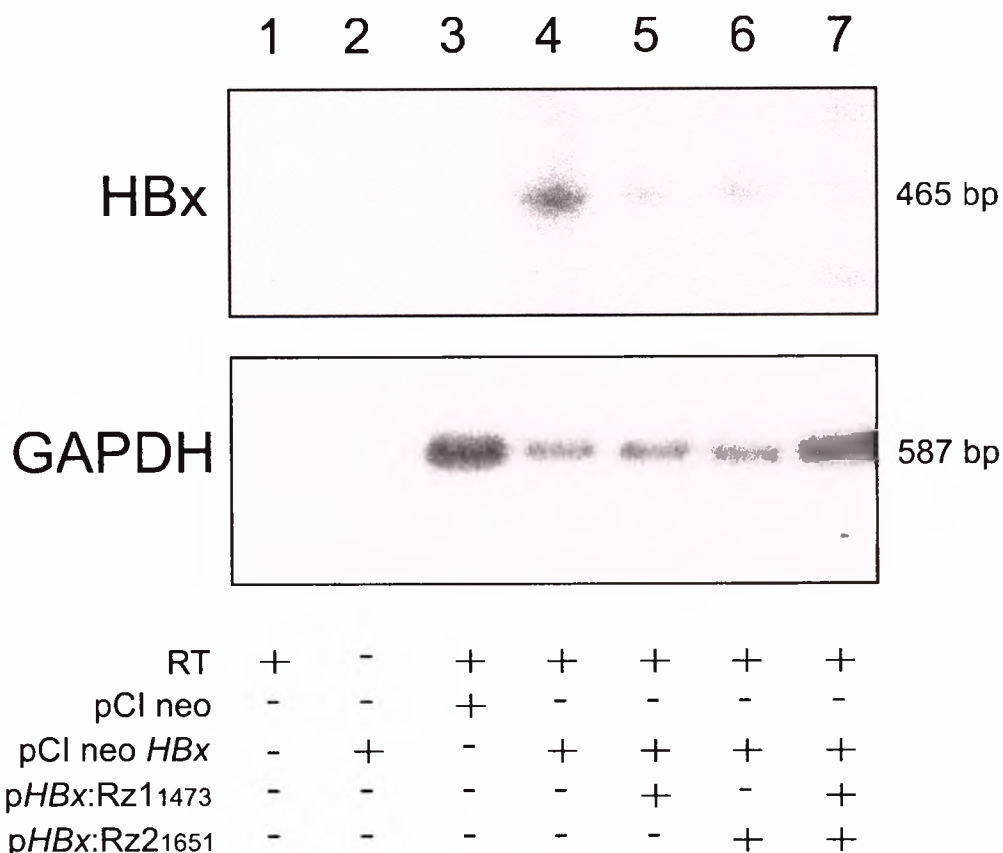


**Figure 2.9** Detection of *HBx* mRNA from Huh7 cells transfected with ribozyme and *HBx*-encoding sequences. Reverse transcriptase (RT) and PCR amplification of *HBx* and *GAPDH* mRNA isolated 72 hours after transfection of Huh7 cells. Autoradiography of 8% polyacrylamide gels demonstrating representative amplified *HBx* and *GAPDH* fragments. Fragments produced during the exponential phase of amplification were analysed. Lane 1, RT-PCR using water as the amplification substrate. Lane 2, PCR amplification of RNA extracted from cells transfected with pCl neo *HBx* without RT treatment. RT-PCR of RNA isolated from cells transfected with pCl neo (lane 3), pCl neo *HBx* (lane 4), pCl neo *HBx* and *pHBx*:Rz1<sub>1473</sub> (lane 5), pCl neo *HBx* and *pHBx*:Rz2<sub>1651</sub> (lane 6), and pCl neo *HBx*, *pHBx*:Rz1<sub>1473</sub> and *pHBx*:Rz2<sub>1651</sub> (lane 7). Again equivalent transfection efficiencies were confirmed in each plate by detecting similar numbers of cells labelled with green fluorescent protein.

transcription and PCR was used to determine the effect of the ribozymes on the concentration of *HBx* mRNA. Radiolabelled *HBx* and standard *GAPDH* DNA fragments produced during the exponential phase of PCR amplification were compared and a representative example of the detected bands is given in Figure 2.9. The amount of amplified *HBx* DNA relative to the *GAPDH* standards indicates that *pHBx:Rz1*<sub>1473</sub> and *pHBx:Rz2*<sub>1651</sub> effectively decrease the *HBx* mRNA concentration in transfected cells (Figure 2.9, lanes 5 and 6). There is a further decrease in the amount of amplified *HBx* DNA when both ribozymes were transfected (Figure 2.9, lane 7). Although this result is only semi-quantitative, the data support previous observations, confirming the inhibitory effects of *pHBx:Rz1*<sub>1473</sub> and *pHBx:Rz2*<sub>1651</sub> on *HBx trans*-activation and indicating that the inhibitory effects are a result of post-transcriptional degradation of target *HBx*-encoding RNA.

## 2.5 Discussion and conclusions

The true accessibility of target RNA for hybridisation by small oligonucleotides is not easily determined *in vivo* since many factors play a role in the folding of RNA (see 5.2.1). As a result, the intracellular mechanism of action involving substrate cleavage by the ribozyme encoding vectors is often difficult to predict. The usual approach is to evaluate the target RNA sequences by computer-aided secondary structure predictions and *in vitro* cleavage assays (Bramlage *et al.*, 1998; Thomson *et al.*, 1997). Of the twelve 5' GUC 3' consensus sequences on the *HBx* ORF, the two sites selected for targeting were only moderately accessible for ribozyme cleavage using the computer program Mfold<sup>®</sup>, a program which is widely used to predict the putative secondary structure of RNA (see Figure 2.4A) (Matzura and Wennborg, 1996; Zuker and Jacobson, 1998). Although the hybridisation regions surrounding both cleavage triplets (Figures 2.1A and C, and 2.4) represent conserved sequences that are unique to hepadnaviruses, the decision to target these specific two sites was largely guided by trial and error. The most important measure of ribozyme efficacy is achieved by inhibiting the function of the translation product of the target sequence, which in this case is the *trans*-activation function of *HBx*. The *in vitro* cleavage data serves more to confirm the functional properties of the designed hammerhead ribozymes.

---



However, for evaluating the accessibility of target RNA for hammerhead ribozyme-mediated cleavage, data obtained through *in vitro* cleavage is usually more reliable than data generated by computer program predictions. To this effect, both hammerhead ribozymes generated *in vitro* were able to cleave their target sequences efficiently and specifically under standard physiological conditions in a cell-free environment (section 2.4.3 and Figure 2.5). Interestingly, computer predictions of the site cleaved by hammerhead ribozyme *HBx:Rz2<sub>1651</sub>* (or the region hybridised by antisense RNA *HBx:At2<sub>1651</sub>*) indicate that it is localised within single-stranded or loop regions, thus making it theoretically more accessible for Watson-Crick hybridisation. However, the *in vitro* cleavage result suggests the opposite, since *HBx:Rz1<sub>1473</sub>* appears to cleave more efficiently. This discrepancy between *in vitro* cleavage data and computer-generated secondary structure predictions has been observed by others (Dropulic and Jeang, 1994) and points to limitations in the use of computer programs as a predictive method in designing target sites for hybridisation.

Ribozymes are thought to be more effective than antisense oligonucleotides at specifically inactivating target RNA since ribozymes possess catalytic activity. Yet the exact mechanism of ribozyme-mediated inactivation of target RNA is difficult to predict in the complex intracellular environment. Information regarding the activity of newly designed ribozymes is largely obtained from *in vitro* cleavage experiments. Since ribozyme activity *in vitro* is assessed in a synthetic environment, these experiments may not necessarily be applicable *in vivo*. Defining the activity of hammerhead ribozyme *trans*-cleavage *in vivo* has proved to be difficult. This is largely owing to the inefficiency of RNA-mediated catalysis in cells and the rapid degradation of reaction products by cellular nucleases (Sullenger and Cech, 1993). Northern blot and nuclease protection assays have been used to detect ribozyme cleavage products. These techniques are laborious and products are often observed close to the detection threshold (approximately 1 pg of RNA) (Bertrand *et al.*, 1994; Sambrook *et al.*, 1989). PCR-based methods are more sensitive and are often used to detect cleavage products (Cantor *et al.*, 1993; Ramezani *et al.*, 1997). However, PCR-based techniques are indirect and ribozyme-mediated cleavage efficiency has been difficult to quantify. Albuquerque-Silva *et al.* (1998) used a modified competitive RT-PCR technique, rapid amplification of cDNA ends (RACE), that results in the



amplification of unknown cDNA 3'-end sequences. In this technique, cDNAs representing 3' ribozyme cleavage products are tailed with a 5' homopolymeric sequence with terminal deoxynucleotidyl transferase prior to PCR amplification. Competitive RACE was used to detect approximately 10 fg (less than 1% of cleaved products) produced by endogenously expressed ribozymes directed to the mumps virus nucleocapsid mRNA in transfected cells (Albuquerque-Silva *et al.*, 1998; Albuquerque-Silva *et al.*, 1999).

A different method for determining the kinetic properties of intracellular hammerhead ribozyme catalysis was developed by Samarsky *et al.* (1999). In this system, a hammerhead ribozyme was localised to the yeast nucleolus by using the U3 small nucleolar RNA (snRNA) as a carrier. The snRNA:ribozyme hybrid (or "snorbozyme") generated cleavage products which, unlike most intracellular ribozyme products, are stable snRNA sequences that can be conveniently measured. This snorbozyme cleaved a target RNA sequence with nearly 100% efficiency *in vivo* in yeast (Samarsky *et al.*, 1999). The methodology employed for this system, which uses a yeast model and snRNA sequences as products of ribozyme cleavage, is unlikely to be generally applicable.

Since the instability of most intracellular ribozyme cleavage products has hampered their direct detection *in vivo*, further alternative approaches have been adopted to distinguish between hammerhead ribozyme cleavage and antisense effects. Indirect measurements using catalytically inactive ribozyme sequences or antisense RNA sequences are used in most cases. Catalytically defective hammerhead ribozymes have sequence changes within the helix II region, which negatively affects catalytic activity. Helical arms I and III remain unchanged allowing complementary hybridisation to the substrate sequence. However, catalytically defective ribozymes/antisense RNAs are still capable of inducing the post-transcriptional inhibition of target RNA, although these effects are usually less pronounced than ribozyme-mediated effects (Dorai *et al.*, 1994; Kintner and Hosick, 1998; Steinecke *et al.*, 1992). In the present study, catalytically inactive ribozymes possessed no cleavage activity *in vitro*, yet antisense RNA expressed from *pHBx:At2<sub>1651</sub>*, which targets the same region as *pHBx:Rz2<sub>1651</sub>* of the *HBx* ORF, induced significant inhibitory effects in transfected PLC/PRF/5 cells (Figure 2.8A and B). In contrast, antisense RNA generated by *pHBx:At1<sub>1473</sub>* was an ineffective inhibitor of *HBx trans*-activation. It is not clear

why the antisense effects generated by *pHBx:At2<sub>1651</sub>* (in combination with *pHBx:At1<sub>1473</sub>*) were better than *pHBx:At1<sub>1473</sub>* alone in inhibiting HBx *trans*-activation function. It is known that maximal antisense effects usually require longer contiguous complementary sequences than the 17 nt present on both antisense molecules (Lieber *et al.*, 1995). The differences may be explained by taking into account that the intracellular secondary and tertiary structure of HBx RNA may preferentially favour the binding of *pHBx:At2<sub>1651</sub>* and *pHBx:Rz2<sub>1651</sub>*. Since *pHBx:Rz1<sub>1473</sub>* has cleavage activity, this may account for its better inhibitory effect *in vivo* than the antisense counterpart *pHBx:At1<sub>1473</sub>*. Although inactivation of HBx mRNA is likely to be at the post-transcriptional level (Figure 2.9), antisense effects are likely to play an important role in the observed inhibition of HBx *trans*-activation by both hammerhead ribozymes, especially for the ribozyme expressed by *pHBx:Rz2<sub>1651</sub>*. Noticeably, there were slight variations in the efficiency of the two ribozyme-encoding vectors *pHBx:Rz1<sub>1473</sub>* and *pHBx:Rz2<sub>1651</sub>* at inhibiting HBx *trans*-activation in Chang and PLC/PRF/5 cells. This can be explained by the fact that hammerhead ribozyme transcripts, which are expressed from a mammalian expression vector, include 5' and 3' vector-derived sequences. These additional sequences may affect the hybridisation of the ribozyme to target RNA, resulting in differing inhibitory effects within the intracellular environment of Chang and PLC/PRF/5.

In conclusion, hammerhead ribozymes, which were functionally active *in vitro*, successfully inactivated HBx mRNA and inhibited HBx *trans*-activation function in transfected liver-derived cells. By inhibiting the expression of HBx mRNA post-transcriptionally, hammerhead ribozymes possess the ability to block translation and decrease the intracellular concentration of HBx, thus concomitantly preventing HBx function *in vivo*. The precise mechanism, however, of ribozyme-derived inhibitory action *in vivo* remains unknown. Antisense hybridisation or antisense effects can elicit the specific degradation of target RNA. This mechanism may be largely responsible for the observed ribozyme-induced inhibitory effects in transfected cells. By inhibiting the function of HBx, which is required for natural viral infection, hammerhead ribozymes or antisense RNAs may interfere with the natural life cycle of the virus. It remains to be determined whether the targeted knockdown of HBx RNA, which must include other viral RNA species, will result in the inhibition of viral gene expression. Since

the HBx sequence is present within viral pregenomic RNA, viral replication and propagation may be directly inhibited with the degradation of this viral replicative intermediate.

---

## 3.0 HAMMERHEAD RIBOZYME-MEDIATED INHIBITION OF HBV GENE EXPRESSION IN Huh7 HEPATOMA CELLS

### 3.1 Summary

The inhibitory activity of the two endogenously expressed hammerhead ribozymes and their catalytically inactive ribozyme controls on HBV gene expression and replication was assessed in Huh7 hepatoma cells. Ribozyme-encoding vectors were co-transfected with the replication-competent HBV vector, pHBV *adw* HTD. Northern blots performed on total cellular RNA extracted from co-transfected cells indicate that the two ribozymes were capable of inhibiting the expression of 2.1 kb preS1/S HBV mRNA species. By contrast, the relative inhibitory activities of the two catalytically inactive variants were significant. Moreover, ribozyme-induced reduction of the 2.1 kb preS2/S mRNA corroborated the measurements of HBsAg and HBeAg secretion from cell culture supernatants, which were obtained from the same plates used to detect viral RNA. This suggests that the two ribozymes pHBx:Rz1<sub>1473</sub> and pHBx:Rz2<sub>1651</sub> possess only a modest antireplicative ability and their inhibitory effects *in vivo* are likely to be generated largely by antisense hybridisation and not necessarily by ribozyme cleavage. When transfected together, the two ribozymes decreased the concentration of 2.1 kb viral RNA to undetectable levels and inhibit the secretion of viral antigens by up to 80%. Similar co-transfections were performed using the vector pCH-EGFP, in which the preS2/S ORF of the modified replication-competent HBV plasmid pCH-9/3091 was replaced by the *EGFP* ORF. Using this vector, both hammerhead ribozymes were able to reduce significantly the number of EGFP fluorescent cells when compared to inactive ribozyme controls. This novel system allowed for the rapid determination *in situ* of anti-HBx ribozyme-mediated inhibition of HBV replication in transfected Huh7 cells. These results were correlated by a reduction in HBsAg when using the replication-competent vector pCH-9/3091.

---

## 3.2 Introduction

Hammerhead ribozymes that are targeted to the *HBx* ORF of HBV should, in theory, be able to inactivate gene expression of all transcribed sequences, including viral pgRNA. On this account, ribozyme-mediated targeting of the *HBx* ORF may be applied therapeutically to abrogate viral replication and propagation in chronically infected individuals. In Chapter 2, the *HBx* sequence was successfully targeted by hammerhead ribozymes *in vitro* and by ribozyme/antisense RNAs in a number of different transfected human hepatoma cell cultures (sections 2.4.3 and 2.4.4). The accessibility of two sites within the *HBx* RNA sequence was confirmed as targets for nucleic acid-based hybridisation. These results are in accord with studies using antisense ODNs/RNAs (Moriya *et al.*, 1996; zu Putlitz *et al.*, 1999), hairpin ribozymes (Welch *et al.*, 1997; zu Putlitz *et al.*, 1998) and hammerhead ribozymes (Kim *et al.*, 1999; Yim *et al.*, 2000) (see section 5.1.1), which indicate the accessibility of the *HBx* sequence as a target for nucleic-acid hybridisation both *in vitro* and in cultured cells. However, the inhibitory effect of hammerhead ribozymes on HBV gene expression and replication has yet to be confirmed in an intracellular context.

Since little is known of the exact mechanism of ribozyme-induced inhibition in mammalian cells, most studies make use of antisense RNAs and catalytically inactive ribozyme variants as additional controls. These controls do not always reveal the exact kinetic mechanism of intracellular inhibition observed by the endogenously expressed ribozymes. It has been technically challenging to measure the actions of ribozymes *in vivo* since target instability after ribozyme cleavage makes detecting the products of ribozyme action difficult. In this chapter, the anti-HBV inhibitory activity of hammerhead ribozyme and inactive ribozyme variants was determined using cell culture models of HBV infection. Ribozyme-mediated effects were determined by measuring a decrease in viral gene expression and the secretion of viral products, HBsAg and HBeAg, into the culture medium. Although ribozyme cleavage activity was not determined *in vivo*, a method was developed for measuring the action of ribozymes targeted to the *HBx* ORF *in situ* in transfected cells. The coding region of EGFP was used to substitute part of the preS2/S ORF in an HBV-encoding vector that expresses all



HBV-derived transcripts. This study demonstrated that the number of transfected cells that express EGFP correlates with the secretion of HBsAg and is an index of the inhibitory effects of the vectors expressing ribozyme sequences. The results presented in this chapter pave the way for the development of improved therapeutic ribozymes that are targeted to the *HBx* ORF of HBV.

### 3.3 Materials and Methods

#### 3.3.1 Target vectors

The target vector pHBV *adw* HTD and the ribozyme vectors have been described previously in sections 2.3.1 and 2.3.2. pCH-9/3091 has been described previously (Nassal *et al.*, 1990) and contains a greater-than-genome-length sequence of HBV subtype *ayw*. In this plasmid, the transcript derived from the CMV promoter generates a 3500 nt pregenomic transcript (Figure 3.1A). To generate pCH-EGFP, the preS2/S ORF of pCH-9/3091 was replaced with a sequence encoding EGFP (Passman *et al.*, 2000) (Figure 3.1B). The EGFP sequence was excised from pCI neo GFP (described in section 2.3.1) with *Xho*I and *Xba*I and inserted into the *Xho*I and *Spe*I sites of pCH-9/3091 to generate pCH-EGFP.

#### 3.3.2 Northern blot

Huh7 cells were transfected with pHBV *adw* HTD together with control or ribozyme plasmids using a procedure similar to that described in section 2.3.3. In summary, cells in 100 mm diameter culture dishes were transfected with a combination of 20  $\mu$ g of pHBV *adw* HTD and 10  $\mu$ g of either pHBx:Rz1<sub>1473</sub>, pHBx:Rz1\*<sub>1473</sub>, pHBx:Rz2<sub>1651</sub>, pHBx:Rz2\*<sub>1651</sub> or pCI neo. Similar quantities (10  $\mu$ g) of the reporter plasmid pCI neo GFP were also included in each transfection to control for equivalent transfection efficiencies. Seventy-two hours after transfection, total cellular RNA was isolated from the cells using the guanidinium thiocyanate method of extraction (see Appendix A3) (Schaller and Fischer, 1991a). For northern blot analysis, 20  $\mu$ g samples of total cellular RNA were separated by electrophoresis in 1.4% formaldehyde-agarose gels. A duplicate gel

was stained with ethidium bromide to ensure for similar amounts of RNA in each lane. Unstained gels were blotted overnight onto Hybond C-extra membranes (Amersham, United Kingdom) and RNA fixed to the membranes by baking for 2 hours at 80°C. Hybridisation was performed in Quickhyb solution (Stratagene, WI, USA) to a multiprime (Amersham, United Kingdom) labelled probe that encompassed the entire HBV genome. See section 3.3.2.1.

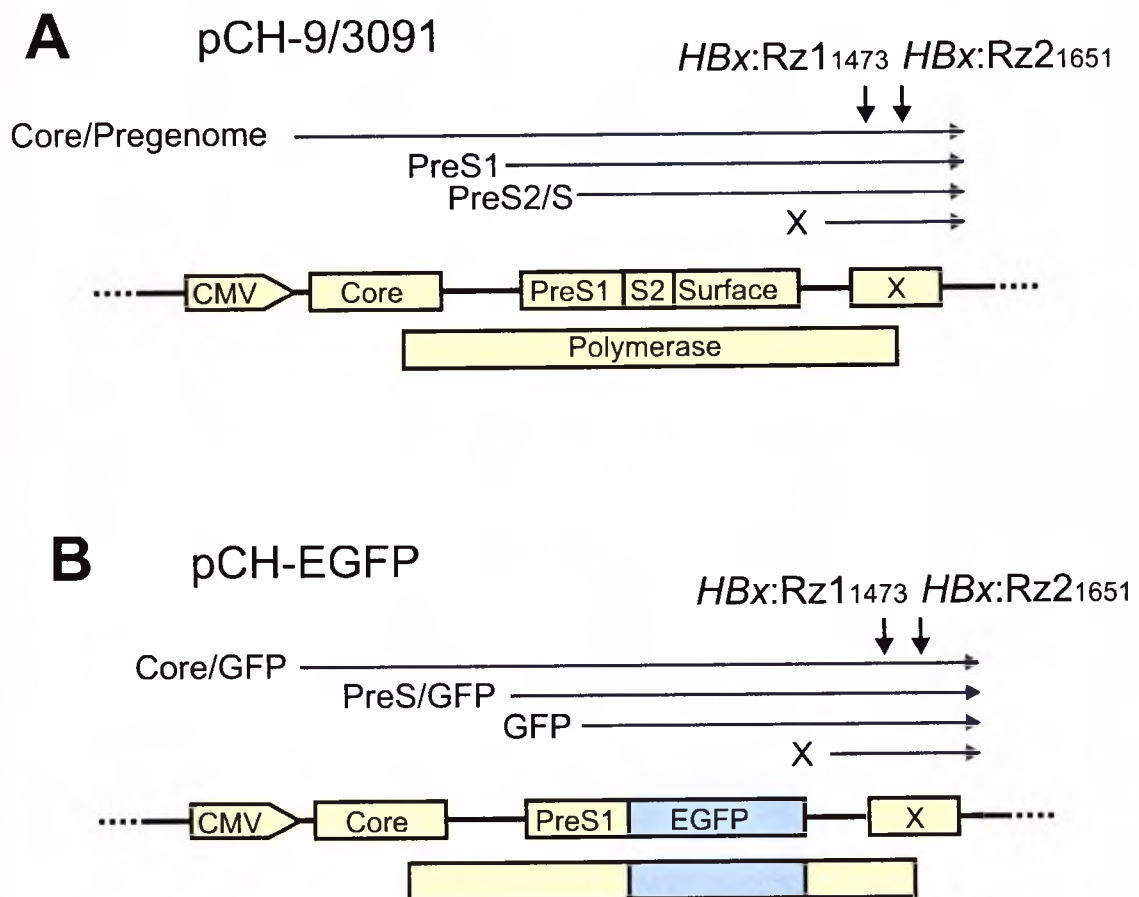


**Figure 3.1** Plasmid constructs pCH-9/3091 (A) and pCH-EGFP (B) showing their open reading frames, respective transcripts and sites targeted by position of cleavage by *pHBx:Rz1<sub>1473</sub>* and *pHBx:Rz2<sub>1651</sub>*. The disrupted polymerase ORF is indicated in light blue.

### 3.3.2.1 Preparation of HBV-specific probe.

pHBV *adw* HTD was digested with *EcoRI* resulting in two fragments. The 3183 bp fragment encompassing the entire HBV genome was eluted from a 1% agarose gel and purified as described in Appendices A4-1 and A4-2. A multiprime random labelling kit (Megaprime DNA Labelling System; Amersham Pharmacia Biotech, England) was used to label the probe to a specific activity of  $2.38 \times 10^6$  cpm/ $\mu$ g.

### 3.3.3 HBsAg and HBeAg secretion from transfected cells

Huh7 cells were transfected with pHBV *adw* HTD (described in section 2.3.2) together with control or ribozyme plasmids (section 3.3.1) in 100 mm diameter culture dishes. HBsAg and HBeAg secretion into the culture supernatants was measured daily for three days using AxSYM (ELISA) immunoassay kits (Abbot Laboratories, IL, USA). The means of HBsAg and HBeAg immunoassay measurements were calculated from two independent transfections.

### 3.3.4 In situ detection of hammerhead ribozyme activity

Huh7 cells were grown, seeded and transfected as described in section 2.3.4 and 2.3.5. Transfections were performed in 60 mm diameter culture dishes. Cells were co-transfected with a combination of 3  $\mu$ g of pCH-EGFP and 6  $\mu$ g of a ribozyme-encoding plasmid: pHBx:Rz1<sub>1473</sub>, pHBx:Rz1\*<sub>1473</sub>, pHBx:Rz2<sub>1651</sub>, pHBx:Rz2\*<sub>1651</sub> or pCl neo (ribozyme-negative control). Similarly, cells in 100 mm diameter culture dishes were co-transfected with a combination of 7  $\mu$ g of pCH-9/3091 and 14  $\mu$ g of a ribozyme encoding plasmid: pHBx:Rz1<sub>1473</sub>, pHBx:Rz1\*<sub>1473</sub>, pHBx:Rz2<sub>1651</sub>, pHBx:Rz2\*<sub>1651</sub> or pCl neo. For the transfections using pCH-9/3091, equivalent transfection efficiencies were confirmed by co-transfection with 10  $\mu$ g of pCl neo GFP followed by fluorescence microscopy (Appendix C2).

Cells labelled with EGFP were detected by fluorescence microscopy three days after transfection. The mean number of fluorescent cells as well as the standard error of the mean (SEM) was calculated from experiments performed in triplicate. HBsAg secretion into the culture supernatants for cells transfected with pCH-9/3091 was measured on three successive days post-transfection similarly

to 3.3.3. The means and SEMs of HBsAg immunoassay measurements were calculated from triplicate transfection experiments. Analysis of variance was calculated using Dunnett's multiple comparisons test.

## 3.4 Results

### 3.4.1 Vectors expressing target sequences

The replication-competent HBV vector, pHBV *adw* HTD, was used to reconstitute HBV infection in transfected Huh7 cells, thus generating all viral mRNA species, including viral pgRNA. This vector was used to determine hammerhead ribozyme inhibitory effects on viral mRNAs, and the secretion of HBsAg and HBeAg into culture supernatants. A sequence encoding EGFP was used to substitute the preS2/S ORF and to generate pCH-EGFP. Transfection of cultured cells with pCH-EGFP allowed fluorescence microscopy to be used to detect marker gene expression *in situ* in living cells. The *HBx* region of HBV is common to naturally-occurring HBV transcripts as well as the mRNA species that are expressed in the target vectors used here. Ribozyme-mediated endonucleolytic cleavage thus includes target sequences on transcripts required for translation of EGFP and HBsAg in pCH-EGFP and pCH-9/3091 respectively.

### 3.4.2 The effects of ribozyme-expressing vectors on HBV RNA expression in transfected cells

HBV RNA was extracted from transfected Huh7 liver cells to determine the effects of the two HBx ribozymes on HBV gene expression. pHBV *adw* HTD in combination with pHBx:Rz1<sub>1473</sub> and pHBx:Rz2<sub>1651</sub> or their catalytically inactive counterparts were used to transfect the established liver cell line. RNA extracted from these cells was measured using northern blot hybridisation (Figure 3.2). The size of the detected RNA (approximately 2.1 kb) indicates that the dominant bands were from the group of transcripts derived from preS1 and preS promoters (Figure 1.2). This observation is consistent with results that suggest these

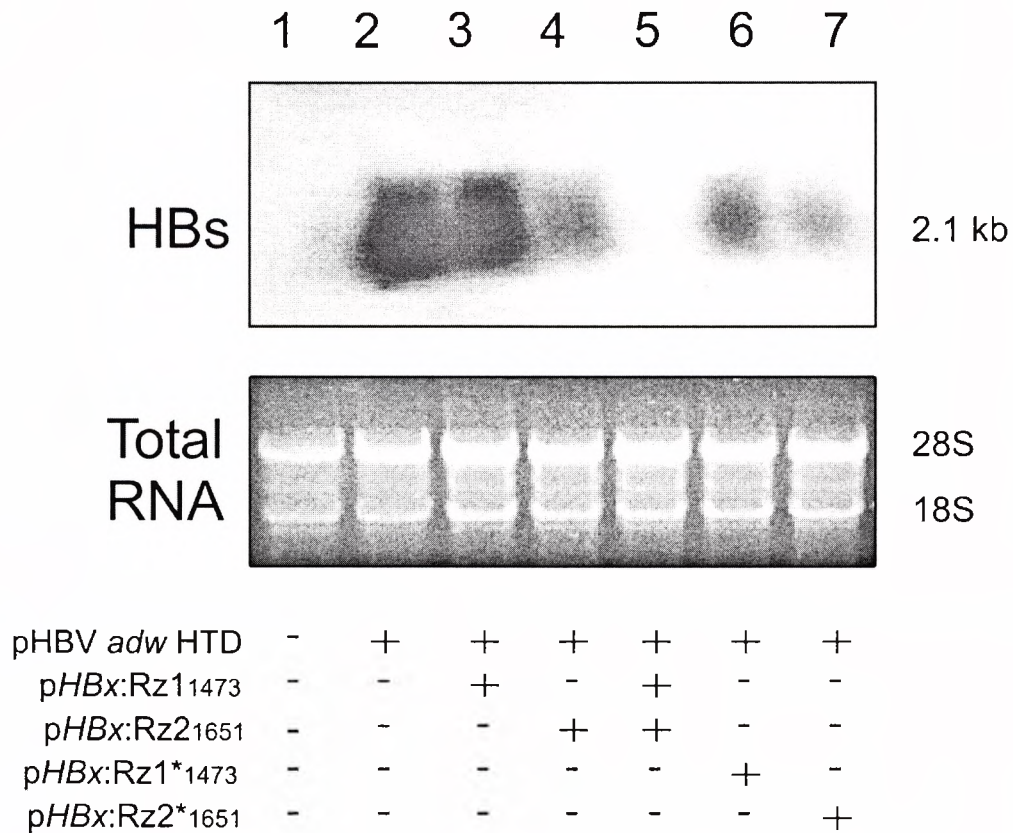


**Figure 3.2** Detection of HBV RNA from Huh7 cells co-transfected with ribozyme vectors and an HBV replication competent vector. Twenty micrograms of total cellular RNA was isolated from Huh7 cells, resolved electrophoretically and subjected to northern blotting with hybridisation to a HBV genomic probe. Cells had been untransfected (lane 1) and transfected with pCI neo GFP, pHBV *adw* HTD and either pCI neo (lane 2), *pHBx*:Rz1<sub>1473</sub> (lane 3), *pHBx*:Rz2<sub>1651</sub> (lane 4), *pHBx*:Rz1<sub>1473</sub> and *pHBx*:Rz2<sub>1651</sub> (lane 5), *pHBx*:Rz1\*<sub>1473</sub> (lane 6) or *pHBx*:Rz2\*<sub>1651</sub> (lane 7). A duplicate gel was stained with ethidium bromide to verify the presence of similar amounts of total cellular RNA on each lane. Equivalent transfection efficiencies were confirmed by detecting similar numbers of transfected cells labelled with green fluorescent protein in each culture plate.



*cis*-elements are the most active HBV transcriptional regulatory sequences (Schaller and Fischer, 1991a). Compared with *pHBx:Rz2*<sub>1651</sub>, *pHBx:Rz1*<sub>1473</sub> is less effective at decreasing the concentration of HBV RNA (Figure 3.2, lanes 3 and 4). This finding is consistent with a diminished effectiveness of *pHBx:Rz1*<sub>1473</sub> as a result of the altered base that is found at the target cleavage triplet of *pHBx:Rz1*<sub>1473</sub> in transcripts from pHBV *adw* HTD. Together, *pHBx:Rz1*<sub>1473</sub> and *pHBx:Rz2*<sub>1651</sub> decrease the detectable 2.1 kb mRNA to a concentration similar to that of the negative control (Figure 3.2, lane 5). Surprisingly, the catalytically inactive ribozymes were also found to decrease the concentration of HBV RNA in the transfected cells. However, this pronounced inhibitory effect was not a consistent observation and was not corroborated by the measurement of HBsAg and HBeAg secretion from transfected cells (see below). The inhibitory effects of *pHBx:Rz1*<sup>\*</sup><sub>1473</sub> and *pHBx:Rz2*<sup>\*</sup><sub>1651</sub> are likely to result from an antisense mechanism that destabilises HBV mRNA.

#### 3.4.3 **Measurements of HBsAg and HBeAg secretion in co-transfected Huh7 cells**

Since *HBx* is common to all HBV transcripts, *pHBx:Rz1*<sub>1473</sub> and *pHBx:Rz2*<sub>1651</sub> should therefore encode ribozymes that act on preC/pregenome, surface as well as *HBx* mRNAs (Figures 1.1, 2.2 and 3.1). As with cellular mRNA, the first ORF is translated most efficiently from HBV transcripts (Schaller and Fischer, 1991a). Translation initiated from the preC initiation codon of the preC/pregenome transcript generates a precursor protein that is modified by proteolysis and is secreted as the HBeAg. The HBsAg is translated from the surface ORF of the preS2/S transcripts. As well as being indicators of translation from preC/pregenome and preS2/S transcripts, HBeAg and HBsAg production are markers of HBV replication in HBV-infected individuals. Therefore the effects of *pHBx:Rz1*<sub>1473</sub> and *pHBx:Rz2*<sub>1651</sub>, as well as their catalytically inactive counterparts, *pHBx:Rz1*<sup>\*</sup><sub>1473</sub> and *pHBx:Rz2*<sup>\*</sup><sub>1651</sub>, on the secretion of HBeAg and HBsAg from transfected Huh7 cells were investigated (Figure 3.3). During a period of three days after transfection, *pHBx:Rz1*<sub>1473</sub> and *pHBx:Rz2*<sub>1651</sub> decreased the secretion of HBeAg and HBsAg into the culture supernatant.

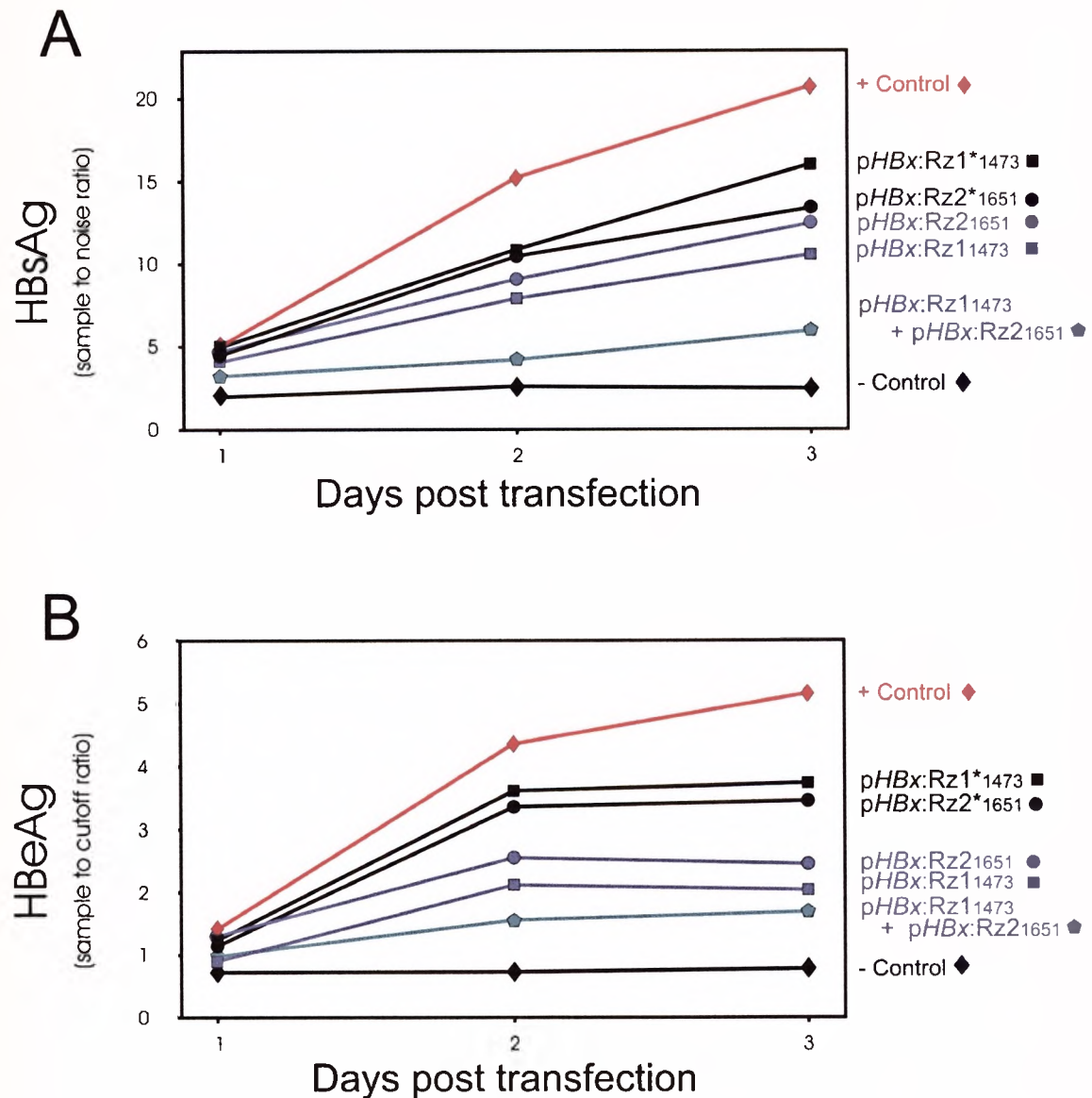


**Figure 3.3** Secretion of HBsAg and HBeAg into the culture supernatant after transfection of Huh7 cells. HBsAg (**A**) and HBeAg (**B**) concentrations in the culture supernatants were measured using the AxSYM immunoassay protocols each day and for three days. The mean ( $n = 3$ ) values of HBsAg and HBeAg were calculated as the sample to noise ratio (HBsAg) or sample to cutoff ratio (HBeAg) according to the supplier's instructions (SEM not shown). Huh7 cells were untransfected (- control) or transfected with pHBV *adw* HTD and pCI neo (+ control), pHBx:Rz1<sub>1473</sub>, pHBx:Rz2<sub>1651</sub>, pHBx:Rz1<sub>1473</sub> and pHBx:Rz2<sub>1651</sub>, pHBx:Rz1\*<sub>1473</sub> or pHBx:Rz2\*<sub>1651</sub>. Equivalent transfection efficiencies were confirmed in each culture plate by detecting similar numbers of cells labelled with green fluorescent protein.

*pHBx:Rz1*<sub>1473</sub> was slightly more effective than *pHBx:Rz2*<sub>1651</sub> despite the altered 5' GUC 3' cleavage motif in the *pHBV adw* HTD vector which renders *pHBx:Rz1*<sub>1473</sub> catalytically inactive (Figure 2.1). This observation confirms the results obtained using antisense RNAs and suggests that an antisense effect of these ribozyme sequences, without substrate cleavage, may be an important mechanism of their action (see section 2.4.4). In combination, the two ribozyme-encoding vectors further inhibited HBsAg and HBeAg secretion to a level that is only slightly higher than that of the negative control. Plasmids *pHBx:Rz1\**<sub>1473</sub> and *pHBx:Rz2\**<sub>1651</sub> exerted modest inhibitory effects on HBsAg and HBeAg secretion. Interestingly, *pHBx:Rz1*<sub>1473</sub> should not be capable of cleaving transcripts derived from *pHBV adw* HTD, yet its effects are diminished by the helix II mutations of *pHBx:Rz1\**<sub>1473</sub>. The reason for this may be a significantly altered secondary structure of *pHBx:Rz1\**<sub>1473</sub>. Helix II is a conserved sequence in hammerhead ribozymes, and mutations in this region are likely to compromise the availability of helix I and helix III sequences for binding to their complementary target bases. This would diminish antisense effects of the anti-HBx ribozymes that have helix II mutations. Taken together with section 3.4.2, the data suggest that the ribozyme sequences inhibit HBV gene expression. However, a dominant antisense effect that results from compromised helix II mutations cannot be excluded.

### **3.4.4 In situ detection of ribozyme activity in transfected Huh7 cells**

#### **3.4.4.1 Ribozyme modulation of EGFP marker gene expression**

The effect of ribozyme sequences on expression from pCH-EGFP was measured *in situ* by quantitation of fluorescent transfected cells expressing EGFP (Figures 3.4 and 3.5). The cells shown in Figure 3.4 are representative fluorescence microscope fields of co-transfections with combinations of pCH-EGFP and pCl neo, *pHBx:Rz1*<sub>1473</sub> or *pHBx:Rz1\**<sub>1473</sub>. The mean and SEM of the number of cells expressing EGFP were calculated at day three from triplicate experiments. The mean of the positive control (cells co-transfected with pCH-EGFP and pCl neo) was normalised to 100% and represents a figure of 972 fluorescent cells per culture dish (Figure 3.5B). The mean percentage of fluorescent cells was significantly decreased when *pHBx:Rz1*<sub>1473</sub> ( $25.5 \pm 5.3\%$ ,  $p < 0.01$ ) or *pHBx:Rz2*<sub>1651</sub> ( $13.3 \pm 3.4\%$ ,  $p < 0.01$ ) was co-transfected with pCH-EGFP.



Substitution of the catalytically inactive counterparts,  $pHBx:Rz1^{*}_{1473}$  or  $pHBx:Rz2^{*}_{1651}$ , resulted in a diminished inhibitory effect on expression of EGFP in transfected cells. Once again, the inhibition by the catalytically inactive vectors may be due to an antisense mechanism that involves hybridisation of helix I and helix III domains to complementary *HBx* sequences. The more marked effects of  $pHBx:Rz1_{1473}$  and  $pHBx:Rz2_{1651}$  suggest that the ribozymes encoded by these vectors operate by intracellular cleavage of the *HBx*-containing substrates. The effect of  $pHBx:Rz1_{1473}$  was more marked than that of  $pHBx:Rz2_{1651}$  and indicates a more favourable interaction between ribozyme and target sequence.

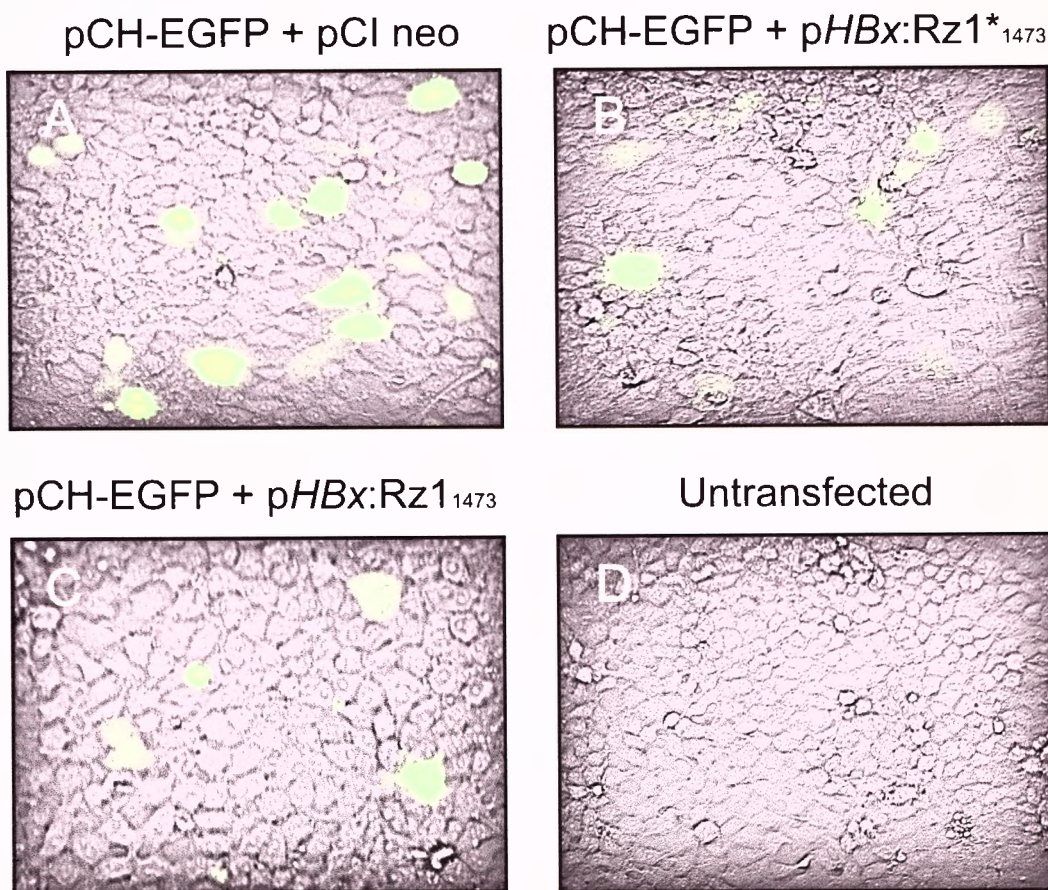


**Figure 3.4** Combined phase contrast and fluorescent microscopic field of Huh7 cells transfected with pCH-EGFP and either pCl neo (A),  $pHBx:Rz1^{*}_{1473}$  (B),  $pHBx:Rz1_{1473}$  (C) as well as untransfected cells (D).

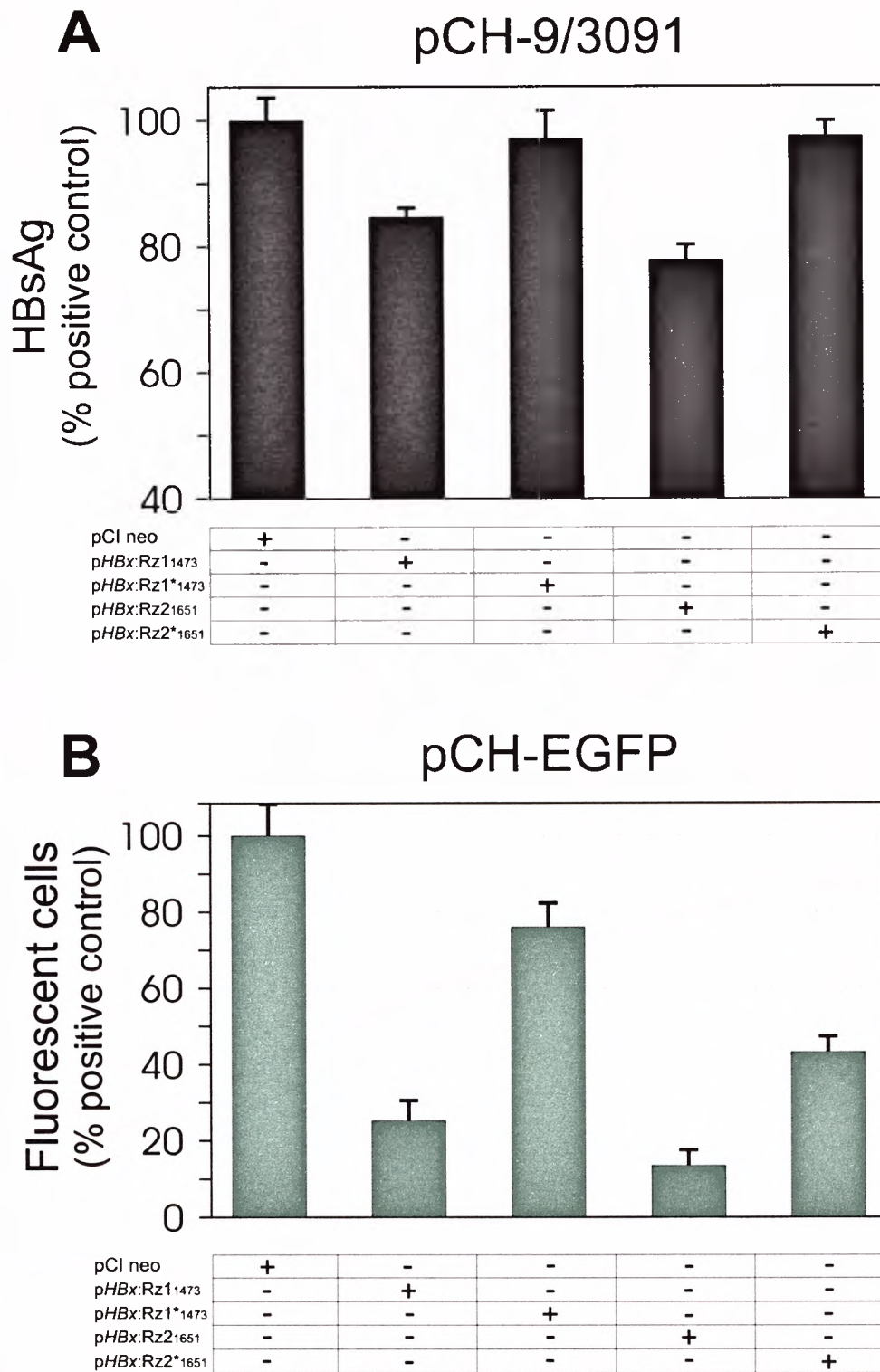


**Figure 3.5** Effect of ribozyme co-transfection on HBsAg production (**A**) and on the number of EGFP positive Huh7 cells (**B**). HBsAg measurements are given as a mean percentage of the positive control with SEM indicated. The plasmids used in the transfection are indicated below each column. The data are given as the mean sample to noise ratio from experiments performed in triplicate.



*Ribozyme effects detected in situ and HBsAg secretion measurements in co-transfected Huh7 cells*

HBsAg concentration in the culture supernatants was measured from cells transfected with pCH-9/3091 together with ribozyme (*pHBx:Rz1<sub>1473</sub>* and *pHBx:Rz2<sub>1651</sub>*) or control vectors (*pCI neo*, *pHBx:Rz1\*<sub>1473</sub>* and *pHBx:Rz2\*<sub>1651</sub>*). A vector constitutively expressing EGFP (*pCI neo GFP*), which is not susceptible to anti *HBx* ribozyme cleavage, was included to confirm equal transfection efficiencies in each of the culture plates. The mean and SEM were calculated from triplicate experiments and the results are depicted in Figures 3.5A and 3.6. In Figure 3.5B, the mean of the positive control has been normalised to 100% to enable comparison to the effects of *pHBx:Rz1<sub>1473</sub>* and *pHBx:Rz2<sub>1651</sub>* on HBsAg secretion. At day 3, HBsAg secretion is significantly lower in the culture plates transfected with *pHBx:Rz1<sub>1473</sub>* ( $84 \pm 2.1\%$ ,  $p < 0.01$ ) and *pHBx:Rz2<sub>1651</sub>* ( $78.3 \pm 2.8\%$ ,  $p < 0.01$ ) when compared to the positive control transfected with *pCI neo*

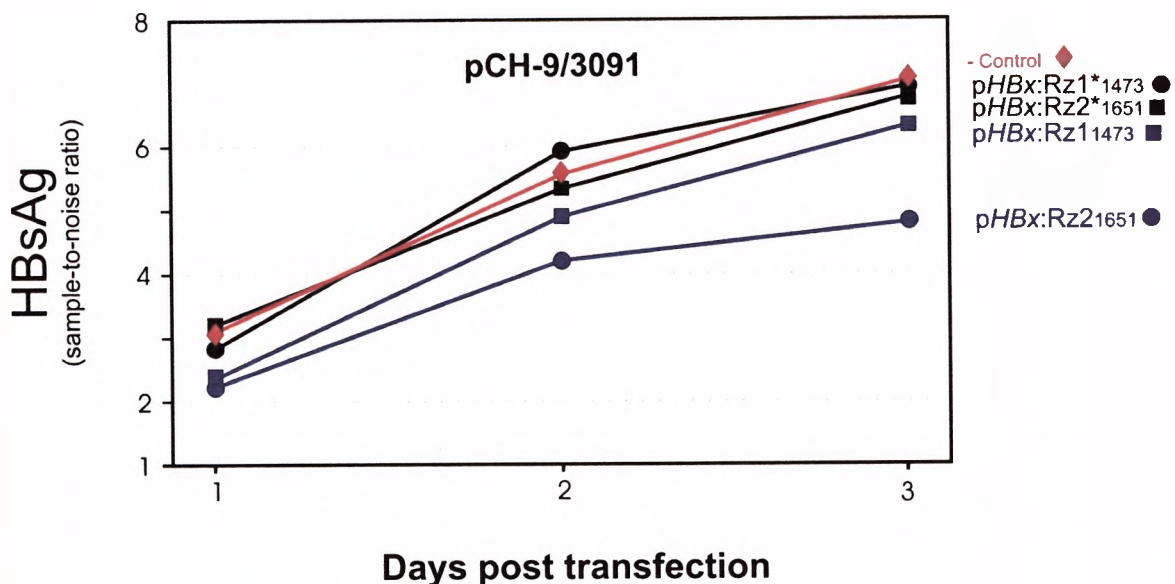


**Figure 3.6** Effect of ribozyme co-transfection on HBsAg production from plasmid pCH-9/3091. Three day time course of HBsAg secretion from transfected Huh7 cells. The data are given as the mean ( $n = 3$ ) sample to noise ratio from experiments performed in triplicate (SEM not shown).

and pCH-9/3091. Daily measurements of HBsAg secretion (Figure 3.6) confirm that the effects of the ribozyme and control vectors follow a similar trend with time. The inhibitory effect is lower in the catalytically inactive vectors and, as with the effect on EGFP expression, pHBx:Rz2<sub>1651</sub> inhibits HBsAg secretion more effectively than does pHBx:Rz1<sub>1473</sub>.

The inhibitory effect of the ribozymes on HBsAg secretion is less marked than on EGFP expression detected *in situ*. However, ribozyme-induced inhibition of HBsAg secretion is less pronounced than earlier results in section 3.4.3. The differences in HBsAg secretion may be a result of using the CMV promoter rather than endogenous HBV promoters to drive the expression of viral mRNA in the vector pCH-9/3091. The correlation between the effects of each of the ribozyme-encoding sequences on HBsAg secretion and EGFP expression demonstrate that *in situ* detection of EGFP expression using the vectors described is an index of HBV gene expression.

### 3.5 Discussion and conclusions

Ribozyme and antisense therapies, which are based on nucleic acid hybridisation, are potentially effective therapeutic agents for the treatment of chronic HBV infection. The selection of therapeutic and target HBV sequences can be determined by measuring efficiently the intracellular action of ribozymes. However, the development and discovery of novel treatment regimens for HBV, including the use of therapeutic hammerhead ribozymes, has been hindered by the lack of cell culture models of viral infection. Most hepatoma cells are not readily receptive to HBV infection. Although primary hepatocytes do respond well to being infected, these cells must remain in the differentiated state (Galle *et al.*, 1989). Since it has been technically difficult to culture primary hepatocytes that are receptive to HBV, alternative *in vitro* systems for the study of HBV replication, utilising continuous cell lines, have been developed. Human HCC cells are transfected with vectors encoding tandem repeats of the viral genome. Expression cassettes that generate greater-than-genome-length HBV RNA sequences result in transient or persistent HBV expression (Sells *et al.*, 1987; Tsurimoto *et al.*, 1987). In HBV-infected hepatocytes, cleavage of pgRNA would prevent the amplification of viral cccDNA. Nevertheless, HBV-encoding vectors,

---

which continuously produce viral pgRNA via foreign promoters or from a replicating plasmid template, represent artificial models of infection. Establishing a cell line capable of being infected by HBV remains important for the development of new therapeutic agents. Existing transfection-based cell culture models of viral infection do, however, offer valuable information regarding the principle and efficacy of new antiviral strategies.

The inhibition of HBV gene expression that was demonstrated in cell culture models of HBV infection is an indicator of promising efficacy of endogenously expressed hammerhead ribozymes *in vivo*. The approach used in this study has been to develop an assay for measuring the inhibitory effects of ribozymes targeted to the *HBx* ORF *in situ* in transfected cells. A modified HBV-derived plasmid, where the preS2/S region is replaced by DNA encoding EGFP, allowed for the *in situ* measurement of hammerhead ribozyme-mediated effects in transfected cells. Since the *HBx* ORF is present downstream of the EGFP coding region on three of the four major viral transcripts, the hammerhead ribozymes presented in this thesis probably inhibited all EGFP-expressing transcripts. Moreover, ribozyme-modulation of EGFP marker gene activity *in situ* was corroborated by measurements of viral HBsAg and HBeAg secretion generated by transfection with a replication-competent HBV vector. This *in situ* assay may thus be a useful marker of the antireplicative effects of ribozymes targeted to the *HBx* ORF. It should be noted that the results presented here reflect an indirect assessment of the inhibition of viral replication in cell culture by hammerhead ribozymes. Ideally, the antireplicative effects of these hammerhead ribozymes should be determined in cell culture systems that permit a complete HBV replication cycle such as, *inter alia*, primary tuapaia hepatocyte cultures and human HepaRG cells.

In conclusion, results presented in this study indicated that hammerhead ribozymes targeted to the *HBx* ORF of HBV were capable of significantly inhibiting viral gene expression and markers of viral replication in an intracellular environment. Once again catalytically inactive ribozymes were shown to be modestly effective in inhibiting viral gene expression and replication in cultured cells. Catalytically-defective ribozyme controls were designed specifically to negate the effects of ribozyme catalytic activity as a means of inactivation. However, since hammerhead ribozymes appear to function under single-turnover

---

conditions *in vivo*, these ribozyme-inactive variants may merely behave like competitive inhibitors and their effects may be largely indistinguishable from their catalytically active counterparts. In fact, the nucleases responsible for antisense effects *in vivo* may be as efficient as ribozyme-mediated endonuclease activity.

Taken on their own, the two ribozyme-expressing vectors do not sufficiently inhibit viral gene expression to the extent necessary for their therapeutic application. Before applying these ribozymes clinically, improvements are needed to increase their intracellular efficacy and specificity. Of particular interest is the fact that ribozyme vectors transfected together do have an additive effect. This suggests that the appropriate therapeutic approach is to target simultaneously more than one sequence using different ribozymes. This may have the dual effect of 1) increasing the intracellular ribozyme concentration, thus improving their efficacy; and 2) preventing the emergence of ribozyme-resistant viral mutants. There are numerous practical constraints that need to be addressed in order to successfully apply different ribozyme-encoding genes simultaneously. These are dealt with in the next chapter.

---

## 4.0 MULTIMERIC *CIS*- AND *TRANS*-ACTING HAMMERHEAD RIBOZYMES THAT TARGET THE HBV *HBx* OPEN READING FRAME

### 4.1 Summary

Vectors were generated to encode multiple hammerhead ribozyme units that simultaneously target three different sites on the *HBx* ORF. The rationale of this study was to improve the inhibitory effects of hammerhead ribozyme *in vivo* by increasing their intracellular concentration; and to prevent the emergence of ribozyme-resistant escape mutants. Each multimeric unit comprises a hammerhead ribozyme sequence flanked by an adjacent upstream complementary ribozyme target sequence and was designed to cleave intramolecularly (in *cis*) and produce 5'- and 3'-processed hammerhead ribozymes that are free to function in *trans*.

Transcripts containing 4-mer, 8-mer and 24-mer *cis*- and *trans*-cleaving ribozyme units efficiently cleaved in *cis* to produce individual processed hammerhead ribozyme monomers *in vitro* that were able to cleave efficiently target *HBx* RNA in *trans* in a site-specific manner. Expression vectors encoding multimeric hammerhead ribozymes were tested for their antireplicative potential in transfected cell culture models of HBV infection. The inhibition of HBsAg and HBeAg secretion was measured along with the inhibition of EGFP fluorescence *in situ*. Vectors expressing 8-mer multimeric *cis*- and *trans*-cleaving hammerhead ribozymes were more effective than their single-unit counterparts at reducing viral HBsAg and HBeAg levels. The 24-mer multimeric ribozyme expression vector, pCI-M24HBx:Rz1,2&3, containing 8-mer units of each of the three anti-HBx ribozymes, reduced EGFP fluorescence by  $\pm 92\%$  and viral antigen secretion by  $\pm 60\%$ . This suggests an additive inhibitory effect when each of the three different ribozymes is targeted simultaneously. Since the multimeric ribozymes are more effective than previously described ribozymes at inhibiting markers of viral replication in transfected cells, these therapeutic agents have a greater potential to be used for the treatment of chronic HBV infection.



## 4.2 Introduction

The data in previous chapters demonstrate that the *HBx* region of HBV is accessible to hammerhead ribozyme hybridisation. These hammerhead ribozymes were successfully applied to inhibit HBx function and suppress HBV gene expression and replication in cultured cells. To date, a number of nucleic acid hybridisation strategies targeting different regions of the virus have been applied *in vitro* and in cell culture investigations with varying success (Beck and Nassal, 1995; Feng *et al.*, 2001a; von Weizsäcker *et al.*, 1992; zu Putlitz *et al.*, 1999). However, within the scope of cell culture models of viral infection, limitations regarding the efficacy of hammerhead ribozymes have emerged that make these agents, as they presently stand, unsuitable for clinical application. Since hammerhead ribozymes behave similarly to antisense RNA *in vivo* (Birikh *et al.*, 1997b), approaches that are aimed at improving the intracellular inhibitory activity of hammerhead ribozymes remain an important medical objective. Since the hybridisation of ribozymes to their complementary target sequence is rate-limiting *in vivo*, hammerhead ribozyme-mediated inhibitory effects may be improved by generating a greater molar excess of ribozyme over target RNA. Moreover, as is evidenced by the data in Chapter 3, a combination of different ribozymes expressed simultaneously may improve their inhibitory efficacy *in vivo*.

Applying many ribozymes simultaneously may be advantageous in other ways. Mutations within the target RNA, especially within the hammerhead ribozyme cleavage triplet sequence, may prevent ribozyme-mediated cleavage, or less severely, affect the accurate hybridisation of ribozyme annealing arms with its target complementary sequence. There have been reports of ribozyme escape mutants generated for HIV-1 infections in cultured cells (Bertrand and Rossi, 1996; Dropulic *et al.*, 1992). Although HBV is far less mutable than HIV, it replicates using the error-prone reverse transcriptase (RT), which lacks a proof-reading function (Preston *et al.*, 1988). Thus, by targeting a single site for ribozyme-mediated cleavage, there exists the real possibility of generating HBV replication variants capable of evading the therapeutic action of ribozymes.

To overcome the problem posed by the mutability of HBV, several ribozymes can be applied to target simultaneously different sites on the HBV sequence. One approach is to use multiple hammerhead ribozyme units that are

---

joined together and expressed on the same transcript (Bai *et al.*, 2001; Chen *et al.*, 1992; Ramezani *et al.*, 1997). But, this method lends itself to steric hindrance between connected ribozymes (Ohkawa *et al.*, 1993a). Various groups have developed systems in which connected ribozymes on the same transcript are liberated through intramolecular ribozyme cleavage (*cis*-cleaving ribozymes) in order to generate *trans*-acting ribozymes (Ohkawa *et al.*, 1993a; Price *et al.*, 1995; Ruiz *et al.*, 1997). This is achieved by using separate *cis*-cleaving 'processing ribozymes', which flank the *trans*-acting ribozyme (Altschuler *et al.*, 1992; Ohkawa *et al.*, 1993a); or by introducing a ribozyme recognition sequence between connected ribozymes such that each ribozyme first cleaves in *cis* before cleaving in *trans* (Ruiz *et al.*, 1997). Since the same ribozyme can be copied many times, and multiple ribozymes can be connected together and expressed from a single transcript, these approaches have the advantage of increasing the intracellular ribozyme concentration.

This chapter describes the construction and application of eukaryotic expression cassettes that encode multiple *cis*- and *trans*-cleaving hammerhead ribozyme sequences. Transcripts expressed from a multimeric hammerhead ribozyme cassette were designed to consist of many ribozyme units bound head-to-tail. Each unit contains a ribozyme target recognition sequence and an upstream complementary ribozyme sequence. From within an expressed transcript, hammerhead ribozymes are theoretically capable of cleaving in *cis* (Figure 4.1A) to generate therapeutic *trans*-acting ribozymes with processed 5' and 3' ends (Figure 4.1B). The aim was to modify the two previously described ribozymes and to introduce a third hammerhead ribozyme targeted to a different site within the *HBx* ORF. Vectors were generated to include multiple copies of the three selected hammerhead ribozyme-encoding sequences (Figure 4.1C). These were tested to inhibit viral gene expression and markers of viral replication in cell culture models of HBV infection.

## 4.3 Materials and Methods

### 4.3.1 Plasmid vectors encoding multimeric ribozyme sequences

#### 4.3.1.1 Plasmids containing single *cis*- and *trans*-cleaving ribozyme units

The *M1HBx:Rz1*<sub>1473</sub>, *M1HBx:Rz2*<sub>1651</sub> and *M1HBx:Rz3*<sub>1607</sub> single-unit *cis*- and *trans*-cleaving hammerhead ribozyme sequences respectively encode the catalytic and annealing sequences of ribozymes *HBx:Rz1*<sub>1473</sub>, *HBx:Rz2*<sub>1651</sub> and *HBx:Rz3*<sub>1607</sub> as well as a downstream target sequence recognised by each ribozyme for *cis*-cleavage. For hammerhead ribozyme *M1HBx:Rz1*<sub>1473</sub>, 5' and 3' flanking arms represent hammerhead ribozyme helices I and III respectively and span regions 1466 to 1479 for internal *cis*-cleavage and regions 1461 to 1484 for *trans*-cleavage. Hammerhead ribozyme *M1HBx:Rz2*<sub>1651</sub> is complementary to HBV *ayw* co-ordinates 1644 to 1658 for *cis*-cleavage and co-ordinates 1639 to 1663 for *trans*-cleavage. Similarly, 5' and 3' flanking arms of *M1HBx:Rz3*<sub>1607</sub> span regions 1600 to 1613 for *cis*-cleavage and regions 1595 to 1618 for *trans*-cleavage (HBV *ayw* sequences: GenBank® accession number J02203) (see Figures 4.1 and 4.2).

With the exception of pBS-*M1HBx:Rz2*<sub>1651</sub>, the construction of each single-unit *cis*- and *trans*-cleaving multimeric ribozyme-encoding plasmid proceeded in two separate cloning operations, since mutant clones were often observed when annealing chemically synthesized fragments larger than 60 nt.

#### Plasmid pBS-*M1HBx:Rz2*<sub>1651</sub>

Two complementary 70-nucleotide oligodeoxynucleotides encoding sense and antisense sequences were synthesized by standard phosphoramidite chemistry using a DNA synthesizer (Ranson Hill, USA). The annealed, dsDNA fragment contains *Xba*I and *Spe*I cohesive ends and encodes a single unit *cis*- and *trans*-cleaving hammerhead ribozyme along with its respective downstream *cis*-cleavage recognition sequence and 5' GUC 3' cleavage site. Sense (S) and antisense (A) oligonucleotide sequences for the single *cis*- and *trans*-cleaving

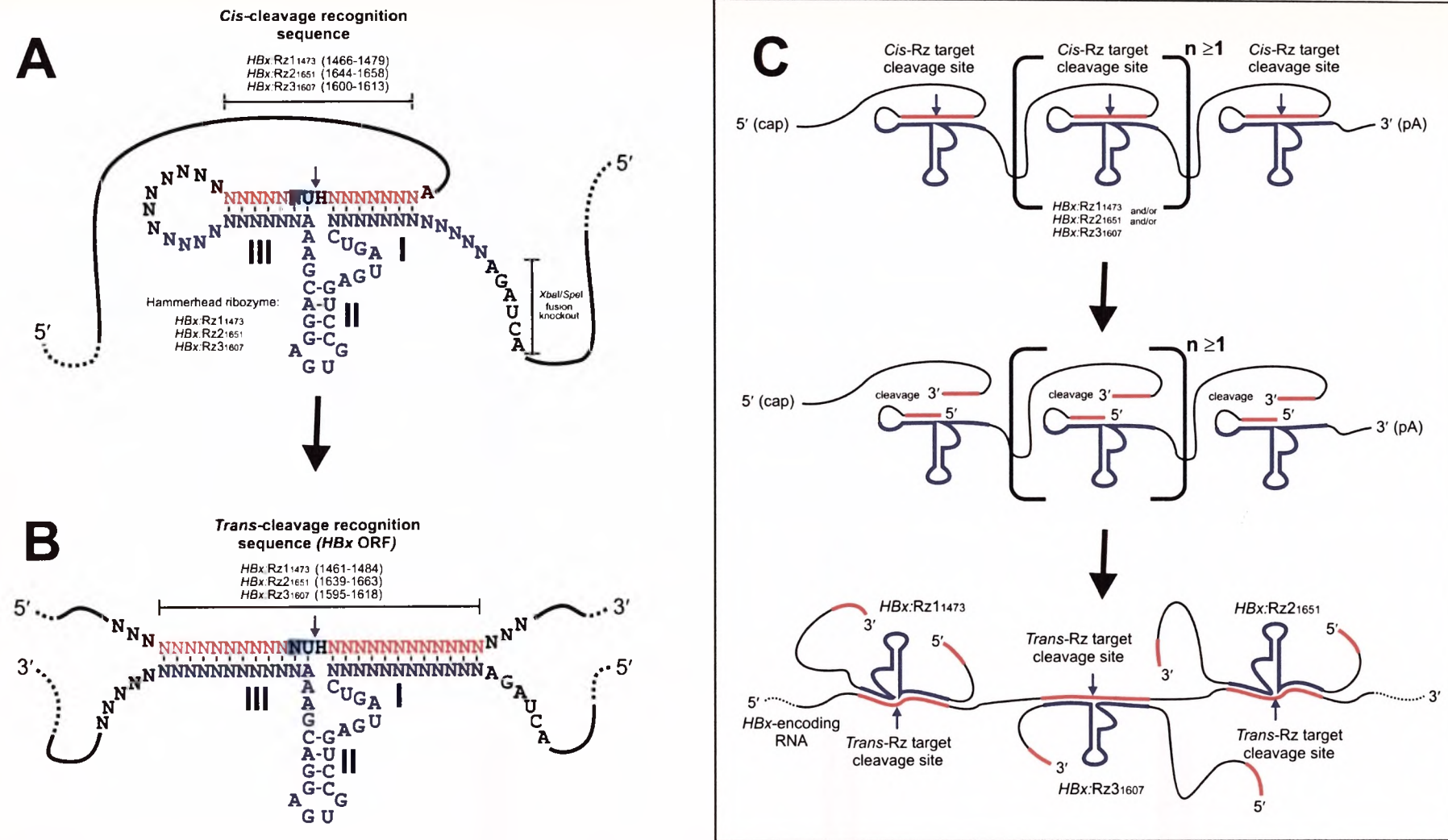
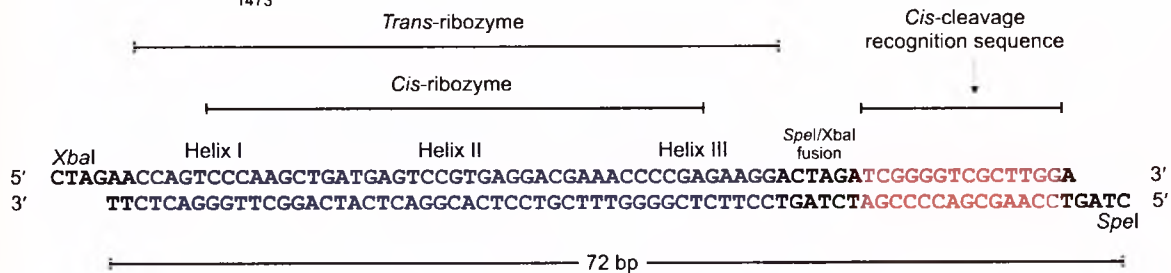


**Figure 4.1** The principle of multimeric hammerhead ribozyme *cis*- and *trans*-cleavage action. **A)** *Cis*-cleavage reaction showing both the *cis*-acting ribozyme sequence (blue) and its *cis*-recognition sequence (red) with a 5' NUH 3' cleavage triplet (shaded). **B)** Ribozyme *trans*-cleavage of *HBx*-encoding RNA (red). The lengths of helices I and III are longer for the *trans*-cleavage reaction. **C)** A precursor transcript comprising several *cis*- and *trans*-cleaving hammerhead ribozyme units. Single-unit ribozymes are released through internal *cis*-cleavage and retain their *trans*-cleaving function to cleave three sites within an *HBx*-encoded RNA sequence.

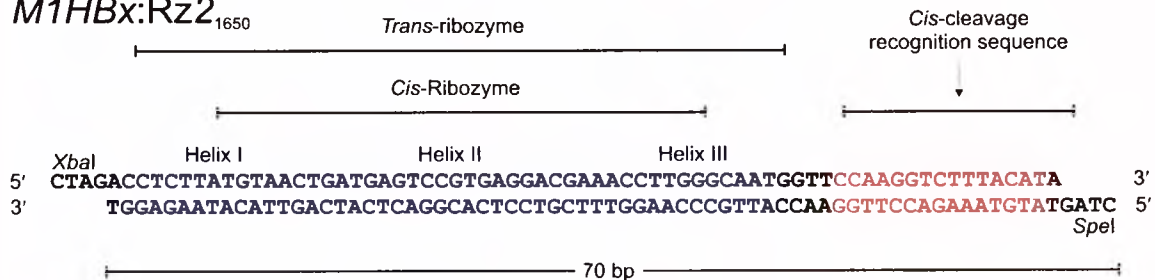


## Single-unit *cis*- and *trans*-cleaving hammerhead ribozyme-encoding oligonucleotide sequences

### M1HBx:Rz1<sub>1473</sub>



### M1HBx:Rz2<sub>1650</sub>



### M1HBx:Rz3<sub>1607</sub>

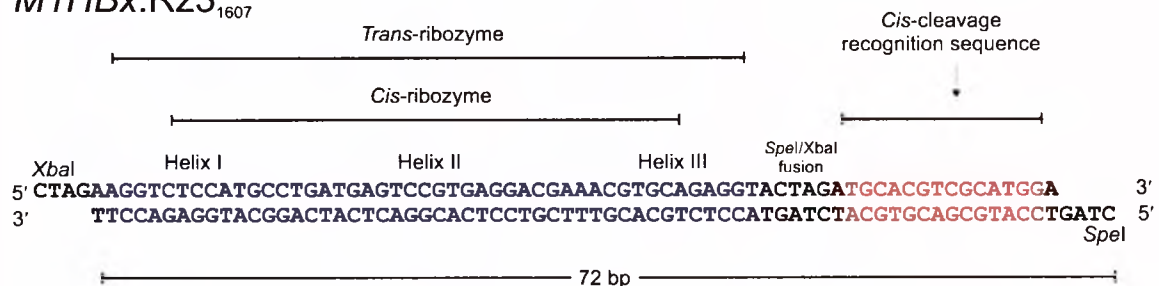


**Figure 4.2** Plus- and minus-strand sequences of a full-length *cis*- and *trans*-cleaving multimeric unit of ribozymes: *HBx*:Rz1<sub>1473</sub> and *HBx*:Rz2<sub>1651</sub> and *HBx*:Rz3<sub>1607</sub>. The restriction sites used for cloning into a pBluescript™ II KS(+) vector are depicted at both 5' and 3' ends. *Trans*- and *cis*-hybridisation arms (for helices I and III) are annotated and bases shown in blue. The sequence length for each *cis*-cleaving hammerhead ribozyme unit is shown. The construction of full-length single-units of *cis*- and *trans*-cleaving ribozymes *HBx*:Rz1<sub>1473</sub> and *HBx*:Rz3<sub>1607</sub> proceeded in a two step cloning operation. The *cis*- and *trans*-cleaving hammerhead ribozyme-encoding sequences were cloned separately from the ribozyme recognition sequence.



multimeric hammerhead ribozyme unit *M1HBx:Rz2<sub>1651</sub>* are represented in Table 4.1.

Complementary oligonucleotides *M1HBx:Rz2<sub>1651</sub> S* and *M1HBx:Rz2<sub>1651</sub> A* were annealed by heating an equimolar mixture (1.3 nmol of each oligonucleotide in 100 µl H<sub>2</sub>O) to 95°C for 5 minutes followed by gradual cooling to room temperature. Once cooled, samples were quantified spectrophotometrically at A<sub>260</sub> (Appendix A4-3) and brought to a final concentration of 30 pmol/µl.

**Table 4.1** Complementary oligonucleotides for single-unit *cis*-cleaving hammerhead ribozyme cassette *M1HBx:Rz2<sub>1651</sub>*

<b><i>M1HBx:Rz2<sub>1651</sub> S</i></b>	5' CTAGACCTCTTATGTAAGTGGTCCGTGAGGACGAAAC CTTGGGCAATGGTCCAAGGTCTTACATA 3'
<b><i>M1HBx:Rz2<sub>1651</sub> A</i></b>	5' CTAGTATGTAAGACCTTGAACCATTGCCCAAGGTTTCGTCCT CACGGACTCATCAGTTACATAAGAGGT 3'

*Xba*I and *Spe*I cohesive ends, which flank the 5' and 3' ends of the annealed fragments, were used to introduce the single-unit ribozyme cassette into the *Xba*I site of cloning vector pBSIIKS(+) to generate plasmid pBS-*M1HBx:Rz2<sub>1651</sub>*. Both *Xba*I and *Spe*I share compatible cohesive ends resulting in bi-directional insertion into an *Xba*I-linearised vector.

Plasmid pBSIIKS(+) was initially digested with *Xba*I and the linearised fragment was excised from a 1% agarose gel and eluted (Appendix A4). A ligation reaction containing a 150:1 fragment to vector molar ratio (30 pmol *M1HBx:Rz2<sub>1651</sub>* fragment insert to 0.158 pmol vector backbone) was conducted at room temperature for 1 hour in a 20 µl total volume that comprised 20 U T4 DNA ligase (New England Biolabs, MA, USA). A 10 µl volume was used to transform 100 µl of competent *E.coli* DH5α, which was plated on ampicillin positive, X-gal, IPTG positive, LB agar plates for α-complementation (Appendix B3-3). Clones were selected and screened by restriction enzyme digestion with *Xho*I and *Xba*I and compared to a 100 bp molecular weight ladder (Promega, WI, USA). Positive orientation candidate clones were then manually sequenced to determine their sequence fidelity (Appendix A5-2).

Plasmids pBS-*M1HBx*:Rz1<sub>1473</sub> and pBS-*M1HBx*:Rz3<sub>1607</sub>

Plasmids pBS-*M1HBx*:Rz1<sub>1473</sub> and pBS-*M1HBx*:Rz3<sub>1607</sub>, each were derived from vectors that contained 'short' and 'long' segments of the complete *cis*- and *trans*-cleaving unit. The pBSIIKS(+)-derived plasmids, pBS-*M1<sub>L</sub>HBx*:Rz1<sub>1473</sub> and pBS-*M1<sub>L</sub>HBx*:Rz3<sub>1607</sub>, encoded the 'long' *HBx*:Rz1<sub>1473</sub> and *HBx*:Rz3<sub>1607</sub> *cis*- and *trans*-cleaving hammerhead ribozyme sequence inserts respectively. Similarly, plasmids pBS-*M1<sub>S</sub>HBx*:Rz1<sub>1473</sub> and pBS-*M1<sub>S</sub>HBx*:Rz3<sub>1607</sub> encoded the 'short' complementary *cis*- target recognition sequence of *HBx*:Rz1<sub>1473</sub> and *HBx*:Rz3<sub>1607</sub> respectively (for a schematic illustration of the cloning, see Appendix C1-1).

Two sets of complementary 28-nt oligonucleotides encoding a 'short' ribozyme target sequence for *HBx*:Rz1<sub>1473</sub> and *HBx*:Rz3<sub>1607</sub> were synthesized. The complementary oligonucleotide sets are designated: *M1<sub>S</sub>HBx*:Rz1<sub>1473</sub> S and *M1<sub>S</sub>HBx*:Rz1<sub>1473</sub> A; and *M1<sub>S</sub>HBx*:Rz3<sub>1607</sub> S and *M1<sub>S</sub>HBx*:Rz3<sub>1607</sub> A (see Table 4.2). Similarly, two sets of complementary 52-nt oligonucleotides encoding the 'long' hammerhead ribozyme region for *HBx*:Rz1<sub>1473</sub> and *HBx*:Rz3<sub>1607</sub> were synthesized. The complementary oligonucleotide pairs are designated: *M1<sub>L</sub>HBx*:Rz1<sub>1473</sub> S and *M1<sub>L</sub>HBx*:Rz1<sub>1473</sub> A; and *M1<sub>L</sub>HBx*:Rz3<sub>1607</sub> S and *M1<sub>L</sub>HBx*:Rz3<sub>1607</sub> A (see Table 4.2). Sequences for both *M1<sub>L</sub>* and *M1<sub>S</sub>* complementary oligonucleotide pairs are represented in Table 4.2.

*Xba*I and *Spe*I restriction sites flank each end of both annealed oligonucleotides sets allowing for their introduction into the cloning vector pBSIIKS(+). Annealed dsDNA fragments *M1<sub>S</sub>HBx*:Rz1<sub>1473</sub> and *M1<sub>S</sub>HBx*:Rz3<sub>1607</sub> were cloned into the *Spe*I site of pBSIIKS(+), whilst fragments *M1<sub>L</sub>HBx*:Rz1<sub>1473</sub> and *M1<sub>L</sub>HBx*:Rz3<sub>1607</sub> were cloned into *Xba*I site of pBSIIKS(+). The construction of vectors pBS-*M1<sub>L</sub>HBx*:Rz1<sub>1473</sub>, pBS-*M1<sub>L</sub>HBx*:Rz3<sub>1607</sub> and pBS-*M1<sub>S</sub>HBx*:Rz1<sub>1473</sub>, pBS-*M1<sub>S</sub>HBx*:Rz3<sub>1607</sub> follows the same method as the construction of pBS-*M1HBx*:Rz2<sub>1651</sub>, as mentioned above. Clones were screened for the correct insert by digestion with *Xho*I and *Xba*I and resolved along with 37 pmol of annealed fragments *M1<sub>S</sub>HBx*:Rz1<sub>1473</sub> and *M1<sub>L</sub>HBx*:Rz1<sub>1473</sub> on a 8% non-denaturing polyacrylamide electrophoretic gel for approximately 1 hour at 100 V. Candidate positive orientation clones were, as mentioned previously, sequenced manually to determine the sequence fidelity (Appendix A5-2).

**Table 4.2** Complementary oligonucleotide sequences for 'long' and 'short' multimeric hammerhead ribozyme units of both *HBx:Rz1<sub>1473</sub>* and *HBx:Rz3<sub>1607</sub>*

<b><i>M1<sub>S</sub>HBx:Rz1<sub>1473</sub> S</i></b>	5' CTAGATCGGGGTCGCTTGGACTAGTCCA 3'
<b><i>M1<sub>S</sub>HBx:Rz1<sub>1473</sub> A</i></b>	5' CTAGTGGACTAGTCCAAGCGACCCCGAT 3'
<b><i>M1<sub>L</sub>HBx:Rz1<sub>1473</sub> S</i></b>	5' CTAGAAGAGTCCCAAGCCTGATGAGTCCGTGAGGACGAAA CCCCGAGAAGGA 3'
<b><i>M1<sub>L</sub>HBx:Rz1<sub>1473</sub> A</i></b>	5' CTAGTCCTTCTCGGGGTTTCGTCCTCACGGACTCATCAGGC TTGGGACTCTT 3'
<b><i>M1<sub>S</sub>HBx:Rz3<sub>1607</sub> S</i></b>	5' CTAGATGCACGTTCGCATGGACTAGTCCA 3'
<b><i>M1<sub>S</sub>HBx:Rz3<sub>1607</sub> A</i></b>	5' CTAGTGGACTAGTCCATGCGACGTGCAT 3'
<b><i>M1<sub>L</sub>HBx:Rz3<sub>1607</sub> S</i></b>	5' CTAGATGGTCTCCATGCCTGATGAGTCCGTGAGGACGAAA CGTGACAGAGGTA3'
<b><i>M1<sub>L</sub>HBx:Rz3<sub>1607</sub> A</i></b>	5' CTAGTACCTCTGCACGTTTCGTCCTCACGGACTCATCAGG CATGGAGACCTT 3'

An additional *SpeI* digestion site was present in both *M1<sub>S</sub>* annealed fragments due to an oversight in the original design of the annealed oligonucleotides. To remove the 8 bp sequence from pBS-*M1<sub>S</sub>HBx:Rz1<sub>1473</sub>* and pBS-*M1<sub>S</sub>HBx:Rz3<sub>1607</sub>*, plasmids were digested with *SpeI*, heat inactivated at 65°C for 30 minutes, and allowed to re-ligate for 20 minutes at room temperature. Transformed colonies were again screened and manually sequenced (Appendix A5-2). The resulting shortened (or truncated) plasmids were named pBS-*M1<sub>ST</sub>HBx:Rz1<sub>1473</sub>* and pBS-*M1<sub>ST</sub>HBx:Rz3<sub>1607</sub>* respectively. Both these plasmids were constructed from a correct-orientation fusion of fragments containing the ribozyme catalytic domain (*M1<sub>L</sub>*) and its corresponding downstream target sequence. The construction of these vectors is illustrated in Appendix C1-1. To generate pBS-*M1<sub>H</sub>HBx:Rz1<sub>1473</sub>* and pBS-*M1<sub>H</sub>HBx:Rz3<sub>1607</sub>* containing complete single unit self-cleaving hammerhead ribozyme cassettes, plasmids pBS-

*M1<sub>ST</sub>HBx*:Rz1<sub>1473</sub> and pBS-*M1<sub>ST</sub>HBx*:Rz3<sub>1607</sub> were digested with *ScaI* and *XbaI* to produce two fragments\* of 1863 and 1112 bp. The 1863 bp fragments contain the target-encoding sequence of both ribozyme *M1<sub>ST</sub>HBx*:Rz1<sub>1473</sub> and *M1<sub>ST</sub>HBx*:Rz3<sub>1607</sub>. Each fragment was eluted from a 1% agarose gel and purified. Plasmids pBS-*M1<sub>L</sub>HBx*:Rz1<sub>1473</sub> and pBS-*M1<sub>L</sub>HBx*:Rz3<sub>1607</sub> were digested with *ScaI* and *SpeI* resulting in two fragments of sizes 1170 and 1843 bp. The 1170 bp fragment containing the hammerhead ribozyme-encoding sequence for both ribozyme *M1<sub>L</sub>HBx*:Rz1<sub>1473</sub> and *M1<sub>L</sub>HBx*:Rz3<sub>1607</sub> was similarly eluted and purified. *M1<sub>ST</sub>* and *M1<sub>L</sub>* fragments were ligated in a 20 µl reaction mixture containing an equimolar ratio of both fragments (2 µg of each fragment). Following ligation at room temperature for an hour, 10 µl of the ligation mixture was used to transform competent *E.coli* DH5α, which were plated on ampicillin positive LB agar plates. Clones were screened by *SpeI* and *XbaI* digestion followed by agarose gel electrophoresis.

#### 4.3.1.2 Multimeric cis- and trans-cleaving hammerhead ribozymes

The construction of multimeric *cis*- and *trans*-cleaving hammerhead ribozymes is illustrated in Appendix C1-2. Plasmids pBS-*M1HBx*:Rz1<sub>1473</sub>, pBS-*M1HBx*:Rz2<sub>1651</sub> and pBS-*M1HBx*:Rz3<sub>1607</sub> were each placed into two separate reaction mixtures. *XbaI* and *ScaI* restriction enzymes were used in the first reaction to yield two fragments of 1112 and 1921 bp for pBS-*M1HBx*:Rz1<sub>1473</sub> and pBS-*M1HBx*:Rz3<sub>1607</sub> respectively (1112 and 1919 bp for pBS-*M1HBx*:Rz2<sub>1651</sub>) (See Table 4.3). *SpeI* and *ScaI* restriction enzymes were used in second reaction to yield fragments of 1190 and 1843 bp for pBS-*M1HBx*:Rz1<sub>1473</sub> and pBS-*M1HBx*:Rz3<sub>1607</sub> respectively (1188 and 1843 bp for pBS-*M1HBx*:Rz2<sub>1651</sub>). Fragment 1190 bp (1186 bp) from the *SpeI*/*ScaI* digest and fragment 1921 bp (1919 bp) from the *XbaI*/*ScaI* digest were eluted from a 1% agarose gel. Each eluted fragment contains a single multimeric hammerhead ribozyme unit. Two micrograms of both eluted fragments (for pBS-*M1HBx*:Rz1<sub>1473</sub>, pBS-*M1HBx*:Rz2<sub>1651</sub> and pBS-*M1HBx*:Rz3<sub>1607</sub>

---

\* Initially, pBS-*M1<sub>ST</sub>HBx*:Rz1<sub>1473</sub> would not digest with *XbaI* due to unexpected methylation of the *XbaI* site following the excision of a 8 bp *SpeI* fragment. The plasmid was then transformed into a DNA adenine methylase negative (*dam*<sup>-</sup>) *E.coli* strain that restored the integrity of the *XbaI* site. Competent *E.coli* GM2929 were transformed with pBS-*M1<sub>ST</sub>HBx*:Rz1<sub>1473</sub> resulting in successful cleavage by *XbaI* following plasmid preparation.

---

respectively) were ligated in a 20  $\mu$ l reaction volume. Following ligation at room temperature for an hour, 10  $\mu$ l of the ligation mixture was used to transform competent *E.coli* DH5 $\alpha$ , which was plated on ampicillin positive LB agar plates. Ten colonies from each plate were grown overnight followed by miniprep plasmid preparation (described in Appendix A2-1). Clones were screened by digestion with *SpeI* and *XbaI* and resolved on 2% agarose gels. Positive clones containing two multimeric *cis*- and *trans*-cleaving ribozyme units (dimer or 2-mer) were named pBS-M2HBx:Rz1<sub>1473</sub>, pBS-M2HBx:Rz2<sub>1651</sub> and pBS-M2HBx:Rz3<sub>1607</sub> respectively. These dimer-containing vectors were again manually sequenced (Appendix A5-2). The same cloning strategy\* was employed to construct plasmids bearing tetramer (4-mer) and octomer (8-mer) multimeric *cis*- and *trans*-cleaving hammerhead ribozyme units. The 4-mer constructs were named pBS-M4HBx:Rz1<sub>1473</sub>, pBS-M4HBx:Rz2<sub>1651</sub> and pBS-M4HBx:Rz3<sub>1607</sub> while the 8-mer constructs were named pBS-M8HBx:Rz1<sub>1473</sub>, pBS-M8HBx:Rz2<sub>1651</sub> and pBS-M8HBx:Rz3<sub>1607</sub>. A 16-mer construct, pBS-M16:Rz1,Rz2, containing 8-mer units of both hammerhead ribozymes HBx:Rz1<sub>1473</sub> and HBx:Rz2<sub>1651</sub> was similarly constructed using the enzyme combinations *XbaI/XhoI* and *SpeI/XhoI* on plasmids pBS-M8HBx:Rz1<sub>1473</sub> and pBS-M8HBx:Rz2<sub>1651</sub> respectively. Employing the same strategy, pBS-M24:Rz1,Rz2,Rz3, a 24-mer construct containing 8-mer units of hammerhead ribozymes HBx:Rz1<sub>1473</sub>, HBx:Rz2<sub>1651</sub> and HBx:Rz3<sub>1607</sub> was constructed by combining the 8-mer fragment of plasmid pBS-M8HBx:Rz3<sub>1607</sub> with the 16-mer fragment of pBS-M16:Rz1,Rz2. (Table 4.3 and Appendix C1-2).

#### 4.3.1.3 Eukaryotic expression vectors producing multi-unit *cis*- and *trans*-cleaving ribozymes

Expression vectors pCI-M8HBx:Rz1<sub>1473</sub>, pCI-M8HBx:Rz2<sub>1651</sub> and pCI-M8HBx:Rz3<sub>1607</sub> were constructed containing 8-mer *cis*- and *trans*-cleaving ribozyme units for hammerhead ribozymes HBx:Rz1<sub>1473</sub>, HBx:Rz2<sub>1651</sub> and

---

\* This cloning technique exploits the fact that fragments produced by digestion with *SpeI* and *XbaI* generate compatible cohesive ends. However, after ligation only *XbaI/XbaI* or *SpeI/SpeI* ligations, and not *XbaI/SpeI* or *SpeI/XbaI* ligations are re-cleaved by either enzyme. This facilitates cloning and screening of multiple fragments in succession since only head-to-tail tandems generate correct fragments upon double-digestion with *XbaI* and *SpeI*.

---



Table 4.3 pBSIIKS(+)-derived multimeric *cis*- and *trans*-cleaving hammerhead ribozyme vectors

Starting plasmids	Enzymes	Fragment sizes produced(bp) <sup>a</sup>	Fragments eluted and ligated (bp)	Resulting plasmid constructs
pBS-M1 <sub>ST</sub> HBx:Rz1 <sub>1473</sub>	<i>Xba</i> I, <i>Scal</i>	1112, 1863	1863	pBS-M1HBx:Rz1 <sub>1473</sub>
pBS-M1 <sub>L</sub> HBx:Rz1 <sub>1473</sub>	<i>Spe</i> I, <i>Scal</i>	1170, 1843	1170	
pBS-M1 <sub>ST</sub> HBx:Rz3 <sub>1607</sub>	<i>Xba</i> I, <i>Scal</i>	1112, 1863	1863	pBS-M1HBx:Rz3 <sub>1607</sub>
pBS-M1 <sub>L</sub> HBx:Rz3 <sub>1607</sub>	<i>Spe</i> I, <i>Scal</i>	1170, 1843	1170	
pBS-M1HBx:Rz1 <sub>1473</sub>	<i>Xba</i> I, <i>Scal</i>	1112, 1921	1921	pBS-M2HBx:Rz1 <sub>1473</sub>
	<i>Spe</i> I, <i>Scal</i>	1190, 1843	1190	
pBS-M1HBx:Rz2 <sub>1651</sub>	<i>Xba</i> I, <i>Scal</i>	1112, 1919	1919	pBS-M2HBx:Rz2 <sub>1651</sub>
	<i>Spe</i> I, <i>Scal</i>	1188, 1843	1188	
pBS-M1HBx:Rz3 <sub>1607</sub>	<i>Xba</i> I, <i>Scal</i>	1112, 1921	1921	pBS-M2HBx:Rz3 <sub>1607</sub>
	<i>Spe</i> I, <i>Scal</i>	1190, 1843	1190	
pBS-M2HBx:Rz1 <sub>1473</sub>	<i>Xba</i> I, <i>Scal</i>	1112, 1999	1999	pBS-M4HBx:Rz1 <sub>1473</sub>
	<i>Spe</i> I, <i>Scal</i>	1268, 1843	1268	
pBS-M2HBx:Rz2 <sub>1651</sub>	<i>Xba</i> I, <i>Scal</i>	1112, 1995	1995	pBS-M4HBx:Rz2 <sub>1651</sub>
	<i>Spe</i> I, <i>Scal</i>	1263, 1843	1264	
pBS-M2HBx:Rz3 <sub>1607</sub>	<i>Xba</i> I, <i>Scal</i>	1112, 1999	1999	pBS-M4HBx:Rz3 <sub>1607</sub>
	<i>Spe</i> I, <i>Scal</i>	1268, 1843	1268	
pBS-M4HBx:Rz1 <sub>1473</sub>	<i>Xba</i> I, <i>Scal</i>	1112, 2155	2155	pBS-M8HBx:Rz1 <sub>1473</sub>
	<i>Spe</i> I, <i>Scal</i>	1424, 1843	1424	
pBS-M4HBx:Rz2 <sub>1651</sub>	<i>Xba</i> I, <i>Scal</i>	1112, 2147	2147	pBS-M8HBx:Rz2 <sub>1651</sub>
	<i>Spe</i> I, <i>Scal</i>	1416, 1843	1416	
pBS-M4HBx:Rz3 <sub>1607</sub>	<i>Xba</i> I, <i>Scal</i>	1112, 2155	2155	pBS-M8HBx:Rz3 <sub>1607</sub>
	<i>Spe</i> I, <i>Scal</i>	1424, 1843	1424	
pBS-M8HBx:Rz1 <sub>1473</sub>	<i>Spe</i> I, <i>Xho</i> I	56, 3523	3523	pBS-M16:Rz1,Rz2
pBS-M8HBx:Rz2 <sub>1651</sub>	<i>Xba</i> I, <i>Xho</i> I	664, 2899	664	
pBS-M8HBx:Rz3 <sub>1607</sub>	<i>Spe</i> I, <i>Xho</i> I	56, 3523	3523	pBS-M24:Rz1,Rz2,Rz3
pBS-M16:Rz1,Rz2	<i>Xba</i> I, <i>Xho</i> I	1288, 2899	1288	

<sup>a</sup>Fragments selected for cloning are shown in italics.

*HBx:Rz3*<sub>1607</sub> respectively (Figure 4.3). A mammalian expression vector containing 24-mer (8-mer of each ribozyme), *cis*- and *trans*-cleaving units for ribozymes *HBx:Rz1*<sub>1473</sub>, *HBx:Rz2*<sub>1651</sub> and *HBx:Rz3*<sub>1607</sub> was also constructed. Plasmids pBS-*M8HBx:Rz1*<sub>1473</sub>, pBS-*M8HBx:Rz2*<sub>1651</sub>, pBS-*M8HBx:Rz3*<sub>1607</sub>, and pBS-*M24HBx:Rz1,Rz2,Rz3* were digested with *Xho*I and *Xba*I. Fragment inserts were separated from vector backbone by elution from a 1% agarose gel (Appendix A4). pCI neo was digested with *Nhe*I and *Xho*I yielding a large vector backbone which was similarly eluted from a 1% agarose gel. A ligation reaction containing a 50:1 annealed fragment to vector molar ratio (30 pmol annealed fragment insert to 0.6 pmol vector backbone) was conducted. Following transformation, overnight growth and plasmid purification (Appendix A2-1), correct plasmid clones were identified by digestion with *Bgl*II and *Spe*I.

### 4.3.2 In vitro transcription and and ribozyme cleavage

#### 4.3.2.1 Preparation of transcription template

pBSIIKS(+)-derived *cis*- and *trans*-cleaving multimeric ribozyme plasmids carrying 1-mer, 2-mer, 4-mer and 8-mer units for ribozymes *HBx:Rz1*<sub>1473</sub>, *HBx:Rz2*<sub>1651</sub> and *HBx:Rz3*<sub>1607</sub> were linearised by digestion with *Pst*I. Single-unit vectors pBS-*M1<sub>L</sub>HBx:Rz1*<sub>1473</sub> and pBS-*M1<sub>L</sub>HBx:Rz3*<sub>1607</sub>, as well as multimeric *cis*- and *trans*-cleaving vectors pBS-*M16HBx:Rz1,Rz2* and pBS-*M24Rz1,Rz2,Rz3* were also linearised with *Pst*I. To generate control antisense transcripts, the above plasmids were also separately linearised by digestion with *Xba*I. Linearised DNA templates were then eluted from a 1% agarose gel and extracted using chloroform/phenol and precipitated with ethanol (Appendix A4-1, A4-2). Pellets were resuspended in H<sub>2</sub>O to a final concentration of 1 µg/µl.

#### 4.3.2.2 Multimeric ribozyme cis-cleavage

Radiolabelled *cis*-cleaving RNA was transcribed at 37°C for 1 hour in a 20 µl reaction mixture containing 2 µg of template DNA, 10 mM dithiothreitol, 40 mM Tris-HCl (pH 8.0), 8 mM MgCl<sub>2</sub>, 2 mM spermidine, 20 U RNasin (Promega, WI, USA), 8 mM ATP, 8 mM TTP, 8 mM UTP, 12.5 µM GTP (Roche, Germany) and

## Multimeric ribozyme cassette design

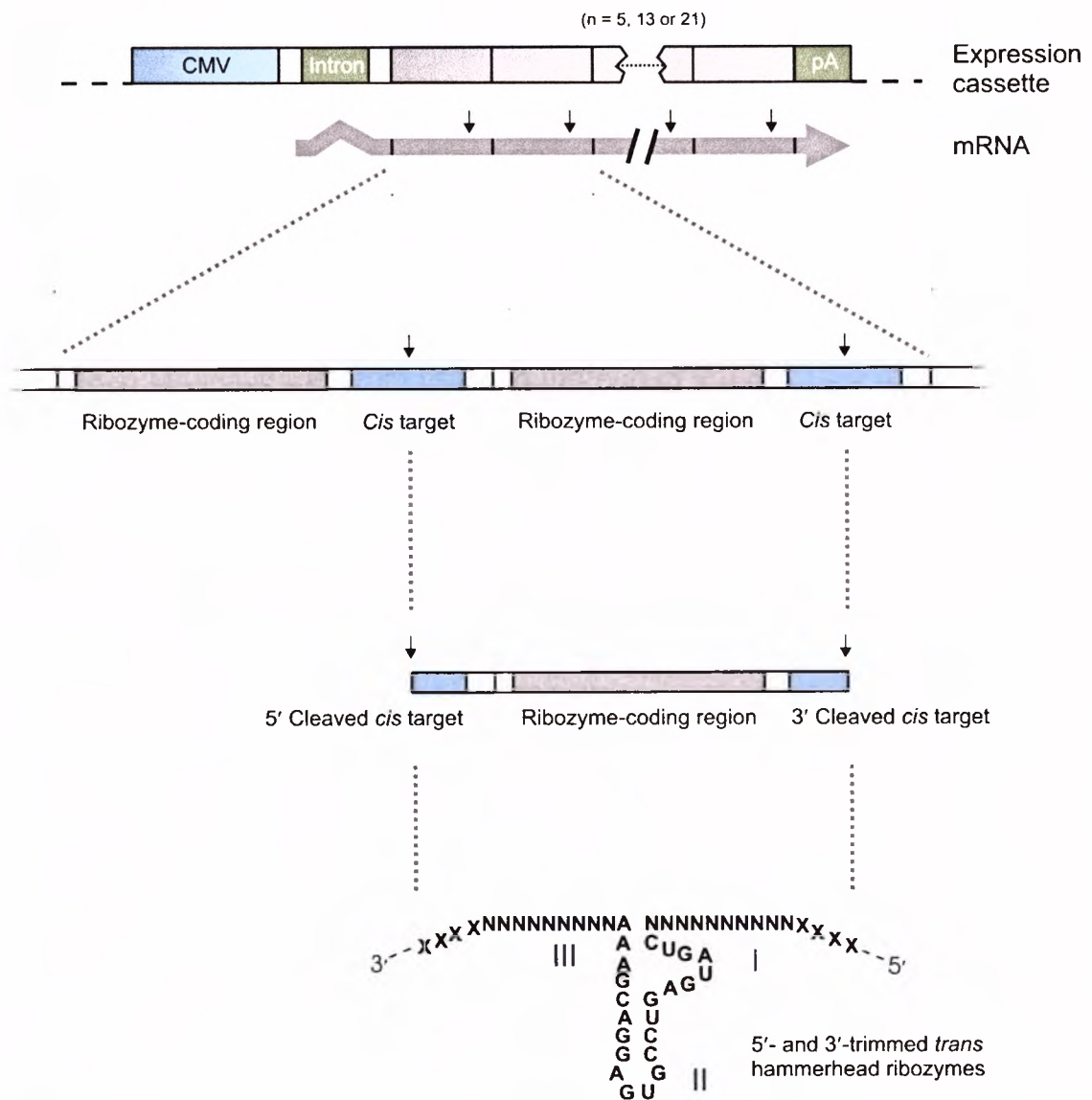


**Figure 4.3** A schematic illustration of the general structure of a multimeric *cis*- and *trans*-cleaving hammerhead ribozyme expression cassette. Transcript sequences encoding multiple ribozymes are under transcriptional control of the CMV promoter/enhancer. The expressed transcript cleaves in *cis* to release 5' and 3'-trimmed monomeric *trans*-cleaving hammerhead ribozymes. The hammerhead ribozyme sequence is displayed. N refers to any base, which forms part of the annealing helices I and III, while X refers to non-annealing bases. The conserved bases of helix II are shown.

20  $\mu\text{Ci}$  of  $\alpha\text{-}^{32}\text{P}$  GTP (3000 Ci/mmol; NEN du Pont, USA) and 20 U of T7 RNA Polymerase (Promega, WI, USA). 20 U of DNase I (Promega, WI, USA) were added to the reaction mixture for 10 minutes at 37°C. RNA fragments were purified using the Qiagen RNeasy (Qiagen, CA, USA) RNA purification kit according to the manufacturer's instructions. The cleavage reaction was carried out in a 40  $\mu\text{l}$  reaction mixture containing radiolabelled *cis*-cleaving multiribozyme transcript RNA. The mixture contained 20 mM  $\text{MgCl}_2$  and 50 mM Tris-Cl (pH 8.0), and was incubated at 37°C. Aliquots (10  $\mu\text{l}$ ) were removed after incubation for 0, 5 and 60 minutes and added to 3  $\mu\text{l}$  of RNA loading buffer (Appendix B2-3). Samples were resolved by 6% denaturing polyacrylamide electrophoresis until the bromophenol blue dye front reached the end of the gel. Gels were subjected to autoradiography for 1 to 12 hours at -70°C.

#### 4.3.2.3 *Multimeric ribozyme trans-cleavage*

Transcription of radiolabelled target RNA (*Xba*I-linearised pBS-X) was performed as described for the multimeric ribozymes above using T3 RNA polymerase. *In vitro* transcription reactions for the multiribozyme templates were performed similarly to that of the single-unit ribozymes. Antisense control pBS-X target RNA was transcribed using T7 RNA polymerase (Promega, WI, USA) from an *Xho*I-linearised pBS-X template. The cleavage reaction was carried out in a 10  $\mu\text{l}$  reaction mixture containing a molar ratio of ribozyme to radiolabelled target RNA of 5:1 in the presence of 20 mM  $\text{MgCl}_2$  and 50 mM Tris-Cl (pH 8.0), and incubated at 37°C. The reaction was stopped after 1 hour with the addition of 3  $\mu\text{l}$  of RNA loading buffer (Appendix B2-3). Samples were resolved as described in section 4.3.2.2.

#### 4.3.3 *In situ detection of multimeric hammerhead ribozyme activity*

Huh7 cells were cultured, seeded and transfected as described in sections 2.3.4 and 2.3.5. In a similar manner to that described in section 3.3.2, transfections were carried out in 100 mm culture dishes and contained a combination of 3  $\mu\text{g}$  of

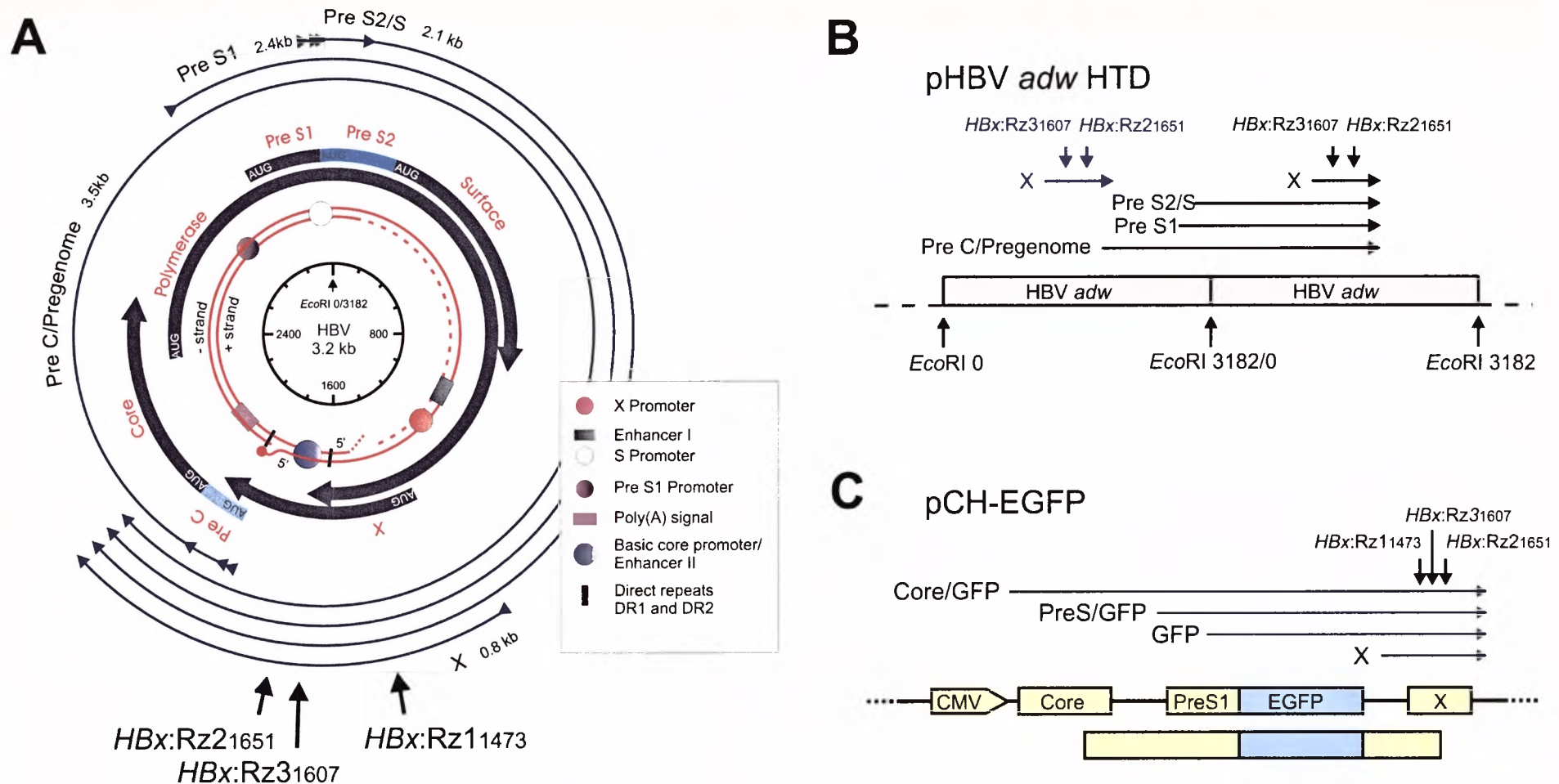


**Figure 4.4** Sequences targeted by three hammerhead ribozymes *HBx:Rz1<sub>1473</sub>*, *HBx:Rz2<sub>1651</sub>*, and *HBx:Rz3<sub>1607</sub>*. **A)** Organisation of the hepatitis B virus genome (strain *ayw*) showing sites targeted by all three hammerhead ribozymes. **B)** The pHBV *adw* HTD plasmid is a HBV replication-competent vector and includes a head-to-tail dimer of the HBV *adw* genome. The HBV transcripts (blue arrows) as well as the targets for ribozymes *HBx:Rz3<sub>1607</sub>* and *HBx:Rz2<sub>1651</sub>* are indicated (black arrows). **C)** Plasmid constructs pCH-EGFP showing their open reading frames, respective transcripts and sites targeted by ribozymes *HBx:Rz1<sub>1473</sub>*, *HBx:Rz2<sub>1651</sub>* and *HBx:Rz3<sub>1607</sub>*. The disrupted polymerase ORF is indicated as a light blue box.



pCH-EGFP (Figure 4.4C) and 6  $\mu$ g of plasmids *pHBx:Rz1*<sub>1473</sub>, *pHBx:Rz1\**<sub>1473</sub>, *pHBx:Rz2*<sub>1651</sub>, *pHBx:Rz2\**<sub>1651</sub>, *pCI-M8HBx:Rz1*<sub>1473</sub>, *pCI-M8HBx:Rz2*<sub>1651</sub>, *pCI-M8HBx:Rz3*<sub>1607</sub>, *pCI-M24HBx:Rz1,Rz2,Rz3* or pCI neo. Cells labelled with EGFP were detected by fluorescence microscopy three days after transfection. The mean number of fluorescent cells as well as the standard error of the mean (SEM) was calculated from experiments performed in triplicate.

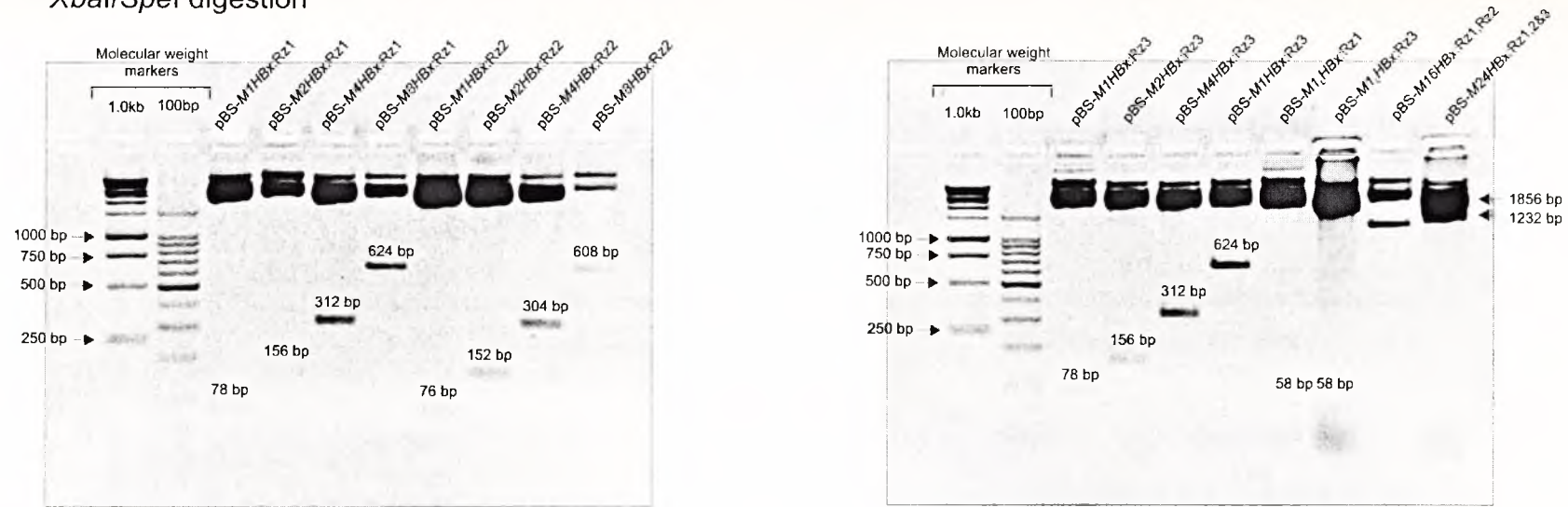
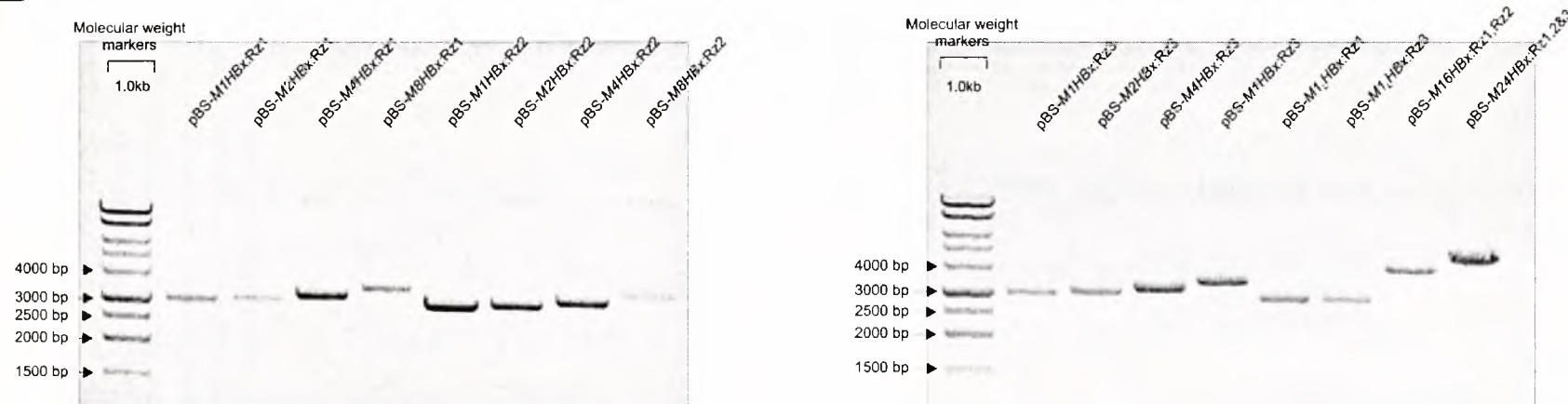
#### 4.3.4 HBsAg and HBeAg assays

Similar to the method described in sections 2.3.2 and 3.3.5, Huh7 cells in 100 mm diameter culture dishes were transfected with a combination of 7  $\mu$ g of pHBV *adw* HTD (Figure 4.4B) and 14  $\mu$ g of *pHBx:Rz1*<sub>1473</sub>, *pHBx:Rz1\**<sub>1473</sub>, *pHBx:Rz2*<sub>1651</sub>, *pHBx:Rz2\**<sub>1651</sub>, *pHBx:At1*<sub>1473</sub>, *pHBx:At2*<sub>1651</sub>, *pCI-M8HBx:Rz1*<sub>1473</sub>, *pCI-M8HBx:Rz2*<sub>1651</sub>, *pCI-M8HBx:Rz3*<sub>1607</sub>, and *pCI-M24HBx:Rz1,Rz2,Rz3*. Following transfection into Huh7 cells, HBsAg and HBeAg secretion into the culture supernatants was measured daily for three days using AxSYM (ELISA) immunoassay kits (Abbot Laboratories, IL, USA). The means of HBsAg and HBeAg measurements were calculated from three independent transfections.

## 4.4 Results

### 4.4.1 Multimeric hammerhead ribozyme vectors

Cloning vectors, which contain the pBluescript II KS(+) backbone, were generated to encode single-unit and multiple-unit *cis*- and *trans*-cleaving hammerhead ribozyme-encoding sequences for hammerhead ribozymes *HBx:Rz1*<sub>1473</sub>, *HBx:Rz2*<sub>1651</sub>, and *HBx:Rz3*<sub>1607</sub>. The construction of head-to-tail multiples of each *cis*- and *trans*-cleaving hammerhead ribozyme sequence was facilitated by the presence of *SpeI* and *XbaI* cohesive ends for each cloned fragment insert. Figure 4.5 shows fragments resolved on agarose gels following digestion with *SpeI* and *XbaI* (Figure 4.5A) and *SpeI* alone (Figure 4.5B). The digest results in different size fragment inserts for each of the multimeric

**A** *Xba*I/*Spe*I digestion**B** *Spe*I digestion

**Figure 4.5** Restriction endonuclease digestion of multimeric hammerhead ribozyme plasmid constructs with *Spe*I and *Xba*I (**A**) to release cloned multimeric hammerhead ribozyme fragment inserts; and with *Spe*I (**B**) to linearise each multiple-unit plasmid. Digested fragments are observed on 1.5% (**A**) and 1% (**B**) agarose gels along with 1 kb and 100 bp markers (Promega, WI, USA).

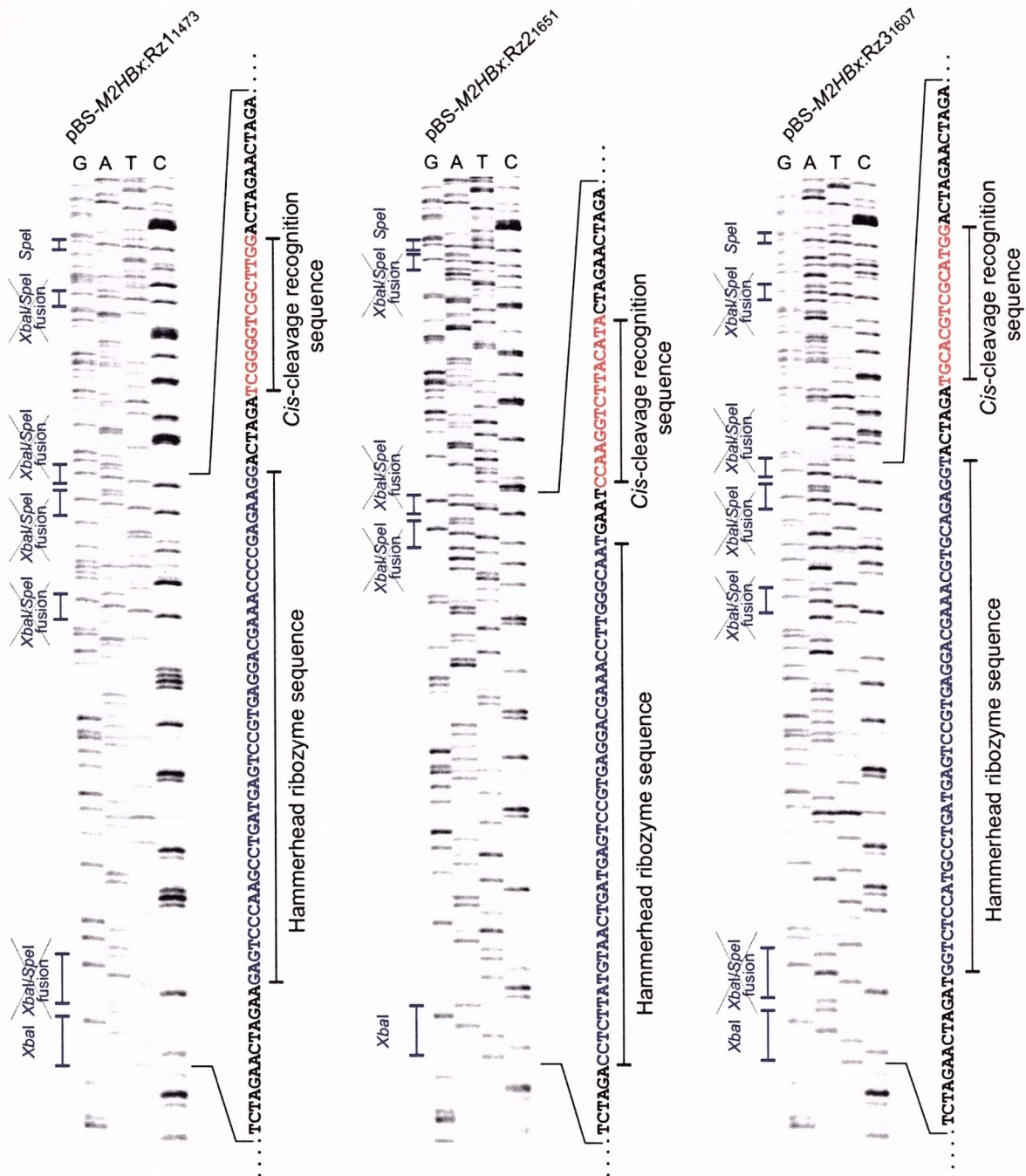


**Figure 4.6** DNA sequences of dimer series pBSKSII(+)-derived *cis*- and *trans*-cleaving hammerhead ribozyme vectors: pBS-M2HBx:Rz1<sub>1473</sub>, pBS-M2HBx:Rz2<sub>1651</sub> and pBS-M2HBx:Rz3<sub>1607</sub>. The 5' hammerhead ribozyme-encoding sequence (blue) is shown along with its respective cleavage recognition sequence (red) for each vector sequence. Annotated to the left of each sequence are the XbaI and SpeI restriction sites and all XbaI/SpeI fusion knockout sites.



hammerhead ribozymes. The 5' ends produced by digestion with *Xba*I and *Spe*I are complementary to each other. However, the re-ligation of *Spe*I-generated 5' ends with *Xba*I-generated 5' ends resulted in sites that are not re-cleaved by either enzyme (Figures 4.5 and 4.6). This approach allowed for the use of both *Xba*I and *Spe*I restriction enzymes to generate vectors encoding up to 24 multimeric ribozyme units bound sequentially head-to-tail (Figures 4.6, 4.7B and Appendix C1).

#### 4.4.2 Proof of multimeric ribozyme efficacy

##### 4.4.2.1 *In vitro* transcription and ribozyme cleavage

Each multimeric ribozyme transcript contains multiples of four (4-mer), eight (8-mer) and twenty-four (24-mer) *cis*-cleaving hammerhead ribozyme units targeted to the three unique HBV sites *HBx*:Rz1<sub>1473</sub>, *HBx*:Rz2<sub>1651</sub>, and *HBx*:Rz3<sub>1607</sub>. To determine the *cis*-cleaving activity of each *cis*- and *trans*-cleaving hammerhead ribozyme unit, RNAs encoding multimeric ribozyme tandems were transcribed *in vitro* from linearised pBluescript II (KS+)-derived vector constructs. Free magnesium ions present in the transcription buffer stimulated ribozyme *cis*-cleavage during transcription. For all transcripts generated from *in vitro* transcription, *cis*-cleavage was very efficient, resulting in 100% monomeric cleavage products before a separate designated cleavage reaction step (Figure 4.7A). To diminish ribozyme *cis*-cleavage during transcription, the ribonucleotide concentration was increased to absorb free Mg<sup>2+</sup> in the transcription buffer. Nevertheless, no full-length transcripts were detectable after transcription (Figure 4.7A) and *cis*-cleavage resulted in approximately 80% single-unit cleavage products. The *cis*-cleavage reaction observed in Figure 4.8A appears to be more efficient than reactions reported by other *cis*-cleaving hammerhead ribozyme constructs (Ohkawa *et al.*, 1993b; Ruiz *et al.*, 1997). Dimer, trimer and tetramer cleavage products were the only remaining multimeric units following *in vitro* transcription (Figure 4.8A). These products underwent further *cis*-cleavage following additional 60 minutes incubation during the cleavage reaction.

The addition of vector-derived sequences, present at the 5' terminus of each transcript, produced single monomer cleavage products of 107 nt in length

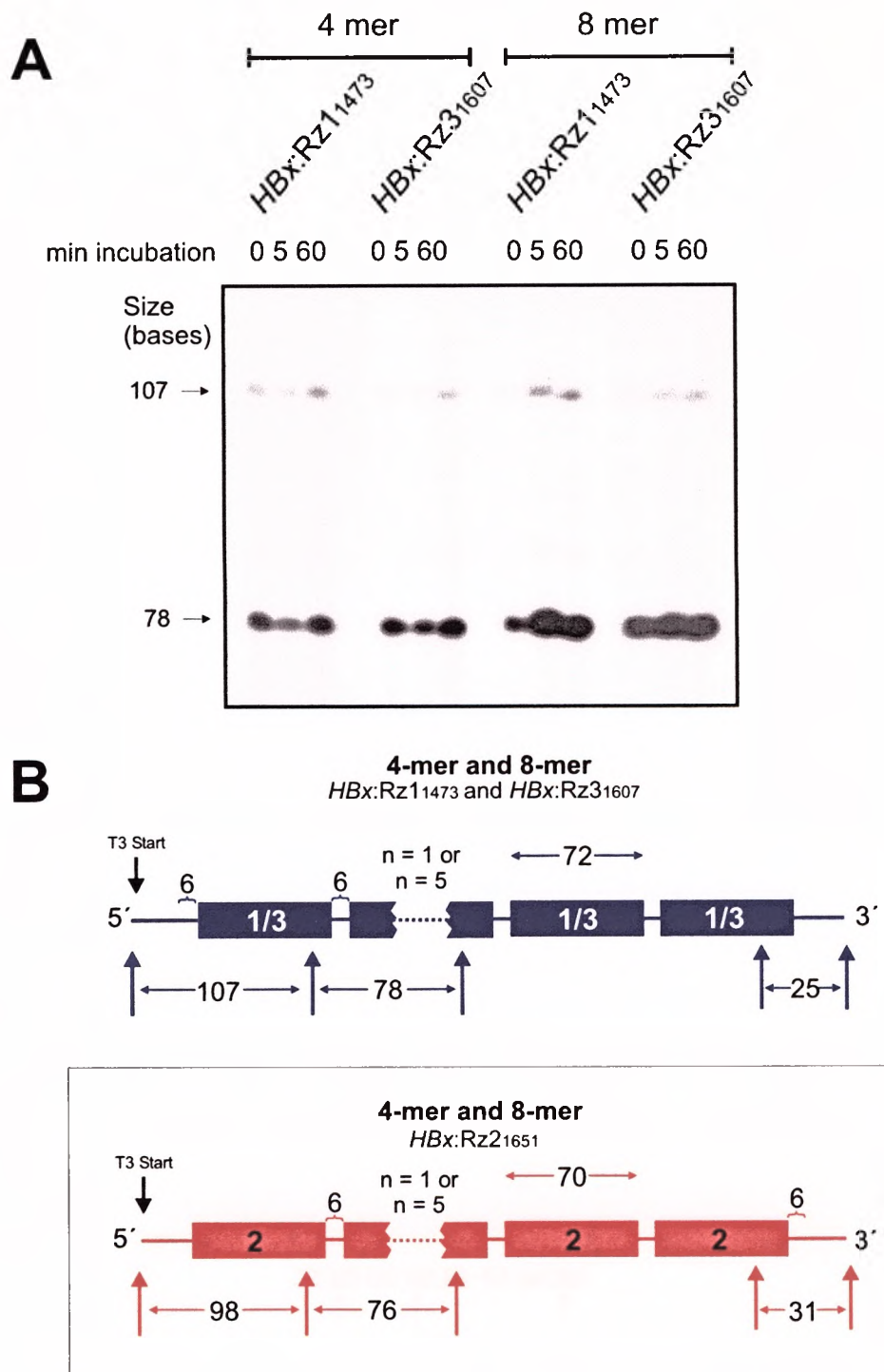


**Figure 4.7** *In vitro cis*-cleavage of multimeric *cis*- and *trans*-cleaving hammerhead ribozymes HBx:Rz1<sub>1473</sub> and HBx:Rz3<sub>1607</sub>. **A)** *Cis*-cleavage showing monomeric cleavage products for 4-mer and 8-mer constructs of ribozyme species HBx:Rz1<sub>1473</sub> and HBx:Rz3<sub>1607</sub>. **B)** Schematic illustration of the cleavage products generated for the 8-mer transcript of all three 8-mer ribozymes. The cleavage products for HBx:Rz2<sub>1651</sub> are included as boxed inset, although the cleavage of fragments is not shown in **A**.



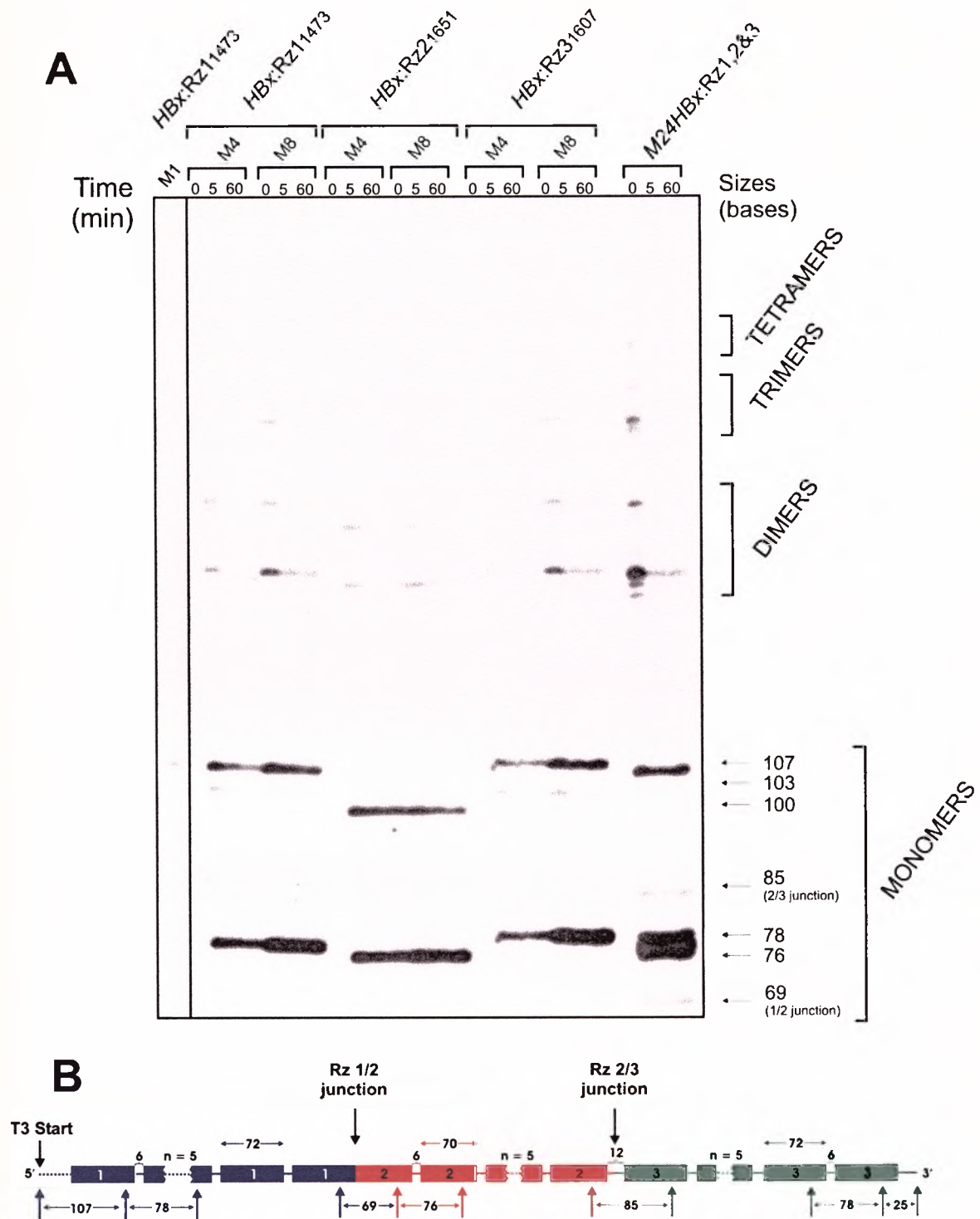


**Figure 4.8** *Cis*-cleavage *in vitro* of transcripts containing multimeric hammerhead ribozymes. **A)** *Cis*-cleavage showing intermediate cleavage products for 4-mer, 8-mer and 24-mer constructs of all three ribozyme species: *HBx:Rz1<sub>1473</sub>*, *HBx:Rz2<sub>1651</sub>* and *HBx:Rz3<sub>1607</sub>*. A single-unit *cis*- and *trans*-cleaving hammerhead ribozyme *M1HBx:Rz1<sub>1473</sub>*, is used as a control to denote a 5' monomeric cleavage product of 107 nt. **B)** Schematic illustration of the cleavage products generated for the 24-mer transcript, *M24HBx:Rz1,2&3*, including the cleavage products generated at the junction of ribozymes 1/2 and 2/3.

for *cis*-cleaving ribozyme constructs containing 4-mer, 8-mer units of ribozymes *HBx*:Rz1<sub>1473</sub> and *HBx*:Rz3<sub>1607</sub>, and 98 nt in length for constructs containing 4-mer and 8-mer units of ribozyme *HBx*:Rz2<sub>1651</sub> (Figures 4.7B and 4.8B). The 107 nt in length monomeric cleavage product generated by the 24-mer multimeric ribozyme transcript, is similar to the sequence at the 5' terminus of the 8-mer multimeric construct of ribozyme *HBx*:Rz1<sub>1473</sub>. This unique 107 nt fragment, produced only once per transcription cycle, can serve as an internal control, enabling a quantitative comparison of products generated by different *cis*-cleaving multimeric ribozyme templates. The most abundant cleavage products were monomer units of individual ribozymes with trimmed 5' and 3' termini. These were observed as a 78 nt band for ribozymes *HBx*:Rz1<sub>1473</sub> and *HBx*:Rz3<sub>1607</sub>, and as a 76 nt band for ribozyme *HBx*:Rz2<sub>1651</sub>. Multimeric constructs containing eight *cis*-cleaving hammerhead ribozyme units (8-mer constructs) produced, as expected, a more intense 78 nt (or 76 nt for *HBx*:Rz2<sub>1651</sub>) band of monomer units when compared to the 4-mer constructs. The autoradiograph in Figure 4.7A shows the difference in the concentration of monomeric units generated between 8-mer and 4-mer multimeric ribozyme transcripts for hammerhead ribozymes *HBx*:Rz1<sub>1473</sub> and *HBx*:Rz3<sub>1607</sub>. This result is also shown for all three ribozymes in Figure 4.8A. The 24-mer transcript, which includes multiples of each of the three hammerhead ribozymes, produced, in addition to the 78 nt and 76 nt monomer units, single monomers of 69 and 85 nt in length. These single cleavage products represent respectively the junction between 8-mer units of ribozymes *HBx*:Rz1<sub>1473</sub> and *HBx*:Rz2<sub>1651</sub>, and between ribozymes *HBx*:Rz2<sub>1651</sub> and *HBx*:Rz3<sub>1607</sub>. Other cleavage products include an array of incomplete reaction intermediates. One such intermediate, visible as a 103 nt product, represents a 78 nt self-cleaved monomer of ribozyme *HBx*:Rz3<sub>1607</sub> with 24 nt of attached, uncleaved 3' terminal vector sequence. These results suggest that *cis*-cleavage is highly efficient and specific for all ribozyme species and that independent liberated ribozymes can be generated to act in *trans*.

---

#### 4.4.2.2 *In vitro trans-cleavage activity of 5'- and 3'-trimmed monomeric ribozymes generated by cis-cleavage*

*Cis*-cleaved 5'- and 3'-trimmed monomeric hammerhead ribozyme units were prepared for a *trans*-cleavage reaction. The processed ribozymes were generated from transcripts containing 1, 2, 4 and 8-mer ribozyme units as described in sections 4.3.1.1 and 4.3.1.2. Sense and antisense target HBV RNA was produced by T7/T3 RNA polymerase using a linearised pBluescript-derived vector, pBS-X, as template. Plasmid pBS-X encodes the *HBx* ORF of HBV. To determine the *trans*-cleavage activity of monomeric ribozymes generated by *cis*-cleavage of a multimeric transcript, target transcript RNA was cleaved in *trans* by each individual processed ribozyme. All multimeric units of each of the three ribozymes were able to cleave target RNA in *trans* to generate two cleavage products: 173 and 411 nt for ribozyme *HBx*:Rz1<sub>1473</sub>; 351 and 233 nt for ribozyme *HBx*:Rz2<sub>1651</sub>; and, 306 and 278 nt for ribozyme *HBx*:Rz3<sub>1607</sub> (Figures 4.9A and 4.9C). Antisense *HBx* template RNA (587 nt), produced by T7 RNA polymerase, was not cleaved by any single-unit or multimeric hammerhead ribozyme (Figure 4.9B). Ribozyme *HBx*:Rz3<sub>1607</sub> proved to be significantly more efficient at cleaving target substrate than both ribozymes *HBx*:Rz1<sub>1473</sub> and *HBx*:Rz2<sub>1651</sub>. This can be deduced from the intensity of the cleaved products and the lack of substrate RNA, represented by a 548 nt band. A 16-mer of *HBx*:Rz1<sub>1473</sub> and *HBx*:Rz2<sub>1651</sub> and a 24-mer containing each of the three ribozyme species also produced all the expected cleavage products (Figure 4.10A).

#### 4.4.3 ***Multimeric ribozyme inhibitory effects on HBV gene expression in transfected liver-derived cells***

In order to observe the effects of the *cis*- and *trans*-cleaving multimeric ribozymes in transfected Huh7 cells, all 8-mer and the 24-mer ribozyme constructs were cloned into the mammalian expression vector pCI neo under control of the immediate/early CMV promoter. This resulted in 8-mer vectors pCI-*M8HBx*:Rz1<sub>1473</sub>, pCI-*M8HBx*:Rz2<sub>1651</sub> and pCI-*M8HBx*:Rz3<sub>1607</sub>, as well as the 24-mer, pCI-*M24HBx*:Rz1,Rz2,Rz3.



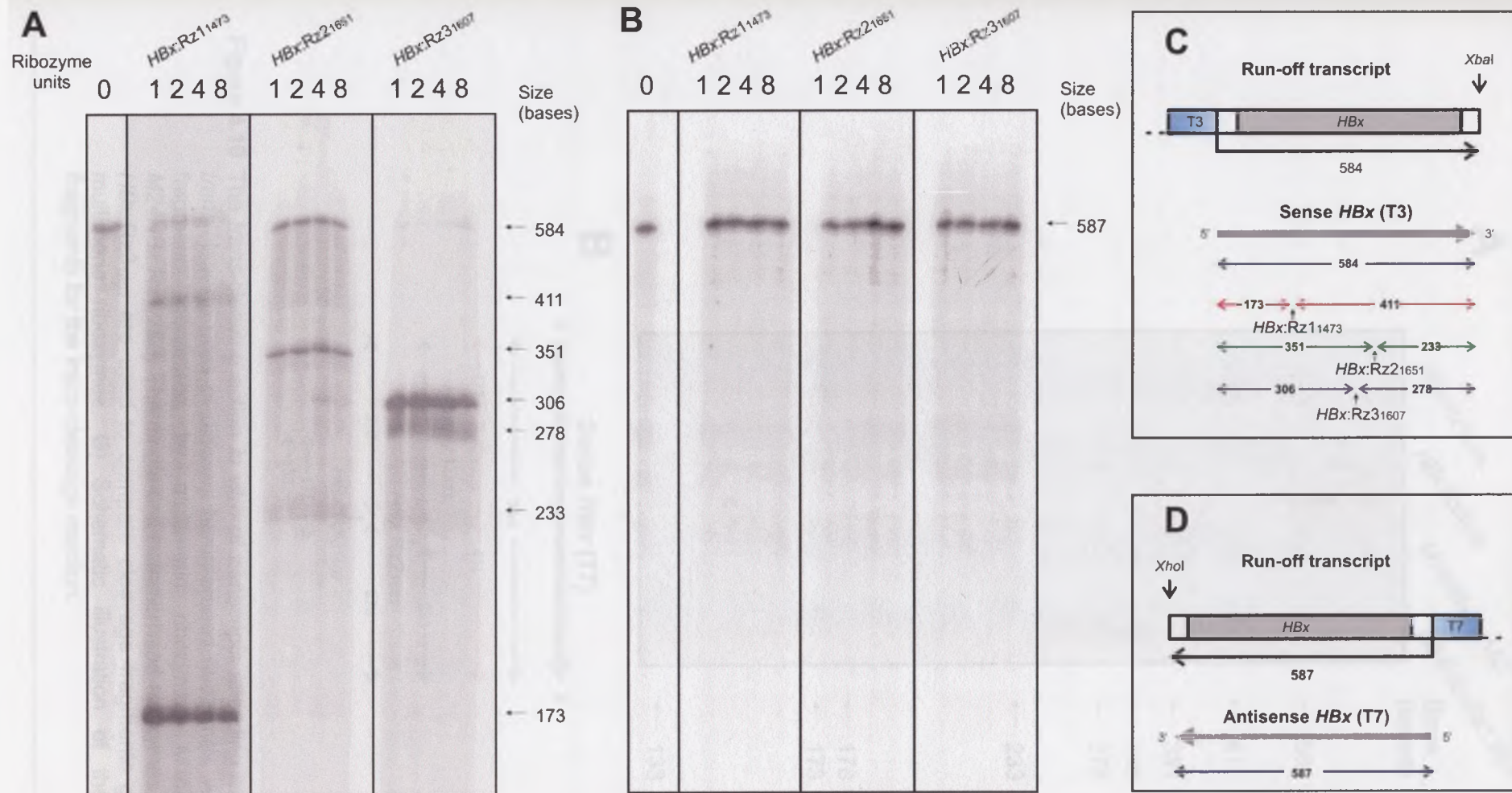


**Figure 4.9** The *trans*-cleaving action *in vitro* of transcripts encoding multimeric *cis*- and *trans*-cleaving units of the same hammerhead ribozymes. **A)** *Trans*-cleavage by various single and multimeric ribozymes on T3 RNA polymerase generated run-off transcripts of HBx. **B)** *Trans*-cleavage of a control antisense transcript produced by T7 RNA polymerase run-off expression of an HBx-encoding fragment. **C)** and **D)** Schematic illustration of the expected size fragments for the *trans*-cleavage reaction using **(C)** T3 (sense) and **(D)** T7 (antisense) generated HBx RNA transcripts.

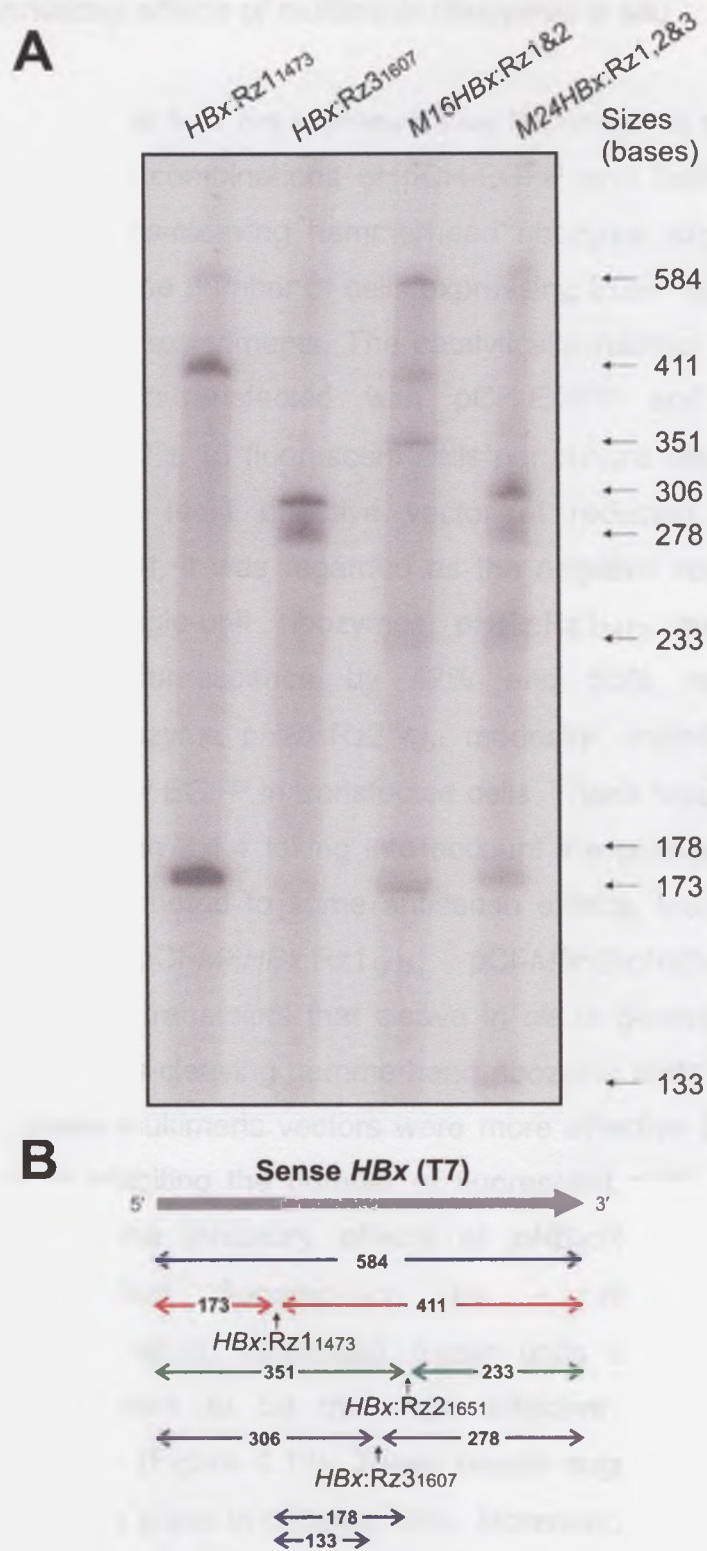


**Figure 4.10** The *trans*-cleaving action *in vitro* of transcripts encoding multimeric *cis*- and *trans*-cleaving units of different hammerhead ribozymes. **A)** *Trans*-cleavage fragments generated by multimeric ribozymes *M16HBx:Rz1&2* and *M24HBx:Rz1,2&3*. The single-unit hammerhead ribozymes *HBx:Rz1<sub>1473</sub>* and *HBx:Rz3<sub>1607</sub>* are used to compare cleavage fragments generated by the multimeric ribozymes. **B)** Schematic illustration of the expected size fragments for the *trans*-cleavage reaction.



#### 4.4.3.1 The inhibitory effects of multimeric ribozymes in situ

The cells shown in Figure 4.11 are representative fluorescence microscope fields of co-transfections with combinations of pCH-EGFP and both single-unit and multimeric *cis*- and *trans*-cleaving hammerhead ribozyme expression vectors. The mean and SEM of the number of cells expressing EGFP were calculated at day three from triplicate experiments. The catalytically-inactive ribozyme control pHBx:Rz1\*<sub>1473</sub> (cells co-transfected with pCH-EGFP and pHBx:Rz1\*<sub>1473</sub>) produced a mean of  $130 \pm 15$  fluorescent cells per culture field. Since plasmid pHBx:Rz1\*<sub>1473</sub> was the least effective vector at reducing the number of fluorescent cells per field, it was regarded as the negative control. Relative to pHBx:Rz1\*<sub>1473</sub> both single-unit ribozymes pHBx:Rz1<sub>1473</sub> and pHBx:Rz2<sub>1651</sub> significantly inhibited fluorescence by 42% and 55% respectively. The catalytically inactive ribozyme pHBx:Rz2\*<sub>1651</sub> modestly inhibited ( $35 \pm 7.6\%$ ,  $p < 0.01$ ) the expression of EGFP in transfected cells. These results correlate with those observed in section 3.4.4 taking into account the possibility that plasmid pHBx:Rz1\*<sub>1473</sub> has contributed to some antisense effects. Multimeric ribozyme expression vectors, pCl-M8HBx:Rz1<sub>1473</sub>, pCl-M8HBx:Rz2<sub>1651</sub> and pCl-M8HBx:Rz3<sub>1607</sub> express transcripts that cleave in *cis* to generate eight (8-mer) individual monomer *trans*-cleaving hammerhead ribozyme units. Apart from pCl-M8HBx:Rz2<sub>1651</sub>, these multimeric vectors were more effective than their single-unit counterparts in inhibiting the number of fluorescent cells per field (Figure 4.12). Compared to the inhibitory effects of pHBx:Rz1\*<sub>1473</sub>, plasmid pCl-M8HBx:Rz3<sub>1607</sub> inhibited fluorescence by  $\pm 60\%$ . Plasmid pCl-M24HBx:Rz1,Rz2,Rz3, which expresses 8-mer units of each of the three ribozyme species, proved to be the most effective vector and inhibited fluorescence by  $\pm 92\%$  (Figure 4.12). These results suggest that both *cis* and *trans* cleavage is taking place in cultured cells. Moreover, the data demonstrate that these multimeric *cis*- and *trans*-cleaving ribozymes are more effective than previous constructs in preventing HBV gene expression, and are thus likely to possess significant antireplicative activities.

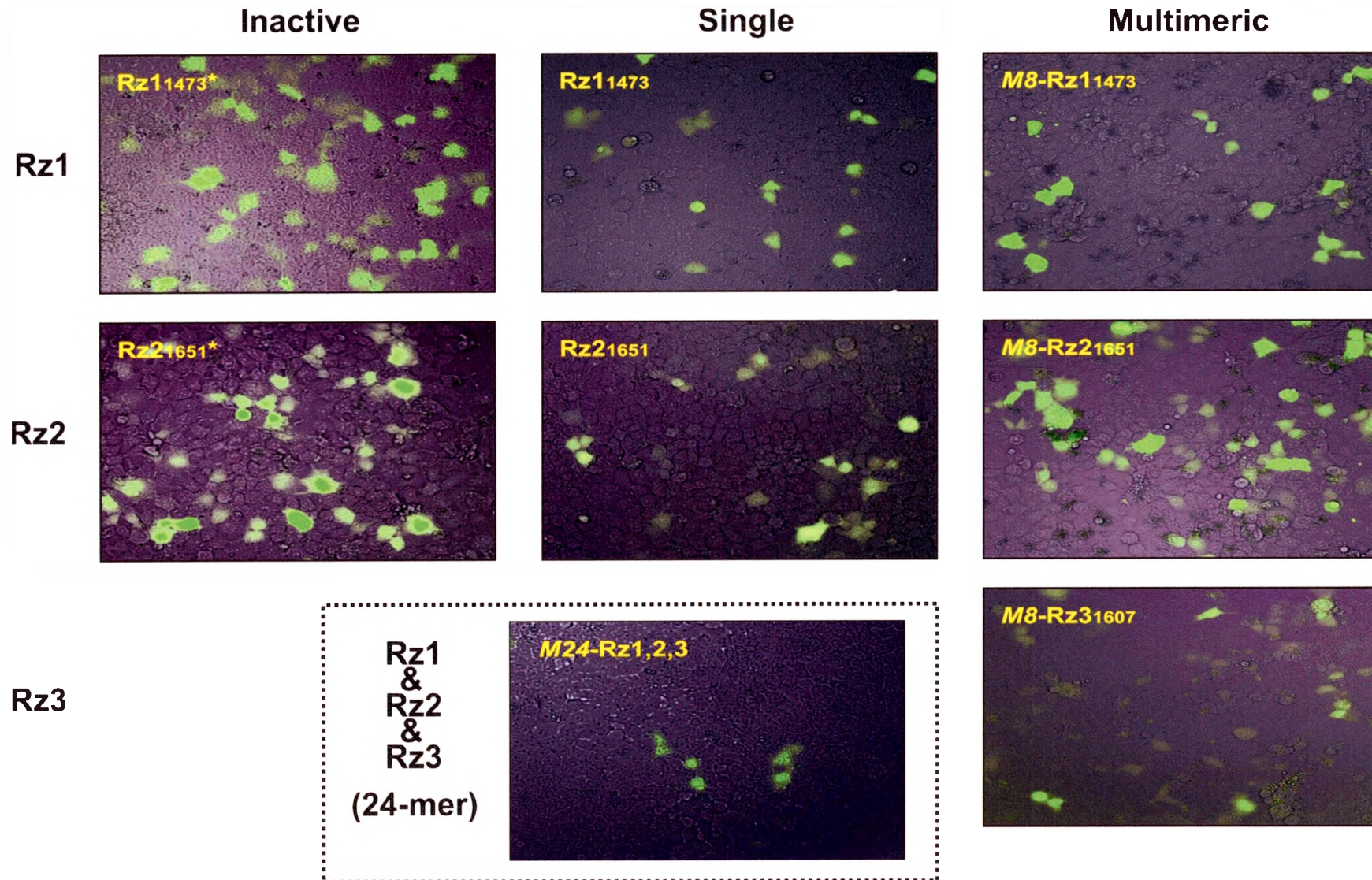


**Figure 4.11** *In situ* ribozyme modulation of EGFP activity in co-transfected Huh7 cells. Combined phase contrast and fluorescence microscopy of Huh7 cells transfected with pCH-EGFP and either single-unit inactive ribozyme controls or various ribozyme-expressing constructs.



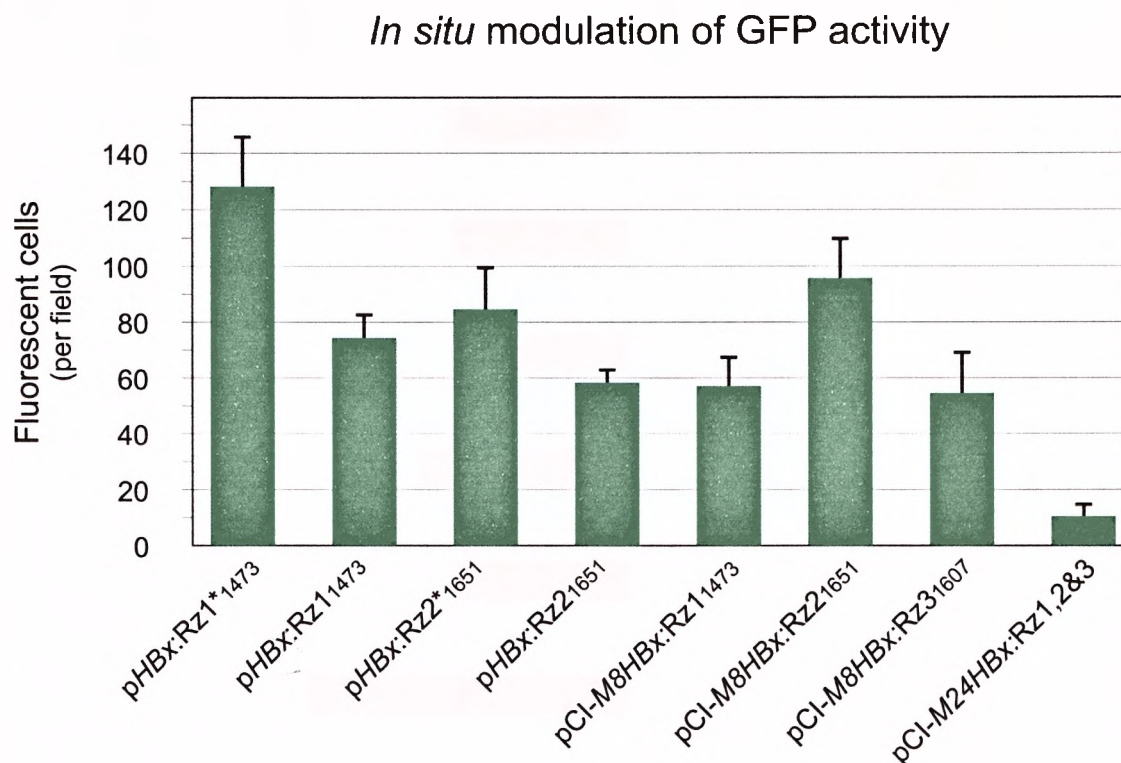


**Figure 4.12** An *in situ* quantitative comparison of the number of EGFP-positive Huh7 cells modulated by the transfection of various ribozyme-encoding expression vectors. Cells were counted from fluorescence microscopy fields of Huh7 cells transfected with pCH-EGFP and either single-unit or multimeric ribozyme-expressing constructs. Single-unit ribozyme-inactive variants were used as negative controls. The data are the mean  $\pm$  SEM of three separate transfections.

#### 4.4.3.2 Effects of multimeric ribozyme on HBV antigen secretion in cell culture supernatants

To assess the effects of single-unit hammerhead ribozymes and multimeric self-cleaving ribozymes on HBsAg and HBeAg secretion, Huh7 cells were co-transfected with ribozyme-encoding vectors and a replication-competent HBV vector, pHBV *adv* HTD (this vector is described in section 2.3.2). Cell culture supernatants were analysed three days after transfection for the secretion of HBsAg and HBeAg (Figure 4.13). All transient co-transfections were performed in triplicate (mean and SEM are indicated) and were normalised to 100% of the positive control. Plate-to-plate variations in transfection efficiencies were

## HBsAg and HBeAg measurements

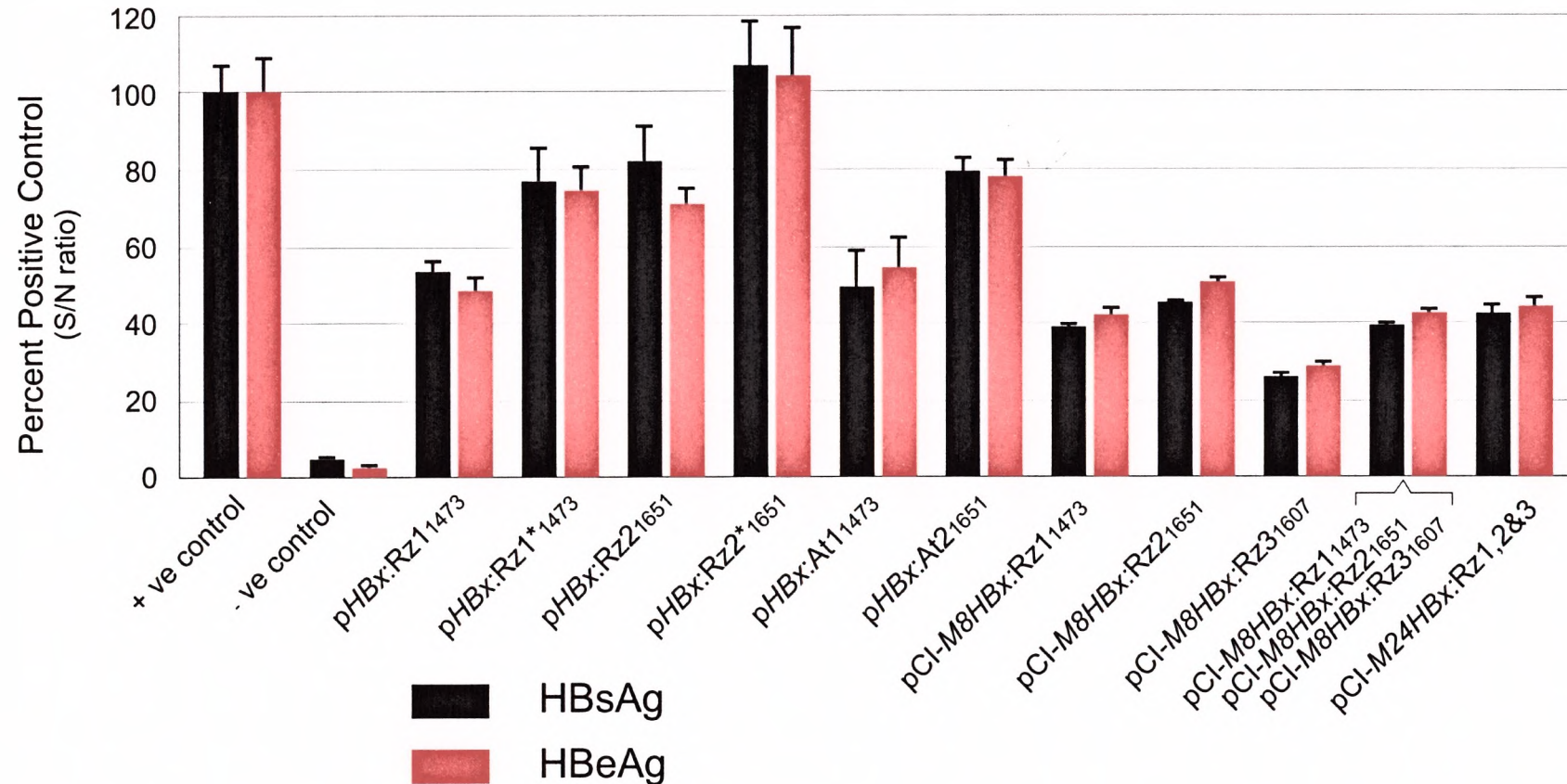


**Figure 4.13** Measurement of HBsAg and HBeAg secretion from Huh7 cells co-transfected with single-unit and multimeric ribozyme vectors (as well as antisense RNA) and a replication-competent HBV vector, pHTD *adv* HBV (Figure 4.4). HBs/HBeAg measurements are given as a mean percentage of the positive control (pHTD *adv* HBV only) with standard error of the mean (SEM). The plasmids used in the transfection are indicated below each column. The data is given as the mean from experiments performed in triplicate and is compared to 100% for the control.

determined by assessing the relative expression of EGFP in each plate (see Appendix C2). As expected, single-unit ribozymes *pHBx:Rz1<sub>1473</sub>* and *pHBx:Rz2<sub>1651</sub>* decreased the secretion of HBeAg and HBsAg into the culture supernatant (Figure 4.13). The catalytically inactive ribozyme control *pHBx:Rz1\*<sub>1473</sub>* had only a modest inhibitory effect on HBsAg and HBeAg secretion whilst the inactive ribozyme control *pHBx:Rz2\*<sub>1651</sub>* was completely ineffective. These results are similar to those obtained in section 3.4.3, suggesting that single-unit ribozymes are only moderately efficacious. Once again, *pHBx:Rz1<sub>1473</sub>*, which cannot cleave RNA sequences generated by the pHBV *adw* HTD vector (see section 3.4.3), was slightly more effective than *pHBx:Rz2<sub>1651</sub>*. To confirm the results observed in the previous chapters, that antisense-effects play a dominant role in inhibiting HBV replication, antisense plasmids *pHBx:At1<sub>1473</sub>* and *pHBx:At2<sub>1651</sub>* were included in this study. The results for both antisense plasmids are similar to each respective single-unit ribozyme. Comparisons between the inactive ribozymes and antisense RNAs suggest that the catalytically inactive ribozymes are not necessarily true antisense controls. The catalytically inactive ribozymes cause only a modest reduction in antigen levels and may only partially elicit the antisense effects seen when using full-length antisense RNA sequences.

Multimeric ribozyme plasmids expressing 8-mer self-cleaving ribozyme units of hammerhead ribozymes *HBx:Rz1<sub>1473</sub>*, *HBx:Rz2<sub>1651</sub>* and *HBx:Rz3<sub>1607</sub>* were largely more effective than their single-unit counterparts in decreasing HBeAg and HBsAg levels (Figure 4.13). *pCI-M8HBx:Rz3<sub>1607</sub>* reduced both HBsAg and HBeAg secretion levels by approximately 75 and 70% respectively. Moreover, *pCI-M8HBx:Rz3<sub>1607</sub>* proved to be more effective than either a combination of all three 8-mer plasmids or the 24-mer plasmid, *pCI-M24HBx:Rz1,Rz2,Rz3*, which simultaneously expresses eight units of each of the three ribozymes. Unlike the results obtained in section 4.4.2, *pCI-M24HBx:Rz1,Rz2,Rz3* reduced the secretion of HBsAg/HBeAg levels by approximately 60%. In conclusion, these results indicate that multimeric ribozymes are more effective at inhibiting viral gene expression than single-unit ribozymes, and implies some degree of ribozyme-mediated cleavage. It is unlikely that multiple, tethered antisense sequences targeting the same site will be more effective than single-unit sequences as multiple antisense sequences are likely to be hindered by steric



effects and competition for the same *trans* target sites and/or *cis*-recognition sequences. However, it may be that *cis*-cleavage is active whilst *trans*-cleavage is ineffective. *In vivo*, hammerhead ribozyme *cis*-cleavage has been shown to be more efficient than *trans*-cleavage (Dropulic *et al.*, 1992; Xing *et al.*, 1995) as both ribozyme and target sequences are co-localised. A molar excess of independent antisense RNA monomers (a situation where *cis*-cleavage takes place but not *trans*-cleavage) could generate similar results to those observed for the multimeric *cis*-cleaving ribozymes. Nevertheless, the results for the multimeric ribozyme constructs in general are encouraging and represent an improvement on previously constructed hammerhead ribozymes. These constructs are capable of significantly inhibiting HBV gene expression and replication in cell culture and are viable agents for further testing in animal models of chronic HBV infection.

#### 4.5 Discussion and conclusions

Most studies to date suggest that ribozyme cleavage activity is relatively inefficient *in vivo* (Castanotto *et al.*, 2000). At present ribozyme research is restricted by a limited understanding of the catalytic activity of hammerhead ribozymes in an intracellular or *in vivo* environment. Few models exist which allow for the design *ex novo* of ribozymes or antisense RNA sequences for use in a clinical setting, let alone for use in treating chronic HBV infection. A number of unresolved issues include the identification of the optimal sequences which need to be targeted, the effect of inhibiting viral and cellular factors, subcellular co-localisation of therapeutic and target sequences, the appropriate length of the hybridising sequences and the efficient delivery of therapeutic sequences to the infected hepatocytes (explored in a detailed discussion, see Chapter 5). Anti-HBV ribozymes produced by others (Beck and Nassal, 1995; Feng *et al.*, 2001a; Feng *et al.*, 2001b; Kim *et al.*, 1999; Welch *et al.*, 1997) confirm the results presented in Chapters 2 and 3 that ribozymes appear less effective when expressed endogenously in transfected cells than in cleavage reactions *in vitro*. Since many factors govern the interactions between RNA molecules in the intracellular physiological environment, improving the efficacy of ribozymes *in vivo* is the primary focus of therapeutic ribozyme development.

---

Ribozymes are distinguished from antisense RNAs in their ability to undergo multiple reactions. They may be applying their therapeutic effects sub-optimally by acting mostly as antisense RNAs *in vivo*. The hammerhead ribozyme catalytic efficiency ( $k_{\text{cat}}$ ) is several orders of magnitude lower *in vivo* compared to *in vitro* (James and Gibson, 1998), and single-turnover conditions prevail. As a result, a greater concentration of hammerhead ribozymes is needed to improve their intracellular efficacy. This has been confirmed by previous studies which indicate that a molar excess of ribozymes over its target substrate RNA is necessary in order to exert an inhibitory biological effect *in vivo* (Cameron and Jennings, 1989; Cotten and Birnstiel, 1989). One of the aims of this study was to increase the number of ribozymes present *in vivo* for cleavage. Various elaborate hammerhead ribozyme constructs have been tested with the specific aim of increasing the number of ribozyme catalytic units per cell, and thereby increasing the intracellular ribozyme concentration. DNA sequences, encoding single transcripts harbouring different ribozymes bound head-to-tail on the same strand, have been constructed to target various sites on *BCR/ABL* mRNA (Leopold *et al.*, 1995), HIV (Bai *et al.*, 2001; Chen *et al.*, 1992; Ohkawa *et al.*, 1993a; Ramezani *et al.*, 1997) and HBV (von Weizsäcker *et al.*, 1992). For these ribozymes, cleavage efficiency was shown to be directly proportional to the number of ribozyme units present on the transcript RNA. However, there is a limit to the number of bound ribozymes which can exert maximal cleavage activity *in vitro*. No increase in cleavage efficiency was observed by adding more than three ribozyme units to the same transcript (Ohkawa *et al.*, 1993a). Ribozymes bound together within a single transcript are catalytically constrained. However, the kinetic mechanism of bound ribozyme units has not been verified *in vivo*.

Ribozymes bound within a single transcript can be released from the parental chain through the action of flanking *cis*-cleaving hammerhead ribozymes present on both the 5' and 3' ends of a *trans*-cleaving ribozyme (Yuyama *et al.*, 1992). Released individual ribozyme monomers are capable of cleaving target RNA in *trans* (Ohkawa *et al.*, 1993a; Ohkawa *et al.*, 1993b; Yuyama *et al.*, 1992; Yuyama *et al.*, 1994). *Trans*-cleaving ribozymes processed from a single transcript are more efficient catalytically than the *trans*-cleaving action of ribozymes bound together on the same transcript (Ohkawa *et al.*, 1993a). Later studies have used several different ribozymes that release themselves from a

single transcript (Taira's "shotgun" ribozymes) (Ohkawa *et al.*, 1993b). In this system, 5' and 3' processed *trans*-cleaving multimeric ribozymes were capable of inhibiting target HIV RNA expression when expressed from retroviral vectors transduced into cultured cells (Xing *et al.*, 1995), but were no more effective than single-unit ribozymes in cell culture.

Taira's shotgun multimeric ribozyme method (Ohkawa *et al.*, 1993a) has been simplified to include multimeric units of both *cis*- and *trans*-cleaving hammerhead ribozymes (Ruiz *et al.*, 1997). In this system each hammerhead ribozyme unit present on the transcript RNA includes a *cis*-cleaving ribozyme recognition sequence. *Cis*-cleaved individual monomeric ribozyme units are then capable of retaining their function to cleave a target RNA in *trans*. The Ruiz model was applied successfully in the present study to target multiple *cis*- and *trans*-cleaving hammerhead ribozymes to different sites of the *HBx* ORF. Although, Ruiz *et al.* (1997) applied their multimeric construct to cleave HBV core RNA sequences *in vitro*, their study made use of a transcript that comprises multiple copies of one hammerhead ribozyme. Moreover, the efficacy of the multimeric ribozymes at inhibiting gene expression in transfected cells was not assessed. The *cis*-cleavage reaction of Ruiz's pentameric hammerhead ribozyme transcript was inefficient and contrasted with the data in Figures 4.7 and 4.8 that show highly efficient *cis*-cleavage using 4-mer, 8-mer and 24-mer ribozyme transcripts. For the *in vitro* transcription/*cis*-cleavage reaction described in 4.4.2.1 (Figure 4.8), efficient cleavage was achieved despite the presence of an increased nucleotide concentration, which sequesters free  $Mg^{2+}$  ions during transcription. This implies either that the hammerhead ribozymes chosen in Chapter 2 show a high specificity for their target, or that the *HBx* ORF is more accessible to the hybridising effects of the ribozyme annealing helices I and III. Since neither ribozyme kinetic studies nor a systematic comparison between different cleavage sites on HBV were performed, any discussion on comparative ribozyme efficiencies must remain speculative.

In the present study, the flanking arms in helices I and III (hybridisation arms) for the *cis*-cleavage reaction span approximately 14 nt of the complementary target sequence. The optimal length of ribozyme-substrate complementary sequences varies between 7 and 20 (Thomson *et al.*, 1997). As, the affinity of the *cis*-cleaving ribozyme for its downstream recognition sequence

is high, ribozyme specificity and catalytic efficiency is less likely to be dependent on hybridisation conditions. Consequently, *cis*-cleavage proceeds optimally under multiple turnover conditions. The *trans*-cleaving hammerhead ribozymes have hybridisation arms which span approximately 24 complementary nt instead of the 16-18 nt used for the same single-unit ribozymes in Chapters 2 and 3. Longer flanking arms were specifically designed to improve intracellular ribozyme specificity. Since the annealing reaction *in vivo* is the rate-limiting step, longer annealing arms often improve the inhibitory effects of the ribozymes (Bertrand and Rossi, 1996). However the higher affinity decreases the catalytic rate constant ( $k_{\text{cat}}$ ) and impedes the cleavage of multiple substrates by a single ribozyme (Hertel *et al.*, 1994). The data generated from cell culture transfections (4.4.3) were not sufficiently sensitive to measure any differences in ribozyme-mediated inhibition due to the length of the annealing arms (see sections 5.2.1 and 5.2.2 for a detailed discussion).

It has been suggested that an alternative reason for the inefficiency of hammerhead ribozymes *in vivo* is the presence of non-hybridising sequences, which are found 5' and 3' of the ribozyme catalytic core sequence (Bramlage *et al.*, 1998; Ohkawa *et al.*, 2000). These auxiliary sequences are usually vector-derived and may interfere with the correct ribozyme secondary structure conformation, resulting in a catalytically compromised ribozyme (He *et al.*, 1993; Ventura *et al.*, 1993). Alternatively, these additional sequences may decrease ribozyme specificity, preventing the annealing arms from hybridising to target complementary sequences. The multimeric *cis*- and *trans*-cleaving hammerhead ribozyme system described in this study has the advantage of generating *trans*-cleaving monomers with defined 5' and 3' ends, thus minimising the presence of additional sequences both upstream and downstream of the ribozyme catalytic core. One serious concern for this multimeric ribozyme system is the question of ribozyme stability post-cleavage. The presence of exposed 5' and 3' ends makes these cleaved ribozyme molecules susceptible to nuclease degradation. It appears, however, that processed ribozyme monomers survive long enough to ensure that they exert their therapeutic effects in an intracellular environment.

In conclusion, the multimeric *cis*- and *trans*-cleaving hammerhead ribozymes are more effective at inhibiting cell culture models of HBV replication than the hammerhead ribozymes described in the previous chapters. There are

---

several advantages associated with using *cis*- and *trans*-cleaving multimeric ribozymes for the future treatment of chronic HBV infection:

- 1) Multimeric *cis*- and *trans*-cleaving hammerhead ribozymes increase the intracellular concentration of hammerhead ribozymes.
- 2) Ribozyme *cis*-cleavage generates trimmed 5' and 3' flanking sequences, thereby removing non-hybridising sequences that may interfere with the stability and antisense action of ribozymes *in vivo*.
- 3) Any number of different individual ribozyme units may be expressed on a single transcript. Simultaneous targeting of different sites within the HBV genome has the advantage of preventing the development of escape mutants (Appendix C3). Viral quasi-species that evade action of single ribozymes are easily selected due to the sensitivity of ribozymes to single base changes within the cleavage recognition sequence.
- 4) Since some cleavage sites within the target RNA remain inaccessible to both ribozyme and antisense action, an approach whereby a number of different sites are targeted simultaneously may prove to be synergistic. The cleavage of an accessible site may make a previously inaccessible region available for targeting.

The results of this study provide a compelling argument for the therapeutic application of these ribozymes in animal models of HBV infection. However, many factors need to be overcome in order to apply ribozyme-encoding genes in a clinical setting. These and other design considerations are discussed in detail in Chapter 5.

---



## 5.0 GENERAL DISCUSSION AND CONCLUSION

The studies presented in this thesis add significantly to the growing body of research on ribozymes targeted to HBV. In most cases, ribozymes have been shown to be specific to their target RNA sequence and are efficient inhibitors of both viral gene expression and replication in cell culture models of HBV infection. The clinical application of hammerhead ribozymes and other therapeutic ribozymes as future therapeutic agents for the treatment of HBV hinges on overcoming two important obstacles. Firstly, since hammerhead ribozymes are expressed endogenously from DNA-encoding sequences, ribozyme expression cassettes need to be effectively delivered to the HBV-infected liver. Secondly, as antiviral agents, therapeutic hammerhead ribozymes must be clinically efficacious and non-toxic *in vivo*. Prospects for overcoming these hurdles are dealt with in the following sections. In addition, important principles for the design of therapeutic hammerhead ribozymes are included.

### 5.1 Hammerhead ribozymes and HBV

#### 5.1.1 *Hammerhead ribozymes targeted to the HBx ORF*

Since the *trans*-activation function of HBx is regarded as a potential risk factor in the development of HBV-associated carcinogenesis, the inactivation of HBx is likely to be important for future approaches to therapy of chronic HBV infection. Hammerhead ribozymes presented in this thesis inhibited endogenous *HBx trans*-activation in primary hepatocellular carcinoma cells, indicating that they have imminent therapeutic potential as agents capable of preventing HBV-associated hepatocellular carcinoma.

Two studies conducted contemporaneously have corroborated the inhibitory effects of hammerhead ribozymes targeted to the *HBx* ORF of HBV described in Chapter 2. Yim *et al.* (2000) generated a yeast expression vector containing a hammerhead ribozyme *in cis* with an *HBx-lacZ* fusion construct under transcriptional control of the yeast copper-inducible chelatin promoter (*CUP1p*). The hammerhead ribozyme, when expressed in transiently transfected yeast cells, was able intermolecularly to cleave the target sequence, thus

---

disrupting the *HBx-LacZ* fusion mRNA. This resulted in histochemically negative (white) colonies on agar plates stained with the chromogenic substrate X-gal. This system, in which both ribozyme and target sequences are present on the same RNA strand, cannot, however, be used to infer the efficacy of hammerhead ribozyme-mediated *trans*-cleavage *in vivo*. In addition, as described earlier for snorbozymes, the intracellular environment of the yeast may be substantially different to that of the hepatocyte. Nevertheless, an interesting feature of this study is the fact that various catalytically inactive ribozyme variants, including an antisense RNA, were able to inhibit *lacZ* expression effectively with results similar to those for the active hammerhead ribozyme (Yim *et al.*, 2000). All these hammerhead ribozyme and antisense RNA variants correspond to the same region as the catalytically active ribozyme. The results in yeast independently suggest that an antisense mechanism without substrate cleavage may be responsible for inhibiting target RNA.

In a very similar experiment to that described in 2.4.3, two hammerhead ribozymes, which target different cleavage sites on the *HBx* ORF to those described here, successfully cleaved target *HBx* RNA *in vitro* (Kim *et al.*, 1999). However, a 100:1 molar ratio of ribozyme to substrate was needed in order to cleave 75% of the substrate in a one-hour reaction under standard *in vitro* cleavage conditions. In this same study, a reporter plasmid pSV2CAT was constructed expressing chloramphenicol acetyl-transferase (CAT) under control of the SV40 early promoter, which is susceptible to *trans*-activation by *HBx* (Twu and Robinson, 1989). The ribozymes constructed by Kim *et al.* (1999) were able to inhibit *HBx trans*-activation function (by reducing CAT activity) in transiently transfected HepG2 human hepatoma cells. This study did not, however, correlate a decrease in *HBx trans*-activation with variations attributed to differences in transfection efficiencies between culture plates. Nevertheless, these results are in agreement with the data presented in sections 2.4.3 and 2.4.4.

### 5.1.2 Hammerhead ribozymes as antiviral agents

Of the two early studies using hammerhead ribozymes targeted to HBV, only Beck and Nassal have tried, albeit unsuccessfully, to observe the *in vivo* effects of hammerhead ribozyme-mediated cleavage of HBV pgRNA (Beck and Nassal,

1995; von Weizsäcker *et al.*, 1992). Since *in vitro* experiments are usually devoid of cellular factors, there is little value in studies aimed at developing therapeutic ribozymes strategies without studying the effects of hammerhead ribozymes in an intracellular environment. Ribozyme activity has been shown to differ remarkably *in vitro* and in cultured cells, often yielding conflicting results (see section 5.2) (Beck and Nassal, 1995; Crisell *et al.*, 1993; Homann *et al.*, 1993; Tabler *et al.*, 1994).

Three studies, which were performed contemporaneously with those presented here, have tried to observe the antireplicative effects of hammerhead ribozymes targeted to HBV. Ribozymes have been targeted to the core region (Feng *et al.*, 2001a), the polyadenylation signal sequence (Feng *et al.*, 2001b) and different sites within the *HBx* ORF (Kim *et al.*, 1999). A hammerhead ribozyme was successfully targeted to the RNA sequence encoding the carboxy-terminus of the core protein in HepG2 cells that were transiently co-transfected with a ribozyme vector, its catalytically inactive counterpart, and a vector containing a replication-competent head-to-tail dimer of HBV (subtype *adr*) (Feng *et al.*, 2001b). Viral DNA extracted from lysed cells and from HBV particles in the culture medium was reduced by approximately 50% by the ribozyme-encoding vector. These results were reflected in similar inhibitions in HBsAg and HBeAg secretion. The inactive ribozyme control showed a 25% reduction in both viral DNA and antigen levels (Feng *et al.*, 2001b). In another study, the same authors targeted the polyadenylation signal region of the viral pgRNA for cleavage using a similar approach to that described for the anti-core ribozyme (Feng *et al.*, 2001a). This hammerhead ribozyme inhibited the production of intracellular viral RNA and DNA levels by approximately 70% compared to a 50% inhibition by the catalytically inactive ribozyme control (Feng *et al.*, 2001a).

The hammerhead ribozymes produced by Feng *et al.* (2001a) are similar in efficiency to those presented in Chapters 2 and 3 as well as by others using hairpin ribozymes, proving that other sites of the viral genome can be targeted successfully in cultured cells to inhibit viral replication. Generally, however, the specificity of hammerhead ribozymes targeted to HBV is low. The multimeric *cis*- and *trans*-cleaving ribozymes described in Chapter 4 represent a significant improvement on existing HBV ribozymes.

A serious concern for the development of any future antiviral strategy,

including the use of ribozymes, is the possibility of developing HBV mutant strains that are resistant to treatment. As was noted for lamivudine and other nucleoside analogues, the HBV genome is flexible enough to sustain substitution changes necessary for the development antiviral-resistant HBV strains. The effects of hammerhead ribozymes are no exception. The ease with which single base substitutions can confer resistance to ribozyme therapy must be a worrying factor for their clinical implementation. A single change within the catalytic site (the 5' GUC 3' cleavage triplet, for instance) can render the ribozyme functionally impotent. Targeting several sites on the HBV genome simultaneously (as was done in Chapter 4) may be the solution since the selective pressure of generating HBV strains that are resistant to a multi-faceted attack is likely to be too great a burden on any replicating virus. Clearly the latter approach represents a suitable option for clinical evaluation of hammerhead ribozymes *in vivo* in animal models of HBV infection.

## 5.2 Designing therapeutic hammerhead ribozymes

### 5.2.1 *The effects of ribozyme flanking sequences*

Hammerhead ribozyme specificity is determined by the flanking sequences of helices I and III, which hybridise to substrate RNA prior to cleavage. Theoretically, the hammerhead ribozyme annealing arms should be long enough to provide structural stability, specificity, and an adequate association rate (Birikh *et al.*, 1997b). Yet the annealing arms must be short enough to ensure reasonable catalytic turnover. Generally, for short unstructured substrate sequences, 7 to 8 nucleotides for each flanking arm provide the most favourable result (Lieber and Strauss, 1995). These ribozymes have been shown to function equally well both *in vitro* and *in vivo* (Bertrand and Rossi, 1994). The hammerhead ribozymes of this study were designed with the intention of ensuring maximal specificity and catalytic turnover.

Hammerhead ribozymes with short hybridising arms are less likely to anneal to sequences with single base changes and thus have a greater potential to discriminate target sequences. Long flanking sequences lack the discriminatory power to distinguish mismatches (Hertel *et al.*, 1996). Should the

---

position of the mismatch be close to the cleavage triplet, ribozyme-target association could be completely obstructed (Werner and Uhlenbeck, 1995). This was observed for ribozymes with hybridising arms of six nucleotides each that target the *tat* gene of HIV-1 in two different strains of the virus. Hammerhead ribozymes targeted to the mutant strain containing an adenosine 3' of the cleavage triplet significantly inhibited viral replication. No such effect was observed for the HIV-1 strain with a guanosine at the same site (Sun *et al.*, 1995).

The length of ribozyme helix III (the 3' arm) is more critical than helix I (5' arm). Asymmetrical hammerhead ribozymes have been constructed with only three nucleotides for helix I and over 100 for helix III. These ribozymes were shown to be effective at cleaving HIV-1 RNA (directed to the long terminal repeat-*gag* region) both *in vitro* and in transfected cells (Tabler *et al.*, 1994).

Some groups have reported that hammerhead ribozymes containing annealing arms greater than 30 nucleotides show effective and rapid cleavage *in vitro* and strong inhibition of target RNA expression in cultured cells (Crisell *et al.*, 1993; Homann *et al.*, 1993; Tabler *et al.*, 1994). The *trans*-cleaving ribozymes of section 4.4.1.2, which have 5' and 3' annealing arms that span 24 nt, produced a greater inhibitory effect than the equivalent ribozymes with shorter arms (16-18 nt). However, it is unclear to what extent the observed inhibition is due to an increased intracellular ribozyme concentration. These latest results appear to conflict with the results of Lieber and Strauss (1995). The rate-limiting step *in vivo* for ribozyme-catalysed reactions is known to be the annealing of the ribozyme arms to complementary sequences on the target RNA. Since single-turnover conditions govern ribozyme action in the intracellular environment, the greater inhibitory power of ribozymes over antisense RNAs lies in their ability to cleave their target once annealed. It appears that target RNA is largely inaccessible in an intracellular environment. Since RNAs *in vivo* are found in varying secondary and tertiary conformations, Bertrand and Rossi (1996) suggest that cellular proteins may facilitate the annealing of ribozymes with long hybridising arms (discussed in section 5.2.2.2). Hammerhead ribozymes which were designed to target the HBV encapsidation signal indicate that longer ribozyme arms facilitate binding by interacting with single-stranded regions that are near the ribozyme cleavage site and which are not accessible to binding with ribozymes comprising

---



shorter flanking arms (Beck and Nassal, 1995). This is supported by the observation that single-stranded cognate sequences are indispensable for successful recognition of ribozyme hybridising arms for the substrate mRNAs (Rittner *et al.*, 1993). At present, there are no clear rules governing the length of annealing arms for intracellular ribozyme action, and each system needs to be determined empirically.

### 5.2.2 Finding suitable target sites for ribozyme cleavage

For long, structured target RNA molecules, which undergo secondary or tertiary folding, the kinetic rate-limiting step is often the association of ribozymes with their target RNA. The RNA secondary structure may hide accessible cleavage sites and prevent effective ribozyme binding, which possibly explains why ribozymes targeted to different sites on the same mRNA strand *in vitro* show varying cleavage activities (Hendrix *et al.*, 1996).

There appears to be an additional disparity between the observed ribozyme effects *in vitro*, and ribozyme function *in vivo* (in cell culture or animal models). Irrespective of these discrepancies, most therapeutic approaches first test newly constructed ribozymes in a chemically isolated environment. Experiments that test ribozyme cleavage parameters *in vitro* still represent the gold standard for ribozyme selection. *In vitro* cleavage experiments may yield important information regarding the catalytic properties of the constructed ribozymes, but often they offer little insight into the intracellular effects of ribozymes on their target RNAs.

Generally, a trial and error approach, although laborious, is often the most effective method to determine which sites will be best suited for ribozyme cleavage (Usman and Stinchcomb, 1996). However, for long mRNA substrates or for target mRNAs suspected of concealing ribozyme-accessible sites, several combinatorial screening techniques have been devised to determine ribozyme-accessible regions and effective cleavage sites.

---

### 5.2.2.1 Probing RNA secondary structure using computer algorithms

RNA folding programs, such as Mfold<sup>®</sup> (Genetics Computer Group, WI, USA) and RNAdraw<sup>™</sup> (Matzura and Wennborg, 1996), are used to predict RNA secondary structures based on global free-energy calculations (Matzura and Wennborg, 1996; Zuker and Jacobson, 1998; Christoffersen *et al.*, 1994; Sczakiel and Tabler, 1997). However, these programs are still in their infancy and, although they predict certain structural properties of RNA, they are currently inept at accurately predicting the correct RNA secondary folding, let alone determining accessible ribozyme cleavage sites. In some cases, predictions generated by such programs contrast directly with experimentally verified sites reported to be susceptible to ribozyme cleavage (Dropulic and Jeang, 1994). Most importantly, these programs fail to predict the secondary and tertiary RNA structure generated by associations with proteins and other factors *in vivo*. Although Mfold was used to determine HBx RNA secondary structure (Chapter 2), the program was unable to predict accurately accessible regions for nucleic acid hybridisation. Hammerhead ribozyme HBx:Rz3<sub>1607</sub> targeted one of the least accessible sites on the HBx ORF and yet proved to be the most effective ribozyme *in vitro* and in cell culture transfections.

### 5.2.2.2 The accessibility of target RNA for ribozyme cleavage *in vivo*

RNAs within the cell associate with an array of proteins. Within the nucleus, heterogeneous nuclear proteins (hnRNPs) and small nuclear proteins (snRNPs) are often complexed to mRNAs. Whilst in the cytoplasm, mRNAs readily combine with hnRNPs, rRNAs and proteins associated with the translation complex. These proteins may either facilitate or inhibit ribozyme binding (Casas-Finet *et al.*, 1993; Khan and Giedroc, 1992; Portman and Dreyfuss, 1994). Proteins such as a peptide polymer derived from the consensus sequence of the carboxy-terminal domain of the hnRNP A1 protein (Herschlag *et al.*, 1994) and HIV-1-encoded NCp7 (Tsuchihashi *et al.*, 1993) were shown to bind non-specifically to RNA. The proteins possess unwinding activity allowing, in some cases, a 1000-fold increase in the hybridisation rate (Bertrand and Rossi, 1994; Herschlag *et al.*, 1994). For the most part, however, proteins associated with mRNAs *in vivo* prevent the

annealing of ribozymes to target sequences and represent a hurdle for the development of effective inhibitory endogenous ribozymes. Recently, Kato *et al.* (2001) developed a ribozyme expression vector, which includes an RNA motif with RNA helicase binding ability linked to a 5' ribozyme-encoding sequence. The unwinding of secondary structures inherent in intracellular target RNA molecules was shown to improve the catalytic efficiency of the designed ribozyme (Kato *et al.* 2001).

### 5.2.2.3 Combinatorial screening techniques for finding ribozyme cleavage sites

Ribozyme activity can be selected from a large ribozyme library with randomised substrate binding sequences (helices I and III for hammerhead ribozymes). A random pool of ribozymes, or ribozyme library, is challenged *in vitro* to cleave target RNA in order to determine susceptible cleavage sites (Lieber and Strauss, 1995). The sites are often selected within an entire transcript and no prior knowledge of the transcript sequence is needed. Cleavage products generated by a random ribozyme library can be tailed, amplified by RT-PCR, and cloned into vectors. Clones can be sequenced to identify the most efficient cleavage sites. Ribozymes discovered using this approach efficiently cleaved human-growth hormone mRNA *in vitro* and strongly inhibited target mRNA expression in transduced cell cultures (Lieber and Kay, 1996; Lieber and Strauss, 1995). An adaptation of this technique was used by zu Putlitz *et al.* (1999) to generate a random hairpin ribozyme library targeted to HBV pregenomic RNA (see section 1.4.3).

Another screening technique utilised a random oligodeoxynucleotide (ODN)-library to probe RNA folded in its secondary structure conformation (Birikh *et al.*, 1997a; Christoffersen *et al.*, 1994). RNase H can be employed to degrade any RNA hybridised to specific ODN probes. The resulting fragments are resolved and identified on denaturing polyacrylamide gels. The fragments generate an RNase H digestion pattern, which is compared to appropriate markers. This technique is a lot simpler than that used by Lieber and Strauss (1995) but reveals only broad hybridisation regions and not necessarily sites specific to ribozyme action.

---

A similar screening technique was used to determine accessible ribozyme cleavage sites in cellular extracts from target RNAs produced endogenously (Castanotto *et al.*, 2000; Scherr and Rossi, 1998). This allows for screening of RNAs in their 'native' state. These target RNAs are folded into secondary structure conformations along with associated cellular proteins. Briefly, antisense ODNs, designed to hybridise to potential ribozyme cleavage sites, can be added to cellular extracts containing exogenously expressed target mRNA. Both RNA-DNA hybrids and ODNs undergo nuclease degradation and the resulting RNA fragments are amplified and quantitated using primers specific for the target mRNA. A direct correlation exists between the degree of antisense ODN-induced target RNA degradation and the accessibility of the respective target site for hammerhead ribozyme cleavage (Scherr *et al.*, 2001; Scherr *et al.*, 2000).

Screening techniques for accessible sites *in vitro* do not necessarily result in improved cleavage *in vivo*. Although Birikh *et al.* (1997) have shown that their method represents a 150-fold improvement on predictions using the Mfold program, target accessibility screening procedures need to incorporate factors that may influence RNA folding *in vivo*.

### 5.2.3 Factors governing *in vivo* ribozyme activity

In addition to the accessibility of the target mRNA for ribozyme cleavage, there are a number of other important factors that influence the ability of ribozymes to inhibit the expression of target RNAs *in vivo*. An important determinant for the optimal endogenous ribozyme production is the nature of the expression system or cassette, which should include elements for regulating intracellular ribozyme concentration and persistence (Yu *et al.*, 1993). The cassette should ensure the correct ribozyme structure and stability *in vivo* (Rossi and Sarver, 1990). Elements within the cassette can also facilitate co-localisation of ribozyme and target RNA in the same cellular compartment (Bertrand and Rossi, 1996; Castanotto *et al.*, 2000; Kawasaki *et al.*, 2000). Since the intracellular concentration appears to be a vital factor for endogenous ribozyme efficacy, the choice of promoter used for RNA expression is a crucial component of the design of a ribozyme expression cassette.

---

Promoters that constitutively express ribozyme-encoding RNAs are obviously desirable since such elements generate an abundance of intracellular RNA. The RNA polymerase II (Pol II) system produces mRNAs necessary for translation into proteins, but has also been widely used for the expression of ribozymes. The cytomegalovirus (CMV) promoter has been used previously to express ribozymes (Weerasinghe *et al.*, 1991) and was used in expression vectors described in this thesis to ensure an equal and persistent expression of ribozyme and target genes in transfected cells. Some Pol II promoters have the advantage of being tissue specific and can be induced or regulated. Other Pol II promoters used to express endogenous ribozymes include retroviral promoters (Leopold *et al.*, 1995), the simian virus 40 (SV40) promoter (Weerasinghe *et al.*, 1991), the  $\beta$ -actin promoter (Ojwang *et al.*, 1992) and the U1 snRNA promoter (Bertrand *et al.*, 1997). Pol II-derived transcripts have ancillary sequences at both 5' and 3' ends, namely 5' and 3' untranslated regions, a 5' m<sup>7</sup>GpppG cap structure and a 3' poly(A) tail. These additional sequences ensure mRNA stability, significantly prolonging mRNA intracellular half-life. Moreover, these sequences may be necessary for cytoplasmic localisation, and for functional recognition by the translation machinery. The multimeric *cis*- and *trans*-cleaving ribozymes produce 5'- and 3'-trimmed RNA monomeric units from a CMV-derived transcript. These ribozymes survive long enough to inhibit target RNA more efficiently than single-unit ribozymes, which possess non-annealing flanking sequences. Thus the stabilising effects of Pol II-derived transcripts appear not to be critical and may in fact hinder ribozyme action *in vivo*. Ancillary nucleotide sequences, which are often hundreds of nucleotides long, may obstruct ribozyme *trans* cleavage by masking hybridisation sequences necessary for the annealing of the ribozyme with its target RNA. Additionally, factors of the riboprotein complex may also bind to Pol II-derived mRNAs, resulting in encumbered transcripts that are less likely to interact freely with target RNAs *in vivo*.

Polymerase III promoters naturally drive the expression of small RNAs such as tRNAs, 5S rRNA and most snRNAs. Transcript expression levels for Pol III promoters are significantly higher (Cotten and Birnstiel, 1989) than for Pol II promoters and only short ancillary sequences are added to each transcript. Pol III promoters have thus been suggested as the optimal promoter choice for the generation of endogenous ribozymes (Kawasaki *et al.*, 2000). However,



questions remain concerning the intracellular stability and half-life of Pol III-derived transcripts.

Anti-HBV hairpin ribozymes generated by zu Putliz *et al.* (1999) made use of both Pol III- and Pol II-derived promoters without any significant difference observed in ribozyme expression or efficacy in Huh7 cells. Similarly, hammerhead ribozymes generated by Beck and Nassal (1995) were derived from a Pol III promoter system and although expression was high, no clear improvement of ribozyme efficacy was observed. In the Beck and Nassal study, increased ribozyme expression was not seen as the reason for failed ribozyme efficacy in transfected cells.

Ribozyme inhibition of gene expression is greatly facilitated by localising both ribozymes and their target RNA to the same intracellular compartment (Arndt and Rank, 1997; Castanotto *et al.*, 2000; Sullenger and Cech, 1993). Each ribozyme application is different, however, and the nature of the target mRNA needs to be carefully studied prior to establishing a co-localisation strategy. Directing target mRNA and ribozymes to the same subcellular region is often achieved by utilising auxiliary sequences which are often promoter-derived. These sequences include: viral packaging signals (Pal *et al.*, 1998; Sullenger and Cech, 1993), and either nuclear localisation signals (Michienzi *et al.*, 2000; Michienzi *et al.*, 1998) or signals which allow co-localisation of ribozymes and their pre-mRNA targets (Lee *et al.*, 1999).

Signals which direct the trafficking of target pre-mRNAs can be attached to ribozymes, enabling co-localisation in the same subcellular compartment. This is best illustrated by the introduction, within the U1 snRNA coding region, of ribozymes that have 3'-end attached sequences which are part of the 3' untranslated regions (UTR) of certain mRNAs. Such ribozyme-encoding transcripts were channelled to 5' splice sites of targeted HIV-1 *rev* pre-mRNAs (Michienzi *et al.*, 1996).

The promoter used to drive expression of ribozyme encoding transcripts can be exploited for its localisation potential (some examples were given in section 1.2.2.3). HIV-1 utilises a tRNA<sup>Lys3</sup> as a specific primer for reverse transcription. Ribozymes incorporated within the tRNA<sup>Lys3</sup> coding region were able to generate a chimeric ribozyme-tRNA<sup>Lys3</sup> transcript which co-packages along with HIV-1 into proviral particles and cleaves HIV RNA simultaneously with

---

reverse transcriptase priming (Welch *et al.*, 1997). Similarly, tRNA<sup>Val</sup> (Yuyama *et al.*, 1992) and Adenoviral VAI (Prisley *et al.*, 1997) Pol III promoters embed regulatory elements within their naturally transcribed regions. Ribozyme sequences can be inserted within stem-loop structures of either tRNA<sup>Val</sup> or Adenoviral VA1 promoter systems to achieve high-level expression, ribozyme structural stability, and either nuclear or cytoplasmic ribozyme localisation.

### 5.2.4 Summary

Presently, the engineering of hammerhead ribozymes as therapeutic molecules represents a challenge with many variables. There are several design constraints when developing therapeutically effective hammerhead ribozymes *in vivo*. Hammerhead ribozymes, which are specifically designed and developed to inactivate the expression of target viral or cellular RNA, must be selected by addressing the following fundamental properties:

- 1) Hammerhead ribozymes should be present in higher molarity than their target RNA within the cell and must possess a functional and stable conformation under intracellular physiological conditions.
- 2) Hammerhead ribozymes must be specific to accessible target sites on the substrate mRNA for efficient cleavage and, if possible, possess catalytic turnover.
- 3) Endogenous hammerhead ribozymes should be constitutively and persistently expressed and directed to the same cellular compartment as their target mRNAs.
- 4) Presynthesized ribozymes or ribozyme-encoding sequences must be efficiently delivered to a large percentage of the target cell population.

### 5.3 Delivery of ribozymes

One of the most important requirements for all nucleic acid-based therapeutic strategies remains that of an efficient delivery mechanism. In order to function as therapeutic agents, ribozymes must be efficiently delivered to the appropriate tissue and cell type. Once inside the cell, ribozyme-encoding genes or

---

presynthesized ribozyme sequences should downregulate their respective target RNA and have pharmacologically significant effects. With regard to hammerhead ribozymes, there are two general methods employed for delivery into target cells *in vivo*. Firstly, ribozymes can be chemically presynthesized as oligoribonucleotides and delivered directly as exogenous agents. Secondly, ribozymes can be encoded as a DNA sequence, incorporated into an expression cassette, and delivered to target cells for endogenous ribozyme gene expression.

Direct or exogenous delivery of presynthesized ribozymes is an attractive therapeutic option. Concerning their pharmacological properties, presynthesized ribozymes are chemotherapeutic agents and in relation to other antiviral agents are considered to possess low cytotoxicity and high target specificity. Nevertheless, these ribozymes need significant chemical modifications in order to function therapeutically. Generally, direct delivery of unmodified RNA is problematic owing to the instability of RNA in bodily fluids. For example, unmodified RNA exhibits a typical half-life of approximately 0.1 to 20 minutes in serum (Beigelman *et al.*, 1995). Presynthesized ribozymes, whether chemically modified or not, are either administered naked or as a conjugate within cationic lipid vesicles. In contrast, endogenous expression of ribozyme-encoding genes usually makes use of a viral vector. Various vector systems, both viral and non-viral, have been utilised to deliver ribozyme-encoding cassettes within cells. Endogenous strategies rely on a biological approach towards achieving effective therapeutic action. Genes are native to any cellular environment and exploit the molecular machinery of the host cell irrespective of their biological origin. Thus, ribozyme-encoding genes can be constructed, produced and tested through the application and malleability of recombinant technology. Additionally, unlike the expression of protein-encoding genes, ribozyme-encoding genes can be expressed from any of the three cellular RNA polymerases. This specifically fine-tunes their intracellular expression and localisation. Irrespective of the present risks associated with the delivery and expression of gene sequences, gene-based approaches offer greater potential as future therapeutic agents owing to their specificity and low toxicity.

At present, delivery strategies for endogenous gene expression are less established for clinical application than exogenous delivery approaches. Significant progress in presynthesized ribozyme research, which utilises a more

orthodox pharmacological approach to therapy, has streamlined these ribozymes for clinical development. Nevertheless, significant progress is being made in developing suitable delivery strategies for gene therapy applications. Most notable is the research conducted in generating cationic liposomes as carriers of expression vectors. Presynthesized ribozymes remain an important component of hammerhead ribozyme therapeutics and deserve further mention prior to a discussion of delivery strategies aimed at endogenous ribozymes.

### 5.3.1 *Presynthesized hammerhead ribozymes*

Presynthesized ribozymes, if chemically modified, can remain free from nucleolytic attack for several days in serum, and for several hours in nuclear extracts (Heidenreich *et al.*, 1994; Heidenreich *et al.*, 1996). In order to retain ribozyme catalytic activity and improve stability, three types of modifications are necessary (Usman and Blatt, 2000; Usman and Stinchcomb, 1996). These include 2'-sugar modifications (Hendry *et al.*, 1992; Perreault *et al.*, 1990), phosphate backbone modifications (Ruffner and Uhlenbeck, 1990; Shimayama *et al.*, 1993) and base change modifications (Grasby *et al.*, 1993; Usman and Stinchcomb, 1996). Terminal (3'-end) stem-loop structures, present on unmodified ribozyme transcripts, have been shown to limit exonuclease degradation *in vivo* (Sioud *et al.*, 1992; Sioud *et al.*, 1994). However, these latter modifications were tested in cell culture and not in serum. The aim in developing optimally designed synthetic hammerhead ribozymes is to generate these agents with the minimum number of chemical modifications to ensure their increased serum longevity and therapeutic efficacy.

There have been two reported clinical trials using nuclease-resistant synthetic hammerhead ribozymes (Usman and Blatt, 2000). A synthetic ribozyme has been developed to inhibit the mRNA of *Flt-1* (VEGF-R1), a high-affinity receptor for Vascular Endothelial Growth Factor (VEGF) that is involved in tumour angiogenesis (Pavco *et al.*, 2000). This ribozyme may be useful in preventing tumour progression and is thus applicable for the treatment of several different cancers. Synthetic ribozymes have also been targeted to the 5'-UTR of the RNA genome of hepatitis C virus (HCV) for treatment of chronic HCV infection (Macejak *et al.*, 2000). Although the trials conducted thus far showed

promising results, there are some concerns regarding the safety of these agents. Their general toxicity following prolonged treatment remains to be determined. Moreover, since synthetic ribozymes are much larger (macromolecules) than conventional pharmacological agents, they possess relatively poor pharmacokinetic properties *in vivo*. These additional drawbacks really need to be overcome for synthetic ribozymes to be used widely as novel therapeutic agents (Usman and Blatt, 2000).

### **5.3.2 Viral-mediated delivery of ribozyme expression cassettes**

Efficient delivery of ribozyme-encoding sequences relies on advances made in the development of viral vectors for gene therapy applications. A number of viral vectors have been studied regarding their ability to introduce genes into target cells (Morgan and Anderson, 1993). Each system has both advantages and disadvantages in their therapeutic application. Discussed below are some of the viral models used thus far for delivery of endogenous ribozymes to target tissues and cells. Viral-mediated delivery of anti-HBV hammerhead ribozymes is included in the discussion.

#### **5.3.2.1 Retroviral vectors**

Retroviral vectors are by far the most widely studied viral delivery vehicle for endogenous ribozyme expression. Retroviruses transduce a plethora of different cell types with high efficiency, and can stably integrate into the host cell genome. Persistence of ribozyme expression can be ensured owing to the maintenance of any introduced genetic material in progenitor cells. Consequently retroviruses are ideally suited for a range of different therapeutic applications (Morgan and Anderson, 1993). The shortcomings of retroviral therapy, however, include the inability to infect non-dividing cells (with the exception of lentiviruses). There are additional concerns regarding the safety of retroviral-delivery strategies since random retroviral integrants may elicit oncogenesis. Retroviruses are known to activate the host immune system by eliciting complement pathways. These pathways may in turn inactivate any transduced retroviruses. Additionally, there exists the possibility of reconstituting an active virus through recombination

---



events within packaging cell lines. These cells are tailored to reconstitute replication-incompetent recombinant retroviruses.

A number of infectious or acquired diseases, such as HIV (Bai *et al.*, 2001) and Moloney murine leukaemia virus infection (Lowenstein and Symonds, 1997; Sun *et al.*, 1994), as well as various cancers (Funato *et al.*, 2000; Halatsch *et al.*, 2000; Kobayashi *et al.*, 2001; Shore *et al.*, 1993) have been targeted using different ribozyme-encoding retroviral vectors. One of the most promising applications of retroviral-delivered ribozyme therapy is for HIV infection, where progenitor T cells are stably transduced with ribozyme-expressing sequences that target HIV RNA. These T cells are then tested for their resistance to HIV infection. Thus far, practical efficacy in a clinical setting has been achieved for the *ex vivo* transduction of ribozyme-encoding sequences into T cells or bone marrow stem cells. These transformed cells, when reintroduced into patients infected with HIV, significantly reduce levels of viraemia in those patients for up to a year post-transplantation (Bertrand and Rossi, 1996). Although these studies are encouraging, *ex vivo* retroviral delivery of ribozymes for chronic HBV infection is not an option. Moreover, since hepatocytes (including those infected with HBV) are largely quiescent, retroviral applications in general are unlikely to prove efficacious. Retroviruses are unsuitable vectors for the delivery of *cis*- and *trans*-acting multimeric ribozyme cassettes since self-cleavage prior to virion packaging would render the construct unviable.

### 5.3.2.2 Adenoviral vectors

Adenoviruses represent a popular alternative to retroviral-mediated delivery of ribozymes. This viral vector system has the advantage of infecting a wide variety of dividing and non-dividing cells without integrating into the host cell genome. Importantly, adenoviral vectors have a propensity for uptake by the liver (Smith *et al.*, 1993). Adenoviruses are present extrachromosomally as epigenetic elements within transduced cells. However, a serious limiting factor for sustained adenoviral therapy remains the transient expression of virally-encoded genes. The intracellular adenoviral vector is diluted-out as a result of repeated cellular division. Repeated administration of adenoviruses fails due to the effects of an efficient immune system clearance of adenoviruses in serum. Both a humoral and

---

cell-mediated response are launched against viral proteins, severely restricting the efficacy of adenoviral gene therapy approaches (Chirmule *et al.*, 1999). In addition, there are concerns regarding the toxicity of adenoviral-mediated delivery approaches.

A number of studies have shown the *in vivo* effects of ribozyme-encoding recombinant adenoviruses (Huang *et al.*, 1997; Patricia *et al.*, 2001; Usui *et al.*, 2001). Ribozyme-expressing adenoviral vectors were infused by vein injection into mice that were transgenic for human growth hormone (hGH). Ribozymes directed against *hGH* mRNA were able to eliminate 96% of the expressed mRNAs in this model (Lieber and Kay, 1996).

A recent application of ribozyme-encoded adenoviral gene therapy involved the use of U1 snRNA-ribozyme chimaeras that targeted the inhibition of the multifunctional growth factor (scatter factor/hepatocyte growth factor [SF/HGF]) and its receptor *c-met*. These have been implicated in multiple human malignancies, including gliomas. Both adenoviral and liposome vectors carrying endogenous ribozymes were able to inhibit the growth of intracranial glioma xenografts in infected/transfected rats, thus prolonging survival (Abounader *et al.*, 2002).

### 5.3.2.3 Adeno-associated viruses (AAVs) and other viral systems

In addition to the two vector systems described above, viral vectors such as the adeno-associated virus (AAVs) and hepatitis delta virus (HDV) (Hsieh and Taylor, 1992) have also been used to transduce ribozyme-encoded expression cassettes. Unlike adenoviruses, AAVs have the advantage of integrating into a specific site on chromosome 19, leading to stable transduction of infected cells. Furthermore, AAVs do not elicit inflammation or a cell-mediated immune response (Hernandez *et al.*, 1999). AAVs are limited to a packaging insert of 4500 nt, which makes them ideally suited for ribozyme gene therapy, since ribozymes occupy a relatively small amount of sequence space. Nevertheless, relative to other viral delivery models, ribozyme-encoding AAVs have only recently been applied. This may be a result of the technical difficulties reported to date in establishing stable packaging cell lines since AAVs usually require co-

---

infection with helper-like adenoviruses or herpes virus. Additionally, producing high titres of recombinant AAVs for further use is inherently difficult.

AAV-encoding ribozymes have been shown to represent a potentially effective therapeutic strategy for dominantly inherited diseases that arise from malfunctional or misfolded protein (Lewin and Hauswirth, 2001). Such is the case for autosomal dominant retinitis pigmentosa (ADRP), which is most commonly associated with mutations in the gene encoding rhodopsin. Seminal studies were conducted using AAVs encoding ribozymes directed to the P23H mutation of rhodopsin. Ribozymes cleaved mutant rhodopsin mRNA and prevented photoreceptor degeneration in transgenic rats (LaVail *et al.*, 2000; Lewin *et al.*, 1998). Ribozyme treatment protected functional vision in these transgenic rats for periods of up to eight months following AAV-ribozyme injection (LaVail *et al.*, 2000).

Ribozymes expressed from AAVs have been tested in cultured cells targeting HIV (Horster *et al.*, 1999) and HCV (Welch *et al.*, 1998). AAVs have also been targeted, in *ex vivo* studies, to both E6 and E7 genes of human papilloma virus (HPV), whose continued expression represents an oncogenic risk factor in HPV-induced human cancers (Kunke *et al.*, 2000).

Other DNA-based viral vectors currently under consideration for the delivery of ribozyme-encoding genes are the herpes simplex virus (HSV) and simian virus 40 (SV40). These vectors may be potentially useful for the delivery of antiviral hammerhead ribozymes to HBV-infected hepatocytes. Although HSV infects quiescent cells and can include a large insert, it has an erratic life cycle. HSV has the propensity to lyse the host cell or enter into a latent phase of infection (Kriskey *et al.*, 1998a; Kriskey *et al.*, 1998b). SV40 is a relatively new viral vector and has yet to be tested completely for safety and efficacy. Nevertheless, SV40 can transduce a broad range of cell types, including quiescent cells. Although SV40 can accommodate only a 5000 nt insert, this may suit future application involving the delivery of ribozyme-encoding genes (Goldstein *et al.*, 2002; Jayan *et al.*, 2001; Strayer, 2000).

---

### 5.3.3 Cationic liposomes and non-viral delivery strategies

Most non-viral delivery strategies employ a transfection-based approach for delivery into mammalian cells. Both presynthesized ribozymes as well as ribozyme-expressing vectors require carrier molecules since naked nucleic acids are either easily degraded or inefficiently transfected. Various cationic liposome formulations have been extensively studied as exogenous and endogenous ribozyme delivery systems. These include cationic lipids for transfecting presynthesized ribozymes (Düzgünes and Felgner, 1993), antisense- and ribozyme-encoding DNA (Akhtar *et al.*, 2000; Castanotto *et al.*, 1997), and antisense RNA (Malone *et al.*, 1989) into mammalian cells. For presynthesized ribozymes, other non-viral delivery strategies can be used, such as the conjugation of oligonucleotides to cholesterol or poly-L-lysine (Leopold *et al.*, 1995).

Various methods have been employed to direct cationic liposomes to target cells by conjugating the liposomes to ligands that interact with receptors on the target cell (Remy *et al.*, 1995). Hepatocyte-specific receptors such as the asialoglycoprotein receptor (Ashwell and Harford, 1982) and the remnant receptor of Apolipoprotein E (Mahley, 1988) may be targeted using appropriate ligand-liposome conjugates for the delivery of anti-HBV therapeutic nucleic acids. However, there have been a number of drawbacks in studies aimed at targeting the asialoglycoprotein receptor (Rensen *et al.*, 1996). These include the preferential uptake of lactosylated particles by the galactose receptor on Kupffer cells, and the decreased density of asialoglycoprotein receptors on hepatocytes of chronically-infected HBV individuals (Sawamura *et al.*, 1984).

Notably, there are additional complications arising from the use of cationic liposomes in general. Nucleic acid-liposome complexes (lipoplexes) are often sequestered into endosomes on entry into target cells, thus diminishing their therapeutic effect. To prevent this, pH-sensitive liposomes are used in addition to membrane-disrupting peptides (Düzgünes *et al.*, 2001) and are incorporated into cationic liposomes in order to disrupt the endosomal membrane and release liposomal contents into the cytoplasm of the target cell. Questions still remain regarding the overall therapeutic efficacy of liposome-based exogenous delivery techniques. At present, cationic liposomes do not efficiently

---

target a particular tissue or cell type and inefficient target non-dividing cells (Düzgünes *et al.*, 2001). This raises concerns regarding their application as delivery vehicles targeting the liver, which is largely composed of quiescent cells. In addition, lipid formulations may have undesirable toxic effects. Although, as yet, non-viral delivery systems lack the cellular specificity of viruses, viral delivery systems are unlikely to be widely used for therapeutic purposes in the near future owing to concerns regarding their safe implementation. Thus, non-viral delivery systems may well prove to be more effective delivery vehicles for anti-HBV hammerhead ribozyme expression vectors. Further refinements are clearly necessary, however, for liposomes to be used successfully in a clinical setting.

## 5.4 Conclusion

The discovery of the catalytic nature of RNA challenges the conception that nucleic acids are merely inert repositories of information. RNA enzymes, or ribozymes, profoundly affect fundamental biochemical processes within the cell. This has prompted the theory of an ancient role for RNA in the evolution of life. Most naturally-occurring RNA catalysts function alongside proteins and other cellular factors. However, a number of small ribozymes discovered in unique organisms can function as independent RNAs and usually only require metal ion cofactors for catalysis.

The group of small ribozymes, which include the hairpin and hammerhead variety, are readily designed to hybridise to a complementary RNA sequence for the site-specific endonucleolytic cleavage in *trans* of the substrate phosphodiester backbone. Cleaved RNAs are thus rendered inactive. Since engineered ribozymes are specific for a target RNA sequence and can inhibit the phenotypic expression and/or the propagation of downstream products of RNA, they are applicable as therapeutic molecules for gene “knockdown” applications. Viral diseases in particular, which replicate and/or express unique RNA sequences, represent ideal targets for the use of therapeutic ribozymes.

Treatment of chronic HBV infection is a global medical objective and since most chemotherapeutic approaches used to date have only a modest effect on clearing viral infection, there exists a need for novel antiviral therapeutic agents. At present, patients treated with existing agents continue to be at risk for

---



cirrhosis and HCC. Future developments of novel nucleoside or nucleotide analogues may prove to be beneficial (Zoulim and Trepo, 1999). However, the emergence of nucleoside analogue-resistant strains of HBV remains a concern should prolonged treatment be necessary for removal of viral infection (Delaney *et al.*, 2001).

In the present study, the *HBx* ORF of HBV was selected as a sequence for the targeting action of endogenously expressed hammerhead ribozymes owing to: 1) the role of HBx in HBV-associated HCC; 2) the presence of HBx-encoding sequences within all viral transcripts, including the viral pregenome; and 3) the multifunctionality of HBx-encoded sequences, which overlap with polymerase and a number of viral *cis*-elements. Hammerhead ribozymes that efficiently cleaved *HBx* RNA *in vitro* significantly inhibited the *trans*-activation function of HBx when produced from an expression cassette in transfected liver-derived cell cultures. This included the inhibition of endogenous HBx *trans*-activator function in primary HCC cells. Apart from preventing the expression of the viral oncogene, HBx, these ribozymes behaved as general antiviral agents and were able to inhibit viral gene expression and markers of viral replication in cell culture models of HBV infection. Use was made of a plasmid containing a modified HBV sequence in which the preS2/S region was replaced by DNA encoding EGFP, thus allowing for the sensitive *in situ* measurement of ribozyme action in transfected cells. Ribozyme-modulation of EGFP activity *in situ* was accurately corroborated by measurements of viral HBsAg and HBeAg secretion. However, the exact mechanism of the ribozyme-induced inhibitory effects remains unclear. Both ribozyme cleavage and antisense-mediated effects may be responsible for the action of hammerhead ribozymes in cultured cells. Different ribozymes when applied simultaneously have an additive effect on the inhibition of viral gene expression. This feature was exploited by a multimeric ribozyme design that produces independent hammerhead ribozyme molecules from a single expressed transcript. The increased inhibitory effect observed by the introduction of multimeric ribozymes *in vivo* was either a result of an increase in ribozyme concentration or due to the simultaneous targeting of different sites on the target RNA. Additionally, independent processed ribozymes possessed trimmed 5' and 3' termini, which may, if uncleaved, interfere with the action of ribozymes *in vivo*. The most elaborate multimeric hammerhead ribozyme

---

---

construct, which contained twenty-four *cis*- and *trans*-cleaving hammerhead ribozyme units (24-mer), was highly effective at reducing markers of viral replication in cell culture. The 24-mer, multimeric ribozyme system, represents a significant improvement on previously constructed single-unit ribozymes or antisense RNAs and can be considered for application in gene therapy clinical trials.

The knowledge obtained from using ribozymes as antiviral agents may add value to other gene-based therapeutic strategies such as the development of dominant-negative mutants and DNA vaccines. The therapeutic potential of hammerhead ribozymes has been clearly shown *in vitro* and in transfected cells. However, it remains important to determine the efficacy of these agents in experimental or established animal models of infection, such as in DHBV, WHV or in transgenic mice. Factors that can be evaluated in these animal models include: the specificity of ribozyme gene therapy for the targeted gene; the stability and potential toxicity of the therapeutic expression cassette and its delivery to, and expression in, infected and non-infected hepatocytes. Moreover, since viral cccDNA has a long intracellular half-life (Whalley *et al.*, 2001), the duration of antiviral therapy required to eradicate viral infection remains unknown. These factors must be addressed when choosing a suitable delivery vehicle.

Throughout the last decade, hammerhead ribozymes have been extensively applied as therapeutic molecules for the inhibition of gene expression in cell culture (Agrawal and Zhao, 1998; Lewin and Hauswirth, 2001). For the treatment of HBV chronic infection, hammerhead ribozymes presented in this thesis may well slow the progression of liver disease and improve the quality of life of chronic carriers by blocking viral gene expression. Additionally, by decreasing the viral load and/or by eliminating the presence of viral proteins such as HBx in infected hepatocytes, the onset of cirrhosis and HCC may be prevented. The delivery of hammerhead ribozyme-encoding genes, however, remains a significant hurdle. The lack of an effective delivery strategy has hampered the application of hammerhead ribozymes *in vivo* in animal models of HBV infection. Nevertheless, many ribozyme applications have, using existing viral and non-viral delivery vehicles, reached clinical evaluation and novel delivery systems continue to be discovered. Once shown to be safe and efficacious in living animals, hammerhead ribozyme gene therapy of HBV

---

infection may act alone or complement existing or future therapeutic strategies, such as interferon alpha, nucleoside/tide analogues, dominant negative mutants and peptide or DNA vaccines. The results presented in this thesis are encouraging and auger well for the future development of therapeutic hammerhead ribozymes for the treatment of chronic HBV infection.

---

## 6.0 APPENDICES

### A Standard Laboratory Methods

#### A1 *Bacterial transformation*

##### A1-1 *Preparing competent E.coli*

200 ml LB medium (Appendix B3-1) was inoculated with glycerol stocks of *E.coli* strains: XL1-Blue, DH5 $\alpha$  or GM2929, and allowed to grow until a spectrophotometric cell density of 0.4 at A<sub>600</sub>. Cells were placed on ice for 10 minutes followed by centrifugation at 4000xg in 50 ml tubes (Nunc, Denmark). Pellets were resuspended in 5 ml sterile Transformation Buffer (Appendix B1-6), pooled into two tubes and placed on ice for 15 minutes. Samples were then centrifuged at 2000xg for 5 minutes. Pellets were resuspended in 0.5 ml Transformation Buffer each and pooled. 100  $\mu$ l aliquots were stored at -70°C.

##### A1-2 *Transformation of competent E.coli*

Competent *E.coli* were transformed as follows: 1  $\mu$ l (0.5  $\mu$ g) of plasmid DNA was added to 100  $\mu$ l of competent bacteria (thawed on ice). Samples were incubated on ice for 20 minutes, followed by a 90 second heat shock at 42°C. Positive transformants were then selected by overnight growth (37°C) on ampicillin-positive LB agar plates (Appendix B3-2).

#### A2 *Plasmid DNA preparation*

##### A2-1 *Plasmid DNA preparation: Alkali lysis and silica matrix adsorption*

Glycerol stock solutions of plasmid-bearing *E.coli* strains, or single colonies from transformed plates, were used to inoculate flasks containing 250 ml ampicillin positive LB medium (flasks with 50 ml LB amp were inoculated for a mini plasmid preparation or "miniprep"). Cultures were grown by incubation and shaking for 24 hours at 37°C. The culture medium was transferred into 250 ml polypropylene tubes (Beckman, CA, USA) and centrifuged at 2000xg for 20 minutes in a

---

Beckman J2-21 Centrifuge (Beckman, CA, USA). For the miniprep method, 50 ml culture samples were centrifuged at 3000xg for 10 minutes in a Heraeus Biofuge *primo* centrifuge (Heraeus instruments, NJ, USA). Cells were collected and resuspended in 5 ml Glucose Resuspension Solution (see Appendix B1-1). SDS-NaOH Denaturing Solution (10 ml) (Appendix B1-1) is then added and mixed thoroughly. Lastly, Potassium Acetate Renaturation Solution (7.5 ml) (Appendix B1-1) is added to form a precipitate. Each solution is added sequentially in a ratio of 1: 2: 0.75 respectively. The mixture was then centrifuged at 1500xg for 10 minutes in a Biofuge *primo* centrifuge. The supernatant was filtered through cheesecloth (nylon cloth) and one volume of isopropanol was added and mixed before incubation at -20°C for 30 minutes. Samples were then centrifuged at 4000xg for 10 minutes. Following recovery of the pellet, samples were resuspended in 400 µl H<sub>2</sub>O containing 0.1 µg/µl DNase-free RNase (Roche, Germany) in autoclaved 1.5 ml microfuge tubes (Eppendorf, Germany) and incubated for 60 minutes at 37°C. Following RNase treatment, 2 volumes (800 µl) sodium iodide solution (Appendix B1-2) and 75 µl silica solution (Appendix B1-3) were added. The samples were left on ice for 10 minutes and then centrifuged briefly (2 to 3 seconds) at 10000xg. The pellet was washed twice with 1 ml Ethanol Washing Buffer (Appendix B1-4) prior the elution of plasmid DNA from the silica matrix by resuspending the pellet in 100 µl H<sub>2</sub>O (50 µl for the miniprep) followed by 5 minutes incubation at 55°C. Samples were then centrifuged at 10000xg for 30 seconds and the supernatant containing the plasmid DNA was retained. Further purification was sometimes necessary depending on the later application of the plasmid DNA (see Appendix A5 and C1).

#### A2-2 *Plasmid preparation: Alkali lysis and PEG precipitation*

This method was similar to Appendix A2-1 up to, and including, the incubation step with RNase A. Samples were then extracted with chloroform-phenol as in Appendix A4-1 prior to being incubated overnight in a 550 µl PEG solution (Appendix B1-11). After centrifugation for 10 minutes, the supernatant was decanted and 190 µl of H<sub>2</sub>O was added. The pellet was dissolved at 45°C for approximately 15 minutes followed by the addition of 200 µl of isopropanol.

---



Tubes were centrifuged for 15 minutes at 13000xg prior to removing the supernatant and air-drying the pellet. Samples were resuspended in 50  $\mu$ l H<sub>2</sub>O and quantified by UV spectrophotometry (Appendix A4-3).

### **A3 RNA extraction and purification**

#### **A3-1 RNA preparation: guanidinium thiocyanate method**

Following the removal of the Huh7 cell culture medium, 1 ml Guanidinium Denaturing Solution (Appendix B1-5) was added directly to each 100 mm dish. The lysate was passed through a syringe several times by continuous aspiration and was divided into two aliquots of 500  $\mu$ l each into two 1.5 ml microfuge tubes. A 50  $\mu$ l volume of sodium acetate (2 M, pH 4) was added and mixed followed by 500  $\mu$ l water-saturated phenol and 100  $\mu$ l of 49:1 chloroform/isoamyl alcohol. The mixture was vortexed for 10 seconds and allowed to stand at 4°C for 15 minutes. Following centrifugation for two minutes at 10000xg at 4°C, the top aqueous phase was transferred to a new 1.5 ml microfuge tube. The RNA was precipitated by adding 500  $\mu$ l (1 volume) of 100% isopropanol and incubated at -20°C for 30 minutes. After centrifugation at 10000xg for 10 minutes, pellets from both tubes were pooled and resuspended in 300  $\mu$ l Guanidinium Denaturing Solution. The RNA was precipitated again with 300  $\mu$ l isopropanol (1 volume) and incubated for 30 minutes at -20°C. Following centrifugation at 10000xg, the RNA pellet was resuspended in 100  $\mu$ l 75% ethanol, vortexed, and allowed to incubate for 10 minutes at room temperature. The samples were centrifuged at 10000xg for 5 minutes and the pellets were air dried and dissolved in 150  $\mu$ l distilled H<sub>2</sub>O (RNase free) for immediate use. Samples were quantitated spectrophotometrically (Appendix A4-3).

### **A4 DNA/RNA purification**

#### **A4-1 Chloroform/phenol extraction of DNA**

The chloroform/phenol method of nucleic acid extraction was routinely used following the elution of fragment DNAs from agarose gels and for general purification purposes. Briefly, DNA solutions were brought to a volume of 500  $\mu$ l

---

with distilled H<sub>2</sub>O in a 1.5 ml microfuge tube. A 500 µl volume of 1:1 phenol:chloroform, (1x volume), was added to the samples which were briefly vortexed for 10 seconds to form an emulsion. The mixture was then centrifuged for 15 seconds at 12000xg in a microfuge at room temperature. Approximately 500 µl of the aqueous phase was transferred to a fresh tube followed by the addition of 1 volume of chloroform. The samples were mixed, briefly vortexed and centrifuged again for 15 seconds at 12000xg at room temperature. The aqueous phase was removed and subjected to further purification by precipitation with ethanol.

#### A4-2 *Ethanol precipitation of DNA/RNA*

Preparations of either DNA or RNA were precipitated using ethanol and further purified. Generally, 0.1 volume of 3 M sodium acetate pH 5.2 was added to the nucleic acid containing solution followed by the addition of 2.5 volumes of 100% ice-cold ethanol. Samples were incubated at -70°C for 30 minutes followed by centrifugation at 13000xg for 15 minutes at 4°C. The pellet was recovered and washed with 70% ethanol (80% for RNA). Samples were air-dried to remove residual ethanol and resuspended in sterile H<sub>2</sub>O.

#### A4-3 *DNA/RNA spectrophotometric quantitation*

Plasmid DNA or RNA concentrations were determined by optical density measurements (Unicam 8625 UV/VIS Spectrometer) at a wavelength ( $\lambda$ ) of 260 nm (At A<sub>260</sub>, 1 absorbance unit  $\approx$  50 µg/ml dsDNA and 40 µg/ml RNA). Protein contamination was determined at  $\lambda = 280$  nm. Generally, DNA (plasmid) or RNA quality was established by resolving samples on an agarose gel alongside 1 µg of commercially available molecular weight markers.

---

**A5 Manual DNA sequencing****A5-1 Sanger sequencing – standard method**

Plasmids were prepared using the silica adsorption method described in Appendix A2-1. All components were supplied within the T7 Sequenase DNA polymerase Kit (Pharmacia Amersham, England). An amount of 0.5 pmol M13 24-mer Forward primer: 5' CGCCACGGTTTTCCCAGTCACGAC 3' was added to a 10  $\mu$ l final annealing reaction mixture. The reaction mixture included 1  $\mu$ g pBSIIKS(+)-derived plasmid DNA (Stratagene, CA, USA) and 2  $\mu$ l T7 Sequenase reaction buffer (5x concentrate). The annealing reaction took place for 2 minutes at 65°C followed by 30 minutes of slow cooling at room temperature. The labelling reaction was performed in a total volume of 15  $\mu$ l by adding the following to the annealed template-primer: 1  $\mu$ l 0.1 M dithiothreitol, 2  $\mu$ l labelling mix, 0.5  $\mu$ l (5  $\mu$ Ci) of  $\alpha$ -<sup>35</sup>S dATP (NEN du Pont, MA, USA) and 3,25 U T7 Sequenase polymerase. The reaction continued for 3 minutes at room temperature. A volume of 3.5  $\mu$ l of the labeling reaction was then transferred to tubes containing 2.5  $\mu$ l of each dideoxy nucleotide termination mixture. Tubes were incubated for a further 5 minutes at 37°C. The reaction was stopped by adding 4  $\mu$ l of stop solution (provided by the manufacturer). After heating at 95°C for 5 minutes, 2  $\mu$ l of each sample was loaded on to a 6% polyacrylamide denaturing gel containing 7 M urea and resolved at 60 W. Gels were fixed in a 10% methanol, 10% acetic acid solution and dried on a gel drier (Bio-rad, Hoefer Scientific Instruments, CA, USA). The dried gel was autoradiographed overnight at room temperature.

**A5-2 Sanger sequencing – cycle sequencing method**

This technique made use of the SequiTherm EXCEL™ II DNA Sequencing Kit (Epicentre Technologies, WI, USA). A “premix” reaction mixture was prepared initially and included: 7.2  $\mu$ l of SequiTherm EXCEL II® Sequencing Buffer, 1.0  $\mu$ l of SequiTherm EXCEL II™ Prelabeling Mix, 2 pmol of unlabelled primer (M13 24-mer Forward primer: 5' CGCCACGGTTTTCCCAGTCACGAC 3'), 0.5  $\mu$ l (5  $\mu$ Ci) of  $\alpha$ -<sup>35</sup>S dATP (NEN du Pont, MA, USA), 1  $\mu$ g of pBS II KS(+)-derived plasmid DNA and 5 U of SequiTherm EXCEL II™ DNA Polymerase. The total reaction volume

---

was 17  $\mu$ l. Primers were allowed to anneal to the template DNA by heating to 95°C for 5 minutes followed by cooling to room temperature for a further 5 minutes. 4  $\mu$ l of the premix were then added to four 0.5 ml microfuge tubes containing 2  $\mu$ l of each dideoxy nucleotide termination mixture. The annealed primers were extended by incubating the mixture for 5 minutes at 65°C. The thermal cycling reaction included 30 cycles of 30 seconds at 95°C and 1 minute at 70°C. A 3  $\mu$ l volume of stop solution (prepared by the manufacturer) was added. Samples (2  $\mu$ l) were loaded onto denaturing polyacrylamide gels and resolved as described in Appendix A5-1.

## **A6        *Histochemical assay using X-gal***

### **A6-1        *$\beta$ -galactosidase detection in transfected mammalian cell culture***

Seventy two hours after transfection, PLC/PRF/5, Huh7, Chang as well as primary HCC cells were fixed for 5 minutes with approximately 400  $\mu$ l (per 35 mm plate) of Fixer Reagent (Appendix B1-8). Cells were then rinsed twice with PBS (Appendix B1-7) prior to the addition of 1 ml X-gal solution (Appendix B1-9) to each plate. These were then incubated for 37°C overnight prior to fixing with a solution containing 1% formaldehyde, 0.5% glycerinaldehyde in 200 ml PBS (Appendix B1-7).  $\beta$ -galactosidase positive cells (blue cells) were observed and counted at 10x magnification on a standard dissecting microscope.

## **A7        *Transfections into mammalian cells***

### **A7-1        *The calcium phosphate method of transfection into mammalian cells***

This method follows closely to that developed by Graham and van der Eb (1973). PLC/PRF/5, Huh7, Chang or primary HCC cultures were seeded at one-tenth their confluent density and allowed to grow overnight. Fresh medium was added to each culture dish approximately 1.5 hours prior to transfection. A transfection solution containing a volume of 1000  $\mu$ l (or one-tenth the volume of medium in each plate) was prepared for each 100 mm dish. Briefly, appropriate volumes of each plasmid were added to 62.5  $\mu$ l 2M CaCl<sub>2</sub> and 500  $\mu$ l 2X HEPES (Appendix B1-10) and made up to a final volume of 1 ml with distilled water. This was gently

---

dispensed onto the cells. The volumes were scaled-down by a factor of five when using six-well dishes. After 16 hours incubation with the DNA/Calcium phosphate precipitate, the spent medium was aspirated and replaced with fresh medium. Using fluorescence microscopy (Zeiss Axiovert 100M, fluorescent microscope, 488 nm), equivalent transfection efficiencies were confirmed by the detection of comparable numbers of EGFP expressing cells in each culture dish (except when using the plasmid pCH-EGFP). Transfected cells were cultured for 24 hours before any medium was collected for further analyses. Cells were used for the extraction of RNA (Appendix A3-1) after three or four days post-transfection.

## **B Solutions, Reagents and Buffers**

### **B1 Solutions**

#### *B1-1 Alkaline lysis buffers for plasmid preparations*

Glucose Resuspension Solution: 50 mM glucose, 25 mM Tris-HCl (pH 8.0) and 10 mM EDTA (pH 8.0).

Denaturing Solution: 0.2 N NaOH (from a 10 N stock) and 1% SDS (from a 10% stock). The solution remained stable at room temperature in a plastic bottle.

Renaturing Solution: 1 litre contains 600 ml of 5 M potassium acetate, 115 ml glacial acetic acid and 285 ml distilled H<sub>2</sub>O. The solution is 3 M with respect to potassium and 5 M with respect to acetate.

#### *B1-2 Sodium Iodide Solution*

Sodium Iodide Solution contains 180 mM sodium iodide (NaI) and 60 mM sodium sulphite (Na<sub>2</sub>SO<sub>3</sub>). The saturated solution was filtered through filter paper to remove any un-dissolved constituents. A further 0.5 g Na<sub>2</sub>SO<sub>3</sub> was added. The solution was stored at 4°C in the dark.

---



*B1-3 Silica Matrix Solution*

Silica powder, 120 g, was resuspended in 400 ml H<sub>2</sub>O and stirred for 1 hour. The solution was allowed to settle for 30 minutes. The supernatant was centrifuged to recover the fine silica particles (800xg for 5 min). The pellet was resuspended in 100 to 200 ml distilled H<sub>2</sub>O, followed by the addition of 50% volume of nitric acid followed by heating (close to boiling) in a fume hood and washed 4 times with an excess of distilled water (800xg for 4 minutes). Lastly, the Silica Solution was stored as a 50% slurry in distilled H<sub>2</sub>O at 4°C.

*B1-4 Ethanol Wash Buffer*

Ethanol wash buffer consists of 10 mM Tris-Cl (pH 7.5), 0.1 M NaCl, and 50% ethanol. The solution was stored at -20°C.

*B1-5 Transformation Buffer*

Transformation buffer consists of 100 mM CaCl<sub>2</sub>, 10 mM PIPES-Cl (pH 7.0), and 15% glycerol. The solution was stored at -20°C.

*B1-6 Guanidinium Thiocyanate Denaturing Solution*

A working solution contains 4 M guanidinium thiocyanate, 25 mM sodium citrate (pH 7), 0.1 M β-mercaptoethanol and 0.5% N-laurylsarcosine (Sarkosyl). A stock solution was prepared without β-mercaptoethanol and was stored for up to 3 months at room temperature. Working solutions were used immediately.

*B1-7 Phosphate-buffered Saline (PBS) Solution*

PBS contains: 8 g of NaCl, 0.2 g of KCl, 1.44 g of Na<sub>2</sub>HPO<sub>4</sub>, and 0.24 g of KH<sub>2</sub>PO<sub>4</sub> in 1000 ml of distilled H<sub>2</sub>O. The pH was adjusted to 7.4 with HCl. The solution was dispensed into 200 ml aliquots and autoclaved for 20 minutes at 15 lb/in<sup>2</sup> on the liquid cycle. Aliquots were stored at room temperature.

---

**B1-8** *Fixer reagent for staining cultured mammalian cells*

The solution contains 1% formaldehyde and 0.5% glutaraldehyde in PBS (Appendix B1-7). 500 ml of fixer was prepared and stored at 4°C.

**B1-9** *X-gal Staining Solution for histochemical assays*

X-gal Staining Solution contains 4 mM potassium ferricyanide, 4 mM potassium ferrocyanide, 2 mM MgCl<sub>2</sub> and 0.4 mg/ml X-gal (5-bromo-4-chloro-3-indolyl-β-D-galactopyranoside, Sigma, MO, USA) in DMSO. Typically, 50 ml X-gal Solution was prepared and stored at 4°C.

**B1-10** *2x HEPES Buffer*

2x HEPES Buffer contains: 280 mM NaCl, 50 mM HEPES and 1.5 mM Na<sub>2</sub>HPO<sub>4</sub>. The buffer was brought to a pH of 7.1 with NaOH and sterilised through a 0.22 mm filter.

**B1-11** *PEG Solution*

A PEG Solution consists of 13% Polyethylene Glycol 8000 and 1.6 M NaCl. The solution was prepared by heating at 56°C until dissolved followed by storage at 4°C.

**B2** *Electrophoresis Buffers (Stock solutions)***B2-1** *50x Tris Acetate EDTA Buffer (TAE)*

A 50x stock solution of TAE buffer contains: 400 mM Tris-acetate (pH 7.6), 50 mM Na<sub>2</sub>.EDTA

**B2-2** *10x Tris Boric Acid EDTA Buffer (TBE)*

A 10x stock solution of TBE buffer contains: 900 mM Tris-borate (pH 8.3), 20 mM Na<sub>2</sub>.EDTA

---

**B2-3**     *RNA Loading Buffer*

A 2x stock solution of RNA Loading Buffer contains: 98% deionized formamide, 1 mM EDTA (pH 8.0), 0.25% bromophenol blue and 0.25% xylene cyanol FF.

**B3**        **Culture Media****B3-1**     *Luria-Bertani medium*

10 g of bacto-tryptone (Oxoid, England), 5 g of bacto-yeast extract (Oxoid, England), and 10 g of NaCl in 1 litre distilled H<sub>2</sub>O. The medium was sterilised by autoclaving for 20 minutes at 121°C and 15 lb/in<sup>2</sup>.

**B3-2**     *Luria-Bertani agar plates with ampicillin*

15 g of bacto-agar (Oxoid, England) was added to 1 litre of dissolved LB medium and sterilised. For ampicillin-agar plates, 1 ml of a 1000x stock solution ampicillin (100 mg/ml made in a 50% ethanol) was added to the agar prior to solidification such that the final ampicillin concentration is 100 µg/ml. Plates were stored at 4°C for up to a month.

**B3-3**     *Luria-Bertani agar plates with X-gal*

A 40 µl volume of X-gal (20 mg/ml stock in dimethyl formamide; Sigma, MO, USA) and 4 µl of IPTG (200 mg/ml aqueous solution; Roche, Germany) were spread on LB agar (ampicillin positive) plates. Plates were air-dried at 37°C for 20 minutes and stored at 4°C for up to a month.

---

## C Other Appendices

### C1 Construction of multimeric cis- and trans-cleaving vectors

#### C1-1 Constructing pBS-M1 series plasmids

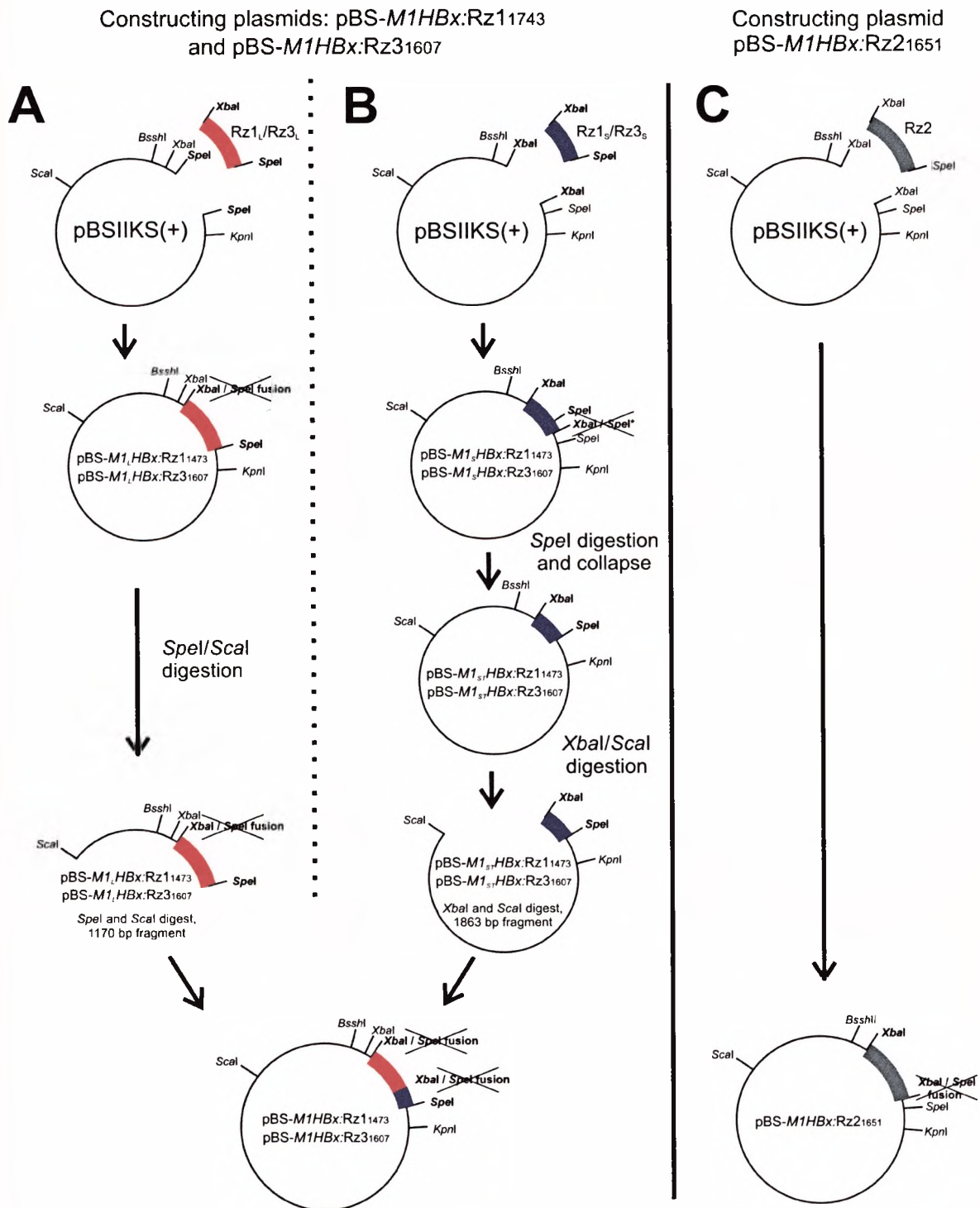


**Figure 6.1** A schematic illustration of the construction of a single-unit (*M1* series) *cis*- and *trans*-cleaving hammerhead ribozyme cloning vector for each of the three hammerhead ribozymes. The construction of plasmid pBS-M1HBx:Rz1<sub>1473</sub> (**A**), pBS-M1HBx:Rz3<sub>1607</sub> (**B**), and pBS-M1HBx:Rz2<sub>1651</sub> (**C**).

## C1-2 Constructing pBS-M2 series plasmids

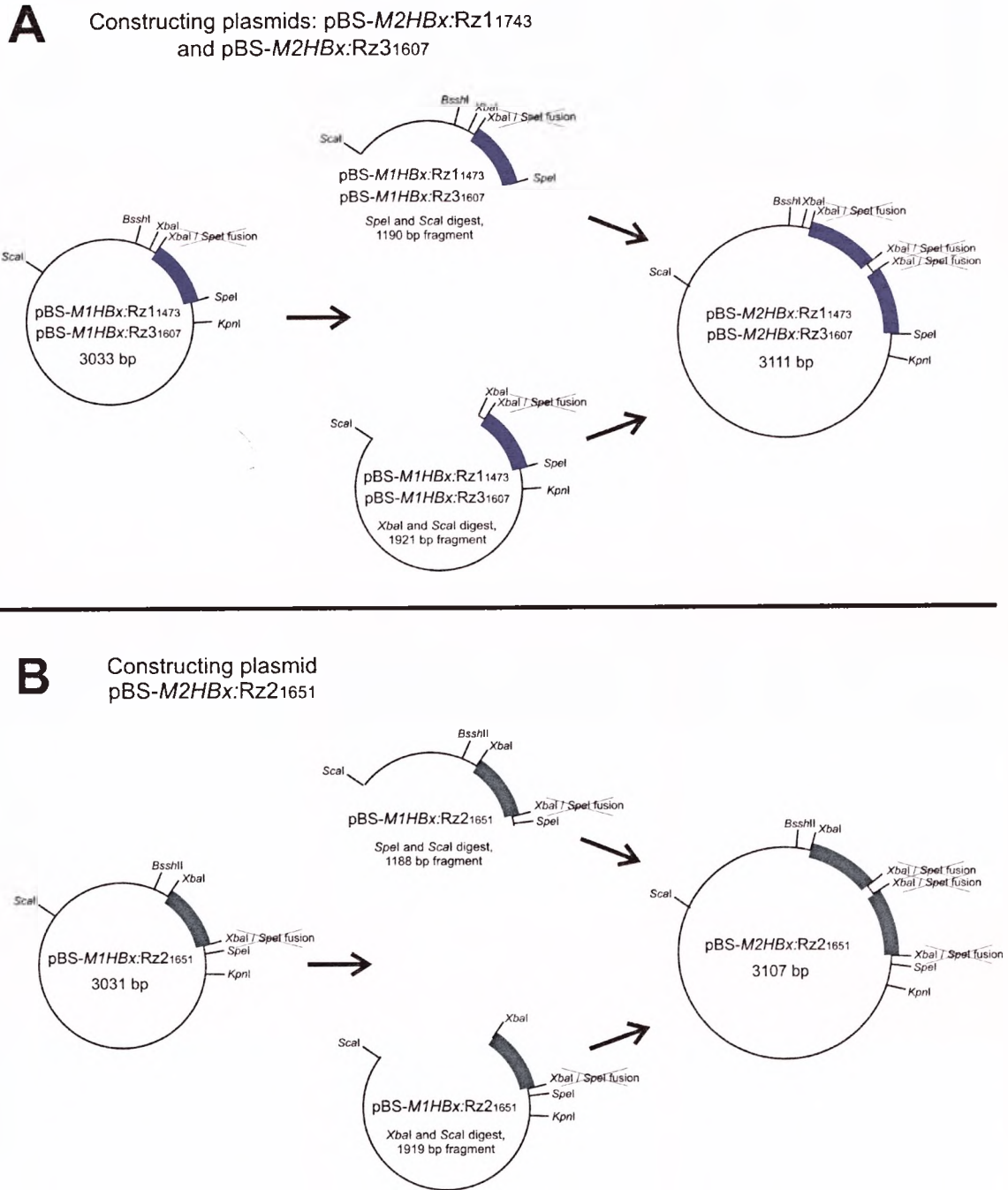


**Figure 6.2** A schematic illustration of the construction of a multiple-unit (*M2* series) *cis*- and *trans*-cleaving hammerhead ribozyme cloning vector for each of the three hammerhead ribozymes.



## C2 Determination of equivalent transfection efficiencies

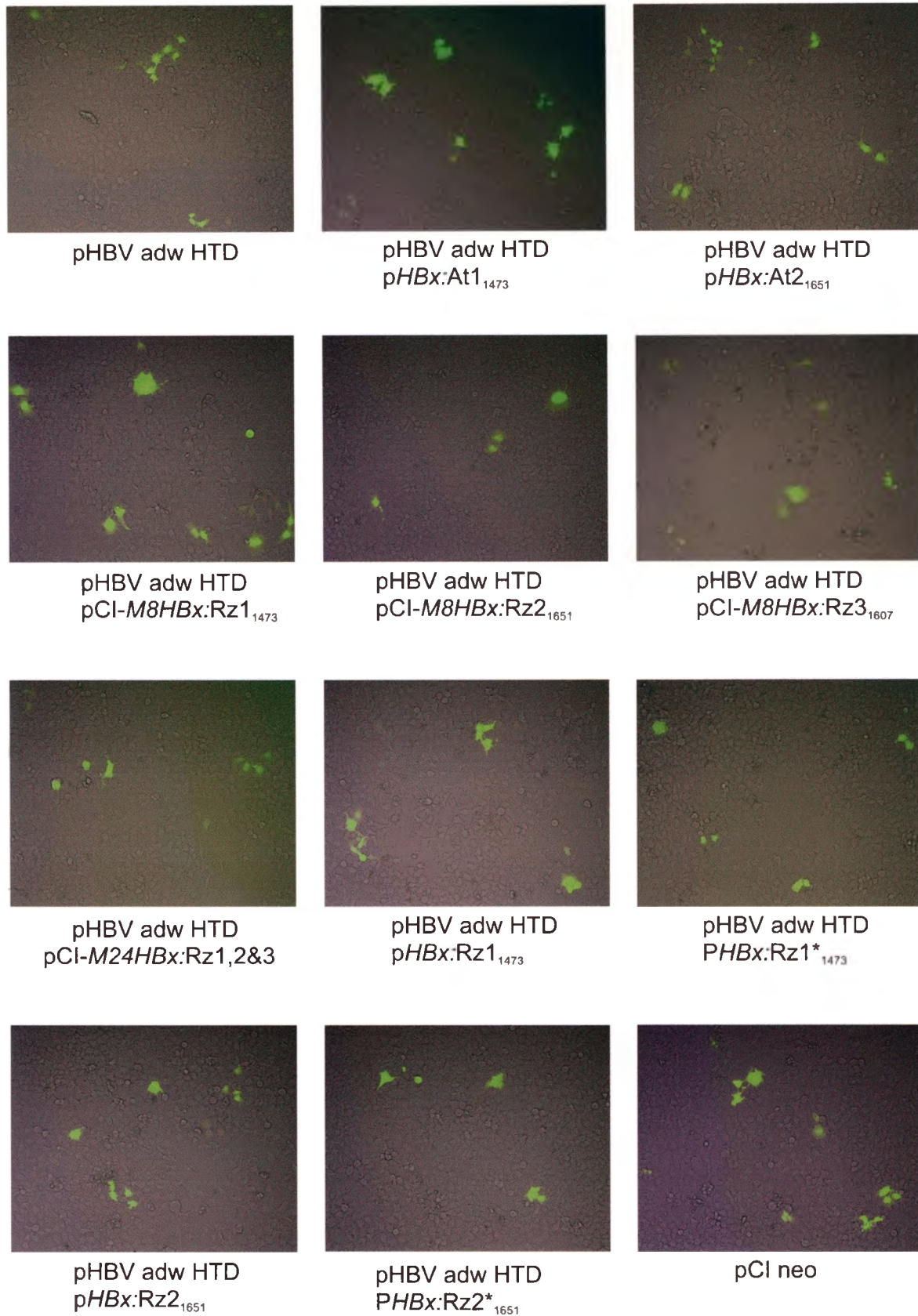


**Figure 6.3** An example of the number of EGFP-expressing Huh7 cells transfected with the plasmid pCI neo GFP for the determination of equivalent transfection efficiencies (transfection reported in 4.4.3.2).

### C3 HBx sequence variation for hammerhead ribozyme hybridisation and cleavage

		<i>HBx:Rz1</i> <sub>1473</sub>	
		↓	
		1460	1485
Serotype ayw	J02203	: CCUUCUCGGGGUCGCUUGGGACUCU	: 25
Genotype D	L27106D	: CCUUCUCGGGGUCGCUUGGGACUCU	: 25
Genotype A	V00866A	: CCCUCUCGGGGCCGCUUGGGACUCU	: 25
Genotype A	M57663AP	: CCCUCGCGAGGCCGCUUGGGACUGU	: 25
Genotype B	D00329B	: CCCUCCCGGGGCCGCUUGGGGCUCU	: 25
Genotype C	X75656C	: CCGUCUCGGGGCCGUUUGGGGAUCU	: 25
Genotype E	X75664E	: CCGUCUCGGGGUCGCUUGGGGAUCU	: 25
Genotype F	X75663F	: CCCUCCCGGGGUCGCUUGGGGCUGU	: 25
Genotype G	AF160501G	: CCCUCCCGGGGCCGUUUGGGGCUCU	: 25

		<i>HBx:Rz2</i> <sub>1651</sub>	
		↓	
		1638	1663
Serotype ayw	J02203	: AUUGCCCAAGGUCUUACAUAAGAGG	: 25
Genotype D	L27106D	: CUUGCCCAAGGUCUUAUUAAGAGG	: 25
Genotype A	V00866A	: CCUGCCCAAGGUCUUACAUAAGAGG	: 25
Genotype A	M57663AP	: CCUGCCCAAGGUCUUACAUAAGAGG	: 25
Genotype B	D00329B	: CCUGCCCAAGGUCUUGCAUAAGAGG	: 25
Genotype C	X75656C	: AUUGCCCAAGGUCUUGCAUAAGAGG	: 25
Genotype E	X75664E	: CUUGCCCAAGGUCUUACAUAAGAGG	: 25
Genotype F	X75663F	: UUUGCCAACAGUCUUACAUAAGAGG	: 25
Genotype G	AF160501G	: UCUGCCAAGGCAGUUAUAUAAG---	: 22

		<i>HBx:Rz3</i> <sub>1607</sub>	
		↓	
		1595	1618
Serotype ayw	J02203	: ACCUCUGCACGUCGCAUGGAGACC	: 24
Genotype D	L27106D	: ACCUCUGCACGUCGCAUGGAGACC	: 24
Genotype A	V00866A	: ACCUCUGCACG <u>UU</u> GCAUGGCGACC	: 24
Genotype A	M57663AP	: ACCUCUGCACG <u>UU</u> GCAUGGAGACC	: 24
Genotype B	D00329B	: ACCUCUGCACGUCGCAUGGAGACC	: 24
Genotype C	X75656C	: ACCUCUGCACGUCGCAUGGAGACC	: 24
Genotype E	X75664E	: ACCUCUGCACGUCGCAUGGAGACC	: 24
Genotype F	X75663F	: ACCUCUGCACGUCGCAUGGAGACC	: 24
Genotype G	AF160501G	: ACCUCUGCACG <u>UU</u> ACAUGGAAACC	: 24

**Figure 6.4** GeneDoc™ alignment of HBV variant RNA sense strand sequences (GenBank® accession numbers indicated) of genotypes A to G with HBV serotype ayw indicating hybridisation regions for ribozymes *HBx:Rz1*<sub>1473</sub>, *HBx:Rz2*<sub>1651</sub> and *HBx:Rz3*<sub>1607</sub>. GUC cleavage triplet sequences are shaded in blue; GUU cleavage triplet sequences are shaded in green (cleavage position is indicated by an arrow). The sequences are numbered according to 1/3182 for the *EcoRI* site of HBV serotype ayw (GenBank® accession no. J02203). The number of aligned nucleotides is indicated to the right of each sequence.

## 7.0 REFERENCES

- Abounader R., Lal B., Luddy C., Koe G., Davidson B., Rosen E. M. and Laterra J. (2002) *In vivo* targeting of SF/HGF and c-met expression via U1snRNA/ribozymes inhibits glioma growth and angiogenesis and promotes apoptosis. *Faseb J* **16**, 108-10.
- Agrawal S. and Zhao Q. (1998) Antisense therapeutics. *Curr Opin Chem Biol* **2**, 519-28.
- Akhtar S., Hughes M. D., Khan A., Bibby M., Hussain M., Nawaz Q., Double J. and Sayyed P. (2000) The delivery of antisense therapeutics. *Adv Drug Deliv Rev* **44**, 3-21.
- Albuquerque-Silva J., Houard S. and Bollen A. (1998) Tailing cDNAs with terminal deoxynucleotidyl transferase in RT-PCR assays to identify ribozyme cleavage products. *Nucleic Acids Res* **26**, 3314-6.
- Albuquerque-Silva J., Milican F., Bollen A. and Houard S. (1999) Ribozyme-mediated decrease in mumps virus nucleocapsid mRNA level and progeny in infected vero cells. *Antisense Nucleic Acid Drug Dev* **9**, 279-88.
- Altschuler M., Tritz R. and Hampel A. (1992) A method for generating transcripts with defined 5' and 3' termini by autolytic processing. *Gene* **122**, 85-90.
- Ananvoranich S. and Perreault J. P. (1998) Substrate specificity of delta ribozyme cleavage. *J Biol Chem* **273**, 13182-8.
- Arbuthnot P., Capovilla A. and Kew M. (2000) Putative role of hepatitis B virus X protein in hepatocarcinogenesis: effects on apoptosis, DNA repair, mitogen-activated protein kinase and JAK/STAT pathways [see comments]. *J Gastroenterol Hepatol* **15**, 357-68.
- Arbuthnot P. and Kew M. (2001) Hepatitis B virus and hepatocellular carcinoma. *Int J Exp Pathol* **82**, 77-100.
- Arndt G. M. and Rank G. H. (1997) Colocalization of antisense RNAs and ribozymes with their target mRNAs. *Genome* **40**, 785-97.
- Ashwell G. and Harford J. (1982) Carbohydrate-specific receptors on the liver. *Annu Rev Biochem* **51**, 531-54.
- Aufiero B. and Schneider R. J. (1990) The hepatitis B virus X-gene product *trans*-activates both RNA polymerase II and III promoters. *Embo J* **9**, 497-504.
-



- Avantaggiati M. L., Natoli G., Balsano C., Chirillo P., Artini M., De Marzio E., Colleparado D. and Levrero M. (1993) The hepatitis B virus (HBV) pX transactivates the c-fos promoter through multiple *cis*-acting elements. *Oncogene* **8**, 1567-74.
- Baglioni C. (1979) Interferon-induced enzymatic activities and their role in the antiviral state. *Cell* **17**, 255-64.
- Bai J., Rossi J. and Akkina R. (2001) Multivalent anti-CCR ribozymes for stem cell-based HIV type 1 gene therapy. *AIDS Res Hum Retroviruses* **17**, 385-99.
- Balsano C., Avantaggiati M. L., Natoli G., De Marzio E., Will H., Perricaudet M. and Levrero M. (1991) Full-length and truncated versions of the hepatitis B virus (HBV) X protein (pX) transactivate the cmyc protooncogene at the transcriptional level. *Biochem Biophys Res Commun* **176**, 985-92.
- Bartenschlager R., Junker-Niepmann M. and Schaller H. (1990) The P gene product of hepatitis B virus is required as a structural component for genomic RNA encapsidation. *J Virol* **64**, 5324-32.
- Bartholomew R. M., Carmichael E. P., Findeis M. A., Wu C. H. and Wu G. Y. (1995) Targeted delivery of antisense DNA in woodchuck hepatitis virus-infected woodchucks. *J Viral Hepat* **2**, 273-8.
- Bartolomé J., Madejon A. and Carreño V. (1995) Ribozymes: structure, characteristics and use as potential antiviral agents. *J Hepatol* **22**, 57-64.
- Beasley R. P. (1988) Hepatitis B virus. The major etiology of hepatocellular carcinoma. *Cancer* **61**, 1942-56.
- Beasley R. P., Hwang L. Y., Lin C. C. and Chien C. S. (1981) Hepatocellular carcinoma and hepatitis B virus. A prospective study of 22 707 men in Taiwan. *Lancet* **2**, 1129-33.
- Beck J. and Nassal M. (1995) Efficient hammerhead ribozyme-mediated cleavage of the structured hepatitis B virus encapsidation signal *in vitro* and in cell extracts, but not in intact cells. *Nucleic Acids Res* **23**, 4954-62.
- Beckel-Mitchener A. and Summers J. (1997) A novel transcriptional element in circular DNA monomers of the duck hepatitis B virus. *J Virol* **71**, 7917-22.
- Becker S. A., Lee T. H., Butel J. S. and Slagle B. L. (1998) Hepatitis B virus X protein interferes with cellular DNA repair. *J Virol* **72**, 266-72.
-

- Been M. D. (1994) Cis- and trans-acting ribozymes from a human pathogen, hepatitis delta virus. *Trends Biochem Sci* **19**, 251-6.
- Beigelman L., McSwiggen J. A., Draper K. G., Gonzalez C., Jensen K., Karpeisky A. M., Modak A. S., Matulic-Adamic J., DiRenzo A. B., Haerberli P. and *et al.* (1995) Chemical modification of hammerhead ribozymes. Catalytic activity and nuclease resistance. *J Biol Chem* **270**, 25702-8.
- Bertrand E., Castanotto D., Zhou C., Carbonnelle C., Lee N. S., Good P., Chatterjee S., Grange T., Pictet R., Kohn D., Engelke D. and Rossi J. J. (1997) The expression cassette determines the functional activity of ribozymes in mammalian cells by controlling their intracellular localization. *Rna* **3**, 75-88.
- Bertrand E., Pictet R. and Grange T. (1994) Can hammerhead ribozymes be efficient tools to inactivate gene function? *Nucleic Acids Res* **22**, 293-300.
- Bertrand E. and Rossi J. J. (1996) Anti-HIV therapeutic hammerhead ribozymes: targeting strategies and optimization of intracellular function. In *Catalytic RNA* (Edited by Eckstein F. and Lilley D. M. J.), Vol. 10, p. 301-313. Springer-Verlag, Berlin.
- Bertrand E. L. and Rossi J. J. (1994) Facilitation of hammerhead ribozyme catalysis by the nucleocapsid protein of HIV-1 and the heterogeneous nuclear ribonucleoprotein A1. *Embo J* **13**, 2904-12.
- Berzal-Herranz A., Joseph S., Chowrira B. M., Butcher S. E. and Burke J. M. (1993) Essential nucleotide sequences and secondary structure elements of the hairpin ribozyme. *Embo J* **12**, 2567-73.
- Birikh K. R., Berlin Y. A., Soreq H. and Eckstein F. (1997a) Probing accessible sites for ribozymes on human acetylcholinesterase RNA. *Rna* **3**, 429-37.
- Birikh K. R., Heaton P. A. and Eckstein F. (1997b) The structure, function and application of the hammerhead ribozyme. *Eur J Biochem* **245**, 1-16.
- Blum H. E., Galun E., Weizsäcker F. and Wands J. R. (1991a) Inhibition of hepatitis B virus by antisense oligodeoxynucleotides. *Lancet* **337**, 1230.
- Blum H. E., Geballe A. P., Stowring A., Figus A., A. H. and Vyas G. (1984) Hepatitis B virus in nonhepatocytes: demonstration of viral DNA in spleen, bile duct epithelium, and vascular elements by *in situ* hybridization. In *Viral hepatitis and liver disease* (Edited by Vyas G. N., Dienstag J. L. and Hoofnagle J. H.), p. 634. Grune & Stratton, New York, N.Y.
-



- Blum H. E., Liang T. J., Galun E. and Wands J. R. (1991b) Persistence of hepatitis B viral DNA after serological recovery from hepatitis B virus infection. *Hepatology* **14**, 56-63.
- Blumberg B. S., Alter H. J. and Visnich S. A. (1965) "new" antigen in leukemia sera. *J Am Med Assoc* **191**, 541-46.
- Bollyky P. L. and Holmes E. C. (1999) Reconstructing the complex evolutionary history of hepatitis B virus. *J Mol Evol* **49**, 130-41.
- Bramlage B., Luzi E. and Eckstein F. (1998) Designing ribozymes for the inhibition of gene expression. *Trends Biotechnol* **16**, 434-8.
- Branch A. D. (1996) A hitchhiker's guide to antisense and nonantisense biochemical pathways. *Hepatology* **24**, 1517-29.
- Branch A. D. (1998) A good antisense molecule is hard to find. *Trends Biochem Sci* **23**, 45-50.
- Bratty J., Chartrand P., Ferbeyre G. and Cedergren R. (1993) The hammerhead RNA domain, a model ribozyme. *Biochim Biophys Acta* **1216**, 345-59.
- Bréchet C., Hadchouel M., Scotto J., Fonck M., Potet F., Vyas G. N. and Tiollais P. (1981) State of hepatitis B virus DNA in hepatocytes of patients with hepatitis B surface antigen-positive and -negative liver diseases. *Proc Natl Acad Sci U S A* **78**, 3906-10.
- Breiner K. M., Urban S. and Schaller H. (1998) Carboxypeptidase D (gp180), a Golgi-resident protein, functions in the attachment and entry of avian hepatitis B viruses. *J Virol* **72**, 8098-104.
- Bruss V. and Gerlich W. H. (1988) Formation of transmembraneous hepatitis B e-antigen by cotranslational *in vitro* processing of the viral precore protein. *Virology* **163**, 268-75.
- Buzayan J. M., Hampel A. and Bruening G. (1986) Nucleotide sequence and newly formed phosphodiester bond of spontaneously ligated satellite tobacco ringspot virus RNA. *Nucleic Acids Res* **14**, 9729-43.
- Cameron F. H. and Jennings P. A. (1989) Specific gene suppression by engineered ribozymes in monkey cells. *Proc Natl Acad Sci U S A* **86**, 9139-43.
- Cantor G. H., McElwain T. F., Birkebak T. A. and Palmer G. H. (1993) Ribozyme cleaves rex/tax mRNA and inhibits bovine leukemia virus expression. *Proc Natl Acad Sci U S A* **90**, 10932-6.
-

- Capovilla A., Carmona S. and Arbutnot P. (1997) Hepatitis B virus X-protein binds damaged DNA and sensitizes liver cells to ultraviolet irradiation. *Biochem Biophys Res Commun* **232**, 255-60.
- Casas-Finet J. R., Smith J. D., Jr., Kumar A., Kim J. G., Wilson S. H. and Karpel R. L. (1993) Mammalian heterogeneous ribonucleoprotein A1 and its constituent domains. Nucleic acid interaction, structural stability and self-association. *J Mol Biol* **229**, 873-89.
- Caselmann W. H. (1996) *Trans*-activation of cellular genes by hepatitis B virus proteins: a possible mechanism of hepatocarcinogenesis. *Adv Virus Res* **47**, 253-302.
- Castanotto D., Bertrand E. and Rossi J. (1997) Exogenous cellular delivery of ribozymes and ribozyme encoding DNAs. *Methods Mol Biol* **74**, 429-39.
- Castanotto D., Scherr M., Lee N. S. and Rossi J. (2000) Targeting and Intracellular Expression Strategies for Therapeutic Ribozymes. In *Ribozyme Biochemistry and Biotechnology* (Edited by Krupp G. and Gaur R. K.), p. 421-440. Eaton Publishing, Natick, MA.
- Cech T. and Golden B. L. (1999) Building a catalytic active site using only RNA. In *The RNA World* (Edited by Cech T.), p. 321-49. Cold Spring Harbor Laboratory Press, New York, NY.
- Cech T. R. (2000) Structural biology. The ribosome is a ribozyme. *Science* **289**, 878-9.
- Cech T. R. and Herschlag D. (1996) Group I ribozymes: substrate recognition, catalytic strategies and comparative mechanistic analysis. In *Catalytic DNA* (Edited by Eckstein F. and Lilley D. M. J.), Vol. 10, p. 1-17. Springer, New York, NY.
- Chang C., Zhou S., Ganem D. and Standring D. N. (1994) Phenotypic mixing between different hepadnavirus nucleocapsid proteins reveals C protein dimerization to be cis preferential. *J Virol* **68**, 5225-31.
- Chang L. J., Pryciak P., Ganem D. and Varmus H. E. (1989) Biosynthesis of the reverse transcriptase of hepatitis B viruses involves de novo translational initiation not ribosomal frameshifting. *Nature* **337**, 364-8.
- Chen C. J., Banerjea A. C., Harmison G. G., Haglund K. and Schubert M. (1992) Multitarget-ribozyme directed to cleave at up to nine highly conserved HIV-1 env RNA regions inhibits HIV-1 replication--potential effectiveness
-

- against most presently sequenced HIV-1 isolates. *Nucleic Acids Res* **20**, 4581-9.
- Chen H. S., Kaneko S., Girones R., Anderson R. W., Hornbuckle W. E., Tennant B. C., Cote P. J., Gerin J. L., Purcell R. H. and Miller R. H. (1993) The woodchuck hepatitis virus X gene is important for establishment of virus infection in woodchucks. *J Virol* **67**, 1218-26.
- Chirmule N., Propert K., Magosin S., Qian Y., Qian R. and Wilson J. (1999) Immune responses to adenovirus and adeno-associated virus in humans. *Gene Ther* **6**, 1574-83.
- Chisari F. V. and Ferrari C. (1995) Hepatitis B virus immunopathogenesis. *Annu Rev Immunol* **13**, 29-60.
- Chowrira B. M., Berzal-Herranz A. and Burke J. M. (1993) Ionic requirements for RNA binding, cleavage, and ligation by the hairpin ribozyme. *Biochemistry* **32**, 1088-95.
- Christoffersen R. E., McSwiggen J. A. and Konings D. (1994) Application of computational technologies to ribozyme biotechnological products. *J Mol Struct. (Theochem)*, 273-284.
- Clouet-D'Orval B. and Uhlenbeck O. C. (1996) Kinetic characterization of two I/II format hammerhead ribozymes. *Rna* **2**, 483-91.
- Collins C. A. and Guthrie C. (2000) The question remains: is the spliceosome a ribozyme? *Nat Struct Biol* **7**, 850-4.
- Conn M. M., Prudent J. R. and Schultz P. G. (1996) Porphyrin metalation catalyzed by a small RNA molecule. *J Am Chem Soc* **118**, 7012-7013.
- Conway J. F., Cheng N., Zlotnick A., Stahl S. J., Wingfield P. T. and Steven A. C. (1998) Localization of the N terminus of hepatitis B virus capsid protein by peptide-based difference mapping from cryoelectron microscopy. *Proc Natl Acad Sci U S A* **95**, 14622-7.
- Cotten M. and Birnstiel M. L. (1989) Ribozyme mediated destruction of RNA *in vivo*. *Embo J* **8**, 3861-6.
- Courouce-Pauty A. M., Plancon A. and Soulier J. P. (1983) Distribution of HBsAg subtypes in the world. *Vox Sang* **44**, 197-211.
- Cremisi F., Scarabino D., Carluccio M. A., Salvadori P. and Barsacchi G. (1992) A new ribozyme: a catalytic activity in search of a function. *Proc Natl Acad Sci U S A* **89**, 1651-5.
-

- Crisell P., Thompson S. and James W. (1993) Inhibition of HIV-1 replication by ribozymes that show poor activity *in vitro*. *Nucleic Acids Res* **21**, 5251-5.
- Dahm S. C., Derrick W. B. and Uhlenbeck O. C. (1993) Evidence for the role of solvated metal hydroxide in the hammerhead cleavage mechanism. *Biochemistry* **32**, 13040-5.
- Dahm S. C. and Uhlenbeck O. C. (1991) Role of divalent metal ions in the hammerhead RNA cleavage reaction. *Biochemistry* **30**, 9464-9.
- Dai X., De Mesmaeker A. and Joyce G. F. (1995) Cleavage of an amide bond by a ribozyme. *Science* **267**, 237-40.
- Dane D. S., Cameron C. H. and Briggs M. (1970) Virus-like particles in serum of patients with Australia-antigen-associated hepatitis. *Lancet* **1**, 695-8.
- Dange V., Van Atta R. B. and Hecht S. M. (1990) A Mn<sup>2+</sup>-dependent ribozyme. *Science* **248**, 585-8.
- Delaney W. E. t., Locarnini S. and Shaw T. (2001) Resistance of hepatitis B virus to antiviral drugs: current aspects and directions for future investigation. *Antivir Chem Chemother* **12**, 1-35.
- Denti M. A., Martinez de Alba A. E., Sagesser R., Tsagris M. and Tabler M. (2000) A novel RNA-binding protein from *Triturus carnifex* identified by RNA- ligand screening with the newt hammerhead ribozyme. *Nucleic Acids Res* **28**, 1045-52.
- Desai S. Y., Patel R. C., Sen G. C., Malhotra P., Ghadge G. D. and Thimmapaya B. (1995) Activation of interferon-inducible 2'-5' oligoadenylate synthetase by adenoviral VAI RNA. *J Biol Chem* **270**, 3454-61.
- Di Giulio M. (1997) On the RNA world: evidence in favor of an early ribonucleopeptide world. *J Mol Evol* **45**, 571-8.
- Dorai T., Kobayashi H., Holland J. F. and Ohnuma T. (1994) Modulation of platelet-derived growth factor-beta mRNA expression and cell growth in a human mesothelioma cell line by a hammerhead ribozyme. *Mol Pharmacol* **46**, 437-44.
- Dropulic B. and Jeang K. T. (1994) Intracellular susceptibility to ribozymes in a tethered substrate-ribozyme provirus model is not predicted by secondary structures of human immunodeficiency virus type 1 RNAs *in vitro*. *Antisense Res Dev* **4**, 217-21.
-

- Dropulic B., Lin N. H., Martin M. A. and Jeang K. T. (1992) Functional characterization of a U5 ribozyme: intracellular suppression of human immunodeficiency virus type 1 expression. *J Virol* **66**, 1432-41.
- Düzgünes N. and Felgner P. L. (1993) Intracellular delivery of nucleic acids and transcription factors by cationic liposomes. *Methods Enzymol* **221**, 303-6.
- Düzgünes N., Simões S., Konopka K., Rossi J. J. and Pedroso De Lima M. C. (2001) Delivery of novel macromolecular drugs against HIV-1. *Expert Opin Biol Ther* **1**, 949-70.
- Ekland E. H. and Bartel D. P. (1996) RNA-catalysed RNA polymerization using nucleoside triphosphates. *Nature* **383**, 192.
- Evans A. A. and London W. T. (1998) Epidemiology of hepatitis B. In *Viral hepatitis* (Edited by Zuckerman A.J. a. T. H. C.), p. 107-114. Harcourt Brace & Co. Ltd, London, United Kingdom.
- Fallows D. A. and Goff S. P. (1995) Mutations in the epsilon sequences of human hepatitis B virus affect both RNA encapsidation and reverse transcription. *J Virol* **69**, 3067-73.
- Fedor M. J. and Uhlenbeck O. C. (1990) Substrate sequence effects on "hammerhead" RNA catalytic efficiency. *Proc Natl Acad Sci U S A* **87**, 1668-72.
- Fedor M. J. and Uhlenbeck O. C. (1992) Kinetics of intermolecular cleavage by hammerhead ribozymes. *Biochemistry* **31**, 12042-54.
- Feng Y., Kong Y. Y., Wang Y. and Qi G. R. (2001a) Inhibition of hepatitis B virus by hammerhead ribozyme targeted to the poly(A) signal sequence in cultured cells. *Biol Chem* **382**, 655-60.
- Feng Y., Kong Y. Y., Wang Y. and Qi G. R. (2001b) Intracellular inhibition of the replication of hepatitis B virus by hammerhead ribozymes. *J Gastroenterol Hepatol* **16**, 1125-30.
- Ferbeyre G., Smith J. M. and Cedergren R. (1998) Schistosoma satellite DNA encodes active hammerhead ribozymes. *Mol Cell Biol* **18**, 3880-8.
- Fernholz D., Galle P. R., Stemler M., Brunetto M., Bonino F. and Will H. (1993) Infectious hepatitis B virus variant defective in pre-S2 protein expression in a chronic carrier. *Virology* **194**, 137-48.
- Ferre-D'Amare A. R., Zhou K. and Doudna J. A. (1998) Crystal structure of a hepatitis delta virus ribozyme. *Nature* **395**, 567-74.
-



- Forster A. C., Davies C., Hutchins C. J. and Symons R. H. (1990) Characterization of self-cleavage of viroid and virusoid RNAs. *Methods Enzymol* **181**, 583-607.
- Forster A. C. and Symons R. H. (1987) Self-cleavage of plus and minus RNAs of a virusoid and a structural model for the active sites. *Cell* **49**, 211-20.
- Fourel G., Trepo C., Bougueleret L., Henglein B., Ponzetto A., Tiollais P. and Buendia M. A. (1990) Frequent activation of N-myc genes by hepadnavirus insertion in woodchuck liver tumours. *Nature* **347**, 294-8.
- Funato T., Ishii T., Kambe M., Scanlon K. J. and Sasaki T. (2000) Anti-K-ras ribozyme induces growth inhibition and increased chemosensitivity in human colon cancer cells. *Cancer Gene Ther* **7**, 495-500.
- Galle P. R., Schlicht H. J., Kuhn C. and Schaller H. (1989) Replication of duck hepatitis B virus in primary duck hepatocytes and its dependence on the state of differentiation of the host cell. *Hepatology* **10**, 459-65.
- Ganem D. (1998) Towards a rational therapy for hepatitis B. *J Clin Invest* **102**, 867-8.
- Gilbert W. (1986) The RNA world. *Nature* **319**, 618.
- Goldstein H., Pettoello-Mantovani M., Anderson C. M., Cordelier P., Pomerantz R. J. and Strayer D. S. (2002) Gene therapy using a simian virus 40-derived vector inhibits the development of *in vivo* human immunodeficiency virus type 1 infection of severe combined immunodeficiency mice implanted with human fetal thymic and liver tissue. *J Infect Dis* **185**, 1425-30.
- Gong S. S., Jensen A. D., Wang H. and Rogler C. E. (1995) Duck hepatitis B virus integrations in LMH chicken hepatoma cells: identification and characterization of new episomally derived integrations. *J Virol* **69**, 8102-8.
- Goodarzi G., Gross S. C., Tewari A. and Watabe K. (1990) Antisense oligodeoxyribonucleotides inhibit the expression of the gene for hepatitis B virus surface antigen. *J Gen Virol* **71**, 3021-5.
- Graham F. L. and van der Eb A. J. (1973) A new technique for the assay of infectivity of human adenovirus 5 DNA. *Virology* **52**, 456-67.
- Grasby J. A., Jonathan P., Butler G. and Gait M. J. (1993) The synthesis of oligoribonucleotides containing O6-methylguanosine: the role of conserved
-

- guanosine residues in hammerhead ribozyme cleavage. *Nucleic Acids Res* **21**, 4444-50.
- Green R., Ellington A. D. and Szostak J. W. (1990) *In vitro* genetic analysis of the Tetrahymena self-splicing intron. *Nature* **347**, 406-8.
- Guerrier-Takada C., Gardiner K., Marsh T., Pace N. and Altman S. (1983) The RNA moiety of ribonuclease P is the catalytic subunit of the enzyme. *Cell* **35**, 849-57.
- Guidotti L. G. and Chisari F. V. (1996) To kill or to cure: options in host defense against viral infection. *Curr Opin Immunol* **8**, 478-83.
- Guidotti L. G., Ishikawa T., Hobbs M. V., Matzke B., Schreiber R. and Chisari F. V. (1996) Intracellular inactivation of the hepatitis B virus by cytotoxic T lymphocytes. *Immunity* **4**, 25-36.
- Guidotti L. G., Morris A., Mendez H., Koch R., Silverman R. H., Williams B. R. and Chisari F. V. (2002) Interferon-regulated pathways that control hepatitis B virus replication in transgenic mice. *J Virol* **76**, 2617-21.
- Guo H. C. and Collins R. A. (1995) Efficient trans-cleavage of a stem-loop RNA substrate by a ribozyme derived from neurospora VS RNA. *Embo J* **14**, 368-76.
- Guo W., Chen M., Yen T. S. and Ou J. H. (1993) Hepatocyte-specific expression of the hepatitis B virus core promoter depends on both positive and negative regulation. *Mol Cell Biol* **13**, 443-8.
- Guo W. T., Bell K. D. and Ou J. H. (1991) Characterization of the hepatitis B virus EnhI enhancer and X promoter complex. *J Virol* **65**, 6686-92.
- Halatsch M. E., Schmidt U., Botefur I. C., Holland J. F. and Ohnuma T. (2000) Marked inhibition of glioblastoma target cell tumorigenicity *in vitro* by retrovirus-mediated transfer of a hairpin ribozyme against deletion-mutant epidermal growth factor receptor messenger RNA. *J Neurosurg* **92**, 297-305.
- Hampel A. and Cowan J. A. (1997) A unique mechanism for RNA catalysis: the role of metal cofactors in hairpin ribozyme cleavage. *Chem Biol* **4**, 513-7.
- Hampel A., Tritz R., Hicks M. and Cruz P. (1990) 'Hairpin' catalytic RNA model: evidence for helices and sequence requirement for substrate RNA. *Nucleic Acids Res* **18**, 299-304.
-

- Haseloff J. and Gerlach W. L. (1988) Simple RNA enzymes with new and highly specific endoribonuclease activities. *Nature* **334**, 585-91.
- Havert M. B. and Loeb D. D. (1997) cis-Acting sequences in addition to donor and acceptor sites are required for template switching during synthesis of plus-strand DNA for duck hepatitis B virus. *J Virol* **71**, 5336-44.
- He Y. K., Lu C. D. and Qi G. R. (1993) In vitro cleavage of HPV16 E6 and E7 RNA fragments by synthetic ribozymes and transcribed ribozymes from RNA-trimming plasmids. *FEBS Lett* **322**, 21-4.
- Heermann K. H., Goldmann U., Schwartz W., Seyffarth T., Baumgarten H. and Gerlich W. H. (1984) Large surface proteins of hepatitis B virus containing the pre-s sequence. *J Virol* **52**, 396-402.
- Heermann K. H., Kruse F., Seifer M. and Gerlich W. H. (1987) Immunogenicity of the gene S and Pre-S domains in hepatitis B virions and HBsAg filaments. *Intervirology* **28**, 14-25.
- Hegg L. A. and Fedor M. J. (1995) Kinetics and thermodynamics of intermolecular catalysis by hairpin ribozymes. *Biochemistry* **34**, 15813-28.
- Heidenreich O., Benseler F., Fahrenholz A. and Eckstein F. (1994) High activity and stability of hammerhead ribozymes containing 2'- modified pyrimidine nucleosides and phosphorothioates. *J Biol Chem* **269**, 2131-8.
- Heidenreich O., Xu X., Swiderski P., Rossi J. J. and Nerenberg M. (1996) Correlation of activity with stability of chemically modified ribozymes in nuclei suspension. *Antisense Nucleic Acid Drug Dev* **6**, 111-8.
- Hendrix C., Anne J., Joris B., Van Aerschot A. and Herdewijn P. (1996) Selection of hammerhead ribozymes for optimum cleavage of interleukin 6 mRNA. *Biochem J* **314**, 655-61.
- Hendry P., McCall M. J., Santiago F. S. and Jennings P. A. (1992) A ribozyme with DNA in the hybridising arms displays enhanced cleavage ability. *Nucleic Acids Res* **20**, 5737-41.
- Hernandez Y. J., Wang J., Kearns W. G., Loiler S., Poirier A. and Flotte T. R. (1999) Latent adeno-associated virus infection elicits humoral but not cell-mediated immune responses in a nonhuman primate model. *J Virol* **73**, 8549-58.
-

- Herschlag D., Khosla M., Tsuchihashi Z. and Karpel R. L. (1994) An RNA chaperone activity of non-specific RNA binding proteins in hammerhead ribozyme catalysis. *Embo J* **13**, 2913-24.
- Hertel K. J., Herschlag D. and Uhlenbeck O. C. (1994) A kinetic and thermodynamic framework for the hammerhead ribozyme reaction. *Biochemistry* **33**, 3374-85.
- Hertel K. J., Herschlag D. and Uhlenbeck O. C. (1996) Specificity of hammerhead ribozyme cleavage. *Embo J* **15**, 3751-7.
- Hertel K. J., Pardi A., Uhlenbeck O. C., Koizumi M., Ohtsuka E., Uesugi S., Cedergren R., Eckstein F., Gerlach W. L., Hodgson R. and *et al.* (1992) Numbering system for the hammerhead. *Nucleic Acids Res* **20**, 3252.
- Hertel K. J. and Uhlenbeck O. C. (1995) The internal equilibrium of the hammerhead ribozyme reaction. *Biochemistry* **34**, 1744-9.
- Heus H. A., Uhlenbeck O. C. and Pardi A. (1990) Sequence-dependent structural variations of hammerhead RNA enzymes. *Nucleic Acids Res* **18**, 1103-8.
- Homann M., Tzortzakaki S., Rittner K., Sczakiel G. and Tabler M. (1993) Incorporation of the catalytic domain of a hammerhead ribozyme into antisense RNA enhances its inhibitory effect on the replication of human immunodeficiency virus type 1. *Nucleic Acids Res* **21**, 2809-14.
- Horster A., Teichmann B., Hormes R., Grimm D., Kleinschmidt J. and Sczakiel G. (1999) Recombinant AAV-2 harboring gfp-antisense/ribozyme fusion sequences monitor transduction, gene expression, and show anti-HIV-1 efficacy. *Gene Ther* **6**, 1231-8.
- Hsieh S. Y. and Taylor J. (1992) Delta virus as a vector for the delivery of biologically-active RNAs: possibly a ribozyme specific for chronic hepatitis B virus infection. *Adv Exp Med Biol* **312**, 125-8.
- Hsu H. C., Wu T. T., Wu M. Z., Sheu J. C., Lee C. S. and Chen D. S. (1988) Tumor invasiveness and prognosis in resected hepatocellular carcinoma. Clinical and pathogenetic implications. *Cancer* **61**, 2095-9.
- Hu K. Q. and Siddiqui A. (1991) Regulation of the hepatitis B virus gene expression by the enhancer element I. *Virology* **181**, 721-6.
- Huang M. and Summers J. (1994) pet, a small sequence distal to the pregenome cap site, is required for expression of the duck hepatitis B virus pregenome. *J Virol* **68**, 1564-72.
-

- Huang S., Stupack D., Mathias P., Wang Y. and Nemerow G. (1997) Growth arrest of Epstein-Barr virus immortalized B lymphocytes by adenovirus-delivered ribozymes. *Proc Natl Acad Sci U S A* **94**, 8156-61.
- Hutchins C. J., Rathjen P. D., Forster A. C. and Symons R. H. (1986) Self-cleavage of plus and minus RNA transcripts of avocado sunblotch viroid. *Nucleic Acids Res* **14**, 3627-40.
- Hyams K. C. (1995) Risks of chronicity following acute hepatitis B virus infection: a review. *Clin Infect Dis* **20**, 992-1000.
- Illangasekare M., Sanchez G., Nickles T. and Yarus M. (1995) Aminoacyl-RNA synthesis catalyzed by an RNA. *Science* **267**, 643-7.
- James H. A. and Gibson I. (1998) The therapeutic potential of ribozymes. *Blood* **91**, 371-82.
- Jayan G. C., Cordelier P., Patel C., BouHamdan M., Johnson R. P., Lisiewicz J., Pomerantz R. J. and Strayer D. S. (2001) SV40-derived vectors provide effective transgene expression and inhibition of HIV-1 using constitutive, conditional, and pol III promoters. *Gene Ther* **8**, 1033-42.
- Jeffries A. C. and Symons R. H. (1989) A catalytic 13-mer ribozyme. *Nucleic Acids Res* **17**, 1371-7.
- Jeong J. K., Yoon G. S. and Ryu W. S. (2000) Evidence that the 5'-end cap structure is essential for encapsidation of hepatitis B virus pregenomic RNA. *J Virol* **74**, 5502-8.
- Ji W. and Si C. W. (1997) Inhibition of hepatitis B virus by retroviral vectors expressing antisense RNA. *J Viral Hepat* **4**, 167-73.
- Johnston W. K., Unrau P. J., Lawrence M. S., Glasner M. E. and Bartel D. P. (2001) RNA-catalyzed RNA polymerization: accurate and general RNA-templated primer extension. *Science* **292**, 1319-25.
- Joyce G. F. (1989) Amplification, mutation and selection of catalytic RNA. *Gene* **82**, 83-7.
- Junker-Niepmann M., Bartenschlager R. and Schaller H. (1990) A short cis-acting sequence is required for hepatitis B virus pregenome encapsidation and sufficient for packaging of foreign RNA. *Embo J* **9**, 3389-96.
- Kamimura T., Yoshikawa A., Ichida F. and Sasaki H. (1981) Electron microscopic studies of Dane particles in hepatocytes with special reference to
-



- intracellular development of Dane particles and their relation with HBeAg in serum. *Hepatology* **1**, 392-7.
- Kane M. (1995) Global programme for control of hepatitis B infection. *Vaccine* **13**, S47-9.
- Kato Y., Kuwabara T., Warashina M., Toda H. and Taira K. (2001) Relationships between the activities in vitro and in vivo of various kinds of ribozyme and their intracellular localization in mammalian cells. *J Biol Chem* **276**, 15378-85.
- Kawasaki H., Koseki S., Yokoyama K. K. and Taira K. (2000) Parameters governing *in vivo* activities of hammerhead ribozymes: construction of intracellularly active ribozyme expression systems. In *Ribozyme Biochemistry and Biotechnology* (Edited by Krupp G. and Guar R. K.), p. 457-482. Eaton Publishing, Natick, MA.
- Kew M. C., Fujita Y., Takahashi H., Coppins A. and Wands J. R. (1986) Comparison between polyclonal and first and second generation monoclonal radioimmunoassays in the detection of hepatitis B surface antigen in patients with hepatocellular carcinoma. *Hepatology* **6**, 636-9.
- Khan R. and Giedroc D. P. (1992) Recombinant human immunodeficiency virus type 1 nucleocapsid (NCp7) protein unwinds tRNA. *J Biol Chem* **267**, 6689-95.
- Kim Y. K., Junn E., Park I., Lee Y., Kang C. and Ahn J. K. (1999) Repression of hepatitis B virus X gene expression by hammerhead ribozymes [published erratum appears in *Biochem Biophys Res Commun* 1999 May 27;259(1):231]. *Biochem Biophys Res Commun* **257**, 759-65.
- Kintner R. L. and Hosick H. L. (1998) Reduction of Cripto-1 expression by a hammerhead-shaped RNA molecule results from inhibition of translation rather than mRNA cleavage. *Biochem Biophys Res Commun* **245**, 774-9.
- Kobayashi H., Takemura Y. and Miyachi H. (2001) Novel approaches to reversing anti-cancer drug resistance using gene-specific therapeutics. *Hum Cell* **14**, 172-84.
- Koizumi M., Hayase Y., Iwai S., Kamiya H., Inoue H. and Ohtsuka E. (1989) Design of RNA enzymes distinguishing a single base mutation in RNA. *Nucleic Acids Res* **17**, 7059-71.
-

- Koizumi M., Iwai S. and Ohtsuka E. (1988) Construction of a series of several self-cleaving RNA duplexes using synthetic 21-mers. *FEBS Lett* **228**, 228-30.
- Korba B. E. and Gerin J. L. (1995) Antisense oligonucleotides are effective inhibitors of hepatitis B virus replication *in vitro*. *Antiviral Res* **28**, 225-42.
- Kore A. R., Vaish N. K., Kutzke U. and Eckstein F. (1998) Sequence specificity of the hammerhead ribozyme revisited; the NHH rule. *Nucleic Acids Res* **26**, 4116-20.
- Kramvis A. and Kew M. C. (1999) The core promoter of hepatitis B virus. *J Viral Hepat* **6**, 415-27.
- Krisky D. M., Marconi P. C., Oligino T. J., Rouse R. J., Fink D. J., Cohen J. B., Watkins S. C. and Glorioso J. C. (1998a) Development of herpes simplex virus replication-defective multigene vectors for combination gene therapy applications. *Gene Ther* **5**, 1517-30.
- Krisky D. M., Wolfe D., Goins W. F., Marconi P. C., Ramakrishnan R., Mata M., Rouse R. J., Fink D. J. and Glorioso J. C. (1998b) Deletion of multiple immediate-early genes from herpes simplex virus reduces cytotoxicity and permits long-term gene expression in neurons. *Gene Ther* **5**, 1593-603.
- Kruger K., Grabowski P. J., Zaug A. J., Sands J., Gottschling D. E. and Cech T. R. (1982) Self-splicing RNA: autoexcision and autocyclization of the ribosomal RNA intervening sequence of Tetrahymena. *Cell* **31**, 147-57.
- Kunke D., Grimm D., Denger S., Kreuzer J., Delius H., Komitowski D. and Kleinschmidt J. A. (2000) Preclinical study on gene therapy of cervical carcinoma using adeno-associated virus vectors. *Cancer Gene Ther* **7**, 766-77.
- Lau G. K. (2000) Use of immunomodulatory therapy (other than interferon) for the treatment of chronic hepatitis B virus infection. *J Gastroenterol Hepatol* **15**, E46-52.
- LaVail M. M., Yasumura D., Matthes M. T., Drenser K. A., Flannery J. G., Lewin A. S. and Hauswirth W. W. (2000) Ribozyme rescue of photoreceptor cells in P23H transgenic rats: long-term survival and late-stage therapy. *Proc Natl Acad Sci U S A* **97**, 11488-93.
-

- Le Bouvier G. L. and McCollum R. W. (1970) Australia (hepatitis-associated) antigen: physicochemical and immunological characteristics. *Adv Virus Res* **16**, 357-96.
- Lee N. S., Bertrand E. and Rossi J. (1999) mRNA localization signals can enhance the intracellular effectiveness of hammerhead ribozymes. *Rna* **5**, 1200-9.
- Lee T. H., Elledge S. J. and Butel J. S. (1995) Hepatitis B virus X protein interacts with a probable cellular DNA repair protein. *J Virol* **69**, 1107-14.
- Leopold L. H., Shore S. K., Newkirk T. A., Reddy R. M. and Reddy E. P. (1995) Multi-unit ribozyme-mediated cleavage of bcr-abl mRNA in myeloid leukemias. *Blood* **85**, 2162-70.
- Lewin A. S., Drenser K. A., Hauswirth W. W., Nishikawa S., Yasumura D., Flannery J. G. and LaVail M. M. (1998) Ribozyme rescue of photoreceptor cells in a transgenic rat model of autosomal dominant retinitis pigmentosa. *Nat Med* **4**, 967-71.
- Lewin A. S. and Hauswirth W. W. (2001) Ribozyme gene therapy: applications for molecular medicine. *Trends Mol Med* **7**, 221-8.
- Lieber A. and Kay M. A. (1996) Adenovirus-mediated expression of ribozymes in mice. *J Virol* **70**, 3153-8.
- Lieber A. and Strauss M. (1995) Selection of efficient cleavage sites in target RNAs by using a ribozyme expression library. *Mol Cell Biol* **15**, 540-51.
- Lieber A. M., Vranken Peeters M. J. T. F. D. and Kay M. A. (1995) Adenovirus-mediated transfer of the amphotropic retrovirus receptor cDNA increases retroviral transduction in cultured cells. *Hum Gene Ther* **6**, 5-11.
- Lin B. and Anderson D. A. (2000) A vestigial X open reading frame in duck hepatitis B virus. *Intervirology* **43**, 185-90.
- Ling R., Mutimer D., Ahmed M., Boxall E. H., Elias E., Dusheiko G. M. and Harrison T. J. (1996) Selection of mutations in the hepatitis B virus polymerase during therapy of transplant recipients with lamivudine. *Hepatology* **24**, 711-3.
- Lo W. Y. and Ting L. P. (1994) Repression of enhancer II activity by a negative regulatory element in the hepatitis B virus genome. *J Virol* **68**, 1758-64.
- Loeb D. D., Hirsch R. C. and Ganem D. (1991) Sequence-independent RNA cleavages generate the primers for plus strand DNA synthesis in hepatitis
-

- B viruses: implications for other reverse transcribing elements. *Embo J* **10**, 3533-40.
- Lok A. S. (2000) Hepatitis B infection: pathogenesis and management. *J Hepatol* **32**, 89-97.
- Lorsch J. R. and Szostak J. W. (1994) *In vitro* evolution of new ribozymes with polynucleotide kinase activity. *Nature* **371**, 31-6.
- Lowenstein P. and Symonds G. (1997) Inhibition of Moloney murine leukaemia virus by a retroviral vector, LNL6, carrying ribozymes targeted to the 5' non-coding sequence. *J Gen Virol* **78**, 2587-90.
- Luzi E., Eckstein F. and Barsacchi G. (1997) The newt ribozyme is part of a riboprotein complex. *Proc Natl Acad Sci U S A* **94**, 9711-6.
- Macejak D. G., Jensen K. L., Jamison S. F., Domenico K., Roberts E. C., Chaudhary N., von Carlowitz I., Bellon L., Tong M. J., Conrad A., Pavco P. A. and Blatt L. M. (2000) Inhibition of hepatitis C virus (HCV)-RNA-dependent translation and replication of a chimeric HCV poliovirus using synthetic stabilized ribozymes. *Hepatology* **31**, 769-76.
- Madon J. and Blum H. E. (1996) Receptor-mediated delivery of hepatitis B virus DNA and antisense oligodeoxynucleotides to avian liver cells. *Hepatology* **24**, 474-81.
- Maguire H. F., Hoeffler J. P. and Siddiqui A. (1991) HBV X protein alters the DNA binding specificity of CREB and ATF-2 by protein-protein interactions. *Science* **252**, 842-4.
- Mahley R. W. (1988) Apolipoprotein E: cholesterol transport protein with expanding role in cell biology. *Science* **240**, 622-30.
- Malone R. W., Felgner P. L. and Verma I. M. (1989) Cationic liposome-mediated RNA transfection. *Proc Natl Acad Sci U S A* **86**, 6077-81.
- Marion P. L., Cullen J. M., Azcarraga R. R., Van Davelaar M. J. and Robinson W. S. (1987) Experimental transmission of duck hepatitis B virus to Pekin ducks and to domestic geese. *Hepatology* **7**, 724-31.
- Marion P. L., Oshiro L. S., Regnery D. C., Scullard G. H. and Robinson W. S. (1980) A virus in Beechey ground squirrels that is related to hepatitis B virus of humans. *Proc Natl Acad Sci U S A* **77**, 2941-5.
- Mason W. S., Seal G. and Summers J. (1980) Virus of Pekin ducks with structural and biological relatedness to human hepatitis B virus. *J Virol* **36**, 829-36.
-

- 
- Matzura O. and Wennborg A. (1996) RNAdraw: an integrated program for RNA secondary structure calculation and analysis under 32-bit Microsoft Windows. *Comput Appl Biosci* **12**, 247-249.
- McKay D. B. and Wedekind J. E. (1999) Small Ribozymes. In *RNA World* (Edited by Cech T.), p. 265-285. Cold Spring Harbor Laboratory Press, New York.
- Michel F., Umesono K. and Ozeki H. (1989) Comparative and functional anatomy of group II catalytic introns--a review. *Gene* **82**, 5-30.
- Michienzi A., Cagnon L., Bahner I. and Rossi J. J. (2000) Ribozyme-mediated inhibition of HIV 1 suggests nucleolar trafficking of HIV-1 RNA. *Proc Natl Acad Sci U S A* **97**, 8955-60.
- Michienzi A., Conti L., Varano B., Prislei S., Gessani S. and Bozzoni I. (1998) Inhibition of human immunodeficiency virus type 1 replication by nuclear chimeric anti-HIV ribozymes in a human T lymphoblastoid cell line. *Hum Gene Ther* **9**, 621-8.
- Michienzi A., Prislei S. and Bozzoni I. (1996) U1 small nuclear RNA chimeric ribozymes with substrate specificity for the Rev pre-mRNA of human immunodeficiency virus. *Proc Natl Acad Sci U S A* **93**, 7219-24.
- Miller R. H. and Robinson W. S. (1986) Common evolutionary origin of hepatitis B virus and retroviruses. *Proc Natl Acad Sci U S A* **83**, 2531-5.
- Miller W. A., Hercus T., Waterhouse P. M. and Gerlach W. L. (1991) A satellite RNA of barley yellow dwarf virus contains a novel hammerhead structure in the self-cleaving domain. *Virology* **183**, 711-720.
- Miyaki M., Sato C., Gotanda T., Matsui T., Mishiro S., Imai M. and Mayumi M. (1986) Integration of region X of hepatitis B virus genome in human primary hepatocellular carcinomas propagated in nude mice. *J Gen Virol* **67**, 1449-54.
- Mojzsis S. J., Krishnamurthy R. and Arrhenius G. (1999) Before RNA and After: Geophysical and Geochemical Constraints on Molecular Evolution. In *The RNA World* (Edited by Cech T. R.), p. 1-45. Cold Spring Harbor Laboratory Press, New York, NY.
- Morgan R. A. and Anderson W. F. (1993) Human gene therapy. *Annu Rev Biochem* **62**, 191-217.
-



- Moriya K., Matsukura M., Kurokawa K. and Koike K. (1996) *In vivo* inhibition of hepatitis B virus gene expression by antisense phosphorothioate oligonucleotides. *Biochem Biophys Res Commun* **218**, 217-23.
- Murray J. B., Seyhan A. A., Walter N. G., Burke J. M. and Scott W. G. (1998) The hammerhead, hairpin and VS ribozymes are catalytically proficient in monovalent cations alone. *Chem Biol* **5**, 587-95.
- Nakazono K., Ito Y., Wu C. H. and Wu G. Y. (1996) Inhibition of hepatitis B virus replication by targeted pretreatment of complexed antisense DNA in vitro. *Hepatology* **23**, 1297-303.
- Nassal M. (1997) Novel molecular approaches toward therapy of chronic hepatitis B. *Arch Virol* **142**, 611-28.
- Nassal M. (1999) Hepatitis B virus replication: novel roles for virus-host interactions. *Intervirology* **42**, 100-16.
- Nassal M., Junker-Niepmann M. and Schaller H. (1990) Translational inactivation of RNA function: discrimination against a subset of genomic transcripts during HBV nucleocapsid assembly. *Cell* **63**, 1357-63.
- Nassal M. and Schaller H. (1993) Hepatitis B virus replication. *Trends Microbiol* **1**, 221-8.
- Negro F., Gerin J. L., Purcell R. H. and Miller R. (1991) Sequence homology between HDV RNA and 7SL RNA: implications for pathogenesis. *Prog Clin Biol Res* **364**, 327-32.
- Negro F., Gerin J. L., Purcell R. H. and Miller R. H. (1989) Basis of hepatitis delta virus disease? *Nature* **341**, 111.
- Nesbitt S., Hegg L. A. and Fedor M. J. (1997) An unusual pH-independent and metal-ion-independent mechanism for hairpin ribozyme catalysis. *Chem Biol* **4**, 619-30.
- Netter H. J., Chassot S., Chang S. F., Cova L. and Will H. (1997) Sequence heterogeneity of heron hepatitis B virus genomes determined by full-length DNA amplification and direct sequencing reveals novel and unique features. *J Gen Virol* **78**, 1707-18.
- Nicoll A. J., Angus P. W., Chou S. T., Luscombe C. A., Smallwood R. A. and Locarnini S. A. (1997) Demonstration of duck hepatitis B virus in bile duct epithelial cells: implications for pathogenesis and persistent infection. *Hepatology* **25**, 463-9.
-

- Niederau C., Heintges T., Lange S., Goldmann G., Niederau C. M., Mohr L. and Haussinger D. (1996) Long-term follow-up of HBeAg-positive patients treated with interferon alfa for chronic hepatitis B. *N Engl J Med* **334**, 1422-7.
- Nissen P., Hansen J., Ban N., Moore P. B. and Steitz T. A. (2000) The structural basis of ribosome activity in peptide bond synthesis. *Science* **289**, 920-30.
- Norder H., Courouce A. M. and Magnius L. O. (1994) Complete genomes, phylogenetic relatedness, and structural proteins of six strains of the hepatitis B virus, four of which represent two new genotypes. *Virology* **198**, 489-503.
- Norder H., Hammas B., Lee S. D., Bile K., Courouce A. M., Mushahwar I. K. and Magnius L. O. (1993) Genetic relatedness of hepatitis B viral strains of diverse geographical origin and natural variations in the primary structure of the surface antigen. *J Gen Virol* **74**, 1341-8.
- Odai O., Kodama H., Hiroaki H., Sakata T., Tanaka T. and Uesugi S. (1990) Synthesis and NMR study of ribo-oligonucleotides forming a hammerhead-type RNA enzyme system. *Nucleic Acids Res* **18**, 5955-60.
- Offensperger W. B., Offensperger S., Walter E., Teubner K., Igloi G., Blum H. E. and Gerok W. (1993) *In vivo* inhibition of duck hepatitis B virus replication and gene expression by phosphorothioate modified antisense oligodeoxynucleotides. *Embo J* **12**, 1257-62.
- Ohkawa J., Takebe Y. and Taira K. (2000) An expression vector for multiple ribozymes. In *Methods in molecular medicine: Therapeutic applications of ribozymes* (Edited by Scanlon K. J.), Vol. 11. Humana Press Inc., Totowa, NJ.
- Ohkawa J., Yuyama N., Takebe Y., Nishikawa S. and Taira K. (1993a) Importance of independence in ribozyme reactions: kinetic behavior of trimmed and of simply connected multiple ribozymes with potential activity against human immunodeficiency virus. *Proc Natl Acad Sci U S A* **90**, 11302-6.
- Ohkawa J., Yuyama N., Takebe Y., Nisikawa S., Homann M., Sczakiel G. and Taira K. (1993b) Multiple site-specific cleavage of HIV RNA by transcribed ribozymes from shotgun-type trimming plasmid. *Nucleic Acids Symp Ser* **90**, 121-2.
-

- Ojwang J. O., Hampel A., Looney D. J., Wong-Staal F. and Rappaport J. (1992) Inhibition of human immunodeficiency virus type 1 expression by a hairpin ribozyme. *Proc Natl Acad Sci U S A* **89**, 10802-6.
- Okamoto H., Tsuda F., Sakugawa H., Sastrosoewignjo R. I., Imai M., Miyakawa Y. and Mayumi M. (1988) Typing hepatitis B virus by homology in nucleotide sequence: comparison of surface antigen subtypes. *J Gen Virol* **69**, 2575-83.
- Ou J. H., Laub O. and Rutter W. J. (1986) Hepatitis B virus gene function: the precore region targets the core antigen to cellular membranes and causes the secretion of the e antigen. *Proc Natl Acad Sci U S A* **83**, 1578-82.
- Pal B. K., Scherer L., Zelby L., Bertrand E. and Rossi J. J. (1998) Monitoring retroviral RNA dimerization *in vivo* via hammerhead ribozyme cleavage. *J Virol* **72**, 8349-53.
- Passman M., Weinberg M., Kew M. and Arbuthnot P. (2000) *In situ* demonstration of inhibitory effects of hammerhead ribozymes that are targeted to the hepatitis Bx sequence in cultured cells. *Biochem Biophys Res Commun* **268**, 728-33.
- Paterlini P., Poussin K., Kew M., Franco D. and Bréchet C. (1995) Selective accumulation of the X transcript of hepatitis B virus in patients negative for hepatitis B surface antigen with hepatocellular carcinoma. *Hepatology* **21**, 313-21.
- Patricia M. K., Natarajan R., Dooley A. N., Hernandez F., Gu J. L., Berliner J. A., Rossi J. J., Nadler J. L., Meidell R. S. and Hedrick C. C. (2001) Adenoviral delivery of a leukocyte-type 12 lipoxygenase ribozyme inhibits effects of glucose and platelet-derived growth factor in vascular endothelial and smooth muscle cells. *Circ Res* **88**, 659-65.
- Pavco P. A., Bouhana K. S., Gallegos A. M., Agrawal A., Blanchard K. S., Grimm S. L., Jensen K. L., Andrews L. E., Wincott F. E., Pitot P. A., Tressler R. J., Cushman C., Reynolds M. A. and Parry T. J. (2000) Antitumor and antimetastatic activity of ribozymes targeting the messenger RNA of vascular endothelial growth factor receptors. *Clin Cancer Res* **6**, 2094-103.
- Pease A. C. and Wemmer D. E. (1990) Characterization of the secondary structure and melting of a self-cleaved RNA hammerhead domain by <sup>1</sup>H NMR spectroscopy. *Biochemistry* **29**, 9039-46.
-

- Peebles C. L., Perlman P. S., Macklenburg K. L., Pertillo M. L., Tabor J. H., Jarrel K. A. and Cheng H. L. (1986) A self-splicing RNA excises an intron lariat. *Cell* **44**, 212-23.
- Perreault J. P., Wu T. F., Cousineau B., Ogilvie K. K. and Cedergren R. (1990) Mixed deoxyribo- and ribo-oligonucleotides with catalytic activity. *Nature* **344**, 565-7.
- Perrillo R., Schiff E., Yoshida E., Statler A., Hirsch K., Wright T., Gutfreund K., Lamy P. and Murray A. (2000) Adefovir dipivoxil for the treatment of lamivudine-resistant hepatitis B mutants. *Hepatology* **32**, 129-34.
- Perrotta A. T. and Been M. D. (1991) A pseudoknot-like structure required for efficient self-cleavage of hepatitis delta virus RNA. *Nature* **350**, 434-6.
- Plenat F. (1996) Animal models of antisense oligonucleotides: lessons for use in humans. *Mol Med Today* **2**, 250-7.
- Pley H. W., Flaherty K. M. and McKay D. B. (1994) Three-dimensional structure of a hammerhead ribozyme. *Nature* **372**, 68-74.
- Pollack J. R. and Ganem D. (1993) An RNA stem-loop structure directs hepatitis B virus genomic RNA encapsidation. *J Virol* **67**, 3254-63.
- Polson A. G., Bass B. L. and Casey J. L. (1996) RNA editing of hepatitis delta virus antigenome by dsRNA-adenosine deaminase. *Nature* **380**, 454-6.
- Portman D. S. and Dreyfuss G. (1994) RNA annealing activities in HeLa nuclei. *Embo J* **13**, 213-21.
- Prange R. and Streeck R. E. (1995) Novel transmembrane topology of the hepatitis B virus envelope proteins. *Embo J* **14**, 247-56.
- Preston B. D., Poiesz B. J. and Loeb L. A. (1988) Fidelity of HIV-1 reverse transcriptase. *Science* **242**, 1168-71.
- Price S. R., Ito N., Oubridge C., Avis J. M. and Nagai K. (1995) Crystallization of RNA-protein complexes. I. Methods for the large-scale preparation of RNA suitable for crystallographic studies. *J Mol Biol* **249**, 398-408.
- Prisley S., Buonomo S. B., Michienzi A. and Bozzoni I. (1997) Use of adenoviral VAI small RNA as a carrier for cytoplasmic delivery of ribozymes. *Rna* **3**, 677-87.
- Pult I., Netter H. J., Bruns M., Prassolov A., Sirma H., Hohenberg H., Chang S. F., Frolich K., Krone O., Kaleta E. F. and Will H. (2001) Identification and analysis of a new hepadnavirus in white storks. *Virology* **289**, 114-28.
-

- Radziwill G., Tucker W. and Schaller H. (1990) Mutational analysis of the hepatitis B virus P gene product: domain structure and RNase H activity. *J Virol* **64**, 613-20.
- Ramezani A., Ding S. F. and Joshi S. (1997) Inhibition of HIV-1 replication by retroviral vectors expressing monomeric and multimeric hammerhead ribozymes. *Gene Ther* **4**, 861-7.
- Reifenberg K., Wilts H., Lohler J., Nusser P., Hanano R., Guidotti L. G., Chisari F. V. and Schlicht H. J. (1999) The hepatitis B virus X protein transactivates viral core gene expression *in vivo*. *J Virol* **73**, 10399-405.
- Remy J. S., Kichler A., Mordvinov V., Schuber F. and Behr J. P. (1995) Targeted gene transfer into hepatoma cells with lipopolyamine-condensed DNA particles presenting galactose ligands: a stage toward artificial viruses. *Proc Natl Acad Sci U S A* **92**, 1744-8.
- Rensen P. C., de Vruet R. L. and van Berkel T. J. (1996) Targeting hepatitis B therapy to the liver. Clinical pharmacokinetic considerations. *Clin Pharmacokinet* **31**, 131-55.
- Rittner K., Burmester C. and Sczakiel G. (1993) In vitro selection of fast-hybridizing and effective antisense RNA directed against the human immunodeficiency virus type 1. *Nucleic Acids Res* **21**, 1381-1387.
- Robaczewska M., Guerret S., Remy J. S., Chemin I., Offensperger W. B., Chevallier M., Behr J. P., Podhajska A. J., Blum H. E., Trepo C. and Cova L. (2001) Inhibition of hepadnaviral replication by polyethylenimine-based intravenous delivery of antisense phosphodiester oligodeoxynucleotides to the liver. *Gene Ther* **8**, 874-81.
- Robinson W. S. (1994) Molecular events in the pathogenesis of hepadnavirus-associated hepatocellular carcinoma. *Annu Rev Med* **45**, 297-323.
- Robinson W. S., Clayton D. A. and Greenman R. L. (1974) DNA of a human hepatitis B virus candidate. *J Virol* **14**, 384-91.
- Rojas A. A., Vazquez-Tello A., Ferbeyre G., Venanzetti F., Bachmann L., Paquin B., Sbordoni V. and Cedergren R. (2000) Hammerhead-mediated processing of satellite pDo500 family transcripts from Dolichopoda cave crickets. *Nucleic Acids Res* **28**, 4037-43.
- Rossi J. J. and Sarver N. (1990) RNA enzymes (ribozymes) as antiviral therapeutic agents. *Trends Biotechnol* **8**, 179-83.
-



- Rossner M. T. (1992) Review: hepatitis B virus X-gene product: a promiscuous transcriptional activator. *J Med Virol* **36**, 101-17.
- Roy G., Ananvoranich S. and Perreault J. P. (1999) Delta ribozyme has the ability to cleave in trans an mRNA. *Nucleic Acids Res* **27**, 942-8.
- Ruffner D. E., Dahm S. C. and Uhlenbeck O. C. (1989) Studies on the hammerhead RNA self-cleaving domain. *Gene* **82**, 31-41.
- Ruffner D. E. and Uhlenbeck O. C. (1990) Thiophosphate interference experiments locate phosphates important for the hammerhead RNA self-cleavage reaction. *Nucleic Acids Res* **18**, 6025-9.
- Ruiz J., Wu C. H., Ito Y. and Wu G. Y. (1997) Design and preparation of a multimeric self-cleaving hammerhead ribozyme. *Biotechniques* **22**, 338-45.
- Ruiz-Opazo N., Chakraborty P. R. and Shafritz D. A. (1982) Evidence for supercoiled hepatitis B virus DNA in chimpanzee liver and serum Dane particles: possible implications in persistent HBV infection. *Cell* **29**, 129-36.
- Russnak R. H. (1991) Regulation of polyadenylation in hepatitis B viruses: stimulation by the upstream activating signal PS1 is orientation-dependent, distance-independent, and additive. *Nucleic Acids Res* **19**, 6449-56.
- Salehi-Ashtiani K. and Szostak J. W. (2001) *In vitro* evolution suggests multiple origins for the hammerhead ribozyme. *Nature* **414**, 82-4.
- Samarsky D. A., Ferbeyre G., Bertrand E., Singer R. H., Cedergren R. and Fournier M. J. (1999) A small nucleolar RNA:ribozyme hybrid cleaves a nucleolar RNA target *in vivo* with near-perfect efficiency. *Proc Natl Acad Sci U S A* **96**, 6609-14.
- Sambrook J., Fritsch E. F. and Maniatis T. (1989) *Molecular cloning: A Laboratory Manual*. Cold Spring Harbout Laboratory Press, Cold Spring Harbour, NY, USA.
- Sanes J. R., Rubenstein J. L. and Nicolas J. F. (1986) Use of a recombinant retrovirus to study post-implantation cell lineage in mouse embryos. *Embo J* **5**, 3133-42.
- Saville B. J. and Collins R. A. (1990) A site-specific self-cleavage reaction performed by a novel RNA in *Neurospora* mitochondria. *Cell* **61**, 685-96.
- Sawamura T., Nakada H. and Hazama H. (1984) Hyperasialoglycoproteinemia in patients with chronic liver diseases and/or liver cell carcinoma:
-

- asialoglycoprotein receptor in cirrhosis and liver cell carcinoma. *Gastroenterology* **87**, 1217-21.
- Sawata S., Shimayama T., Komiyama M., Kumar P. K., Nishikawa S. and Taira K. (1993) Enhancement of the cleavage rates of DNA-armed hammerhead ribozymes by various divalent metal ions. *Nucleic Acids Res* **21**, 5656-60.
- Schaller H. and Fischer M. (1991a) Transcriptional control of hepadnavirus gene expression. In *Hepadnaviruses: Molecular Biology and Pathogenesis* (Edited by Mason M. S. and Seeger C.), p. p.21-39. Springer-Verlag, Berlin.
- Schaller H. and Fischer M. (1991b) Transcriptional control of hepadnavirus gene expression. *Curr Top Microbiol Immunol* **168**, 21-39.
- Scherr M., LeBon J., Castanotto D., Cunliffe H. E., Meltzer P. S., Ganser A., Riggs A. D. and Rossi J. J. (2001) Detection of antisense and ribozyme accessible sites on native mRNAs: application to NCOA3 mRNA. *Mol Ther* **4**, 454-60.
- Scherr M. and Rossi J. J. (1998) Rapid determination and quantitation of the accessibility to native RNAs by antisense oligodeoxynucleotides in murine cell extracts. *Nucleic Acids Res* **26**, 5079-85.
- Scherr M., Rossi J. J., Sczakiel G. and Patzel V. (2000) RNA accessibility prediction: a theoretical approach is consistent with experimental studies in cell extracts. *Nucleic Acids Res* **28**, 2455-61.
- Scott W. G., Finch J. T. and Klug A. (1995) The crystal structure of an all-RNA hammerhead ribozyme: a proposed mechanism for RNA catalytic cleavage. *Cell* **81**, 991-1002.
- Sczakiel G. and Nedbal W. (1995) The potential of ribozymes as antiviral agents. *Trends Microbiol* **3**, 213-7.
- Sczakiel G. and Tabler M. (1997) Computer-aided calculation of the local folding potential of target RNA and its use for ribozyme design. *Methods Mol Biol* **74**, 11-5.
- Seeger C., Ganem D. and Varmus H. E. (1986) Biochemical and genetic evidence for the hepatitis B virus replication strategy. *Science* **232**, 477-84.
- Seeger C. and Mason W. S. (2000) Hepatitis B virus biology. *Microbiol Mol Biol Rev* **64**, 51-68.
-

- Seifer M., Hohne M., Schaefer S. and Gerlich W. H. (1991) *In vitro* tumorigenicity of hepatitis B virus DNA and HBx protein. *J Hepatol* **13**, S61-5.
- Sells M. A., Chen M. L. and Acs G. (1987) Production of hepatitis B virus particles in Hep G2 cells transfected with cloned hepatitis B virus DNA. *Proc Natl Acad Sci U S A* **84**, 1005-9.
- Sherlock S., Fox R. A., Niazi S. P. and Scheuer P. J. (1970) Chronic liver disease and primary liver-cell cancer with hepatitis-associated (Australia) antigen in serum. *Lancet* **1**, 1243-7.
- Shimayama T., Nishikawa F., Nishikawa S. and Taira K. (1993) Nuclease-resistant chimeric ribozymes containing deoxyribonucleotides and phosphorothioate linkages. *Nucleic Acids Res* **21**, 2605-11.
- Shimayama T., Nishikawa S. and Taira K. (1995) Generality of the NUX rule: kinetic analysis of the results of systematic mutations in the trinucleotide at the cleavage site of hammerhead ribozymes. *Biochemistry* **34**, 3649-54.
- Shore S. K., Nabissa P. M. and Reddy E. P. (1993) Ribozyme-mediated cleavage of the BCRABL oncogene transcript: *in vitro* cleavage of RNA and *in vivo* loss of P210 protein-kinase activity. *Oncogene* **8**, 3183-8.
- Sioud M., Natvig J. B. and Forre O. (1992) Preformed ribozyme destroys tumour necrosis factor mRNA in human cells. *J Mol Biol* **223**, 831-5.
- Sioud M., Opstad A., Zhao J. Q., Levitz R., Benham C. and Drlica K. (1994) *In vivo* decay kinetic parameters of hammerhead ribozymes. *Nucleic Acids Res* **22**, 5571-5.
- Smith T. A., Mehaffey M. G., Kayda D. B., Saunders J. M., Yei S., Trapnell B. C., McClelland A. and Kaleko M. (1993) Adenovirus mediated expression of therapeutic plasma levels of human factor IX in mice. *Nat Genet* **5**, 397-402.
- Spandau D. F. and Lee C. H. (1988) *Trans*-activation of viral enhancers by the hepatitis B virus X protein. *J Virol* **62**, 427-34.
- Sprengel R., Kaleta E. F. and Will H. (1988) Isolation and characterization of a hepatitis B virus endemic in herons. *J Virol* **62**, 3832-9.
- Staprans S., Loeb D. D. and Ganem D. (1991) Mutations affecting hepadnavirus plus-strand DNA synthesis dissociate primer cleavage from translocation and reveal the origin of linear viral DNA. *J Virol* **65**, 1255-62.
- Stein C. A. (1995) Does antisense exist? *Nat Med* **1**, 1119-21.
-

- Steinecke P., Herget T. and Schreier P. H. (1992) Expression of a chimeric ribozyme gene results in endonucleolytic cleavage of target mRNA and a concomitant reduction of gene expression *in vivo*. *Embo J* **11**, 1525-30.
- Strayer D. S. (2000) SV40-based gene therapy vectors: turning an adversary into a friend. *Curr Opin Mol Ther* **2**, 570-8.
- Stuyver L., De Gendt S., Van Geyt C., Zoulim F., Fried M., Schinazi R. F. and Rossau R. (2000) A new genotype of hepatitis B virus: complete genome and phylogenetic relatedness. *J Gen Virol* **81**, 67-74.
- Su Q., Schroder C. H., Hofmann W. J., Otto G., Pichlmayr R. and Bannasch P. (1998) Expression of hepatitis B virus X protein in HBV-infected human livers and hepatocellular carcinomas. *Hepatology* **27**, 1109-20.
- Sullenger B. A. and Cech T. R. (1993) Tethering ribozymes to a retroviral packaging signal for destruction of viral RNA. *Science* **262**, 1566-9.
- Summers J. and Mason W. S. (1982) Replication of the genome of a hepatitis B-like virus by reverse transcription of an RNA intermediate. *Cell* **29**, 403-15.
- Summers J., Smolec J. M. and Snyder R. (1978) A virus similar to human hepatitis B virus associated with hepatitis and hepatoma in woodchucks. *Proc Natl Acad Sci U S A* **75**, 4533-7.
- Sun L. Q., Wang L., Gerlach W. L. and Symonds G. (1995) Target sequence-specific inhibition of HIV-1 replication by ribozymes directed to tat RNA. *Nucleic Acids Res* **23**, 2909-13.
- Sun L. Q., Warrilow D., Wang L., Witherington C., Macpherson J. and Symonds G. (1994) Ribozyme-mediated suppression of Moloney murine leukemia virus and human immunodeficiency virus type I replication in permissive cell lines. *Proc Natl Acad Sci U S A* **91**, 9715-9.
- Symons R. H. (1992) Small catalytic RNAs. *Annu Rev Biochem* **61**, 641-71.
- Tabler M., Homann M., Tzortzakaki S. and Sczakiel G. (1994) A three-nucleotide helix I is sufficient for full activity of a hammerhead ribozyme: advantages of an asymmetric design. *Nucleic Acids Res* **22**, 3958-65.
- Takada S., Gotoh Y., Hayashi S., Yoshida M. and Koike K. (1990) Structural rearrangement of integrated hepatitis B virus DNA as well as cellular flanking DNA is present in chronically infected hepatic tissues. *J Virol* **64**, 822-8.
-

- Takagi Y. and Taira K. (1995) Temperature-dependent change in the rate-determining step in a reaction catalyzed by a hammerhead ribozyme. *FEBS Lett* **361**, 273-6.
- Takagi Y., Warashina M., Stec W. J., Yoshinari K. and Taira K. (2001) SURVEY AND SUMMARY: Recent advances in the elucidation of the mechanisms of action of ribozymes. *Nucleic Acids Res* **29**, 1815-1834.
- Takahashi K., Mishiro S. and Prince A. M. (2001) Novel Hepatitis B Virus Strain from a Chimpanzee of Central Africa (*Pan troglodytes troglodytes*) with an Unusual Antigenicity of the Core Protein. *Intervirology* **44**, 321-6.
- Tarasow T. M., Tarasow S. L. and Eaton B. E. (1997) RNA-catalysed carbon-carbon bond formation. *Nature* **389**, 54-7.
- Tavis J. E., Perri S. and Ganem D. (1994) Hepadnavirus reverse transcription initiates within the stem-loop of the RNA packaging signal and employs a novel strand transfer. *J Virol* **68**, 3536-43.
- Thomson J. B., Tuschl T. and Eckstein F. (1997) The hammerhead ribozyme. In *Catalytic RNA* (Edited by Eckstein F. and Lilley D. M. J.), p. 173-196. Springer-Verlag, Berlin.
- Tiollais P., Charnay P. and Vyas G. N. (1981) Biology of hepatitis B virus. *Science* **213**, 406-11.
- Tiollais P., Pourcel C. and Dejean A. (1985) The hepatitis B virus. *Nature* **317**, 489-95.
- Toh H., Hayashida H. and Miyata T. (1983) Sequence homology between retroviral reverse transcriptase and putative polymerases of hepatitis B virus and cauliflower mosaic virus. *Nature* **305**, 827-9.
- Tsuchihashi Z., Khosla M. and Herschlag D. (1993) Protein enhancement of hammerhead ribozyme catalysis. *Science* **262**, 99-102.
- Tsurimoto T., Fujiyama A. and Matsubara K. (1987) Stable expression and replication of hepatitis B virus genome in an integrated state in a human hepatoma cell line transfected with the cloned viral DNA. *Proc Natl Acad Sci U S A* **84**, 444-8.
- Tuschl T., Gohlke C., Jovin T. M., Westhof E. and Eckstein F. (1994) A three-dimensional model for the hammerhead ribozyme based on fluorescence measurements. *Science* **266**, 785-9.
-

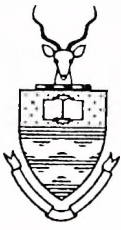


- Twu J. S., Lai M. Y., Chen D. S. and Robinson W. S. (1993) Activation of protooncogene c-jun by the X protein of hepatitis B virus. *Virology* **192**, 346-50.
- Twu J. S. and Robinson W. S. (1989) Hepatitis B virus X gene can transactivate heterologous viral sequences. *Proc Natl Acad Sci U S A* **86**, 2046-50.
- Twu J. S. and Schloemer R. H. (1987) Transcriptional *trans*-activating function of hepatitis B virus. *J Virol* **61**, 3448-53.
- Uhlenbeck O. C. (1987) A small catalytic oligoribonucleotide. *Nature* **328**, 596-600.
- Urban S., Breiner K. M., Fehler F., Klingmuller U. and Schaller H. (1998) Avian hepatitis B virus infection is initiated by the interaction of a distinct pre-S subdomain with the cellular receptor gp180. *J Virol* **72**, 8089-97.
- Usman N. and Blatt L. M. (2000) Nuclease-resistant synthetic ribozymes: developing a new class of therapeutics. *J Clin Invest* **106**, 1197-202.
- Usman N. and Stinchcomb D. T. (1996) Design, synthesis, and function of therapeutic hammerhead ribozymes. In *Catalytic RNA* (Edited by Eckstein F. and Lilley D. M. J.), p. 243-246. Springer-Verlag, Berlin.
- Usui T., Hara M., Satoh H., Moriyama N., Kagaya H., Amano S., Oshika T., Ishii Y., Ibaraki N., Hara C., Kunimi M., Noiri E., Tsukamoto K., Inatomi J., Kawakami H., Endou H., Igarashi T., Goto A., Fujita T., Araie M. and Seki G. (2001) Molecular basis of ocular abnormalities associated with proximal renal tubular acidosis. *J Clin Invest* **108**, 107-15.
- Ventura M., Wang P., Ragot T., Perricaudet M. and Saragosti S. (1993) Activation of HIV-specific ribozyme activity by self-cleavage. *Nucleic Acids Res* **21**, 3249-55.
- Vilcek J. and Sen G. C. (1996) Interferons and other cytokines. In *Fields virology* (Edited by Fields B. N., Knipe D. M. and Howley P. M.), Vol. 1, p. 375-399. Lippincott-Raven, Philadelphia, Pa.
- von Weizsäcker F., Blum H. E. and Wands J. R. (1992) Cleavage of hepatitis B virus RNA by three ribozymes transcribed from a single DNA template. *Biochem Biophys Res Commun* **189**, 743-8.
- von Weizsäcker F., Wieland S., Kock J., Offensperger W. B., Offensperger S., Moradpour D. and Blum H. E. (1997) Gene therapy for chronic viral
-

- hepatitis: ribozymes, antisense oligonucleotides, and dominant negative mutants. *Hepatology* **26**, 251-5.
- Walter P. and Blobel G. (1982) Signal recognition particle contains a 7S RNA essential for protein translocation across the endoplasmic reticulum. *Nature* **299**, 691-8.
- Wands J. R., Geissler M., Putlitz J. Z., Blum H., Weizsäcker F. V., Mohr L., Yoon S. K., Melegari M. and Scaglioni P. P. (1997) Nucleic acid-based antiviral and gene therapy of chronic hepatitis B infection. *J Gastroenterol Hepatol* **12**, S354-69.
- Wang C. and Stiles C. D. (1994) Platelet-derived growth factor alpha receptor gene expression: isolation and characterization of the promoter and upstream regulatory elements. *Proc Natl Acad Sci U S A* **91**, 7061-5.
- Wang G. H. and Seeger C. (1993) Novel mechanism for reverse transcription in hepatitis B viruses. *J Virol* **67**, 6507-12.
- Weerasinghe M., Liem S. E., Asad S., Read S. E. and Joshi S. (1991) Resistance to human immunodeficiency virus type 1 (HIV-1) infection in human CD4+ lymphocyte-derived cell lines conferred by using retroviral vectors expressing an HIV-1 RNA-specific ribozyme. *J Virol* **65**, 5531-4.
- Welch P. J., Tritz R., Yei S., Barber J. and Yu M. (1997) Intracellular application of hairpin ribozyme genes against hepatitis B virus. *Gene Ther* **4**, 736-43.
- Welch P. J., Yei S. and Barber J. R. (1998) Ribozyme gene therapy for hepatitis C virus infection. *Clin Diagn Virol* **10**, 163-71.
- Werner M. and Uhlenbeck O. C. (1995) The effect of base mismatches in the substrate recognition helices of hammerhead ribozymes on binding and catalysis. *Nucleic Acids Res* **23**, 2092-6.
- Whalley S. A., Murray J. M., Brown D., Webster G. J., Emery V. C., Dusheiko G. M. and Perelson A. S. (2001) Kinetics of acute hepatitis B virus infection in humans. *J Exp Med* **193**, 847-54.
- Wiegand T. W., Janssen R. C. and Eaton B. E. (1997) Selection of RNA amide synthases. *Chem Biol* **4**, 675-83.
- Wilson C. and Szostak J. W. (1995) *In vitro* evolution of a self-alkylating ribozyme. *Nature* **374**, 777-82.
- World Health Organisation. (1998) World Health Report. World Health Organisation (WHO).
-

- Wu G. Y. and Wu C. H. (1992) Specific inhibition of hepatitis B viral gene expression *in vitro* by targeted antisense oligonucleotides. *J Biol Chem* **267**, 12436-9.
- Wu H. N., Lin Y. J., Lin F. P., Makino S., Chang M. F. and Lai M. M. (1989) Human hepatitis delta virus RNA subfragments contain an autocleavage activity. *Proc Natl Acad Sci U S A* **86**, 1831-5.
- Wu J. and Gerber M. A. (1997) The inhibitory effects of antisense RNA on hepatitis B virus surface antigen synthesis. *J Gen Virol* **78**, 641-7.
- Xing Z., Mahadeviah S. and Whitton J. L. (1995) Antiviral activity of RNA molecules containing self-releasing ribozymes targeted to lymphocytic choriomeningitis virus. *Antisense Res Dev* **5**, 203-12.
- Xiong X., Yang H., Westland C. E., Zou R. and Gibbs C. S. (2000) In vitro evaluation of hepatitis B virus polymerase mutations associated with famciclovir resistance. *Hepatology* **31**, 219-24.
- Yang W. and Summers J. (1995) Illegitimate replication of linear hepadnavirus DNA through nonhomologous recombination. *J Virol* **69**, 4029-36.
- Yao Z., Zhou Y., Feng X., Chen C. and Guo J. (1996) In vivo inhibition of hepatitis B viral gene expression by antisense phosphorothioate oligodeoxynucleotides in athymic nude mice. *J Viral Hepat* **3**, 19-22.
- Yim S. H., Park I., Ahn J. K. and Kang C. (2000) Translational suppression by hammerhead ribozymes and inactive variants in *S. cerevisiae*. *Biomol Eng* **16**, 183-9.
- Yu M., Ojwang J., Yamada O., Hampel A., Rapaport J., Looney D. and Wong-Staal F. (1993) A hairpin ribozyme inhibits expression of diverse strains of human immunodeficiency virus type 1. *Proc Natl Acad Sci U S A* **90**, 6340-4.
- Yu X. and Mertz J. E. (1996) Promoters for synthesis of the pre-C and pregenomic mRNAs of human hepatitis B virus are genetically distinct and differentially regulated. *J Virol* **70**, 8719-8726.
- Yuyama N., Ohkawa J., Inokuchi Y., Shirai M., Sato A., Nishikawa S. and Taira K. (1992) Construction of a tRNA-embedded-ribozyme trimming plasmid. *Biochem Biophys Res Commun* **186**, 1271-9.
- Yuyama N., Ohkawa J., Koguma T., Shirai M. and Taira K. (1994) A multifunctional expression vector for an anti-HIV-1 ribozyme that produces
-

- a 5'- and 3'-trimmed *trans*-acting ribozyme, targeted against HIV-1 RNA, and *cis*-acting ribozymes that are designed to bind to and thereby sequester *trans*-activator proteins such as Tat and Rev. *Nucleic Acids Res* **22**, 5060-7.
- Zeuzem S. and Carreno V. (2001) Interleukin-12 in the treatment of chronic hepatitis B and C. *Antiviral Res* **52**, 181-8.
- Zhou D. X., Taraboulos A., Ou J. H. and Yen T. S. (1990) Activation of class I major histocompatibility complex gene expression by hepatitis B virus. *J Virol* **64**, 4025-8.
- Zoulim F., Saputelli J. and Seeger C. (1994) Woodchuck hepatitis virus X protein is required for viral infection *in vivo*. *J Virol* **68**, 2026-30.
- Zoulim F. and Seeger C. (1994) Reverse transcription in hepatitis B viruses is primed by a tyrosine residue of the polymerase. *J Virol* **68**, 6-13.
- Zoulim F. and Trepo C. (1999) New antiviral agents for the therapy of chronic hepatitis B virus infection. *Intervirol* **42**, 125-44.
- Zoumadakis M. and Tabler M. (1995) Comparative analysis of cleavage rates after systematic permutation of the NUX consensus target motif for hammerhead ribozymes. *Nucleic Acids Res* **23**, 1192-6.
- zu Putlitz J., Wieland S., Blum H. E. and Wands J. R. (1998) Antisense RNA complementary to hepatitis B virus specifically inhibits viral replication. *Gastroenterology* **115**, 702-13.
- zu Putlitz J., Yu Q., Burke J. M. and Wands J. R. (1999) Combinatorial screening and intracellular antiviral activity of hairpin ribozymes directed against hepatitis B virus. *J Virol* **73**, 5381-7.
- Zuker M. and Jacobson A. B. (1998) Using reliability information to annotate RNA secondary structures. *Rna* **4**, 669-679.
-



## UNIVERSITY OF THE WITWATERSRAND, JOHANNESBURG

---

Medical School, 7 York Road  
Parktown, Johannesburg 2193  
South Africa

☎ 27-11-647-2561  
Fax 27-11-647-2395 or  
27-11-643-4318

24 June 2002

Mr Marc S. Wienberg  
Molecular Medicine & Haematology  
Medical School  
University

Dear Mr Weinberg

This letter serves to confirm that the Chairman of the Committee for Research on Human Subjects (Medical) has acknowledged that your proposal entitled "Nucleic Acid-Based Targeting of the Hepatitis B Virus X Open Reading Frame: Inactivating Viral Gene Expression And Replication" does not require ethics approval.

Should you require any further information, please do not hesitate to contact me.

Yours sincerely,

Anisa Keshav (Ms)  
Secretary  
Committee for Research on Human Subjects (Medical)





FORM CRHS (2002)

UNIVERSITY OF THE WITWATERSRAND, JOHANNESBURG

APPLICATION TO THE COMMITTEE FOR RESEARCH ON HUMAN SUBJECTS (MEDICAL) FOR CLEARANCE OF RESEARCH INVOLVING HUMAN SUBJECTS, OR PATIENT RECORDS.

CLEARANCE NUMBER (for office use only):

no ethics clearance needed [Signature] 10-502

Awsa Kesteven 717 1234 10th floor West House

This application must be typed or handwritten in capitals

NAME: Prof/Dr/Mr/Miss/Ms MARC SAUL WEINBERG
PROFESSIONAL STATUS (if student, year of study) ASSOCIATE LECTURER / PHD 4
UNIVERSITY DEPARTMENT MOLECULAR MEDICINE AND HAEMATOLOGY
HOSPITAL/INSTITUTION WHERE EMPLOYED UNIVERSITY OF THE WITWATERSRAND
FULL-TIME OR PART-TIME FULL-TIME marc.saul@wits.ac.za
TELEPHONE AND EXTENSION 72362 FAX NO 72395

TITLE OF RESEARCH PROJECT: (Use no abbreviations)
NUCLEIC ACID-BASED TARGETING OF THE HEPATITIS B VIRUS X OPEN READING FRAME : INACTIVATING VIRAL GENE EXPRESSION AND REPLICATION
WHERE WILL THE RESEARCH BE CARRIED OUT? (Please furnish name of hospital/institution and particular department) WITS UNIVERSITY, MEDICAL SCHOOL DEPT. MOLECULAR MEDICINE

All the following sections must be completed. Please tick all relevant boxes.

- 1. PURPOSE OF THE RESEARCH: postgraduate: degree/diploma (state which) [X] PhD undergraduate: degree/diploma (state which) [ ] not for degree purposes [ ]

- 2. OBJECTIVES OF THE RESEARCH (please list): SEE ATTACHMENT

1. Unless received by the 15th of the month, applications will be carried over to the next month for consideration. 2. If not employed by the University or one of the University's teaching hospitals, please indicate clearly where correspondence should be sent. 3. This requirement holds even if, to assist the Committee, a protocol detailing the background to the research, the design of the investigation and all procedures, is submitted with the application.